

UNIVERSIDADE FEDERAL DO RIO GRANDE DO SUL
INSTITUTO DE CIÊNCIAS BÁSICAS DA SAÚDE

PROGRAMA DE PÓS-GRADUAÇÃO EM CIÊNCIAS BIOLÓGICAS: BIOQUÍMICA

Juciano Gasparotto

A função mediadora do receptor para produtos finais de glicação avançada (RAGE) na neuroinflamação e neurodegeneração em diferentes modelos *in vivo*

Porto Alegre, 2017

Juciano Gasparotto

A função mediadora do receptor para produtos finais de glicação avançada (RAGE) na neuroinflamação e neurodegeneração em diferentes modelos *in vivo*

Tese submetida ao Programa de Pós-Graduação em Ciências Biológicas: Bioquímica, como requisito para obtenção do título de Doutor.

Orientador: Prof. Dr. Daniel Pens Gelain

Porto Alegre, 2017

CIP - Catalogação na Publicação

Gasparotto, Juciano

A função mediadora do receptor para produtos finais de glicação avançada (RAGE) na neuroinflamação e neurodegeneração induzida por diferentes modelos in vivo / Juciano Gasparotto. -- 2018.

118 f.

Orientador: Daniel Pens Gelain.

Tese (Doutorado) -- Universidade Federal do Rio Grande do Sul, Instituto de Ciências Básicas da Saúde, Programa de Pós-Graduação em Ciências Biológicas: Bioquímica, Porto Alegre, BR-RS, 2018.

1. RAGE. 2. Neuroinflamação. 3. Neurodegeneração.
I. Pens Gelain, Daniel, orient. II. Título.

Elaborada pelo Sistema de Geração Automática de Ficha Catalográfica da UFRGS com os dados fornecidos pelo(a) autor(a).

Dedicatória

Dedico esta tese com a mais pura alegria e satisfação à minha amada Geovana, por estar presente na minha vida em todos os momentos.

Agradecimento

Agradeço a Universidade Federal do Rio Grande do Sul, ao Programa de Pós-Graduação em Ciências Biológicas-Bioquímica, em especial, as pessoas da secretaria: Cléia, Claudia, Serginho, Giordano e Douglas, por fornecer toda a estrutura e amparo necessário para a realização desta tese.

Às agências financiadoras brasileiras e rio grandense de fomento à pesquisa e de bolsas de pós-graduação- CAPES, CNPq, PROPESQ-UFRGS e FAPERGS;

Ao meu orientador, por conceder a total liberdade para aprimorar nossos estudos (intelectualmente e estruturalmente), pela disponibilidade em discutir os resultados, pelos ricos momentos de troca de ideias, pela competência em orientar e pela parceria tanto dentro do laboratório quanto fora. Muito obrigado Daniel, faltam palavras para descrever minha gratidão.

Ao professor Zé que me abriu as portas do laboratório me dando a oportunidade de realizar um sonho.

A todos os colegas do Lab. 32 que me auxiliaram na concretização do mestrado e doutorado.

Aos queridos colegas e amigos Rafael, Vitor e Nauana, pela amizade e pelo conhecimento que trocamos diariamente. É muito bom estar perto de pessoas como vocês.

Aos bolsistas de iniciação científica sou muito grato por todo o auxílio. Espero ter contribuído tanto quanto contribuíram comigo. Foram fundamentais para a construção desta tese.

Aos meu pais, Jaci (*In memoriam*) e Ana, pelo carinho, incentivo, esforço e dedicação em me ajudar sempre. Muito obrigado por tudo. Amo vocês.

A Gabe e a Marilu pelo apoio, parceria, carinho e por estarem sempre perto dispostas a ajudar. Amo vocês.

Um agradecimento mais que especial à pessoa fundamental para que todo este trabalho fosse concretizado, minha esposa, Geovana, minha maior incentivadora, seja no trabalho ou na vida, presente nos momentos mais delicados e nos mais felizes. Companheira de todas horas, essencial na minha vida. Te amo Giuzinha.

A ciência nunca resolve um problema sem
criar pelo menos outros dez

George Bernard Shaw

SUMÁRIO

Parte 1

I. Resumo	1
II. Abstract.....	2
III. Lista de abreviaturas e siglas	3
IV. Introdução.....	5
V. Objetivos.....	21

Parte 2

Resultados	23
------------------	----

Capítulo I: Increased tau phosphorylation and receptor for advanced glycation endproducts (RAGE) in the brain of mice infected with *Leishmania amazonensis*.... 23

Capítulo II: Anti-RAGE antibody selectively blocks acute systemic inflammatory responses to LPS in serum, liver, CSF and striatum

Capítulo III: Receptor for advanced glycation end products mediates sepsis-triggered amyloid- β accumulation, tau phosphorylation, and cognitive impairment... 49

Capítulo IV: Targeted inhibition of RAGE in substantia nigra of rats blocks 6-OHDA-induced dopaminergic denervation..... 69

Parte 3

Discussão	84
Conclusões	95
Perspectivas	96
Referências Bibliográficas.....	98

Lista de figuras

Figura 1. Estrutura do RAGE.....	6
Figura 2. Isoformas do RAGE.....	9
Figura 3. Mecanismo do <i>looping de feed back</i> positivo do RAGE.....	12
Figura 4. Estrutura do antagonista do RAGE.....	18
Figura 5. A inibição do RAGE bloqueia a neuroinflamação e a neurodegeneração induzida pela interação com seus ligantes.....	93

Apresentação

A presente tese de doutorado está organizada em três partes, conforme segue:

Parte 1: Resumo, *abstract*, lista de abreviaturas, introdução e objetivos;

Parte 2: Resultados apresentados na forma de 4 artigos científicos;

Parte 3: Discussão, conclusões, perspectivas e referências bibliográficas.

Parte 1

I. Resumo

O RAGE é um receptor transmembrana, imunoglobulina-*like* que existe em múltiplas isoformas e interage com um amplo repertório de ligantes extracelulares. O RAGE é expresso em níveis baixos na maioria das células, porém o aumento da presença de seus ligantes no domínio extracelular faz com que o RAGE inicie uma cascata de sinalização intracelular complexa, resultando em estresse oxidativo, ativação do fator de transcrição NF- κ B, aumento da expressão de citocinas, além da indução de sua própria expressão. O envolvimento do RAGE neste amplo espectro de sinalização vincula este receptor a diversas condições patológicas. Nesta tese utilizamos 3 modelos experimentais que induzem inflamação sistêmica (*Leishmania amazonensis*, Lipopolissacarídeo e sepse) e 1 modelo experimental que mimetiza a denervação neuronal (modelos experimentais *in vivo*). Além disso utilizamos diferentes abordagens de bloqueio do RAGE a fim de elucidar a função deste receptor. Com base em nossos resultados os modelos experimentais foram eficientes em induzir o aumento do RAGE e sua sinalização no sistema nervoso central, desencadeando a síntese e liberação de moléculas pró-inflamatórias e o aumento do estresse oxidativo, culminando em neuroinflamação e neurodegeneração. As intervenções de bloqueio do RAGE foram eficientes em inibir as vias de sinalização intracelular mediadas pelo receptor, comprovando a via de ação. Levando em conta nossos principais resultados concluímos que: **a)** RAGE atua como mediador da perda neuronal em resposta ao insulto inflamatório em diversas estruturas do SNC, **b)** está presente no corpo dos neurônios dopaminérgicos e envolvido na morte destes neurônios; **c)** o aumento do RAGE é tempo-dependente e a morte dos neurônios está vinculada a ação deste receptor.

Palavras chave: RAGE; neuroinflamação; neurodegeneração

II. Abstract

RAGE is a transmembrane, immunoglobulin-like receptor that exists in multiple isoforms and interacts with a broad repertoire of extracellular ligands. RAGE is expressed at low levels in most cells, but the increased presence of its ligands initiates a complex intracellular signaling cascade resulting in oxidative stress, activation of transcription factor NF- κ B, increased expression of cytokines in addition to concomitant upregulation of RAGE itself. In this thesis we used 3 experimental models which induce systemic inflammation (*Leishmania amazonensis*, Lipopolysaccharide and sepsis) and 1 experimental model that mimics neuronal denervation (experimental models *in vivo*). In addition, different approaches to block RAGE were used to elucidate the function of this receptor. Based on our results the experimental models were efficient in inducing the increase of RAGE and its signaling in the central nervous system, triggering the synthesis and release of proinflammatory molecules and the increase of oxidative stress, culminating in neuroinflammation and neurodegeneration. The RAGE blocking interventions were effective in inhibiting receptor-mediated signaling, proving the signaling pathway. Considering our main results, we conclude that: **a)** RAGE acts as a mediator of neuronal loss triggered by inflammatory insults in various CNS structures; **b)** RAGE is present in the body of dopaminergic neurons and is involved in the death of these neurons; **c)** the increase of RAGE is time-dependent, and the neuronal death is dependent on the action of this receptor.

Key words: RAGE; neuroinflammation; neurodegeneration

III. Lista de abreviaturas e siglas

6-OHDA: 6-hidroxidopamina

AKT ou **PKB:** proteína cinase B

ADAM10: proteína desintegrina e metaloproteínase 10, do inglês: *disintegrin and metalloproteinase domain-containing protein 10*

AGE: produto final de glicação avançada, do inglês: *advanced glycation end-products*

AGER: Gene humano do RAGE, do inglês: *advanced glycation end-products receptor*

CDC42: proteína de controle de divisão celular 42, do inglês: *cell division control protein 42 homolog*

CLP: Ligadura e Perfuração Cecal, do inglês: *cecal ligation puncture*

CML: N ϵ - (carboximetil) lisina

DAMP: Padrão molecular associado ao dano, do inglês: *damage-associated molecular pattern*

DIAPH1: proteína diáfano 1, do inglês: *protein diaphanous homolog 1*

DN-RAGE: RAGE dominante negativo, do inglês: *dominant negative - receptor for advanced glycation end products*

ERO: espécie reativa de oxigênio

FL-RAGE: versão completa do RAGE, do inglês: *full length - receptor for advanced glycation end-products*

FPS-ZM1: *N*-Benzil-*N*-ciclo-hexil-4-clorobenzamida

HMGB1: grupo de alta mobilidade 1, do inglês: *high mobility group box 1*

HSP70: proteína de choque térmico 70, do inglês: *high shock protein 70*

IL-1 β : interleucina 1 β

JAK: janus cinase

LPS: lipopolissacarídeo

MIP-1 α : proteína inflamatória de macrófagos 1 α , do inglês: *macrophage inflammatory protein 1 α*

MIP-1 β : proteína inflamatória de macrófagos 1 β , do inglês: *macrophage inflammatory protein 1 β*

MMP9: metaloproteínase 9

N-CAM: moléculas de adesão celular neural, do inglês: *neural cell adhesion molecule*

N-RAGE: RAGE N-truncado, do inglês: N-truncated: *receptor for advanced glycation end-products*

SAPK/JNK: proteína cinase ativadas por estresse/cinases jun amino-terminais, do inglês: *stress-activated protein kinases/Jun amino-terminal kinases*

sRAGE: RAGE solúvel, do inglês: *soluble receptor for advanced glycation end products*

MAPK: proteína-cinases ativadas por mitógenos, do inglês: *mitogen-activated protein kinase*

MHC: complexo principal de histocompatibilidade, do inglês: *major histocompatibility complex*

mTOR: proteína alvo da rapamicina em mamíferos, do inglês: *mammalian target of rapamycin*

NF- κ B: fator nuclear kappa B, do inglês: *nuclear factor kappa B*

RAGE: receptor para produtos finais de glicação avançada - do inglês: *receptor for advanced glycation end products*

SNC: sistema nervoso central

STAT: transdutor de sinal e ativador de transcriptoma, do inglês: *signal transducer and activator of transcription*

TH: tirosina hidroxilase

TLR4: receptor tipo toll 4, do inglês: *toll-like receptor 4*

TNF- α : fator de necrose tumoral- α , do inglês: *tumor necrosis factor- α*

IV. Introdução

Estrutura do RAGE

A exposição de proteínas a açúcares redutores resulta em glicação através de ação não enzimática, formando os produtos finais de glicação avançada (AGEs). Em 1992 (Schmidt *et al.*, 1992) ao tentar identificar o mecanismo pelo qual os AGEs modulam as funções celulares no pulmão de bovinos os investigadores descreveram a presença de um aceptor de alta afinidade presente na superfície das células. Este aceptor foi posteriormente purificado e definido como o receptor para produtos finais de glicação avançada (RAGE) (Schmidt *et al.*, 1992; Schmidt *et al.*, 1996). Desde então o RAGE vem sendo intensamente investigado.

RAGE é um receptor transmembrana que pertence a superfamília das imunoglobulinas. Este receptor possui múltiplas isoformas com capacidade multiligante surpreendente e é considerado um receptor de reconhecimento de padrões (Chavakis *et al.*, 2003). O gene humano do RAGE (*AGER*) está localizado no cromossomo 6 na região de classe III do complexo principal de histocompatibilidade que contém 11 exons. Estruturalmente, o RAGE consiste de 404 aminoácidos com uma massa molecular de 50 kDa (Neeper *et al.*, 1992). O RAGE na versão completa consiste de **uma estrutura extracelular**, que possui uma sequência na região N-terminal (aminoácidos 1-22), um domínio imoglobulina-*like* do tipo-V (aminoácidos 23-116), e uma sequência de dois domínios imoglobulina-*like* de tipo-C (aminoácidos 124-221 e 227-317, respectivamente). **Um domínio transmembrana único** (aminoácidos 343-363). E **uma cauda citoplasmática** intracelular curta (C-terminal) altamente carregada (aminoácidos 364-404) (Neeper *et al.*, 1992).

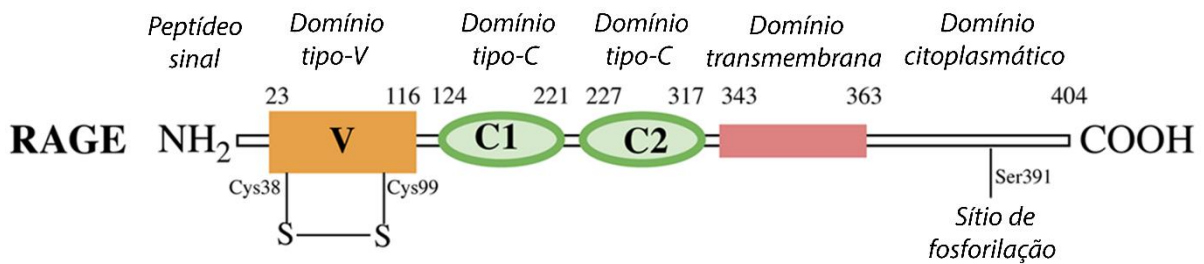


Figura 1. Estrutura do RAGE. Adaptado de (Bongarzone *et al.*, 2017).

O domínio do tipo-V apresenta estrutura secundária e consiste de duas folhas β conectadas por uma ponte dissulfeto, uma pequena hélice α e uma *random coil* que não possui uma estrutura secundária definida (Yatime e Andersen, 2013). É o principal sítio de ligação para ligantes que interagem com RAGE em nível micromolar (Matsumoto *et al.*, 2008). Os outros domínios também apresentam capacidade de ligar moléculas, por exemplo, a proteína S100B liga-se a ambos domínios V e C1, enquanto que S100A6 se liga aos domínios C1 e C2 (Leclerc *et al.*, 2007).

O domínio C1 se dobra (*fold*) em um domínio de Ig do tipo-C clássico (Dattilo *et al.*, 2007; Yatime e Andersen, 2013). A superfície molecular dos domínios V e C1 é coberta por uma cavidade hidrofóbica e áreas carregadas positivamente. Várias ligações de hidrogênio e interações hidrofóbicas ocorrem entre os domínios V e C1 formando uma unidade estrutural integrada para reconhecimento do ligantes (VC1) (Dattilo *et al.*, 2007).

Estudos demonstraram que o ectodomínio VC1 articulado, está implicado na interação com uma gama diversificada de ligantes do RAGE que possuem característica ácida (carregado negativamente), como AGEs, HMGB1 (grupo de alta mobilidade 1) e β -amilóide (Hori *et al.*, 1995; Xue *et al.*, 2014).

O RAGE pode sofrer dimerização ou oligomerização multimodal mediada por auto associação de domínios V-V ou C1-C1 (Koch *et al.*, 2010; Zong *et al.*, 2010; Yatime e Andersen, 2013). O domínio VC1 é anexado ao domínio C2 por uma ligação flexível (Kislinger *et al.*, 2001). O domínio C2 consiste de duas folhas- β estabilizadas por pontes dissulfeto, além de possuir uma grande superfície carregada negativamente com resíduos ácidos direcionados para a superfície básica do oligômero VC1 (Yatime e Andersen, 2013).

O domínio extracelular (VC1C2) do RAGE humano (UniProtKB Q15109) compartilha uma identidade de sequência de 79,2% (Q62151) com ratos (*Rattus norvegicus*) e 96,5% (Q63495) com primatas (*Rhesus macaque*, F1ABQ1) (Rodriguez Gonzalez-Moro *et al.*, 2009). Os resíduos carregados positivamente envolvidos na ligação de AGE a RAGE, são conservados nas 3 espécies sugerindo um padrão de ligação comum (Rodriguez Gonzalez-Moro *et al.*, 2009; Xue *et al.*, 2014). O domínio transmembrana do RAGE é uma estrutura helicoidal que pode promover a homodimerização hélice-hélice do receptor e, portanto, pode estar envolvida na transdução de sinal (Yatime e Andersen, 2013). A cauda citoplasmática do RAGE é dividida em pelo menos três partes: um domínio de 17 aminoácidos proximal a membrana, rica em aminoácidos básicos (Arg366, Arg368, Arg369 e Glu371), um domínio central de 17 aminoácidos contendo ácidos glutâmicos e um local de fosforilação em Ser391 e um domínio C-terminal não estruturado (Rai *et al.*, 2012). Esta pequena cauda citoplasmática na região C-terminal é crucial para a interação do domínio citoplasmático do RAGE com moléculas efetoras que disparam sinalização intracelular.

A cauda citoplasmática é absolutamente essencial para sinalização intracelular do RAGE (Ding e Keller, 2005), na ausência da cauda, RAGE é capaz de reconhecer

e ligar seus ligantes, porém não dispara a sinalização intracelular (Hofmann *et al.*, 1999).

A ligação RAGE-ligante dispara a sinalização de várias proteínas incluindo, diáfano-1 (DIAPH1), proteína-cinases ativadas por mitógenos (MAPKs), - proteína de controle de divisão celular 42 (CDC42) e Janus cinase (JAK)/ transdutores de sinal e ativadores de transcriptomas (STATs) e subsequente ativação da via do NF- κ B (Hudson *et al.*, 2008; Ramasamy *et al.*, 2008; Rai *et al.*, 2012).

Isoformas do RAGE

Até o momento estão documentadas 22 isoformas do RAGE em seres humanos, 12 das quais são encontradas no cérebro (Lopez-Diez *et al.*, 2013). Estas isoformas variam por splicing alternativo, que inclui a forma solúvel, além dos receptores ligados a membrana celular (Lopez-Diez *et al.*, 2013).

As 4 isoformas principais do RAGE são (figura 2):

1) RAGE na forma completa, *full-length* (FL-RAGE): contém todos os principais componentes do receptor e representa a sua forma ativa para transduzir o sinal intracelular.

2) RAGE dominante negativo (DN-RAGE): está ancorado na membrana, porém não apresenta a cauda intracelular, portanto não há mediação de sinalização entre o lado interno e externo da célula;

3) RAGE N-truncado (N-RAGE): apesar de não possuir o domínio do tipo-V, os restantes dos domínios estão ancorados na membrana possuindo capacidade de ligação de seus ligantes nos domínios do tipo-C;

4) RAGE C-truncado, secretado/solúvel (sRAGE): o domínio C-terminal está ausente, mas contém todos os domínios das imunoglobulinas da versão completa do RAGE. A forma solúvel do RAGE é secretada extracelularmente como resultado do *splicing* alternativo do mRNA do RAGE ou também pela ação de metaloproteínas (ADAM10 e MMP9) que clivam o RAGE resultando na liberação de sRAGE (Ramasamy *et al.*, 2016).

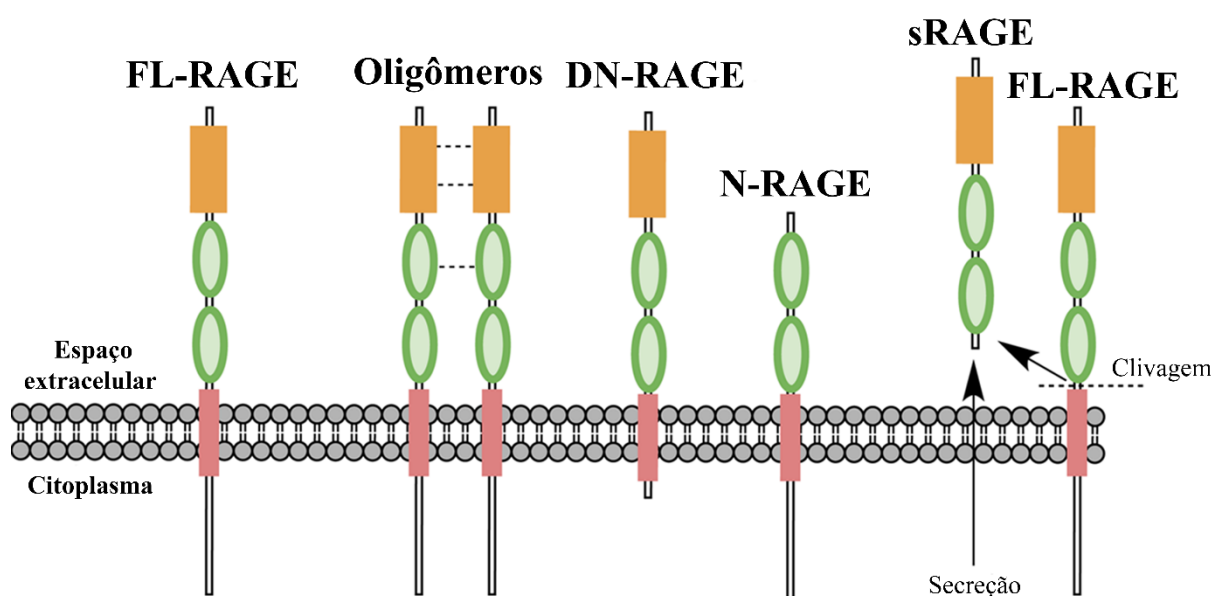


Figura 2. Isoformas do RAGE. As isoformas chave do RAGE na ilustração inclui: (a partir da esquerda) FL-RAGE; oligômeros do RAGE; DN-RAGE; N-RAGE; e sRAGE. Adaptado de (Bongarzone *et al.*, 2017).

Papel fisiológico e sinalização do RAGE

RAGE é altamente expresso durante o desenvolvimento embrionário e durante o período pós-natal onde possui função constitutiva em uma ampla variedade de células (Brett *et al.*, 1993). Na fase adulta, em condições fisiológicas, a expressão do RAGE em células diferenciadas como cardiomiócitos, neurônios e em outros tipos

celulares é reprimida (Brett *et al.*, 1993; Schmidt *et al.*, 1993). Em células da pele e do pulmão, que apresentam características distintas aos demais tipos celulares, a expressão do RAGE é constitutiva e altos níveis do RAGE durante o desenvolvimento e fase adulta são normais e provavelmente benéficas para manter a homeostase (Buckley e Ehrhardt, 2010; Chuah *et al.*, 2013).

RAGE contribui para o metabolismo dos ossos, é expresso tanto em osteoclastos quanto em osteoblastos. RAGE é essencial na maturação, funcionamento e função dos osteoclastos além de auxiliar na remodelação óssea (Zhou *et al.*, 2006). Camundongos RAGE^(-/-) tem osteoclastos com morfologia e funcionalidades comprometidas levando as células ao fenótipo osteopetrose-*like*. A ausência do RAGE induz falha na diferenciação osteoclástica e redução da sinalização de adesão celular mediada por integrina em macrófagos de medula óssea, além de diminuir a pre-fusão de osteoclastos. Em ratos RAGE^(-/-) tanto a densidade mineral óssea quanto a força biomecânica são afetadas com a diminuição no número de osteoclastos (Ding *et al.*, 2006; Zhou *et al.*, 2006).

A presença do RAGE nos axônios em baixas concentrações já está bem estabelecida e sua presença é importante como promotor de crescimento e regeneração de neuritos em condições saudáveis (Rong, Trojaborg, *et al.*, 2004; Rong, Yan, *et al.*, 2004).

Em situações de estresse, o acúmulo ou o aumento da circulação dos ligantes do RAGE induz a expressão do receptor em células que o RAGE estava reprimido ou diminuído (Cheng *et al.*, 2005; Chuah *et al.*, 2013). A interação de um ligante no domínio extracelular do receptor desencadeia uma complexa cascata de sinalização intracelular, resultando na produção de espécies reativas de oxigênio (ERO), induzindo efeitos imunoinflamatórios, modulando a proliferação celular, alterando a

movilidade/migração celular e estimulando a expressão de genes pró-inflamatório, além do concomitante aumento do RAGE (Ramasamy et al., 2008). Além disso o RAGE possibilita as células a habilidade de aderir a componentes da matriz extracelular e também a aderir a outras células através de interações homofílicas (Sessa et al., 2014), pois apresenta alto grau de homologia estrutural a moléculas de adesão celular neural (N-CAM) (Song et al., 2014).

Em alguns transtornos neurológicos como na doença de Alzheimer já é bem comprovada a interação do peptídeo β -amilóide com o RAGE, conduzindo principalmente à inflamação e ao estresse oxidativo (Kim et al., 2013; Chen et al., 2014). Já a interação entre RAGE/HMGB1 e RAGE/S100B são conhecidas por estarem envolvidas em funções neuronais como o crescimento de neuritos e diferenciação celular (Huttunen et al., 2000). No entanto, a concentração de ligantes é um fator importante na predição do efeito do RAGE na homeostase celular. As baixas concentrações levam a eventos mais benéficos (crescimento de neuritos) e altas concentrações, induzem eventos mais deletérios (sinalização inflamatória) (Huttunen et al., 2000). Além da concentração, o tipo de célula parece ser importante. Nos neurônios, a ligação do HMGB1 resulta em crescimento de neuritos, enquanto que na microglia HMGB1 induz sinalização inflamatória potencialmente nociva (Ding e Keller, 2005).

O aumento exacerbado dos níveis do RAGE também é tempo-dependente e estudos demonstram que durante o envelhecimento há o aumento da expressão do RAGE em diversos tecidos (Simm et al., 2004; Srikanth et al., 2011). Este aumento do RAGE durante o envelhecimento é devido ao acúmulo de ligantes do RAGE, que por sua vez elevam a expressão do receptor em um *looping* de *feed back* positivo (figura 3) (Li e Schmidt, 1997).

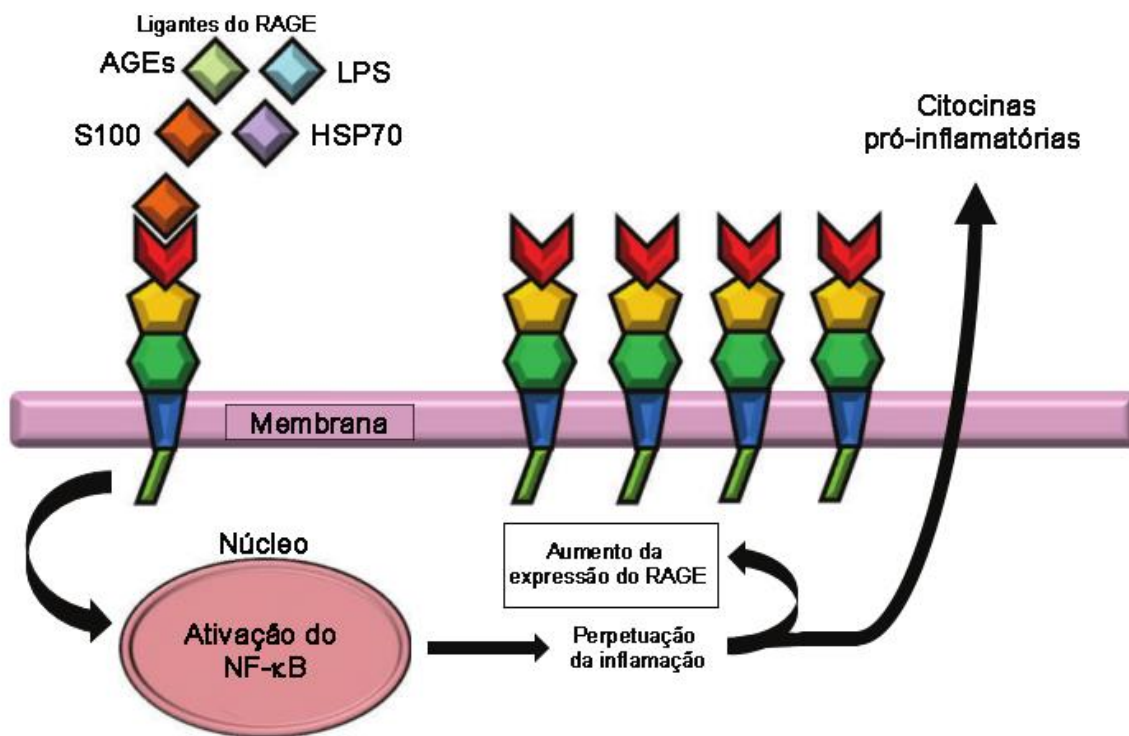


Figura 3. Mecanismo do *looping de feed back* positivo do RAGE. Adaptado de Chuah *et al.*, 2013.

Em contraste, sRAGE tem níveis menores no plasma durante o envelhecimento (Fujii e Nakayama, 2010). Níveis elevados de sRAGE no plasma são correlacionados com longevidade humana (Geroldi *et al.*, 2006), visto que sRAGE pode atuar como agente bloqueador do RAGE, evitando que outros ligantes interajam com RAGE ou com outros receptores de superfície celular (Zhang *et al.*, 2008). Em pacientes com doença arterial coronariana, baixos níveis plasmáticos de sRAGE foram evidenciados em um evento agudo, esse fenômeno ocorre pela alta demanda do receptor na membrana. A alta interação AGE-RAGE amplifica a sinalização do RAGE e mais ligantes são recrutados levando a um aumento da produção de ERO e da resposta inflamatória (Falcone *et al.*, 2013).

A função ambígua do RAGE em células neuronais é complexa, em baixas concentrações é capaz de aumentar a sobrevivência celular e favorecer a

diferenciação neuronal e por outro lado sua ativação pode induzir estresse oxidativo e levar à morte neuronal (Huttunen *et al.*, 2000). Esses efeitos contraditórios parecem não estar relacionados aos tipos de ligantes do RAGE, visto que diferentes ligantes são capazes de induzir ambos os tipos de resposta celular. Provavelmente o que diferencia de um caso para outro é a intensidade e a duração do estímulo e fundamentalmente as características específicas das células (Huttunen *et al.*, 2000; Piras *et al.*, 2016).

RAGE e inflamação

Inicialmente, o RAGE foi considerado importante na patogênese da diabetes e suas complicações, visto que diabéticos apresentam acúmulos de AGEs nas paredes dos vasos sanguíneos, plasma e tecidos (Ruderman *et al.*, 1992). Atualmente RAGE é considerado o receptor chave no eixo de inflamação, pois além de ser ativado por AGEs tem capacidade de ligar um amplo repertório de agonistas com preferência por ligantes propensos a agregação e modificações pós-tradução (oxidação, glicosilação, etc.) denominados padrões moleculares associados ao dano celular (DAMPs), presentes em proteínas como o peptídeo β -amilóide, proteínas da família S100, HMGB1, HSP70, N ϵ -(carboximetil) lisina (CML), LPS e uma série de outras moléculas/proteínas relacionadas com condições patológicas (Yan *et al.*, 2009; Dal-Pizzol *et al.*, 2012).

Um dos efeitos intracelulares mais pronunciados da ativação do RAGE é a ativação redox-dependente de NF- κ B e a indução de vias pró-inflamatórias controladas por esse fator de transcrição (Janssen-Heininger *et al.*, 2000). A ativação de NF- κ B é normalmente induzida por mecanismos transitórios de ação, como a

ativação de cascatas de fosforilação e oxidação de grupamentos tióis de proteínas redox-sensíveis. Tais eventos acabam induzindo a fosforilação de proteínas cinases da subunidade inibitória I κ B α (IKKs). Esta subunidade é responsável pela integridade do complexo I κ B-p50-p65, que é inativo. No entanto, a fosforilação de I κ B α por IKKs resulta na dissociação das subunidades p50-p65, as quais podem formar homo e/ou heterodímeros e atuarem como fatores de transcrição de genes pró-inflamatórios (Sarnico *et al.*, 2012).

A interação do RAGE com seus ligantes em locais de lesão ou inflamação induzem a ativação intracelular de NF- κ B. O gene *AGER* tem um elemento responsivo ao NF- κ B, uma vez que possui sítio de ligação funcional ao NF- κ B em seu promotor proximal (Li e Schmidt, 1997). A sinalização entre RAGE/ NF- κ B está interligada, isso garante a manutenção e a amplificação do sinal pró-inflamatório caracterizando a perpetuação da inflamação. Tal mecanismo de retroalimentação positiva possibilita ao RAGE aumentar sua própria expressão.

RAGE é expresso em numerosas células do sistema imune, incluindo neutrófilos, monócitos/macrófagos, linfócitos e células dendríticas (Brett *et al.*, 1993). Camundongos RAGE^{-/-} estão protegidos dos efeitos letais do choque séptico, que é em grande parte baseado na resposta imune inata. Os camundongos RAGE^{-/-} tem inflamação local diminuída e também menor ativação de NF- κ B nos órgãos alvo de choque séptico (Liliensiek *et al.*, 2004). O bloqueio do RAGE provoca um adiamento na resposta inflamatória através da diminuição da rota de sinalização da inflamação no SNC (Hofmann *et al.*, 1999; Kislinger *et al.*, 2001). Quando o RAGE está ativo no endotélio, fagócitos mononucleares e linfócitos desencadeiam sinalização celular, com liberação dos principais mediadores pró-inflamatórios (Hofmann *et al.*, 1999).

RAGE e doenças neurodegenerativas

O aumento do RAGE tem sido implicado em inúmeras condições patológicas – diabetes, doenças cardiovasculares, doença inflamatória renal, arteriosclerose, doença inflamatória intestinal e também doenças neurodegenerativas, como doença de Alzheimer, polineuropatia amilóide familiar, neuropatia diabética, doença de Parkinson e doença de Huntington (Uttara *et al.*, 2009; Chuah *et al.*, 2013; Juranek *et al.*, 2015).

A expressão do RAGE está presente em neurônios, células vasculares, micróglia e astrócitos, sugerindo-lhe um papel chave no SNC (Ding e Keller, 2005). A ação do RAGE nessas células depende da isoforma e seus níveis de concentração na superfície celular (Ding e Keller, 2005). A ligação entre RAGE/AGE ou RAGE/ β -amilóide nos neurônios resulta em aumento do estresse oxidativo e ativação de NF- κ B (Yan *et al.*, 1996; Mattson e Camandola, 2001) enquanto que em células mononucleares e linfócitos a ligação RAGE/S100 desencadeia a síntese de mediadores pró-inflamatórios (Hofmann *et al.*, 1999).

Na doença de Alzheimer, por exemplo, há um aumento na expressão do RAGE no SNC, e de forma co-localizada com as placas amilóides, estruturas histopatológicas constituídas por *cross-links* do peptídeo β -amilóide (Zhang *et al.*, 2009). Em um estudo (*post mortem*) com cérebros de pacientes afetados pela doença de Alzheimer e diabetes foram encontrados níveis elevados do RAGE, sugerindo a participação deste receptor no mecanismo de dano celular contribuindo na progressão da doença pela geração permanente de estresse oxidativo (Valente *et al.*, 2010).

Já na doença de Parkinson, apesar de também estar bem estabelecido que a ativação pró-inflamatória é um componente importante na progressão da morte dos

neurônios dopaminérgicos, o papel do RAGE neste processo ainda é obscuro e precisa ser estudado.

O bloqueio do RAGE como potencial terapêutico

O crescente número de evidências conectando RAGE a uma série de doenças despertou o interesse na investigação do RAGE como um alvo para intervenção terapêutica. O RAGE solúvel (sRAGE) é um dos modelos utilizados para bloquear o RAGE, dado que sRAGE atua como antagonista inibindo a ativação da sinalização do RAGE. Ratos tratados com sRAGE mostraram uma redução significativa na infiltração de neutrófilos, índice de permeabilidade pulmonar e atividade de NF- κ B, bem como a produção de várias citocinas pró-inflamatórias incluindo TNF- α e proteína inflamatória de macrófagos (MIP-1 α e MIP-1 β) em modelo induzido por LPS (Zhang *et al.*, 2008). Muitos estudos vêm evidenciando que sRAGE tem capacidade de bloqueio do RAGE e que a inibição do receptor acarreta em proteção contra várias doenças (Chen *et al.*, 2004; Chen *et al.*, 2007; Ramasamy *et al.*, 2008).

Estudos conduzidos com camundongos *knock-out* demonstraram que a deleção genética do RAGE forneceu proteção e melhorou a sobrevivência em situações de patologias como a sepse e aterosclerose (Lutterloh *et al.*, 2007; Ramasamy *et al.*, 2008). Em camundongos *knock-out* para RAGE, a ativação de NF- κ B e morte celular em neurônios e células gliais causadas pela indução de modelo da doença de Parkinson por injeção da neurotoxina MPTP (1-metil-4-fenil-1,2,3,6-tetrahidropiridina) é revertida aos níveis de animais controle (Teismann *et al.*, 2012). Resultados semelhantes foram observados com animais *knock-out* para S100B, nos quais a indução de doença de Parkinson com MPTP produziu uma microgliose

significativamente menor, com diminuída expressão do RAGE e de TNF- α , e consequente diminuição da perda celular dopaminérgica (Sathe *et al.*, 2012).

Estudos que investigaram doenças neurodegenerativas em ratos, como a neuropatia periférica diabética e doença de Alzheimer mostraram que o tratamento farmacológico ou o bloqueio genético do RAGE atenua as complicações associadas ao diabetes e a formação de placa nos neurônios (Bierhaus *et al.*, 2004; Cho *et al.*, 2009).

O bloqueio do RAGE com o anticorpo anti-RAGE em células endoteliais do cérebro humano reduziu o transporte de sA β 1-40 através da membrana (transcitose), melhorando as condições gerais dessas células (Mackic *et al.*, 1998). Outro estudo revelou o possível envolvimento do RAGE na biologia da amiloidose, onde foi demonstrado que RAGE liga tanto o peptídeo β -amilóide quanto seus agregados. O bloqueio do RAGE resultou na supressão da expressão esplênica de citocinas pró-inflamatórias, ativação NF- κ B e acúmulo de β -amilóide (Yan *et al.*, 2000). Em modelo de sepse grave a inibição do RAGE com o anti-RAGE aumentou a sobrevivência dos animais (Lutterloh *et al.*, 2007).

A inibição da interação RAGE-anfoterina diminuiu o crescimento e a metástase em camundongos com tumores implantados e tumores que se desenvolvem espontaneamente em camundongos susceptíveis. A ativação das MAPK-p44/p42, p38 e proteínas cinases ativadas por estresse/cinases Jun amino-terminais (SAPK/JNK) e de metaloproteinases foram reprimidas pelo bloqueio do RAGE (Taguchi *et al.*, 2000).

Dentre todas estratégias de bloqueio do RAGE, o *N*-Benzil-*N*-ciclo-hexil-4-clorobenzamida, ou FPS-ZM1, vem despertando mais interesse da comunidade científica. Este antagonista foi selecionado através da triagem de 5000 compostos na

busca por de inibidores do RAGE (Deane *et al.*, 2012). FPS-ZM1 é um bloqueador multimodal do RAGE que bloqueia o domínio tipo-V do receptor *in vitro* e *in vivo* (Deane *et al.*, 2012). Os recursos associados a ligação a RAGE são (1) um núcleo central de amida terciária, (2) um benzeno deficiente em elétrons, (3) uma fração hidrofóbica e (4) um anel de benzeno rico em elétrons ligado à amida com um espaçador de alquilo (Deane *et al.*, 2012; Cary *et al.*, 2016).

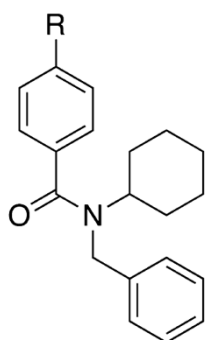


Figura 4. Estrutura do antagonista do RAGE, N-Benzil-N-ciclo-hexil-4-clorobenzamida (FPS-ZM1)

Em um estudo com camundongos o FPS-ZM1 controlou efetivamente a progressão da disfunção cerebral mediado por β -amilóide melhorando o desempenho cognitivo (Deane *et al.*, 2012).

Com base nos expressivos resultados obtidos de estudos *in vitro* e *in vivo*, o bloqueio ou a eliminação do RAGE parece ter grande potencial farmacoterapêutico no contexto clínico. Portanto delinear as ligações moleculares entre os complexos caminhos de sinalização do RAGE e disfunção neuronal é essencial para a compreensão básica dos mecanismos envolvidos nas doenças neurodegenerativas.

Modelos experimentais para estudo de dano neuronal

Infecções bacterianas e virais são fatores de risco para várias doenças neurodegenerativas, como a doença de Alzheimer e doença de Parkinson (De Chiara *et al.*, 2012). A infecção leva à ativação de processos inflamatórios e respostas imunes

do hospedeiro, que atua como mecanismo de defesa, mas também pode causar danos às funções neuronais, infecções no SNC podem levar a múltiplos danos em células infectadas e células vizinhas (Alam *et al.*, 2017). Esses efeitos podem atuar em combinação com outros fatores, como envelhecimento, doenças metabólicas e a composição genética do hospedeiro (Alam *et al.*, 2017).

No capítulo I é demonstrada a ligação entre a infecção sistêmica induzida pelo modelo de *L. Amazonensis* e alterações de parâmetros envolvidos em processos neurodegenerativos através da ativação do RAGE em camundongos. Vários patógenos bacterianos e virais são relacionados com a produção e acúmulo de agregados de proteínas, estresse oxidativo, processos autofágicos deficientes, sinaptopatias e consequente morte neuronal (Alam *et al.*, 2017).

No capítulo II foi utilizado o modelo de LPS de maneira aguda em ratos Wistar com intuito de realizar um mapeamento entre a inflamação sistêmica e seus efeitos em diferentes estruturas do sistema nervoso central. A imunoneutralização do RAGE foi empregada para investigar o papel deste receptor na mediação da resposta inflamatória sistêmica e no SNC.

A injeção sistêmica de LPS em ratos é um modelo surpreendentemente fisiológico para o estudo do papel da inflamação no desenvolvimento de doenças neurodegenerativas. Uma única injeção intraperitoneal pode induzir uma diminuição progressiva (cerca de 50%) na quantidade de neurônios dopaminérgicos da substância negra em tratamento de longo prazo (Qin *et al.*, 2007). Essas características são muito similares ao processo lento e gradual de evolução da neurodegeneração em pacientes, sendo que os animais apresentam evolução similar de sintomas motores. Além disso, esse efeito foi observado ser significativamente

menor em ratas fêmeas, o que é consistente com a maior incidência de Doença de Parkinson em homens do que em mulheres (Miller e Cronin-Golomb, 2010).

No capítulo III investigamos os efeitos da inflamação no SNC induzida por modelo de sepse cronicamente. Utilizamos o método de imunoneutralização do RAGE aplicado diretamente no hipocampo de ratos Wistar com objetivo de elucidar o papel deste receptor em uma doença que acomete milhares de pessoas pelo mundo. A sepse é um problema de saúde pública, é definida como uma disfunção orgânica com risco de vida causada por respostas desreguladas do hospedeiro frente a uma infecção grave, até 71% dos pacientes sépticos desenvolvem disfunção cerebral irreversível (Widmann e Heneka, 2014). Mesmo sendo uma condição induzida por inflamação sistêmica, sem infecção no cérebro (porém com inflamação), a sepse tem como característica a diminuição do metabolismo cerebral, diminuição da atenção, desorientação, delírio ou coma (Semmler *et al.*, 2008).

Na intenção de comprovar o envolvimento do RAGE nas doenças que conduzem à disfunção/morte neuronal, no capítulo IV o modelo de 6-OHDA foi empregado com concomitante administração do antagonista farmacológico (FPS-ZM1) do RAGE. Dentre os diversos modelos que já foram utilizados para elucidar os mecanismos que desencadeiam doenças neurodegenerativas a 6-OHDA apresenta a denervação neuronal do eixo nigroestriatal muito semelhante à aquela encontrada na doença de Parkinson. Este modelo foi utilizado para investigar a morte neuronal à nível celular, diferentemente dos outros modelos citados anteriormente, que envolvem toda a complexidade fisiológica do organismo.

Nesta tese utilizamos 4 modelos experimentais *in vivo*, com diferentes abordagens metodológicas de indução de inflamação, com intenção de elucidar o

papel do RAGE na inflamação sistêmica, na neuroinflamação e na degeneração de neurônios do SNC.

V. Objetivos

Justificativa e objetivos

Esclarecer o papel do RAGE na progressão da morte neuronal é emergente. A elucidação do mecanismo de ação do RAGE pode estabelecer este receptor como alvo terapêutico para o desenvolvimento de terapias efetivas voltadas às causas das doenças. Para determinar tais respostas foi consolidada uma rede interdisciplinar de cooperação entre instituições de pesquisa, ensino e saúde do Brasil e do exterior (Universidade Federal do Rio Grande do Sul - UFRGS, Fundação Oswaldo Cruz - FIOCRUZ, Universidade do Extremo Sul Catarinense - UNESC e *The University of Newcastle-AUS*), de forma a reunir e agregar conhecimento para nossa investigação.

Considerando: i) a relevância da modulação pró-inflamatória na morte neuronal e progressão de doenças neurodegenerativas; ii) A importância do RAGE na resposta inflamatória crônica e morte celular neuronal em processos desse tipo; iii) A falta de conhecimento sobre o papel do RAGE em doenças neurodegenerativas, **o objetivo central desta tese foi o de determinar a função do RAGE em diferentes modelos de inflamação e morte neuronal *in vivo***, tendo como objetivo específicos:

- a) **Determinar alterações do RAGE no cérebro de camundongos infectados com *Leishmania amazonensis*.**

- b) Avaliar os efeitos do bloqueio do RAGE na resposta inflamatória aguda induzida por LPS em ratos Wistar.**

- c) Investigar o papel mediador do RAGE no acúmulo de β -amilóide na fosforilação de tau e no comprometimento cognitivo de ratos Wistar submetidos a sepse.**

- d) Determinar os efeitos do bloqueio do RAGE na denervação dopaminérgica induzida por 6-hidroxidopamina em ratos Wistar.**

- e) Identificar o subtipo celular responsável pela expressão do RAGE nos modelos *in vivo*.**

Parte 2

Resultados

Capítulo I

Increased tau phosphorylation and receptor for advanced glycation endproducts (RAGE) in the brain of mice infected with *Leishmania amazonensis*

Publicado em: **Brain, Behavior, and Immunity (2015)**



ELSEVIER

Contents lists available at ScienceDirect

Brain, Behavior, and Immunity

journal homepage: www.elsevier.com/locate/ybrbi

Increased tau phosphorylation and receptor for advanced glycation endproducts (RAGE) in the brain of mice infected with *Leishmania amazonensis*



Juciano Gasparotto^a, Mario Roberto Senger^b, Alice Kunzler^a, Adriana Degrossoli^b, Salvatore Giovanni de Simone^b, Rafael Calixto Bortolin^a, Nauana Somensi^a, Carolina Saibro Girardi^a, Celeste da Silva Freitas de Souza^b, Kátia da Silva Calabrese^b, Felipe Dal-Pizzol^c, José Claudio Fonseca Moreira^a, Floriano Paes Silva-Jr^b, Daniel Pens Gelain^{a,*}

^a Centro de Estudos em Estresse Oxidativo, Departamento de Bioquímica, Instituto de Ciências Básicas da Saúde, Universidade Federal do Rio Grande do Sul, Porto Alegre, RS, Brazil

^b Fundação Oswaldo Cruz, Instituto Oswaldo Cruz, Laboratório de Bioquímica de Proteínas e Peptídeos, 21040-360 Rio de Janeiro, RJ, Brazil

^c Laboratório de Fisiopatologia Experimental, Programa de Pós-Graduação em Ciências da Saúde, Universidade do Extremo Sul Catarinense, Criciúma, SC, Brazil

ARTICLE INFO

Article history:

Received 31 March 2014

Received in revised form 20 June 2014

Accepted 30 June 2014

Available online 8 July 2014

Keywords:

Leishmaniasis

Tau phosphorylation

RAGE

Oxidative stress

Neurodegeneration

ABSTRACT

Leishmaniasis is a parasitosis caused by several species of the genus *Leishmania*, an obligate intramacrophagic parasite. Although neurologic symptoms have been observed in human cases of leishmaniasis, the manifestation of neurodegenerative processes is poorly studied. The aim of the present work was to investigate if peripheral infection of BALB/c mice with *Leishmania amazonensis* affects tau phosphorylation and RAGE protein content in the brain, which represent biochemical markers of neurodegenerative processes observed in diseases with a pro-inflammatory component, including Alzheimer's disease and Down syndrome. Four months after a single right hind footpad subcutaneous injection of *L. amazonensis*, the brain cortex of BALB/c mice was isolated. Western blot analysis indicated an increase in tau phosphorylation (Ser³⁹⁶) and RAGE immunoccontent in infected animals. Brain tissue TNF- α , IL-1 β , and IL-6 levels were not different from control animals; however, increased protein carbonylation, decreased IFN- γ levels and impairment in antioxidant defenses were detected. Systemic antioxidant treatment (NAC 20 mg/kg, i.p.) inhibited tau phosphorylation and recovered IFN- γ levels. These data, altogether, indicate an association between impaired redox state, tau phosphorylation and RAGE up-regulation in the brain cortex of animals infected with *L. amazonensis*. In this context, it is possible that neurologic symptoms associated to chronic leishmaniasis are associated to disruptions in the homeostasis of CNS proteins, such as tau and RAGE, as consequence of oxidative stress. This is the first demonstration of alterations in biochemical parameters of neurodegeneration in an experimental model of *Leishmania* infection.

© 2014 Elsevier Inc. All rights reserved.

1. Introduction

Leishmaniasis is a parasitosis caused by several species of the genus *Leishmania*, an obligate intramacrophagic parasite. Endemic leishmaniasis transmission occurs in at least 98 countries (Alvar et al., 2012). There are three main human syndromes caused by *Leishmania*: cutaneous disease, the least severe form of disease; mucocutaneous disease, which can be due the extension or metastasis of local skin lesions; and visceral leishmaniasis, also known as Kala-azar, the most severe form (Desjeux, 2004). The outcome of

each is determined by the species of infecting parasite and the genetic susceptibility of the host (McGwire and Satoskar, 2013). *Leishmania amazonensis* causes different diseases depending on the host and parasitic virulence factors (Souza et al., 2011). Commonly, *L. amazonensis* infection is more associated to cutaneous leishmaniasis (Murray et al., 2005), but parasites have been also isolated from patients with the entire spectrum of the disease, including localized and diffuse cutaneous lesions, mucosal and visceral leishmaniasis (Barral et al., 1991). Recently, *L. amazonensis* was also associated with disseminate cutaneous leishmaniasis, an intermediate clinical form (David and Craft, 2009).

Although neurologic symptoms have been largely observed in human cases of the disease, the manifestation of degenerative

* Corresponding author. Address: Rua Ramiro Barcelos, 2600 – anexo, CEP 90035-003 Porto Alegre, RS, Brazil. Tel.: +55 51 3308 5577; fax: +55 51 3308 5535.

E-mail address: dgelain@yahoo.com.br (D.P. Gelain).

<http://dx.doi.org/10.1016/j.bbi.2014.06.204>

0889-1591/© 2014 Elsevier Inc. All rights reserved.

processes associated with the central nervous system (CNS) in leishmaniasis is poorly studied. Cutaneous leishmaniasis is known to cause a peripheral neuropathy by direct or close parasite involvement with the nerve or nerve sheath (Petersen and Greenlee, 2011). In this form of the disease, parasites in the skin and draining lymph nodes are thought to cause an endocrine imbalance as a consequence of cytokines action on the CNS (de Moura et al., 2005). More recently, patients with cutaneous leishmaniasis were reported to exhibit an immune–endocrine imbalance with reduction of plasma levels of dehydroepiandrosterone-S, prolactin and testosterone (Baccan et al., 2011). Together with the observation that *L. amazonensis* may cross the blood–brain barrier and induce significant pathologic changes in the CNS (Abreu-Silva et al., 2003), these data indicate that relevant neurodegenerative processes may occur in the course of leishmaniasis.

The microtubule-stabilizing protein tau is mainly expressed in central nervous system (CNS) neurons and is essential for axon architecture and synaptic function. Initially, the aberrant hyperphosphorylation of tau was observed to be associated with the formation of neurotoxic histological structures in the CNS known as neurofibrillary tangles, characteristic of Alzheimer's disease (AD) (Sonnen et al., 2008). Later, tau hyperphosphorylation was detected in at least twenty-two different CNS related pathologies, including prionic diseases, amyotrophic lateral sclerosis and Down's syndrome (Spires-Jones et al., 2009). These conditions have been referred to as "tauopathies", in which tau aberrant phosphorylation is thought to exert a causative role in synapse impairment and progression of neuronal cell death. Although the molecular detailing of the steps coupling tau aberrant phosphorylation and neuronal death are currently not completely understood, it is clear that disruption of tau homeostasis is associated with an impairment of neural circuits and cognitive deficits (Gendron and Petrucelli, 2009).

The receptor for advanced glycation endproducts (RAGE) is a multiligand membrane receptor that exerts crucial roles in the development of chronic inflammatory processes (Srikanth et al., 2011). RAGE was initially observed to be associated with late diabetic complications, where the accumulation of advanced glycation endproducts (AGE) on the endothelial surface triggers its expression and activation. Further studies have characterized RAGE as a damage-associated molecular pattern (DAMP) receptor, as other molecules with pro-inflammatory and pro-apoptotic activities were observed to act as RAGE ligands (Coughlan et al., 2007). These include the extracellular forms of HMGB1 and members of the S100/calgranulin family, such as S100B and S100A7 (Bopp et al., 2008; Leclerc et al., 2007). RAGE activation induces the expression of pro-inflammatory cytokines and NADPH oxidase activation, which in turn stimulate reactive species (RS) production, causing oxidative damage to biomolecules and sustaining local inflammation and tissue damage (Maczurek et al., 2008). In the brain, a prominent role of RAGE in the contribution to neurodegenerative processes has been emerging since the earlier observations that the β -amyloid peptide function as a RAGE ligand (Arancio et al., 2004; Du Yan et al., 1997). Since then, extensive data have been indicating a key role for RAGE in the chronic pro-inflammatory axis responsible for the progression of neuronal death observed in AD (Yan et al., 2009). On the other hand, the involvement of RAGE in other neuroinflammatory states potentially associated with neurodegeneration is poorly studied. In the present work, we investigated the phosphorylation of tau and the modulation of the immunocentent of RAGE in the brain cortex of BALB/c mice infected with *L. amazonensis*. We also analyzed oxidative stress and inflammatory parameters in order to study the possible relationship of RS production and inflammation in the modulation of neurodegeneration parameters in leishmaniasis.

2. Materials and methods

2.1. Chemicals

Glycine, H₂O₂ (hydrogen peroxide), catalase (CAT, EC 1.11.1.6), superoxide dismutase (SOD, EC 1.15.1.1), thiobarbituric acid, epinephrine, AAPH (2,2'-azobis[2-methylpropionamide]dihydrochloride), trichloroacetic acid (TCA), 2,4-dinitrophenylhydrazine (DNPH), 5,5'-dithionitrotris 2-nitrobenzoic acid (DTNB), Bile salts, sodium dodecyl sulfate, DNP polyclonal antibody and monoclonal TNF- α antibody were purchased from Sigma–Aldrich® (St. Louis, USA). Electrophoresis and immunoblot reagents were from Bio-Rad (Hercules, USA), GE Healthcare Brazilian Headquarter (São Paulo, Brazil) and Sigma–Aldrich® RAGE polyclonal antibody, phosphorylated tau polyclonal antibody, total tau polyclonal antibody, β -actin polyclonal antibody, IL-1 β polyclonal antibody and anti-rabbit immunoglobulin linked to peroxidase were from Cell Signalling technology® (Beverly, USA). ELISA microplates were from Greiner Bio-One (Monroe, USA) and ELISA TMB spectrophotometric detection kit was from BD Biosciences (San Diego, USA). Immunoblot chemiluminescence detection was carried out with the West Pico detection kit from Thermo Scientific Pierce Protein Biology Products (Rockford, USA). MilliQ-purified H₂O was used for preparing solutions. All other reagents used in this study were of analytical or HPLC grade.

2.2. Ethics statement

All experimental procedures were performed in accordance with the National Institute of Health Guide for the Care and Use of Laboratory Animals (NIH publication number 80-23 revised 1996) and the Brazilian Society for Neuroscience and Behavior recommendations for animal care. The experimental protocols were approved by the Oswaldo Cruz Foundation Committee of Ethics for the Use of Animals (CEUA–Fiocruz) protocol number P-36/11-3.

2.3. Parasite strain and infection

L. amazonensis (MHOM/BR/75/JOSEFA) were maintained by regular passage in BALB/c mice. Amastigotes were purified from the footpad lesions of mice as previously described (Barbieri et al., 1993). Female BALB/c mice (6 weeks old) were obtained from Centro de Criação de Animais de Laboratório (CECAL)–Fiocruz, Rio de Janeiro, RJ, Brazil, and injected subcutaneously in the right hind footpad with 10⁵ amastigotes (Arrais-Silva et al., 2006). Four months post-infection the animals were euthanized, the brain cortex was removed and maintained in liquid nitrogen until the assays were performed. Additional groups of mice received a systemic antioxidant therapy (*N*-acetylcysteine 20 mg/kg b.w., one daily injection, i.p.) for five consecutive days before euthanasia. During the post-infection period, animals show apathy and diminished eating behavior. To estimate parasite burden in the lesions, the entire infected footpads were removed and amastigotes were recovered from the lesions and counted. Inflammatory parameters in liver and serum (TNF- α and IL-1 β) were measured to confirm systemic inflammation. In all assays five animals per group ($n = 5$) were utilized.

2.4. Antioxidant enzymes activities

Samples were homogenized in phosphate buffer (PB) 50 mM (KH₂PO₄ and K₂HPO₄, pH-7.4) and the protein content was determined by Bradford method (Bradford, 1976). Catalase (CAT; E.C. 1.11.1.6) activity was evaluated by following the rate of decrease in hydrogen peroxide (H₂O₂) absorbance in a spectrophotometer

at 240 nm (Aebi, 1984). Results are expressed as units of CAT/mg of protein. The activity of superoxide dismutase (SOD; EC 1.15.1.1) was measured by quantifying the inhibition of superoxide-dependent adrenaline auto-oxidation in a sample buffer; adrenochrome formation was monitored at 480 nm for 10 min (32 °C) in a spectrophotometer (Misra and Fridovich, 1972). Results are expressed as units of SOD/mg of protein.

2.5. Oxidative damage to proteins (carbonyl)

As an index of protein oxidative damage, the carbonyl groups were determined as previously described (Levine et al., 1990). The homogenate were divided into two aliquots of 300 μ L (1 mg of protein). Proteins were precipitated by the addition of 150 μ L of 20% TCA for 5 min on ice and centrifuged at 4000g for 5 min. The pellet was dissolved with 100 μ L of sodium hydroxide (NaOH) (200 mM) and 100 μ L of hydrochloric acid (HCl) (2 M) was added in blanks. DNPH (10 mM) was added for carbonyl groups derivatization. Samples were maintained for 30 min at room temperature. Proteins were precipitated with 20% TCA and washed three times with 500 μ L of 1:1 ethanol:ethyl acetate with 15 min standing periods to remove the excess DNPH. Samples were dissolved in 200 μ L of urea (8 M) pH 2.3, and the absorbance was read at 370 nm.

2.6. Western blot detection of dinitrophenyl (DNP)-labeled protein carbonyls

Tissue samples were homogenized in 1 volume of radio-immunoprecipitation assay (RIPA) buffer (20 mM Tris-HCl at pH 7.5, 150 mM NaCl, 1 mM Na₂ EDTA, 1 mM EGTA, 1% NP-40, 1% sodium deoxycholate, 2.5 mM sodium pyrophosphate, 1 mM β -glycerophosphate, 1 mM Na₃VO₄, 1 μ g/mL leupeptin), centrifuged (14,000g for 10 min at 4 °C) and the pellet proteins were quantified. Proteins were dissolved in 6% sodium dodecyl sulfate (SDS) and derivatized with an equal volume of DNPH 10 mM in 10% trifluoroacetic acid for 1 h (Shacter et al., 1994). Samples were subjected to SDS-polyacrylamide gel electrophoresis for Western blot detection of DNP-derivatized proteins with an antibody against DNP as described below.

2.7. Sulfhydryl groups quantification

Oxidative status of thiol groups were assessed by quantification of total reduced sulfhydryl (SH) groups in samples (Ellman, 1959). Briefly, for total SH content measurement, 60 μ g sample aliquot was diluted in phosphate-buffered saline (PBS) (NaCl, Na₂HPO₄, KH₂PO₄), and 5,5'-dithionitro bis 2-nitrobenzoic acid (10 mM), and read in a spectrophotometer at 412 nm after 60 min of incubation in room temperature.

2.8. Index of lipid peroxidation (TBARS)

The quantification of thiobarbituric acid reactive substances (TBARS) was performed for evaluation of an index of lipoperoxidation, as previously described (Draper and Hadley, 1990). Brain cortex tissue was homogenized in ice-cold Tris-HCl 15 mM (pH 7.4) and reacted with an equal volume of 40% trichloroacetic acid (TCA), followed by centrifugation and addition of 0.67% TBA. Samples were then incubated at 100 °C for 25 min. After cooling, samples were centrifuged (750g/10 min) and supernatant absorbance was read at 535 nm.

2.9. Total reactive antioxidant potential (TRAP assay)

The total reactive antioxidant potential (TRAP) was used as an index of non-enzymatic antioxidant capacity. This assay is based on the quenching of peroxy radicals generated by AAPH (2,2 azo-bis[2-amidinopropane]) by antioxidants present in a given sample (Lissi et al., 1992). Briefly, a chemical system that generates peroxy radicals at a constant rate (an AAPH-containing buffer) is coupled to a luminescent reactant (luminol) which emits photons proportionally to its oxidation. The samples were homogenized with glycine buffer (pH-8.6). The reaction was initiated by injecting luminol to the 0.1 M glycine buffer containing AAPH that resulted in steady luminescence emission. Equal amounts of samples are then added to this reaction system, and the luminescence emission at the moment following this addition ($t = 0$) is recorded. This initial emission reflects the production of free radicals by AAPH at the first moment right after sample addition and is related to the endogenous oxidant state of the sample. Following incubation, the thermal decomposition of AAPH produces luminescence at a constant rate ("system"), and the presence of free radical scavengers in the added sample will decrease this rate according to its content of non-enzymatic antioxidants. We followed TRAP luminescence emission for 80 min and calculated the area under the curve (AUC) relative to the system without samples (which was considered as 100% of luminescence emission at all time points). The addition of the homogenate samples decreases or facilitates the luminescence emission proportionally to its redox state. The luminescence emission was recorded in a MicroBeta[®] luminescence counter (Perkin Elmer, USA).

2.10. TNF- α , IL-1 β , IFN- γ , IL-6 and nitrotyrosine levels (ELISA)

TNF- α , IL-1 β , IFN- γ , IL-6 and nitrotyrosine were quantified by indirect ELISA. Brain cortex homogenate was placed in ELISA plates. After 24 h incubation, plates were washed three times with Tween-Tris buffered saline (TTBS, 100 mM Tris-HCl, pH 7.5, containing 0.9% NaCl, and 0.1% Tween-20). Subsequently, 200 μ L of anti-TNF- α , anti-IL-1 β , anti-IFN- γ , anti-IL-6 or anti-nitrotyrosine (1:1000) were added and incubation was carried for 24 h at 4 °C. The plates were washed three times with TTBS and incubated with rabbit or mouse IgG peroxidase-linked secondary antibody (1:1000) for 2 h. After washing the plate three times with TTBS, 200 μ L of substrate solution (TMB spectrophotometric ELISA detection kit) were added to each well and incubated for 15 min. The reaction was terminated with 50 μ L/well of 12 M sulfuric acid stopping reagent and the plate read at 450 nm.

2.11. Immunoblot detection of phosphorylated tau and RAGE

To perform immunoblot experiments, the tissue was homogenated with 1X RIPA buffer, centrifuged (10,000g for 5 min at 4 °C) and the pellet proteins were measured by the Bradford method (Bradford, 1976). Laemmli-sample buffer (62.5 mM Tris-HCl, pH 6.8, 1% (w/v) SDS, 10% (v/v) glycerol) was added to complete volume according the protein content of each sample and equal amounts of cell protein (30 μ g/well) were fractionated by SDS-PAGE and electro-blotted onto nitrocellulose membranes with Trans-Blot[®] SD Semi-Dry Electrophoretic Transfer Cell, Bio-Rad (Hercules, CA, USA). Protein loading and electro-blotting efficiency were verified through Ponceau S staining, and the membrane was washed with Tween-Tris buffered saline (Tris 100 mM, pH 7.5, 0.9% NaCl and 0.1% Tween-20). Membranes were incubated 20 min at room temperature in SNAP i.d.[®] 2.0 Protein Detection System Merck Millipore (Billerica, MA, USA) with each primary antibody (anti-RAGE, anti-phospho-tau, anti-tau, anti- β -actin – 1:500 dilution range each) and then washed with TTBS. Anti-rabbit

or mouse IgG peroxidase-linked secondary antibody (1:5000 dilution range) was incubated with membranes for additional 20 min in SNAP i.d. system (Millipore, Billerica, MA, USA), washed again and the immunoreactivity was detected by enhanced chemiluminescence using Supersignal West Pico Chemiluminescent kit from Thermo Scientific (Luminol/Enhancer and Stable Peroxide Buffer). Densitometric analysis of the films was performed with Image J software. Blots were developed to be linear in the range used for densitometry.

2.12. Statistical analysis

Statistical analysis was performed with GraphPad 5.0 software. Student's *t* test (two-tailed) was applied for simple comparisons between control and infected animals in each assay. For comparison of multiple means, ANOVA with Tukey's post hoc was performed. The results of measurements were expressed as mean \pm standard error of the mean (SEM). Differences were considered significant when $p < 0.05$. The tissue protein content was measured by Bradford method for data normalization in all assays (Bradford, 1976).

3. Results

Tau may be phosphorylated by diverse protein kinases at approximately 25 different sites (Wang et al., 2013). However, phosphorylation of tau on Ser396 is one of the earliest events leading to neurofibrillary tangles formation in AD and Down syndrome and it was suggested to play a key role in the formation of paired helical filaments, the major component of neurofibrillary tangles (Mondragon-Rodriguez et al., 2014). We evaluated the content of phosphorylated and total tau isoforms in the brain cortex of mice infected by *L. amazonensis* by Western blot. An increase in the content of phospho-tau (Ser396) was detected, but the content of total tau was not changed (Fig. 1A). This result indicates that tau phosphorylation in infected animals is increased by a mechanism that is not associated with modulation of tau expression.

We next evaluated the immunoccontent of RAGE in these samples of brain cortex. In animals infected by *L. amazonensis*, the total content of RAGE was significantly increased compared to control animals (Fig. 1B). In AD, both tau aberrant phosphorylation and RAGE up-regulation are strongly implicated in the molecular mechanisms underlying the progression of neuronal death (Li et al., 2012; Yan et al., 2009). RAGE has been suggested to be the key component of the chronic pro-inflammatory axis responsible

for microglia activation and reactive species production that ultimately leads to neuronal cell death in AD and also in other neurodegenerative processes (Maczurek et al., 2008). For this reason, we next sought to evaluate parameters of inflammation and oxidative/nitrosative stress in the brain cortex of mice infected with *L. amazonensis*.

The levels of TNF- α and IL-1 β were evaluated by ELISA. These cytokines are considered markers of acute pro-inflammatory activation and have been associated with modulation of tau phosphorylation and RAGE expression in some neuropathological states (Krstic et al., 2012; Roe et al., 2011). Although an increase in TNF- α levels was detected in other organs, such as liver (data not shown), no significant changes in the levels of both TNF- α and IL-1 β were detected in brain cortex of infected animals (Fig. 2A and B). Thus, our results indicate that tau phosphorylation and RAGE upregulation are not associated with TNF- α and IL-1 β in leishmaniasis.

We next evaluated parameters of oxidative and nitrosative damage in biomolecules of brain cortex samples from mice infected with *L. amazonensis*. We quantified levels of nitrotyrosine, a marker of peroxynitrite-mediated protein nitration, in brain cortex samples by ELISA. Besides, the quantification of free (reduced) thiol groups indicates the redox state of proteins and peptides containing sulfhydryl groups that may undergo oxidation or reduction and form disulfide bonds. No changes in the levels of nitrotyrosine and free thiol groups were observed between control and infected animals (Fig. 3A and B). On the other hand, the levels of TBARS were significantly increased in infected animals, suggesting an elevated status of brain lipid peroxidation (Fig. 3C). Besides, the Western blot analysis of DNP-reactive proteins indicated that protein carbonylation in infected animals was increased (Fig. 3D), which was also confirmed by quantification of carbonyl groups in the samples (Fig. 3E).

The antioxidant status of brain cortex samples was also analyzed. The activities of the antioxidant enzymes CAT and SOD were measured. A decrease in CAT activity was observed in infected animals, indicating impaired H₂O₂ detoxification capacity in brain cortex (Fig. 4A). SOD activity did not differ between control and infected animals (Fig. 4B). Also, the analysis of the non-enzymatic antioxidant status by the TRAP assay showed that mice infected by *L. amazonensis* had a decreased status in non-enzymatic antioxidant defense, indicating a diminished antioxidant capacity compared to control animals (Fig. 4C and D).

Finally, to verify whether tau phosphorylation was associated to the elevated status of oxidative stress in the brain cortex, mice infected with *L. amazonensis* were subjected to a daily i.p.

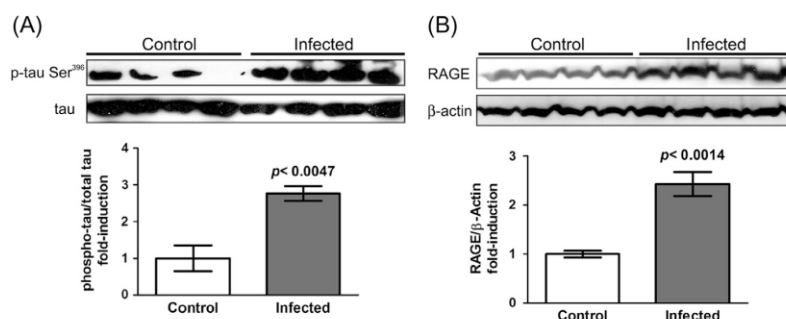


Fig. 1. Tau phosphorylation and RAGE content in brain cortex of mice infected with *L. amazonensis*. Four months after infection, brain cortex tissue from infected and control animals was removed and proteins were subjected to SDS-PAGE/Western blot analysis. (A) Representative immunoblots of tau phosphorylated at Ser396 (p-tau Ser³⁹⁶, upper panel) and total tau (lower panel) from four control and four infected animals. Bar graph corresponds to mean \pm SEM quantification values of the p-tau/total tau ratio from all samples. (B) Representative immunoblots of RAGE content from four control and four infected animals (upper panel). Lower panel corresponds to β -actin immunoccontent used as control for protein constitutive expression. Bar graph corresponds to mean \pm SEM quantification values of the RAGE/ β -actin ratio from all samples. Values for *p* depicted were obtained by applying two-tailed student's *t* test.

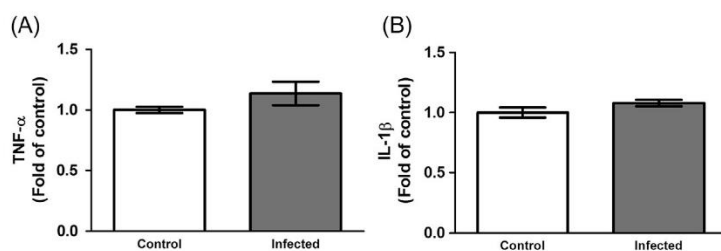


Fig. 2. Levels of TNF- α and IL-1 β in brain cortex from mice infected with *L. amazonensis*. Four months after infection, brain cortex tissue from infected and control animals was removed and proteins were subjected to ELISA detection of (A) TNF- α and (B) IL-1 β internal levels. Values represent mean \pm SEM of five samples from each group. No statistical differences were detected using two-tailed student's *t* test (for $p = 0.005$).

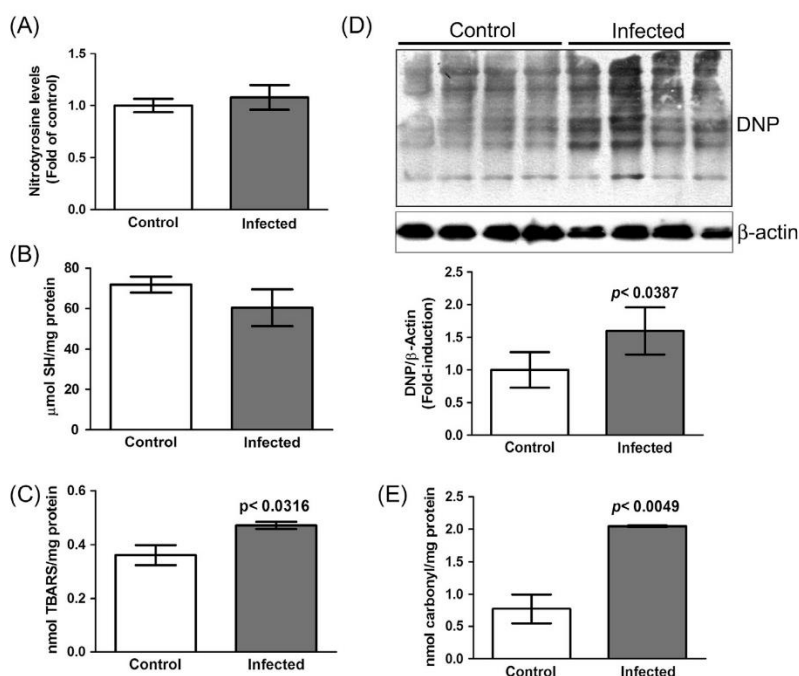


Fig. 3. Parameters of protein oxidative and nitrosative modifications in brain cortex from mice infected with *L. amazonensis*. (A) Protein samples from control and infected animals were subjected to nitrotyrosine detection by ELISA. (B) Free thiol (sulfhydryl; SH) groups quantification in brain cortex samples from control and infected animals. (C) Quantification of thiobarbituric acid reactive substances was performed as an index of lipoperoxidation. (D) Western blot detection of carbonyl groups was also performed by analysis of total protein fraction of samples previously derivatized with DNP. Polyclonal anti-DNP was used to detect DNP-carbonyl derivatized proteins (upper gel panel) and β -actin immunoprecipitated used as control for protein constitutive expression (lower gel panel). Bar graph corresponds to mean \pm SEM quantification values of the DNP/ β -actin ratio from all samples. (E) Spectrophotometric quantification of carbonyl groups was performed in the same samples. Bar graphs in A, B, C and E correspond to mean \pm SEM quantification values from all samples. Values for p were obtained by applying two-tailed student's *t* test and are shown only when $p < 0.005$.

administration with the antioxidant NAC (20 mg/kg) for five consecutive days before euthanasia. Infected animals that received NAC had decreased levels of phosphorylated tau compared to infected animals that did not receive antioxidant therapy (Fig. 5A and B), indicating a role for reactive species in tau phosphorylation. Additionally, we compared the levels of IFN- γ and IL-6, plus TNF- α and IL-1 β , between control and infected animals receiving NAC. The levels of IFN- γ were decreased in infected animals, while the infected animals that received NAC recovered IFN- γ levels to control values (Fig. 5C), which indicates a role for oxidative stress in the modulation of IFN- γ in the brain cortex of animals infected with *L. amazonensis*. We did not observe any effect on IL-6 levels at any group of animals (Fig. 5D). Besides, infected animals receiving NAC presented decreased TNF- α levels compared to infected

animals that did not receive antioxidant therapy (Fig. 5E). No variations in IL-1 β levels were observed in all groups (Fig. 5F).

4. Discussion

Oxidative stress is an important factor in the course of *Leishmania* infection. *L. amazonensis* was reported to contain a cluster of genes expressing META1 and META2 proteins, which were found to be responsible for resistance of the parasite against heat shock and oxidative stress (Ramos et al., 2011). These characteristics probably evolved as a parasite's strategy of resistance against the oxidizing agents generated by inflammatory cells aimed to kill intracellular and extracellular pathogens. However, depending on

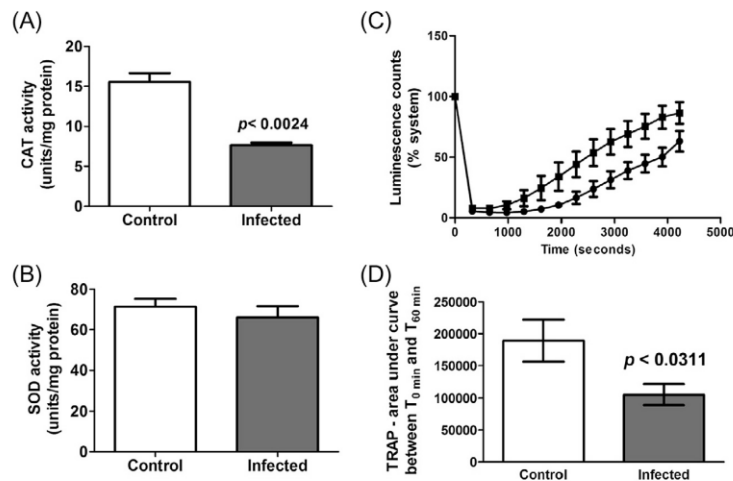


Fig. 4. Antioxidant capacity in brain cortex samples from mice infected with *L. amazonensis*. The activities of antioxidant enzymes and the non-enzymatic antioxidant potential in brain cortex samples from animals 4 months after infection were measured. (A) Catalase (CAT) activity. (B) Superoxide dismutase (SOD) activity. (C) Total reactive antioxidant parameter (TRAP) kinetic assay: square dots represent control and circle dots represent samples from infected animals. (D) Quantification of the area under the curve between time points 0 min and 60 min of the kinetic assay (arbitrary units are shown). Bar graphs correspond to mean \pm SEM quantification values from all samples. Values for *p* were obtained by applying two-tailed student's *t* test and are shown only when *p* < 0.005.

the parasite's ability to cope with the oxidative stress generated by the host, the inflammatory response may be further intensified in order to kill more resistant micro-organisms. The intensification of the production of oxidizing agents during this response may affect cells and tissues of the host, thus contributing to further development of the disease. The observation of oxidative damage to proteins in the CNS of mice infected with *L. amazonensis* reported here may bring new information for the understanding of neurological symptoms in cutaneous leishmaniasis and related parasitic infections. In previous studies, alterations in the redox state of liver were observed only in visceral leishmaniasis caused by infection of hamsters with *Leishmania chagasi* (Oliveira and Cecchini, 2000).

Oxidative stress in patients and experimental models of leishmaniasis is generally analyzed in the context of infected cells or focusing on the microenvironment (tissue) of the injury. Granulomatous inflammatory reaction is associated with the presence of amastigotes within macrophages, reflecting in the function of organs such as liver, spleen, lymph nodes and bone marrow. Cells of the mononuclear phagocyte system are present in these organs (Baneth and Aroch, 2008; Engwerda et al., 2004). In a previous study conducted with the same animal model and infection protocol used here, it was observed that BALB/c mice infected with *L. amazonensis* displayed inflammatory infiltrates of mononuclear cells and neutrophils without parasites in the meninges and the presence of macrophages containing parasites in the cerebral parenchyma (Abreu-Silva et al., 2003). However, as observed in studies with human subjects, the mere presence of parasites in skin and draining lymph nodes (as in localized cutaneous leishmaniasis) affects several neuroendocrine axes, and these effects are believed to emerge as consequences of the actions of pro-inflammatory factors released by peripheral tissues on the CNS (Baccan et al., 2011).

Inflammation and oxidative stress are important components in several neurodegenerative conditions. In AD and related tauopathies, tau phosphorylation and RAGE up-regulation are unequivocally stimulated. These characteristics are strongly believed to be associated with the activation of RS production caused by factors that sustain a chronic state of local inflammatory activation in

CNS. However, we did not observe any changes in the levels of TNF- α , IL-1 β and IL-6 in the brain cortex of infected animals. These cytokines are associated with acute inflammatory responses, while RAGE is considered a marker of chronic pro-inflammatory development (Ibrahim et al., 2013). TNF- α promotes the induction of IL-6 and IL-1 β , and high levels of these cytokines in macrophages of rats acutely infected with *Leishmania braziliensis* have been previously reported (Brelaz-de-Castro et al., 2012). However, in leishmaniasis, the action of these cytokines is more pronounced at either acute phases or advanced stages of the chronic disease (Oliveira et al., 2014). On the other hand, the levels of IFN- γ were decreased in the brain of infected animals, and the antioxidant therapy with NAC recovered IFN- γ status to control levels. IFN- γ is associated to the Th1 response, which is a necessary step of an adequate immune response to control the parasite. A Th1 predominant response is considered a good prognosis for control of the infection with most species of *Leishmania*, while Th2-predominant response is associated to the evolution of the disease (Pereira and Alves, 2008). Nonetheless, infections caused by *L. amazonensis* were observed to downregulate IFN- γ levels in lymph node cells to a greater extent compared to other *Leishmania* species (Maioli et al., 2004), and this was suggested to be part of a specific mechanism by which the parasite modulates the host immune system, as INF- γ -mediated induction of macrophage activation is essential for control of the parasite (Alexander and Bryson, 2005). Inhibition of IFN- γ production in leishmaniasis is directly associated to increased lesion size. The shift between Th1 and Th2 responses is influenced in different ways by the parasite at earlier and later stages of the disease, in order to couple the host immune response with the progression of the parasite's cycle and its change from amastigote to promastigote forms (Pereira and Alves, 2008).

Interestingly, infected mice that received NAC presented decreased TNF- α levels in the brain cortex compared to infected animals that were not treated with NAC. Variations in the levels of this cytokine were not observed between control and infected animals, but the antioxidant treatment was able to reduce this pro-inflammatory mediator in the brain of both control and infected mice. At systemic level, an increase in IL-4 production caused *L. amazonensis* promotes a Th2 response and downregulates

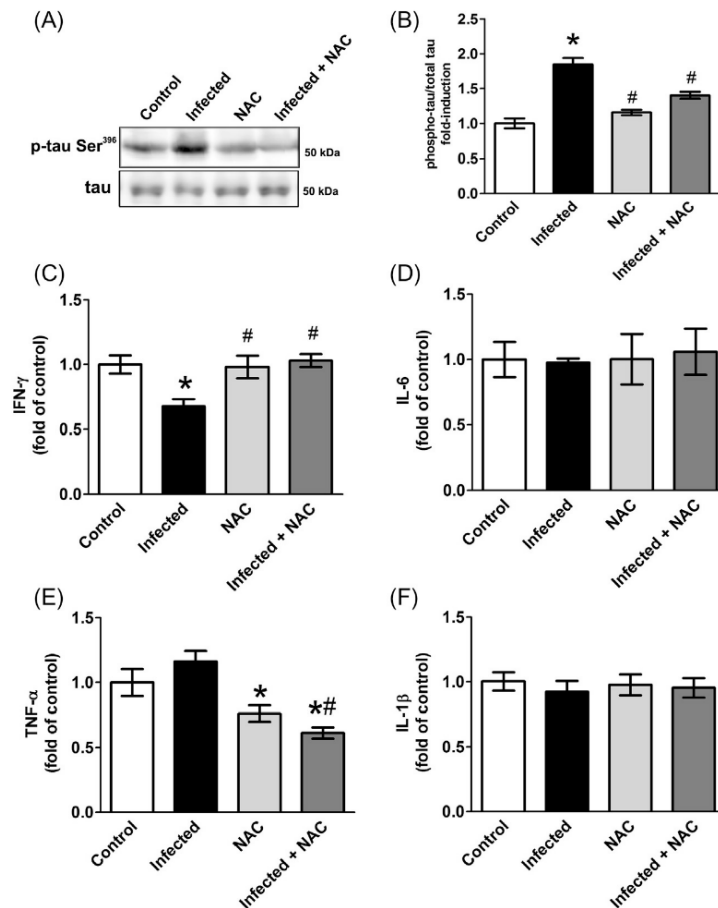


Fig. 5. Effects of antioxidant therapy with NAC in tau phosphorylation and brain cortex cytokines. Uninfected and infected animals were subdivided into groups that received one daily i.p. injection of N-acetylcysteine (NAC) 20 mg/kg for five consecutive days before the day of euthanasia. (A) Representative Western blots of brain cortex samples incubated with antibodies to tau phosphorylated at Ser396 (p-tau Ser³⁹⁶, upper panel) and total tau (lower panel). (B) Mean \pm SEM quantification values of the p-tau/total tau ratio from all samples. Relative quantification of cytokine levels was assessed by ELISA in samples from the same groups. (C) IFN- γ , (D) IL-6, (E) TNF- α and (F) IL-1 β levels were analyzed. Values represent mean \pm SEM of all samples from each group. ANOVA with Tukey's post hoc analysis was performed. * denotes difference from control group; # denotes difference from infected group ($p = 0.005$).

IFN- γ production. These effects are believed to be directly related to the decrease of macrophage activation and TNF- α production associated to the progression of leishmaniasis, as these events would be a consequence of the shift from Th1 to Th2 response caused by the parasite (Pereira and Alves, 2008). Thus, it is surprising that TNF- α levels are not decreased along with IFN- γ in infected animals. However, the changes in the levels of these cytokines caused by NAC treatment suggest that redox-dependent mechanisms are a key factor in the regulation of pro-inflammatory mediators at CNS level in leishmaniasis. It is possible that the pro-oxidant environment in the brain cortex of infected animals is responsible for maintaining TNF- α levels unaltered compared to control animals, instead of an expected decrease in the levels of this cytokine, since Th1 response is supposed to be suppressed.

In AD, accumulated evidence shows that stimulation of the amyloidogenic pathway results in the activation of innate immune system mainly by pattern recognition receptors (PRRs), including RAGE (Salminen et al., 2009). In the amyloidogenic pathway, beta-amyloid peptide release in CNS stimulates oligomers and fibril accumulation (early steps of amyloid plaques formation), which may act as danger-associated molecular patterns (DAMPs).

DAMPs stimulate the up-regulation and activation of PRRs such as Toll-like receptors, NOD-like receptors and RAGE (Maczurek et al., 2008; Salminen et al., 2009). RAGE activation, in turn, triggers a wide array of cellular responses relevant to neurodegenerative progression in AD, such as the transcriptional activation of NF- κ B-regulated genes (which include several genes associated with pro-inflammatory activation, oxidative stress and cell survival-associated responses), MAPK activation (which regulates both cell survival/death responses as well as inflammatory activation) and NADPH oxidase activation (which leads to microglia recruitment/activation, increased RS production and modulation of redox-sensitive protein kinases and transcription factors) (Arancio et al., 2004; Kojro and Postina, 2009; Maczurek et al., 2008; Sims et al., 2010; Yan et al., 2009).

Oxidative stress-related protein carbonylation, nitrotyrosination and thiol oxidation favor the formation of intra- and intermolecular protein cross-links, which leads to conformational changes increasing hydrophobicity and aggregation. These oxidative alterations favor the formation of protein cross-links, inducing generalized cellular dysfunction (Halliwell, 2006). Although we did not detect changes in thiol oxidation or nitrotyrosine formation

here, protein carbonylation was significantly increased in infected animals. This oxidative modification is responsible for the impairment in several protein functions by causing disruption of proteasome-mediated protein turnover and generation of aberrant conformations (Kastle and Grune, 2011). We also observed that the non-enzymatic antioxidant potential in the brain cortex of infected animals was decreased, suggesting a state of enhanced RS production. These observations, altogether, strongly suggest that the increase in tau phosphorylation and RAGE protein content in the brain cortex of animals infected with *L. amazonensis* is associated with a state of oxidative stress in the CNS caused by the infection. It is possible brain oxidative stress may be a sustained response to acute pro-inflammatory activation induced in early stages of the infection, contributing later to the evolution of the chronic disease. Also, as previously stated, it is important to note that even when the presence of the parasite within the CNS is not certain, *Leishmania* spp. infection have been reported by different works to exert neurologic effects as consequence of systemic alterations originated by local inflammatory responses in organs such as liver and spleen (Melo et al., 2013; Petersen and Greenlee, 2011). In human patients with localized cutaneous leishmaniasis, plasma levels of cortisol, estradiol or prolactin positively correlated with at least one clinical parameter of the disease (lesion size, dose used to reach cure and time to cure), indicating a reflect in neuroendocrine regulation (Baccan et al., 2011). It is possible that such modifications may contribute to brain oxidative stress, since neuroendocrine hormones may exert significant changes in the redox state of the CNS (Mancini et al., 2010).

It is reasonable to suggest, based on our present data, that the increase in tau phosphorylation and RAGE immuncontent is a consequence of the oxidative stress in brain cortex. Tau phosphorylation and RAGE expression have been previously observed to be regulated by pro-inflammatory cytokines, including TNF- α and IL-1 (Li et al., 2003; Shi et al., 2011). We observed that levels of TNF- α in infected animals treated with NAC are decreased compared to infected animals that were not treated with NAC. These data indicate that a participation of TNF- α in the induction of tau aberrant phosphorylation may not be completely ruled out. On the other hand, we must consider that the decrease in IFN- γ levels could be involved in this effect, as the levels of this cytokine were recovered in infected animals subjected to antioxidant treatment. The inhibitory effect of NAC treatment on tau phosphorylation was very clear in our experimental model. These data, altogether with the effects observed other cytokines with NAC treatment, strongly suggests that aberrant tau phosphorylation is caused primarily by a redox-dependent mechanism in the brain of animals infected with *L. amazonensis*.

Several evidence associate increased RS production and oxidative damage to biomolecules to both tau aberrant phosphorylation and RAGE up-regulation/activation (de Bittencourt Pasquali et al., 2013; Mondragon-Rodriguez et al., 2014, 2013). In AD, there is a clear role of oxidative stress in the progression of neurodegeneration, and both tau phosphorylation and aggregation are involved in RS-dependent neuronal death in the course of the disease (Schmitt et al., 2012). RAGE up-regulation in response to oxidative stress was observed in different diseases where increased RS production is a characteristic, including diabetes, atherosclerosis and AD (Guo et al., 2008; Kojro and Postina, 2009). In AD, RAGE is believed to contribute in maintaining an elevated state of RS production by stimulating NADPH oxidase (Kojro and Postina, 2009), enhance tau phosphorylation via the ERK1/2-GSK3 β pathway (Barroso et al., 2013; Li et al., 2012) and amyloid translocation through blood-brain barrier (Candela et al., 2010). In this context, it is possible that neurologic symptoms associated with chronic leishmaniasis are related to disruptions in the homeostasis of CNS proteins, such as tau and RAGE, as consequence of oxidative stress

which in turn may be originated initially by systemic infection. This is the first demonstration of alterations in biochemical parameters of neurodegeneration in an experimental model of *Leishmania* infection. The relationship between the regulation of RAGE expression and function in the course of leishmaniasis and its relationship with modulation of Th1/Th2 responses arises from this work as an interesting issue to be addressed in future studies.

This was an exploratory study and, as such, more detailed evaluations aiming to understand mechanistic relationships or propose intervention procedures could not be performed at this stage. Therefore, it is important to point some limitations inherent to this study. First, although data presented here strongly indicate an association of oxidative stress with modulation of tau phosphorylation and RAGE in leishmaniasis, this relationship would only be fully established if administration of antioxidants is able to reverse the effects of *L. amazonensis* infection on these parameters. Also, we did not explore the full complexity of the inflammatory response, as we focused on biochemical parameters more commonly observed in inflammatory diseases of the CNS and in neurodegenerative conditions. Thus, the absence of increase in TNF- α and IL-1 β levels do not necessarily mean absence of brain inflammation. A detailed study focused on a longitudinal evaluation of neurological, neurodegenerative and pro/anti-inflammatory parameters (including a wider range of Th1/Th2 mediators) must be performed for a full comprehension of the mechanisms involved in the etiology of CNS damage in leishmaniasis. Nonetheless, this is the first observation of classic neurodegenerative parameters in this disease, which is not only clinically relevant as it also opens perspectives of new mechanistic and intervention studies.

Acknowledgements

The Brazilian research funding agencies FAPERGS (PqG 12099/8) CAPES (PROCAD 066/2007), CNPq (PVE 400437/2013-9), PRO-PESQ-UFRGS and FAPERJ supported this work. A.D. was the recipient of Visiting Research Fellow (Postdoctoral Fellow)-CNPq/Fiocruz. M.R.S. was the recipient of a fellowship PAPDRJ – CAPES/FAPERJ.

References

- Abreu-Silva, A.L., Calabrese, K.S., Tedesco, R.C., Mortara, R.A., Goncalves da Costa, S.C., 2003. Central nervous system involvement in experimental infection with *Leishmania (Leishmania) amazonensis*. Am. J. Trop. Med. Hyg. 68, 661–665.
- Aebi, H., 1984. Catalase in vitro. Methods Enzymol. 105, 121–126.
- Alexander, J., Bryson, K., 2005. T helper (h)1/Th2 and Leishmania: paradox rather than paradigm. Immunol. Lett. 99, 17–23.
- Alvar, J., Velez, I.D., Bern, C., Herrero, M., Desjeux, P., Cano, J., Jannin, J., den Boer, M., 2012. Leishmaniasis worldwide and global estimates of its incidence. PLoS One 7, e35671.
- Arancio, O., Zhang, H.P., Chen, X., Lin, C., Trinchese, F., Puzzo, D., Liu, S., Hegde, A., Yan, S.F., Stern, A., Luddy, J.S., Lue, L.F., Walker, D.G., Roher, A., Buttini, M., Mucke, L., Li, W., Schmidt, A.M., Kindy, M., Hyslop, P.A., Stern, D.M., Du Yan, S.S., 2004. RAGE potentiates Abeta-induced perturbation of neuronal function in transgenic mice. EMBO J. 23, 4096–4105.
- Arrais-Silva, W.W., Pinto, E.F., Rossi-Bergmann, B., Giorgio, S., 2006. Hyperbaric oxygen therapy reduces the size of *Leishmania amazonensis*-induced soft tissue lesions in mice. Acta Trop. 98, 130–136.
- Baccan, G.C., Oliveira, F., Sousa, A.D., Cerqueira, N.A., Costa, J.M., Barral-Netto, M., Barral, A., 2011. Hormone levels are associated with clinical markers and cytokine levels in human localized cutaneous leishmaniasis. Brain Behav. Immun. 25, 548–554.
- Baneth, G., Aroch, I., 2008. Canine leishmaniasis: a diagnostic and clinical challenge. Vet. J. 175, 14–15.
- Barbieri, C.L., Giorgio, S., Merjan, A.J., Figueiredo, E.N., 1993. Glycosphingolipid antigens of *Leishmania (Leishmania) amazonensis* amastigotes identified by use of a monoclonal antibody. Infect. Immun. 61, 2131–2137.
- Barral, A., Pedral-Sampaio, D., Grimaldi Junior, G., Momen, H., McMahon-Pratt, D., Ribeiro de Jesus, A., Almeida, R., Badaro, R., Barral-Netto, M., Carvalho, E.M., et al., 1991. Leishmaniasis in Bahia, Brazil: evidence that *Leishmania amazonensis* produces a wide spectrum of clinical disease. Am. J. Trop. Med. Hyg. 44, 536–546.

- Barroso, E., del Valle, J., Porquet, D., Vieira Santos, A.M., Salvado, L., Rodriguez-Rodriguez, R., Gutierrez, P., Anglada-Huguet, M., Alberch, J., Camins, A., Palomer, X., Pallas, M., Michalik, L., Wahli, W., Vazquez-Carrera, M., 2013. Tau hyperphosphorylation and increased BACE1 and RAGE levels in the cortex of PPARbeta/delta-null mice. *Biochim. Biophys. Acta* 1832, 1241–1248.
- Bopp, C., Bierhaus, A., Hofer, S., Bouchon, A., Nawroth, P.P., Martin, E., Weigand, M.A., 2008. Bench-to-bedside review: the inflammation-perpetuating pattern-recognition receptor RAGE as a therapeutic target in sepsis. *Crit. Care* 12, 201.
- Bradford, M.M., 1976. A rapid and sensitive method for the quantitation of microgram quantities of protein utilizing the principle of protein-dye binding. *Anal. Biochem.* 72, 248–254.
- Brelaz-de-Castro, M.C., de Almeida, A.F., de Oliveira, A.P., de Assis-Souza, M., da Rocha, L.F., Pereira, V.R., 2012. Cellular immune response evaluation of cutaneous leishmaniasis patients cells stimulated with *Leishmania (Viannia) braziliensis* antigenic fractions before and after clinical cure. *Cell. Immunol.* 279, 180–186.
- Candela, P., Gosselet, F., Saint-Pol, J., Sevin, E., Boucau, M.C., Boulanger, E., Cecchelli, R., Fenart, L., 2010. Apical-to-basolateral transport of amyloid-beta peptides through blood-brain barrier cells is mediated by the receptor for advanced glycation end-products and is restricted by P-glycoprotein. *J. Alzheimers Dis.* 22, 849–859.
- Coughlan, M.T., Cooper, M.E., Forbes, J.M., 2007. Renal microvascular injury in diabetes: RAGE and redox signaling. *Antioxid. Redox Signal.* 9, 331–342.
- David, C.V., Craft, N., 2009. Cutaneous and mucocutaneous leishmaniasis. *Dermatol. Ther.* 22, 491–502.
- de Bittencourt Pasquali, M.A., Gelain, D.P., Zeidan-Chulia, F., Pires, A.S., Gasparotto, J., Terra, S.R., Moreira, J.C., 2013. Vitamin A (retinol) downregulates the receptor for advanced glycation endproducts (RAGE) by oxidant-dependent activation of p38 MAPK and NF- κ B in human lung cancer A549 cells. *Cell. Signal.* 25, 939–954.
- de Moura, T.R., Novais, F.O., Oliveira, F., Clarencio, J., Noronha, A., Barral, A., Brodskyn, C., de Oliveira, C.I., 2005. Toward a novel experimental model of infection to study American cutaneous leishmaniasis caused by *Leishmania braziliensis*. *Infect. Immun.* 73, 5827–5834.
- Desjeux, P., 2004. Leishmaniasis: current situation and new perspectives. *Comp. Immunol. Microbiol. Infect. Dis.* 27, 305–318.
- Draper, H.H., Hadley, M., 1990. Malondialdehyde determination as index of lipid peroxidation. *Methods Enzymol.* 186, 421–431.
- Du Yan, S., Zhu, H., Fu, J., Yan, S.F., Roher, A., Tourtellotte, W.W., Rajavashisth, T., Chen, X., Godman, G.C., Stern, D., Schmidt, A.M., 1997. Amyloid-beta peptide-receptor for advanced glycation endproduct interaction elicits neuronal expression of macrophage-colony stimulating factor: a proinflammatory pathway in Alzheimer disease. *Proc. Natl. Acad. Sci. U. S. A.* 94, 5296–5301.
- Ellman, G.L., 1959. Tissue sulfhydryl groups. *Arch. Biochem. Biophys.* 82, 70–77.
- Engwerda, C.R., Ato, M., Kaye, P.M., 2004. Macrophages, pathology and parasite persistence in experimental visceral leishmaniasis. *Trends Parasitol.* 20, 524–530.
- Gendron, T.F., Petrucelli, L., 2009. The role of tau in neurodegeneration. *Mol. Neurodegen.* 4, 13.
- Guo, Z.J., Niu, H.X., Hou, F.F., Zhang, L., Fu, N., Nagai, R., Lu, X., Chen, B.H., Shan, Y.X., Tian, J.W., Nagaraj, R.H., Xie, D., Zhang, X., 2008. Advanced oxidation protein products activate vascular endothelial cells via a RAGE-mediated signaling pathway. *Antioxid. Redox Signal.* 10, 1699–1712.
- Halliwel, B., 2006. Oxidative stress and neurodegeneration: where are we now? *J. Neurochem.* 97, 1634–1658.
- Ibrahim, Z.A., Armour, C.L., Phipps, S., Sukkar, M.B., 2013. RAGE and TLRs: relatives, friends or neighbours? *Mol. Immunol.* 56, 739–744.
- Kastle, M., Grune, T., 2011. Protein oxidative modification in the aging organism and the role of the ubiquitin proteasomal system. *Curr. Pharm. Des.* 17, 4007–4022.
- Kojro, E., Postina, R., 2009. Regulated proteolysis of RAGE and AbetaPP as possible link between type 2 diabetes mellitus and Alzheimer's disease. *J. Alzheimers Dis.* 16, 865–878.
- Krstic, D., Madhusudan, A., Doehner, J., Vogel, P., Notter, T., Imhof, C., Manalastas, A., Hilfiker, M., Pfister, S., Schwerdel, C., Riether, C., Meyer, U., Knuesel, I., 2012. Systemic immune challenges trigger and drive Alzheimer-like neuropathology in mice. *J. Neuroinflamm.* 9, 151.
- Leclerc, E., Fritz, G., Weibel, M., Heizmann, C.W., Galichet, A., 2007. S100B and S100A6 differentially modulate cell survival by interacting with distinct RAGE (receptor for advanced glycation end products) immunoglobulin domains. *J. Biol. Chem.* 282, 31317–31331.
- Levine, R.L., Garland, D., Oliver, C.N., Amici, A., Climent, I., Lenz, A.G., Ahn, B.W., Shalitel, S., Stadtman, E.R., 1990. Determination of carbonyl content in oxidatively modified proteins. *Methods Enzymol.* 186, 464–478.
- Li, X.H., Lv, B.L., Xie, J.Z., Liu, J., Zhou, X.W., Wang, J.Z., 2012. AGES induce Alzheimer-like tau pathology and memory deficit via RAGE-mediated GSK-3 activation. *Neurobiol. Aging* 33, 1400–1410.
- Li, Y., Liu, L., Barger, S.W., Griffin, W.S., 2003. Interleukin-1 mediates pathological effects of microglia on tau phosphorylation and on synaptophysin synthesis in cortical neurons through a p38-MAPK pathway. *J. Neurosci.* 23, 1605–1611.
- Lissi, E., Pascual, C., Del Castillo, M.D., 1992. Luminol luminescence induced by 2,2'-Azo-bis(2-amidinopropane) thermolysis. *Free. Radic. Res. Commun.* 17, 299–311.
- Maczurek, A., Shanmugam, K., Munch, G., 2008. Inflammation and the redox-sensitive AGE-RAGE pathway as a therapeutic target in Alzheimer's disease. *Ann. N. Y. Acad. Sci.* 1126, 147–151.
- Maioli, T.U., Takane, E., Arantes, R.M., Fietto, J.L., Afonso, L.C., 2004. Immune response induced by New World *Leishmania* species in C57BL/6 mice. *Parasitol. Res.* 94, 207–212.
- Mancini, A., Festa, R., Di Donna, V., Leone, E., Littarru, G.P., Silvestrini, A., Meucci, E., Pontecorvi, A., 2010. Hormones and antioxidant systems: role of pituitary and pituitary-dependent axes. *J. Endocrinol. Invest.* 33, 422–433.
- McGwire, B.S., Satoskar, A.R., 2013. Leishmaniasis: clinical syndromes and treatment. *QJM* 107, 7–14.
- Melo, G.D., Seraguci, T.F., Schweigert, A., Silva, J.E., Grano, F.G., Peiro, J.R., Lima, V.M., Machado, G.F., 2013. Pro-inflammatory cytokines predominate in the brains of dogs with visceral leishmaniasis: a natural model of neuroinflammation during systemic parasitic infection. *Vet. Parasitol.* 192, 57–66.
- Misra, H.P., Fridovich, I., 1972. The role of superoxide anion in the autoxidation of epinephrine and a simple assay for superoxide dismutase. *J. Biol. Chem.* 247, 3170–3175.
- Mondragon-Rodriguez, S., Perry, G., Luna-Munoz, J., Acevedo-Aquino, M.C., Williams, S., 2014. Phosphorylation of tau protein as the link between oxidative stress, mitochondrial dysfunction, and connectivity failure: implications for Alzheimer's disease. *Oxid. Med. Cell. Longev.* 2013, 940603.
- Murray, H.W., Berman, J.D., Davies, C.R., Saravia, N.G., 2005. Advances in leishmaniasis. *Lancet* 366, 1561–1577.
- Oliveira, F.J., Cecchini, R., 2000. Oxidative stress of liver in hamsters infected with *Leishmania (L.) chagasi*. *J. Parasitol.* 86, 1067–1072.
- Oliveira, W.N., Ribeiro, L.E., Schrieffer, A., Machado, P., Carvalho, E.M., Bacellar, O., 2014. The role of inflammatory and anti-inflammatory cytokines in the pathogenesis of human tegumentary leishmaniasis. *Cytokine* 66, 127–132.
- Pereira, B.A., Alves, C.R., 2008. Immunological characteristics of experimental murine infection with *Leishmania (Leishmania) amazonensis*. *Vet. Parasitol.* 158, 239–255.
- Petersen, C.A., Greenlee, M.H., 2011. Neurologic manifestations of *Leishmania* spp. *Infection J. Neuroparasitol.* 2, 10–20.
- Ramos, C.S., Yokoyama-Yasunaka, J.K., Guerra-Giraldez, C., Price, H.P., Mortara, R.A., Smith, D.F., Uliana, S.R., 2011. *Leishmania amazonensis* MET2A protein confers protection against heat shock and oxidative stress. *Exp. Parasitol.* 127, 228–237.
- Roe, A.D., Staup, M.A., Serrats, J., Sawchenko, P.E., Rissman, R.A., 2011. Lipopolysaccharide-induced tau phosphorylation and kinase activity-modulation, but not mediation, by corticotropin-releasing factor receptors. *Eur. J. Neurosci.* 34, 448–456.
- Salminen, A., Ojala, J., Kauppinen, A., Kaarniranta, K., Suuronen, T., 2009. Inflammation in Alzheimer's disease: amyloid-beta oligomers trigger innate immunity defence via pattern recognition receptors. *Prog. Neurobiol.* 87, 181–194.
- Schmitt, K., Grimm, A., Kazmierczak, A., Strosznajder, J.B., Gotz, J., Eckert, A., 2012. Insights into mitochondrial dysfunction: aging, amyloid-beta, and tau-A deleterious trio. *Antioxid. Redox Signal.* 16, 1456–1466.
- Shacter, E., Williams, J.A., Lim, M., Levine, R.L., 1994. Differential susceptibility of plasma proteins to oxidative modification: examination by western blot immunoassay. *Free Radic. Biol. Med.* 17, 429–437.
- Shi, J.Q., Shen, W., Chen, J., Wang, B.R., Zhong, L.L., Zhu, Y.W., Zhu, H.Q., Zhang, Q.Q., Zhang, Y.D., Xu, J., 2011. Anti-TNF-alpha reduces amyloid plaques and tau phosphorylation and induces CD11c-positive dendritic-like cell in the APP/PS1 transgenic mouse brains. *Brain Res.* 1368, 239–247.
- Sims, G.P., Rowe, D.C., Rietdijk, S.T., Herbst, R., Coyle, A.J., 2010. HMGB1 and RAGE in inflammation and cancer. *Annu. Rev. Immunol.* 28, 367–388.
- Sonnen, J.A., Breitner, J.C., Lovell, M.A., Markesbery, W.R., Quinn, J.F., Montine, T.J., 2008. Free radical-mediated damage to brain in Alzheimer's disease and its transgenic mouse models. *Free Radic. Biol. Med.* 45, 219–230.
- Souza, V.L., Veras, P.S., Welby-Borges, M., Silva, T.M., Leite, B.R., Ferraro, R.B., Meyer-Fernandes, J.R., Barral, A., Costa, J.M., de Freitas, L.A., 2011. Immune and inflammatory responses to *Leishmania amazonensis* isolated from different clinical forms of human leishmaniasis in CBA mice. *Mem. Inst. Oswaldo Cruz* 106, 23–31.
- Spire-Jones, T.L., Stoothoff, W.H., de Calignon, A., Jones, P.B., Hyman, B.T., 2009. Tau pathophysiology in neurodegeneration: a tangled issue. *Trends Neurosci.* 32, 150–159.
- Srikanth, V., Maczurek, A., Phan, T., Steele, M., Westcott, B., Juskiw, D., Munch, G., 2011. Advanced glycation endproducts and their receptor RAGE in Alzheimer's disease. *Neurobiol. Aging* 32, 763–777.
- Wang, J.Z., Xia, Y.Y., Grundke-Iqbal, I., Iqbal, K., 2013. Abnormal hyperphosphorylation of tau: sites, regulation, and molecular mechanism of neurofibrillary degeneration. *J. Alzheimers Dis.* 33 (Suppl. 1), S123–S139.
- Yan, S.D., Bierhaus, A., Nawroth, P.P., Stern, D.M., 2009. RAGE and Alzheimer's disease: a progression factor for amyloid-beta-induced cellular perturbation? *J. Alzheimers Dis.* 16, 833–843.

Capítulo II

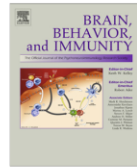
**Anti-RAGE antibody selectively blocks acute systemic inflammatory responses
to LPS in serum, liver, CSF and striatum**

Publicado em: **Brain, Behavior, and Immunity (2017)**



Contents lists available at ScienceDirect

Brain, Behavior, and Immunity

journal homepage: www.elsevier.com/locate/ybrbi

Full-length Article

Anti-RAGE antibody selectively blocks acute systemic inflammatory responses to LPS in serum, liver, CSF and striatum



Juciano Gasparotto^{a,*}, Camila Tiefensee Ribeiro^a, Rafael Calixto Bortolin^a, Nauana Somensi^a, Henrique Schaan Fernandes^a, Alexsander Alves Teixeira^a, Marcelo Otavio Rodrigues Guasselli^a, Crepin Aziz Jose O. Agani^a, Natália Cabral Souza^b, Mateus Grings^c, Guilhian Leipnitz^c, Henrique Mautone Gomes^a, Matheus Augusto de Bittencourt Pasquali^b, Peter R. Dunkley^d, Phillip W. Dickson^d, José Claudio Fonseca Moreira^a, Daniel Pens Gelain^{a,*}

^a Centro de Estudos em Estresse Oxidativo, Departamento de Bioquímica, Instituto de Ciências Básicas da Saúde, Universidade Federal do Rio Grande do Sul, Porto Alegre, RS, Brazil

^b Centro de Tecnologia e Recursos Naturais, Universidade Federal de Campina Grande, Campina Grande, PB, Brazil

^c Programa de Pós-Graduação em Ciências Biológicas: Bioquímica, Departamento de Bioquímica, Instituto de Ciências Básicas da Saúde, Universidade Federal do Rio Grande do Sul, Porto Alegre, RS, Brazil

^d School of Biomedical Sciences and Pharmacy and Hunter Medical Research Institute, University of Newcastle, Australia

ARTICLE INFO

Article history:

Received 14 October 2016

Received in revised form 10 January 2017

Accepted 10 January 2017

Available online 11 January 2017

Keywords:

RAGE

Neuroinflammation

Systemic inflammation

LPS

Striatum

Neurodegeneration

ABSTRACT

Systemic inflammation induces transient or permanent dysfunction in the brain by exposing it to soluble inflammatory mediators. The receptor for advanced glycation endproducts (RAGE) binds to distinct ligands mediating and increasing inflammatory processes. In this study we used an LPS-induced systemic inflammation model in rats to investigate the effect of blocking RAGE in serum, liver, cerebrospinal fluid (CSF) and brain (striatum, prefrontal cortex, ventral tegmental area and substantia nigra). Intraperitoneal injection of RAGE antibody (50 µg/kg) was followed after 1 h by a single LPS (5 mg/kg) intraperitoneal injection. Twenty-four hours later, tissues were isolated for analysis. RAGE antibody reduced LPS-induced inflammatory effects in both serum and liver; the levels of proinflammatory cytokines (TNF- α , IL-1 β) were decreased and the phosphorylation/activation of RAGE downstream targets (ERK1/2, I κ B and p65) in liver were significantly attenuated. RAGE antibody prevented LPS-induced effects on TNF- α and IL-1 β in CSF. In striatum, RAGE antibody inhibited increases in IL-1 β , Iba-1, GFAP, phospho-ERK1/2 and phospho-tau (ser202), as well as the decrease in synaptophysin levels. These effects were caused by systemic RAGE inhibition, as RAGE antibody did not cross the blood-brain barrier. RAGE antibody also prevented striatal lipoperoxidation and activation of mitochondrial complex II. In conclusion, blockade of RAGE is able to inhibit inflammatory responses induced by LPS in serum, liver, CSF and brain.

© 2017 Elsevier Inc. All rights reserved.

1. Introduction

The importance of systemic inflammation as a causative factor to the development of brain functional impairment, cognitive decline and neurodegeneration has been recognized. Clinical and experimental data indicate that both chronic and acute systemic proinflammatory processes affect central nervous system (CNS) function, leading to either transient or permanent dysfunction (Cunningham and Hennessy, 2015). Chronic medical conditions with activated proinflammatory signalling, such as diabetes, obesity and atherosclerosis, have been associated with increased incidence of Alzheimer's disease (AD) and dementia (Holt et al.,

2009; Nguyen et al., 2014). In systemic inflammation induced by sepsis delirium is a common CNS manifestation during the acute phases, while a significant number of patients on recovery develop long-term functional impairment of the brain similar to neurodegeneration associated with brain trauma (Pandharipande et al., 2013; Widmann and Heneka, 2014).

The receptor for advanced glycation endproducts (RAGE) is a multi-ligand receptor associated with distinct cell responses depending on the tissue of origin and developmental stage. RAGE is known to interact with a variety of ligands that may be classified as danger- or pathogen-associated molecular pattern molecules (DAMPs and PAMPs), including the S100 family proteins, HMGB1, amyloid- β peptide (A β), bacterial lipopolysaccharide (LPS) and several advanced glycation endproducts (AGEs), among others (Xie et al., 2013). RAGE is present only in mammals, where it is constitutively expressed in lungs and endothelial cells, but it may be

* Corresponding authors at: Rua Ramiro Barcelos, 2600 – anexo, CEP 90035-003 Porto Alegre, RS, Brazil.

E-mail address: daniel.gelain@ufrgs.br (D.P. Gelain).

<http://dx.doi.org/10.1016/j.bbi.2017.01.008>

0889-1591/© 2017 Elsevier Inc. All rights reserved.

up-regulated in most other cell types by DAMPs and PAMPs that evoke proinflammatory signalling (Creagh-Brown et al., 2010). In such situations, RAGE-activated signalling induces the transcription of proinflammatory cytokines and also enhances its own transcription, establishing a positive feedback axis of proinflammatory signalling (Lukic et al., 2008). Since its activation enhances its own expression, RAGE exerts a key role in the sustained proinflammatory states that occur with chronic diseases. This role has been well documented in diabetes, atherosclerosis, cancer, autoimmune diseases and some neurodegenerative conditions (Guo et al., 2008; Maczurek et al., 2008; Martens et al., 2012; Sims et al., 2010). Microglial RAGE activation by β is believed to sustain the proinflammatory/neurodegenerative axis in AD (Yu and Ye, 2015) and RAGE activation in brain is associated to memory impairment (Mazarati et al., 2011). RAGE is also suggested to play a central role in the development of diabetic neuropathy and other neurodegenerative comorbidities of diabetes (Juraneck et al., 2015; Sugimoto et al., 2008).

RAGE blocking, using antibodies against RAGE or soluble isoform (sRAGE) that sequesters circulating ligands, is protective against systemic proinflammatory insults induced by sepsis and LPS endotoxemia (Lutterloh and Opal, 2007; Lutterloh et al., 2007; van Zoelen and van der Poll, 2008; Yamamoto et al., 2011). Immune neutralization of RAGE has been successfully performed with polyclonal, monoclonal or Fab fragments *in vivo* and *in vitro* (Bro et al., 2008; Lutterloh et al., 2007; Tekabe et al., 2015). In rodents, systemic injection of polyclonal antibodies against RAGE has been applied to inhibit RAGE signalling and was demonstrated to inhibit acute liver injury and fibrosis in a rat bile duct ligation model (Xia et al., 2016), and experimental endotoxaemic liver failure induced by galactosamine and LPS in mice (Kuhla et al., 2013). Abdominal sepsis induced by *Escherichia coli* was also observed to be significantly attenuated by polyclonal anti-RAGE (van Zoelen et al., 2009), and *in situ* studies demonstrated that it is possible to achieve specific blocking of RAGE using polyclonal antibodies (Marsche et al., 2007; Origlia et al., 2014). RAGE inhibition has also been suggested to be a potential molecular mechanism to alleviate neuroinflammation and neurodegeneration in AD, Parkinson's disease (PD), Huntington's disease (HD) and other similar conditions (Kim et al., 2015; Maczurek et al., 2008; Ray et al., 2016; Teismann et al., 2012).

In rodent models of systemic inflammation induced by LPS, neuroinflammation and neurodegeneration are observed in brain structures related to dopaminergic function (Bodea et al., 2014; Qin et al., 2013). Proinflammatory cytokines produced peripherally, such as liver TNF- α , are involved in the genesis and progression of neurodegenerative processes observed several months after a single LPS injection (Qin et al., 2007). Episodes of acute systemic inflammation seem to play a major role in brain disease pathogenesis. In the present work, we investigated the role of RAGE in the short-term (up to 24 h) in serum, liver and CSF and the neurotoxicity-related effects induced by acute systemic inflammation in prefrontal cortex, striatum, substantia nigra (SN) and ventral tegmental area (VTA). Intraperitoneal administration of anti-RAGE IgG (RAGE-Ab) prior to LPS inhibited changes in proinflammatory, oxidative and neurotoxicity parameters that occurred in tissue specific manner 24 h after induction of systemic inflammation. All brain regions responded to LPS, but the striatum cytokine response was most susceptible to inhibition by RAGE-Ab. The present results suggest that RAGE exerts an important role in the propagation of acute systemic inflammation in the striatum within 24 h.

2. Materials and methods

2.1. Chemicals

Glycine, H₂O₂ (hydrogen peroxide), thiobarbituric acid, bile salts and sodium dodecyl sulfate (SDS) were from Sigma-Aldrich®

(St. Louis, USA). Electrophoresis and immunoblot apparatus and reagents were from Bio-Rad (Hercules, USA) and GE Healthcare Brazilian Headquarter (Sao Paulo, Brazil). Polyclonal and monoclonal antibodies from Cell Signalling Technology® (MA, USA) were: p-ERK-44/42 (Thr202/Tyr204) (9101), ERK-44/42 (9102), I κ B α (4812), p-I κ B (9246), NF κ B-p65 (8242), p-NF κ B-p65 (3033), GFAP (3670), synaptophysin (5461) and p-tau ser202 (11834). anti- β -actin (A1978) anti-Iba-1 (SAB2500042) were from Sigma-Aldrich® (St. Louis, USA). Antibodies against nitrotyrosine (ab7048), TNF- α (ab6671), IL-1 β (ab9722), 4-hydroxynonenal (ab46545), RAGE (AB37647) and TLR4 (ab8376) were obtained from Abcam® (Cambridge, UK). For RAGE blocking, anti-RAGE rat IgG (SC5563) from Santa Cruz Biotechnology, Inc. (Texas, USA) was used. Other antibodies used here are described below. ELISA kits to TNF- α (RAB0479) and IL-1 β (RAB0272) were from Sigma-Aldrich® (St. Louis, USA). anti-rabbit IgG, peroxidase conjugated (AP132P) and anti-mouse IgG, peroxidase conjugated (AP124P) were from Merck Millipore (MA, EUA). Immunoblot chemiluminescence detection was carried out with the West Pico detection kit from Thermo Scientific Pierce Protein Biology Products (Illinois, USA). All other reagents used in this study were of analytical or HPLC grade.

2.2. Animals and drug treatments

Male Wistar rats (60-days old) were obtained from our breeding colony ($n = 6$ per group). They were caged in groups of four animals with free access (*ad libitum*) to water and standard commercial food (Chow Nuvilab CR-1 type; Curitiba, PR, Brazil). Rats were maintained in a twelve-hour light-dark cycle in a temperature-controlled colony room (21 °C). Animals were handled for 7 days (adaptation period) to reduce stress caused by subsequent manipulation and weighting. After this adaptation period blood was sampled from the lateral tail vein (Lee and Goosens, 2015). Rats were separated into four groups: a) control group – received one saline injection and one hour later a second saline injection; b) RAGE-Ab group – received one RAGE antibody (RAGE-Ab) injection and one hour later a saline injection; c) LPS group – received one saline injection and one hour later one LPS injection; d) RAGE-Ab+LPS group – received one RAGE-Ab injection and one hour later one LPS injection. In some experiments, isotype anti-rat IgG was used as control for specificity of RAGE-Ab.

All injections were administered *i.p.* The RAGE-Ab concentration (50 μ g/kg) was selected based on previous reports (Kuhla et al., 2013; van Zoelen et al., 2009; Xia et al., 2016) and modified according our pilot experiments. We tested concentrations of RAGE-Ab up to 250 μ g/kg and selected the lowest effective dose inhibiting liver ERK1/2 and serum TNF- α and IL-1 β induced by systemic inflammation (unpublished data). The LPS dose of 5 mg/kg and via of administration (intraperitoneal) were applied based on results of previous works demonstrating acute changes in blood-brain barrier (BBB) permeability followed by neurodegenerative progression over time using this procedure (Hoban et al., 2013; Qin et al., 2013, 2007), plus data from pilot experiments to assess mortality in the animals used in this study (Suppl. Fig. 1A and B). After 24 h, animals were anesthetized and the blood-free cerebrospinal fluid (CSF) was collected from the *cisterna magna* (Nirogi et al., 2009). An average volume of 100 μ L of blood traces-free CSF per animal was obtained. Animals were euthanized by decapitation. The liver, serum, and brain structures (prefrontal cortex, striatum, SN and VTA) were isolated for analyses (see Fig. 1). Serum was separated from whole blood and used for ELISA as described below. Liver and brain were removed and the brain was quickly dissected using a rat brain matrix slicer and promptly homogenized. Tissue aliquots were homogenized in separate buffers according the respective procedure to follow, as described

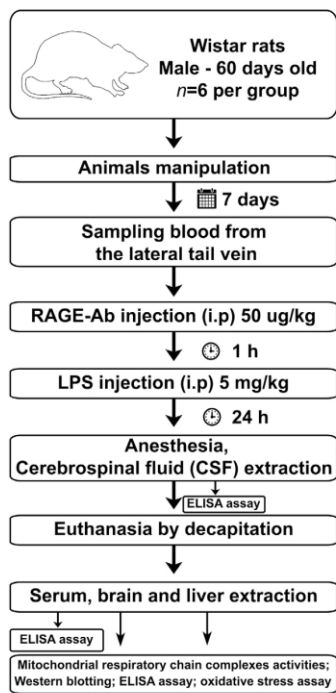


Fig. 1. Experimental design.

separately below. For brain immunofluorescence, animals were subjected to a different protocol of tissue preparation and isolation (see details below). To evaluate RAGE-Ab translocation through BBB, RAGE-Ab was conjugated to Alexa-Fluor 555 dye according kit's manufacturer instructions (Thermo Fisher, A20187) prior to i.p. injection procedure described above. In these animals, collected CSF was used to determine fluorescence intensity corresponding to Alexa-Fluor 555-conjugated RAGE-Ab. Alexa-Fluor 555-conjugated anti-rat IgG was used as control for RAGE-Ab. Repeated experiments with different animals were independently performed to obtain samples for multiple assays when required; the number of animals in each group (6) was always maintained.

2.3. Ethics statement

All experimental procedures were performed in accordance with the guidelines of the National Institutes of Health (NIH, 1985) and the Brazilian Society for Neuroscience and Behavior recommendations for animal care. Our research protocol was approved by the Ethical Committee for Animal Experimentation of the Universidade Federal do Rio Grande do Sul- Brazil (CEUA-UFRGS) under the project number #27683.

2.4. In vivo Evans blue dye (EBD) injection and dye extraction

In order to determine the effect of LPS on BBB permeability an EBD perfusion assay was performed as previously described (Dal-Pizzol et al., 2013). Injection of EBD is peripheral and its detection in brain is associated to BBB disruption, due to its high molecular weight (around 960 kDa). Twenty-four hours after LPS administration, the lateral tail vein was cannulated. EBD (4% solution in 0.9% saline), was injected as a single bolus dose of 2 mL/kg via cannula. After 120 min to enable uniform blood distribution, each rat was anaesthetized and thoroughly perfused with 0.9% saline to rid

circulation of remaining dye, and the perfused brain was collected. For extraction, the right and left sides of each striatum were placed in 50% trichloroacetic acid (TCA), at a ratio of 30–35 mg striatum to 200 μ L, and then homogenized for 5 min. The TCA brain extracts were centrifuged at 10,000g for 20 min to remove debris. The supernatants were added to a 96-well plate (30 μ L per well, each plate supplemented with 90 mL of 95% ethanol and thoroughly mixed by pipetting) for detection of EBD emission of fluorescence in a microplate reader (620 nm/680 nm) (Wang and Lai, 2014). The intensity of the EBD fluorescence leaking into the striatum provided an indication of the increased permeability of the BBB.

2.5. Enzyme-linked immunosorbent assay (ELISA) determination of cytokines and oxidative damage

TNF- α and IL-1 β were quantified with commercial kits and 4-hydroxynonenal (4-HNE) and nitrotyrosine were assessed by indirect assay. Liver and brain tissues were homogenized in phosphate buffer 50 mM (KH_2PO_4 and K_2HPO_4 , pH 7.4) and protein content measured. Tissue homogenate samples (30 μ g protein/well), CSF and blood serum samples (100 μ L) were placed in ELISA plates. For TNF- α , and IL-1 β quantification, kit manufacturer protocol was followed. For indirect ELISA, samples were incubated for 24 h in plates, and then washed three times with Tween-Tris buffered saline (TTBS, 100 mM Tris - HCl, pH 7.5, containing 0.9% NaCl, and 0.1% Tween-20). Subsequently, 200 μ L of primary antibody against 4-HNE or nitrotyrosine (1:1000) were added and incubation was carried for 24 h at 4 $^\circ\text{C}$. The plates were washed three times with TTBS and incubated with rabbit or mouse IgG peroxidase-linked secondary antibody (1:1000) for 2 h. After washing the plate three times with TTBS, 200 μ L of substrate solution (TMB spectrophotometric ELISA detection kit) were added to each well and incubated for 15 min. The reaction was terminated with 50 μ L/well of 12 M sulfuric acid stopping reagent and the plate read at 450 nm in a microplate. The results are expressed in percentage to control.

2.6. Measurement of total thiol content

For total reduced sulfhydryl (-SH) content measurement, samples were homogenized in phosphate buffer and protein content measured. A sample aliquot (50 μ L making 50 μ g protein/well) was diluted with 120 μ L of 50 mM PBS at pH 7.4 (NaCl , Na_2HPO_4 , KH_2PO_4) and 30 μ L of a buffer pH 8.5 (boric acid 100 mM and EDTA 0.2 mM) mixed with 10 μ L of 5,5'-dithiobis (2-nitrobenzoic acid) 10 mM. The reaction was read in a spectrophotometer at 412 nm after 60 min of incubation at room temperature (Ellman, 1959).

2.7. Mitochondrial respiratory chain complexes activities

Tissues were homogenized (1:10, w/v) with SETH buffer (250 mM sucrose, 2 mM EDTA, 10 mM Tris-HCl, 50 IU/ml heparin, pH 7.4). The homogenates were centrifuged at 800g for 10 min at 4 $^\circ\text{C}$ and protein content measured. Samples (6 μ g protein/ μ L in 500 μ L) were submitted to three freeze-thaw cycles to fully expose the enzymes to substrates. Ten microliters of supernatant (60 μ g protein) were applied per well to measure the activities of succinate-2,6-dichloroindophenol (DCIP)-oxidoreductase (succinate dehydrogenase), succinate:cytochrome c oxidoreductase (complexes II:III), NADH dehydrogenase:cytochrome c oxidoreductase (complexes I:III) and cytochrome c oxidase (complex IV) were determined by spectrophotometry kinetic measurements according previously described (Fischer et al., 1985; Rustin et al., 1994; Schapira et al., 1990) with modifications (da Silva et al., 2002).

2.8. Antioxidant enzymes activities

Catalase (CAT, EC 1.11.1.6), superoxide dismutase (SOD, EC 1.15.1.1) and glutathione peroxidase (GPx, EC 1.11.1.9) activities were quantified in tissue samples previously homogenized in phosphate buffer (pH 7.4) and normalized to 1 µg protein/µL. CAT activity was evaluated by determining the rate of H₂O₂ absorbance decrease at 240 nm (Aebi, 1984). In brief, 5 µL of each sample were added per well and mixed with 195 µL of phosphate buffer 50 mM at pH 7.4 (Na₂HPO₄, KH₂PO₄). Hydrogen peroxide 1 mM (5 µL) was added to start the reaction and kinetic was monitored in a spectrophotometer. The activity of SOD was measured by quantifying the inhibition of superoxide-dependent adrenaline autoxidation to adrenochrome, which was monitored at 480 nm for 10 min (32 °C) in spectrophotometer (Misra and Fridovich, 1972). In brief, 5 µL of catalase (10 µM) were added in each well, followed by 10 µL of sample and 180 µL of glycine buffer (50 mM, pH 10.2). Epinephrine (60 mM, 5 µL) was added to start reaction. To determine GPx activity, the rate of NADPH oxidation was measured in the presence of reduced glutathione (GSH), *tert*-butyl hydroperoxide, and glutathione reductase as previously described (Flohe and Gunzler, 1984). Ten microliters of sample were added per well, followed by 20 µL of NADPH (5 mM) and 170 µL of phosphate buffer (Na₂HPO₄, KH₂PO₄ -20 mM, pH 7.7). The microplate was incubated during 10 min in 37 °C then 10 µL of glutathione reductase (40 U/mL) + 10 µL glutathione (40 mM) + 20 µL of *tert*-butyl hydroperoxide (1 µL/mL) were added in each well. The reaction was monitored in spectrophotometer at 340 nm during 6 min.

2.9. Lipid peroxidation

The quantification of thiobarbituric acid reactive substances (TBARS) was performed for lipoperoxidation evaluation, as previously described (Draper and Hadley, 1990). Liver and striatum were homogenized in phosphate buffer (pH 7.4) and protein content normalized for 1 mg/mL. Samples were mixed with 0.6 mL of 10% TCA and centrifuged (10,000g for 10 min). Supernatant was mixed with 0.5 mL of 0.67% thiobarbituric acid and heated in boiling water for 25 min. TBARS were determined by the absorbance in a spectrophotometer at 532 nm. Results were expressed as nmol TBARS/mg protein.

2.10. Total reactive antioxidant potential (TRAP assay)

The total reactive antioxidant potential (TRAP) assay was applied to assess the non-enzymatic antioxidant capacity of samples. This assay is based on the quenching of peroxy radicals generated by addition of AAPH to samples (Lissi et al., 1992) and was performed as optimized by (Dresch et al., 2009). In brief, samples were homogenized in phosphate-buffered saline and protein content normalized to 1 µg/µL in glycine buffer (100 mM, pH 8.6). Supernatant is isolated and used for TRAP measurement. In separate vials, a chemical system that generates peroxy radicals at a constant rate (AAPH 10 mM dissolved in glycine buffer, 4 mL) is coupled to a luminescent reactant (luminol 4 mM, 10 µL) which emits photons in proportion to its oxidation. The addition of the homogenate samples either decreases or facilitates the luminescence emission in proportion to its content of non-enzymatic antioxidants. The luminescence emission was recorded in a MicroBeta[®] luminescence counter (Perkin Elmer, USA).

2.11. Western blotting

To perform immunoblot experiments, the tissues were prepared using an radioimmunoprecipitation assay buffer protocol

(Gasparotto et al., 2015). The proteins (30 µg/well) were electrophoresed by SDS-PAGE and electroblotted onto nitrocellulose membranes with trans-Blot Semi-Dry Electrophoretic Transfer Cell (Bio-Rad, CA, USA). Protein loading and electroblotting efficiency were verified through Ponceau S staining, and the membranes were washed with TTBS. Membranes were incubated for 20 min at room temperature in SNAP i.d. 2.0 Protein Detection System (Merck Millipore, MA, USA) with each primary antibody (all antibodies incubated at 1:500 dilution) and subsequently washed with TTBS. anti-rabbit or mouse IgG peroxidase-linked secondary antibody was incubated for an additional 20 min in SNAP (1:5000 dilution) and washed again, and the immunoreactivity was detected by enhanced chemiluminescence using Supersignal West Pico Chemiluminescent kit. The chemiluminescence was captured with an ImageQuant LAS 4000 (GE Healthcare). Densitometric analysis of the images was performed using ImageJ software (ImageJ v1.49, National Institute of Health, USA). Blots were developed to be linear in the range used for densitometry. All results were expressed as a relative ratio to β-actin or total isoform of the protein.

2.12. Reporter gene (Luciferase) assay

RAW 264.7 macrophage cells (obtained in the Rio de Janeiro Cell Bank, RJ, Brazil) were plated in 96-well plates and after 24 h transfected with 100 ng of a vector containing a responsive element to NF-κB driving firefly luciferase (pGL4.32 Luc2P-NF-κB[®] Promega) and 10 ng constitutive *Renilla*-luciferase construct (pRL-TK[®] Promega) per well. The transfection was carried by ViaFect[®] reagent (Promega) and Opti-MEM. Cells were also transfected with GFP vector to monitor the efficiency of transfection, and an empty vector was used as negative control. When more than 60% of cells display green fluorescence, NF-κB-luciferase and *Renilla* transfected cells were treated. Cells were pre-treated with RAGE-Ab at 20 µg/mL and treated with LPS 1 µg/mL for 1 h. At the end of treatments, the cells were lysed and luciferase activity was assessed using the Dual-Glo[®] Luciferase Assay System (Promega). Results are expressed in ratio Luciferase/*Renilla* luminescence relative to control groups.

2.13. Immunofluorescence

Rats were perfused via the vascular system with descendent aorta clamped. Sterile saline was administered during 10 min followed by 10 min with paraformaldehyde (PFA) solution 4% in PBS (7.4). The brains were then carefully extracted and maintained in PFA 4% for 24 h at 4 °C, then placed in sucrose 15% for 24 h at 4 °C and placed for 24 h at 4 °C in sucrose 30%. Brains were slightly dried and frozen in -20 °C. After 24 h the striatum was sectioned in slices of 15 µm on the coronal plane using a cryostat at -20 °C (Jung Histoslide 2000R; Leica; Heidelberg, Germany). A total of 20–30 slices per rat containing the striatum were collected in PBS containing Triton x100 0.1% (PBS-0.1%). The free-floating sections were incubated with albumin 5% during 2 h to block nonspecific binding sites. The antibody was incubated during 48 h at 4 °C. Antibody dilution and catalogue number: Iba-1 (1:500; 019-19741) is from Wako Chemicals USA, Inc. (VA, USA). GFAP (1:500; #3670) is from Cell Signalling. DAPI for nucleic acid staining (1:500; D9542) is from Sigma-Aldrich[®] (MO, USA). Antibodies were diluted in PBS containing bovine serum albumin (2%). After washing four times with PBS-0.1%, tissue sections were incubated with secondary antibody according to reactive species (anti-rabbit or mouse Alexa 488 or 555 from Cell Signalling Technology[®]), all diluted 1:500 in PBS and BSA 2%. After 1 h at room temperature the slices were washed several times in PBS-0.1%, transferred to gelatinized slides, mounted with FluorSave[™] (345789 – Merck Millipore; MA, USA) and covered with coverslips. The images were obtained with a

Microscopy EVOS® FL Auto Imaging System (AMAFD1000 – Thermo Fisher Scientific; MA, USA).

2.14. Protein assay

Total protein was quantified by Bradford assay and used to normalize all data (Bradford, 1976).

2.15. Statistical analysis

Statistical analysis was performed with GraphPad Prism version 5.04 (GraphPad Software Inc., San Diego, USA). Data were evaluated by one-way ANOVA analysis and followed by Tukey's Multiple Comparison post hoc test. Differences were considered significant when $p < 0.05$.

3. Results and discussion

Systemic LPS induces peripheral inflammation, oxidative stress and neuroinflammation, followed by progressive neurodegeneration over a period of ten months (Hoban et al., 2013; Qin et al., 2007). This model has been used to investigate the role of inflammation in the onset of neurodegenerative processes in the brain, and also has been applied to induce Parkinson's disease- and major depression-like changes (Duty and Jenner, 2011; O'Sullivan et al., 2009; Qin et al., 2013), thus constituting a suitable model

to investigate the role of RAGE in systemic inflammation-induced CNS damage. We first evaluated inflammatory markers in serum and determined the effects of pretreatment with anti-RAGE rabbit polyclonal IgG (RAGE-Ab). Previous works using polyclonal anti-RAGE for immune neutralization in rodents applied doses varying from 200 µg/kg to 1000 µg/kg and above (Kuhla et al., 2013; van Zoelen et al., 2009; Xia et al., 2016). Although unspecific binding of the blocking antibody was not reported in such studies, we tested a lower range of RAGE-Ab doses (from 50 up to 250 µg/kg) and selected the lowest concentration effective in inhibiting liver ERK1/2 phosphorylation induced by systemic inflammatory shock (unpublished data), as we wanted to avoid potential binding of RAGE-Ab to other proteins that could result from the use of higher doses.

LPS injection has been shown to initiate an inflammatory response that leads to the activation of macrophages, and other white blood cells (WBC). This in turn leads to the production of proinflammatory cytokines and a burst of NADPH oxidase activation with consequent generation of reactive species (Qin et al., 2013). LPS (5 mg/kg) increased both serum TNF-α and serum IL-1β 24 h after injection into rats (Fig. 2A and B). At 24 h, rats had lost approximately 10% of their body weight (Suppl. Fig. 1C) and further increases in the dose of LPS (7.5 and 10 mg/kg) caused 100% of mortality 1 h after injection (Suppl. Fig. 1 A and B). LPS (5 mg/kg) also increased serum 4-HNE and serum nitrotyrosine 24 h after injection (Fig. 2C and D) and this is consistent with an oxidative

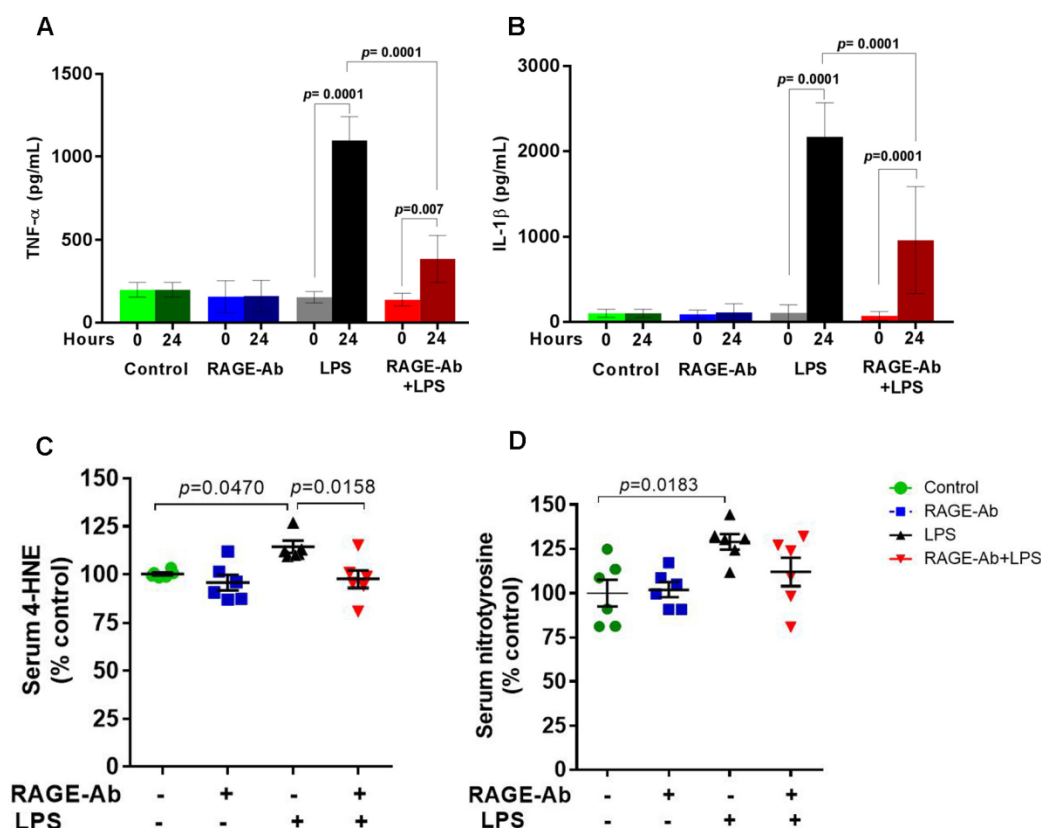


Fig. 2. Effects of systemic administration of RAGE-Ab and LPS on serum cytokines and oxidative stress markers. Wistar rats received a single dose of RAGE-Ab (50 µg/kg i.p.) and after 1 h a single dose of LPS (5 mg/kg i.p.); control group received saline. A) TNF-α and B) IL-1β levels were compared before injections (0 h) and 24 h after LPS injection. C) 4-HNE (4-hydroxynonenal) and D) nitrotyrosine relative levels were evaluated 24 h after LPS injection. Values represent mean ± SEM of samples obtained from six rats per group. One-way analysis of variance and Bonferroni Multiple Comparison post hoc analysis were applied for all data. The p values are embedded in the figures.

stress response. Prior treatment with RAGE-Ab significantly reduced the production of the proinflammatory cytokines and serum 4-HNE and it reduced the mean level of serum nitrotyrosine (Fig. 2A–D). Overall these serum results indicate that LPS induces a substantial inflammatory response in rats and suggests that LPS also induces RAGE activation, which in turn facilitates many of these LPS induced inflammatory responses. Importantly, the use of a polyclonal isotype antibody not directed to RAGE (rabbit anti-rat IgG) was not able to produce an effect similar to RAGE-Ab over serum cytokines (Suppl. Fig. 1D and E), confirming the specific activity of RAGE-Ab. Previous works observed that serum cytokines may present decreased levels compared to control 24 h after systemic injection with different doses of LPS (Fischer et al., 2015; Ong et al., 2016). This is expected as the serum cytokine response to systemic LPS may vary according the dose and bacterial origin of LPS utilized. Systemic inflammatory response induced by LPS or pathogens is constituted by an acute proinflammatory activation followed by a counter-regulatory anti-inflammatory response, which may be even more harmful than the proinflammatory phase (Kumar et al., 2009; Van Amersfoort et al., 2003; Xu et al., 2012). In our model, serum cytokines at 24 h were still increased compared to control levels, but their levels were declining compared to 1 h after injection (Suppl. Fig. 1A and B).

The increase in oxidative stress markers in serum is often associated to organ damage and release to the bloodstream. Previously, it was demonstrated that systemic injection of LPS to mice induced long-term neurodegeneration by a mechanism that was triggered by liver inflammation and secretion of TNF- α (Qin et al., 2007). In order to thoroughly investigate the inflammatory effects of LPS and the mechanisms whereby RAGE activation facilitates many of these LPS induced responses we chose liver as our model tissue. This is because liver is one of the main tissue targets during systemic inflammation and it is a major source of systemic proinflammatory mediators, which when released can affect other organs, including the brain (Romero-Gomez et al., 2015). The level of RAGE in liver was significantly increased by LPS 24 h after injection (Fig. 3A). Prior treatment with RAGE-Ab decreased basal levels of liver RAGE and completely blocked the increase in RAGE induced by LPS confirming the utility of this approach. These results indicate that RAGE participates in maintenance of its own basal levels in liver during LPS induction of systemic inflammation. Classically, following ligand binding, RAGE activates NF- κ B transcriptional activity and an increase in RAGE expression is induced, since the RAGE gene (*AGER*) possess a responsive element for NF- κ B (Maczurek et al., 2008). RAGE ligand binding increases RAGE availability, whereas RAGE inhibition decreases RAGE expression and protein levels. In this context, downregulation of RAGE expression generally evidences that RAGE signalling is inhibited, and these results indicate that the positive feedback axis of RAGE activation and up-regulation was successfully blocked.

Immune neutralization of RAGE with antibodies or Fab fragments has been extensively applied to inhibit RAGE, as a pharmacological inhibitor was not available until recently. Generally, the use of Fab fragments or monoclonal antibodies may present evident advantages compared to full-length polyclonal antibodies for this type of approach, as polyclonal antibodies recognize multiple epitopes and could potentially bind to other scavenger receptors that may share one or more epitopes. Besides, potential induction of receptor internalization could “mask” the expected blockade of the receptor. Nonetheless, this blocking approach of RAGE using polyclonal antibody was previously applied in different rodent models of systemic inflammation, being demonstrated to successfully block RAGE activation and other proinflammatory effects related to RAGE signalling in similar conditions (Kuhla et al., 2013; Origlia et al., 2008; van Zoelen et al., 2009; Xia et al., 2016). It is important to note, however, that LPS binds to multiple

receptors (including RAGE) and trigger similar intracellular effects that are associated to proinflammatory activation, including NF- κ B activation. In this context, the use of unspecific antibodies to neutralize RAGE could also inhibit other receptors, potentially Toll-like receptor 4 (TLR4), which is one of the main receptors to recognize and translate LPS proinflammatory signals. We tested the blocking effect of RAGE-Ab over NF- κ B activation by LPS in a macrophage cell line through a luciferase-reporter transactivation assay and observed that RAGE-Ab significantly, but not completely, inhibited LPS-mediated NF- κ B activity (Suppl. Fig. 1F). This result is expected for macrophage cells that express both RAGE and TLR4 and are exposed to LPS, as selective blocking of RAGE would not inhibit TLR4-mediated NF- κ B activation by LPS.

To further characterize the effect of RAGE blockade on LPS systemic inflammation, parameters related to LPS and RAGE signalling in liver were analyzed. The content of TLR4 was significantly increased by LPS in liver, and RAGE-Ab significantly, but not completely, inhibited this effect (Fig. 3B). The Extracellular-signal Regulated Kinases 1 and 2 (ERK1/2) are intracellular downstream targets of both RAGE and TLR4. ERK1/2 are also activated in response to oxidative stress (Son et al., 2013). Phosphorylated ERK1/2 levels were increased in the liver by LPS, and RAGE-Ab significantly, but not completely, inhibited this effect (Fig. 4C). Overall these liver results indicate that RAGE signalling facilitates the up-regulation of TLR4 and activation of ERK1/2 that occurs during systemic inflammation induced by LPS. Importantly, the use of a polyclonal isotype antibody not directed to RAGE was not able to produce a similar inhibitory effect over liver ERK1/2 phosphorylation by LPS, evidencing the specificity of RAGE blocking in this effect (Suppl. Fig. 1G). Both RAGE and TLR4 trigger NF- κ B activation during inflammatory stimulation. ERK1/2 are known to modulate the amplification of proinflammatory signalling resulting from RAGE and TLR4 ligand binding by causing NF- κ B-dependent gene transcription activation (Mandrekar and Szabo, 2009; Ott et al., 2014). NF- κ B is a multi-subunit protein complex regulated by various mechanisms that affect interaction between the different subunits, which may culminate in translocation of the p50 and p65 transcriptional subunits to the nucleus. In unstimulated conditions, p50 and p65 subunits are sequestered in the cytosol in an inactive state by the inhibitory I κ B subunits, which prevent nuclear translocation and consequent activation of gene transcription by p50/p65. Activation and modulation of NF- κ B may occur through phosphorylation and/or ubiquitination of I κ B subunits, which leads to dissociation from p50/p65 and proteasomic degradation; phosphorylation of p65 itself also positively modulates transcriptional activity (Viatour et al., 2005). Systemic injection of LPS induced a significant increase in I κ B phosphorylation, which was significantly, but not completely, inhibited in animals pre-treated with RAGE-Ab (Fig. 3D). This increase in phosphorylation was despite the total I κ B level being significantly decreased in LPS-treated animals (Fig. 3E). LPS also caused a significant increase in p65 phosphorylation, which was significantly, but not completely, inhibited in animals pre-treated with RAGE-Ab (Fig. 3F). This increase in phosphorylation was despite the total p65 level being significantly decreased in LPS-treated animals (Fig. 3G). Overall these results suggest that, during systemic inflammation induced by LPS, activation of NF- κ B through I κ B and p65 regulatory mechanisms in liver results from multiple pathways, with RAGE participating in I κ B and p65 phosphorylation and RAGE-independent pathways leading to I κ B and p65 degradation.

LPS increased liver levels of TNF- α and IL-1 β (Fig. 4A and B). Prior treatment with RAGE-Ab had no effect on the basal levels of these proinflammatory markers, but completely blocked the LPS induced increases in TNF- α and IL-1 β . Overall these results indicate that RAGE activation significantly facilitates the effects of LPS on liver cytokine production. LPS increased liver levels of

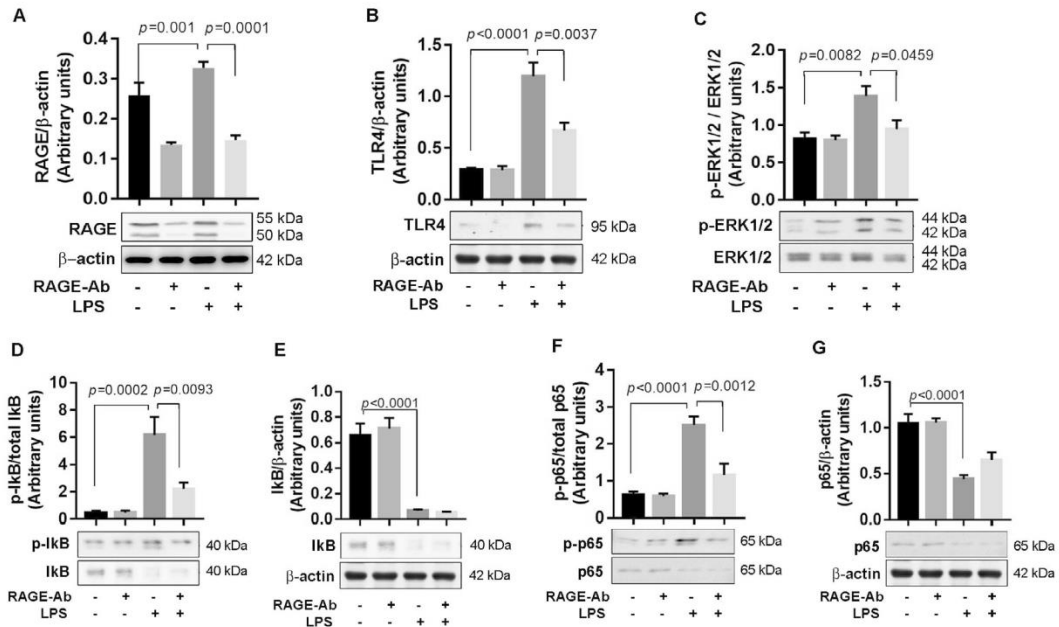


Fig. 3. Effects of systemic administration of RAGE-Ab and LPS on liver RAGE, TLR4, ERK1/2, IκB and p65. Wistar rats received a single dose of RAGE-Ab (50 μg/kg i.p.) followed by a single dose of LPS (5 mg/kg i.p.); control group received saline. Twenty-four hours after LPS injection, liver was isolated for western blot determination of the content of A) RAGE B) TLR4 C) phospho-ERK1/2 D) phospho-IκB E) IκB/β-actin F) phospho-p65 G) p65/β-actin. Representative western blots images are disposed under the graphs. Content of RAGE, TLR4, IκB and p65 was normalized relative to β-actin levels; content of phosphorylated isoforms of ERK1/2, IκB and p65 was normalized relative their total isoforms. Values represent mean ± SEM of samples obtained from six rats/group. One-way analysis of variance and Bonferroni Multiple Comparison post hoc analysis were applied for all data. The *p* values are embedded in figures.

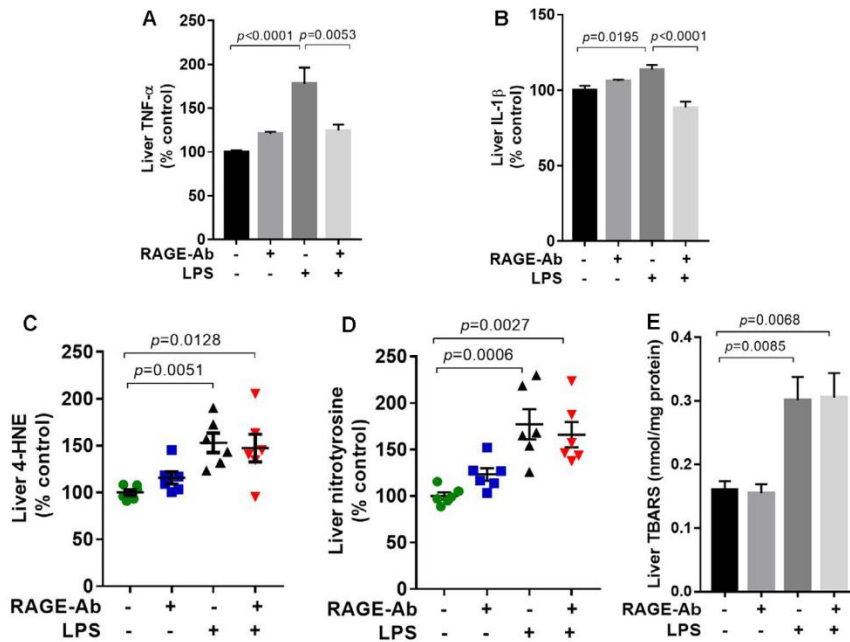


Fig. 4. Effects of systemic administration of RAGE-Ab and LPS on liver cytokines and oxidative stress markers. Wistar rats received a single dose of RAGE-Ab (50 μg/kg i.p.) followed by a single dose of LPS (5 mg/kg i.p.); control group received saline. Twenty-four hours after LPS injection, liver was isolated for determination of the content of A) TNF-α, B) IL-1β, C) 4-HNE (4-hydroxynonenal) and D) nitrotyrosine by ELISA and E) lipoperoxidation by TBARS quantification. Values represent mean ± SEM of samples obtained from six rats/group. One-way analysis of variance and Bonferroni Multiple Comparison post hoc analysis were applied for all data. The *p* values are embedded in figures.

4-HNE (marker for lipoperoxidation) and nitrotyrosine (marker of protein nitrosative damage) (Fig. 4C and D). Prior treatment with RAGE-Ab did not block the LPS induced increase in liver 4-HNE and only minimally reduced the mean level of liver nitrotyrosine. Damage to lipids is the main cause of cell rupture and release of many proteases and toxic substances, affecting other cells. We therefore also measured lipid damage in liver through the TBARS assay and observed that LPS increased TBARS, but this was also not reversed by RAGE-Ab (Fig. 4E). Overall these results indicated that, unlike in serum, liver oxidative stress during acute systemic inflammation induced by LPS is not dependent on RAGE signalling. This suggested also that the liver is not the main source of 4-HNE and nitrotyrosine observed in serum, as RAGE-Ab blocked the increase in these markers in the circulation. It could also be possible that RAGE-Ab pre-treatment inhibited the release of these molecules from this tissue to the bloodstream, but this hypothesis should be examined in more details.

LPS has been used to induce neurodegeneration both by systemic or intracranial injection (Bodea et al., 2014; Qin et al., 2007). In order to understand the role of RAGE in neuroinflammation triggered by systemic inflammation, we first evaluated parameters of proinflammatory activation in CSF, prefrontal cortex, striatum, SN and VTA. Systemic LPS administration increased TNF- α by 10-fold and IL-1 β by 35-fold in CSF, and these effects were blocked in animals pre-treated with RAGE-Ab (Fig. 5A and B). Control experiments with anti-IgG isotype injection

instead of RAGE-Ab failed to produce this inhibition, confirming the specificity of RAGE-Ab effect (Suppl. Fig. 1H and I). As this effect was similar to what we observed in serum, it is possible that the increase in TNF- α and IL-1 β in CSF is related to an influx of systemic cytokines via passage across the choroid plexus, or indirectly by passage across impaired blood–brain barrier (BBB) (Nirogi et al., 2009; Shen et al., 2004). Cytokines can also be transported across the BBB by saturable transport systems, which are able to directly affect central nervous system functions (Liu and Bing, 2011). We observed an increase in BBB permeability in animals subjected to systemic LPS injection by using the Evans blue translocation assay (Fig. 5C), suggesting that this route was likely to have contributed to the CSF cytokine levels.

Local production of inflammatory cytokines by different brain structures were analyzed separately. TNF- α was not changed in any brain region after systemic LPS injection (Fig. 5D), while IL-1 β was increased in striatum, prefrontal cortex and VTA (Fig. 5E). The increase in IL-1 β in the striatum was inhibited by pre-treatment with RAGE-Ab, but there was no effect of RAGE-Ab on prefrontal cortex and VTA IL-1 β levels. The fact that prefrontal cortex and VTA levels of IL-1 β were not altered by RAGE-Ab, while the CSF levels were, suggests that IL-1 β was produced locally in these regions. However, for the striatum which showed changes in BBB permeability, these results suggest that systemic inhibition of RAGE prior to LPS injection blocks either the local production of IL-1 β in the striatum or migration of this cytokine into the striatum

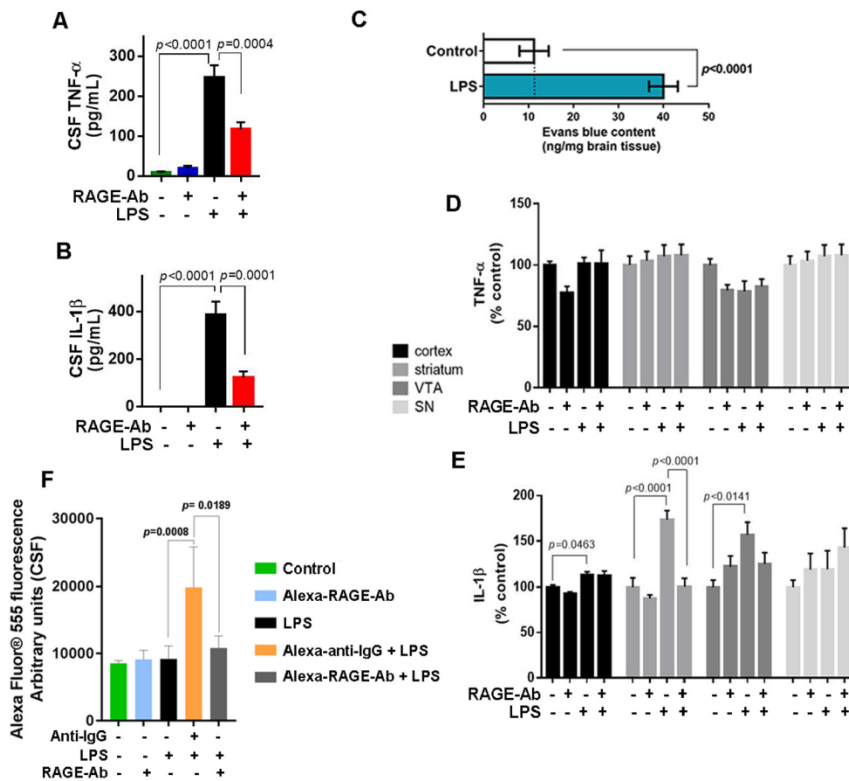


Fig. 5. Effects of systemic administration of RAGE-Ab and LPS on brain cytokines and BBB permeability. Wistar rats received a single dose of RAGE-Ab (50 μ g/kg i.p.) followed by a single dose of LPS (5 mg/kg i.p.); control group received saline. Twenty-four hours after LPS injection, CSF was obtained for determination of the content of A) TNF- α and B) IL-1 β by ELISA. The brain of these rats was isolated for analysis of D) TNF- α and E) IL-1 β in cortex, striatum, VTA and SN by ELISA. For C) Evans blue-based BBB permeability assay, rats were cannulated and perfused before brain extraction according description in “material and methods” section. Evans blue-fluorescence in striatum was determined in control vs. LPS-treated animals. F) Passage of RAGE-Ab across the BBB was analyzed by evaluating the presence of RAGE-Ab conjugated with Alexa-fluor[®] fluorescent probe in CSF; conjugated anti-IgG was used for specificity control. Values represent mean \pm SEM of samples obtained from six rats/group. One-way analysis of variance and Bonferroni Multiple Comparison post hoc test were applied for all data. The *p* values are embedded in figure.

from the CSF. LPS was previously observed to alter A β transport across BBB and this effect was not associated to BBB disruption, although it was not associated to changes in RAGE expression either (Jaeger et al., 2009). In this context, it seemed important to determine whether systemically injected RAGE-Ab could translocate into the CNS in our model, in order to establish if any potential effects observed at CNS level could be ascribed to local RAGE blocking. We thus evaluated the translocation of RAGE-Ab across the BBB by pre-injecting animals with RAGE-Ab conjugated to a fluorescent probe (Alexa Fluor[®]) and evaluating the presence of fluorescent probe in the CSF. Fluorescent conjugated RAGE-Ab is not detected in the CSF of animals treated with LPS, indicating that RAGE-Ab does not cross the BBB (Fig. 5F). Using conjugated anti-rat IgG isotype as control, CSF fluorescence is significantly increased in animals treated with LPS. These results confirm that effects of systemic RAGE-Ab injection over the CNS are not due to RAGE inhibition in the brain, as RAGE-Ab did not have access to the CNS in our experimental conditions. Besides, this result suggests that RAGE-Ab prevents BBB disruption by LPS, since, opposite to RAGE-Ab, anti-rat IgG is detected in the CSF of LPS-treated animals.

The effects of systemic LPS and RAGE-Ab on the striatum were investigated further in order to determine which of the major cell

types (microglia, astrocytes or neurons) were activated and what mechanisms were operating in this tissue. Unlike with the liver, there were no significant effects of systemic LPS on striatal RAGE levels 24 h after injection (Fig. 6A) and RAGE-Ab did not significantly reduce basal RAGE levels in the striatum. This reinforces the hypothesis that effects of RAGE-Ab in the striatum were not due to local blocking of RAGE. Brain RAGE has been implicated in neurodegeneration in previous studies (Ray et al., 2016), but these works examined much longer-term effects than 24 h. The microglial protein Iba-1, which is used as a marker of microglia activation, was increased in the striatum of animals subjected to systemic LPS and this increase was significantly inhibited by RAGE-Ab (Fig. 6B and G). Microglia are key innate immune cells in brain homeostasis and are constantly scavenging the CNS for damaged or unnecessary neurons and infectious agents (Gehrmann et al., 1995). The communication between peripheral inflammation and brain inflammation can result in the propagation of cytokines and chemokines within the brain by action of microglia (Chen et al., 2012; Norden et al., 2016) and microglia are known to be activated by systemic LPS (Qin et al., 2007). Glial fibrillary acidic protein (GFAP) expression is increased in activated astrocytes during neuroinflammation and is considered to be a marker for astrogliosis (Niranjan et al., 2010). Systemic LPS

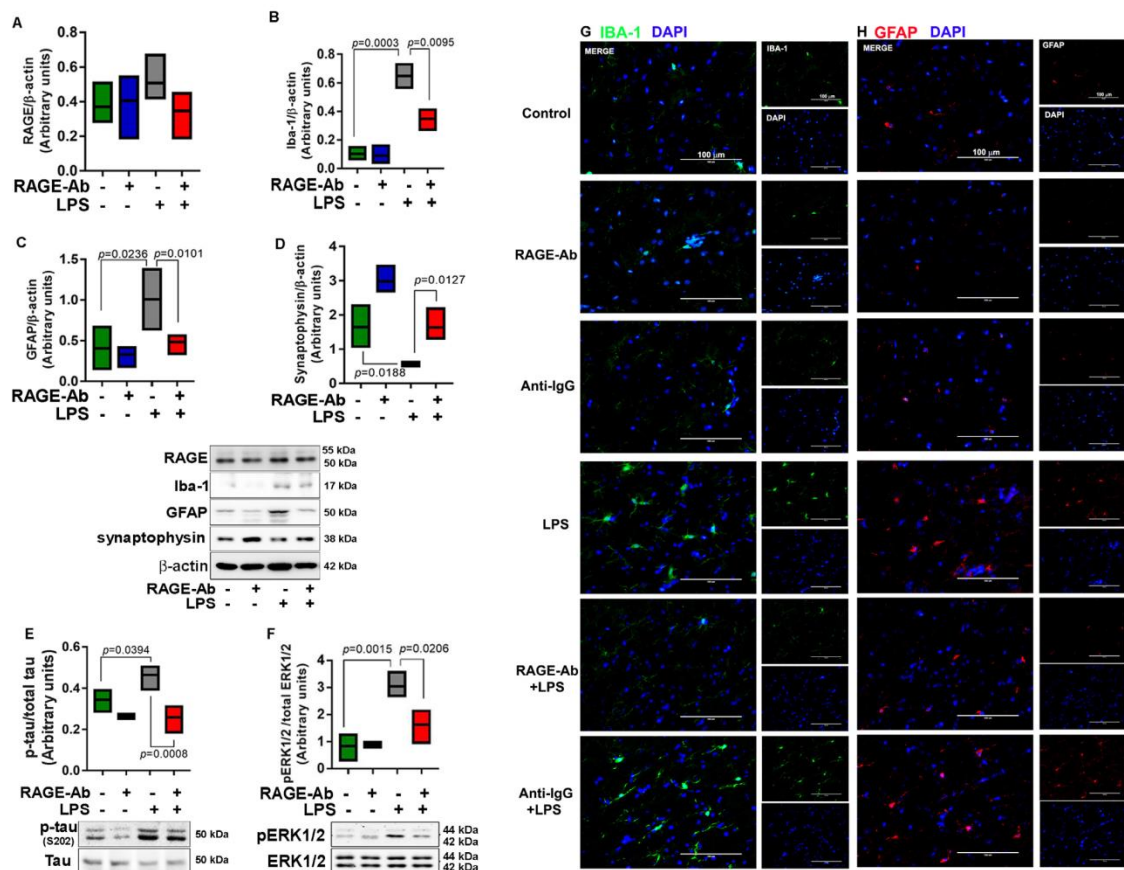


Fig. 6. Effects of systemic administration of RAGE-Ab and LPS on striatum. Wistar rats received a single dose of RAGE-Ab (50 μ g/kg i.p.) followed by a single dose of LPS (5 mg/kg i.p.); control group received saline or anti-rat IgG at the same concentration of RAGE-Ab. The contents of A) RAGE, B) Iba-1, C) GFAP, D) synaptophysin, E) phosphorylated tau (ser202) and F) phosphorylated ERK1/2 were quantified by western blot. Representative western blot bands are depicted. Immunofluorescence visualization of G) Iba-1 and H) GFAP in animals treated with anti-IgG for control of RAGE-Ab activity was performed in striatum; DAPI was used for nucleus staining. Representative images of analyzed samples from three rats/group are demonstrated. Values represent mean \pm SEM of samples obtained from six rats/group. One-way analysis of variance and Bonferroni Multiple Comparison post hoc test were applied for all data. The *p* values are embedded in figure.

injection significantly increased GFAP levels in striatum, and this effect was completely blocked by RAGE-Ab (Fig. 6C and H). Finally, we compared the effect of RAGE-Ab with isotype anti-rat IgG over Iba-1 and GFAP immunolocalization to assess the inhibitory specificity of RAGE-Ab over microglia and astrocyte activation by LPS, which was confirmed as anti-IgG had no effect over LPS-induced Iba-1 and GFAP immunoreactivity (Fig. 6G and H).

The levels of synaptophysin, a protein marker of functional synapses in neurons (Tarsa and Goda, 2002), was significantly decreased in LPS-treated animals (Fig. 6D), suggesting that the activity of striatal neurons was markedly altered. Synaptophysin expression is changed in response to various stimuli that affect the architecture of neuronal interconnections where functional synapses are established. RAGE-Ab pre-treatment conserved the level of synaptophysin in LPS treated animals. RAGE activation in brain has been suggested to affect synaptophysin levels in response to A β (Arancio et al., 2004). Nonetheless, as our results indicate, the decrease in synaptophysin by LPS is very likely to be a consequence of systemic inflammation, as systemic RAGE-Ab rescued synaptophysin levels without crossing the BBB. In this context, it is possible that the action of RAGE over the modulation of peripheral proinflammatory mediators may be the cause, direct or not, of synaptophysin downregulation and consequent synaptic dysfunction in the striatum. Several studies have been indicating that neuroinflammation correlates with synaptic loss, and NMDA-related excitotoxicity in response to IL-1 β , TNF- α , IL-6 and chemokines released by activated microglia and astrocytes during a major proinflammatory event. As our data indicated, systemic inflammation by LPS affected the BBB integrity, which allowed the passage of proinflammatory mediators to striatum and consequent glia activation. This has been proposed as a poten-

tial mechanism responsible by synaptophysin downregulation in major inflammatory insults (Rao et al., 2012) and our data suggests that systemic RAGE blocking probably prevented BBB integrity disruption by LPS and consequent microglia/astrocyte activation.

An increase in protein phosphorylation can indicate enzyme activation in cells due to increased protein kinase activity. Tau phosphorylation is increased in activated neurons as tau regulates neuron microtubule assembly and stabilization in response to phosphorylation by diverse serine/threonine kinases (Wang et al., 2012). Hyperphosphorylated states of tau for extended periods are also associated with the formation of dense hydrophobic aggregates leading to neurofibrillary tangles, contributing to neurodegeneration in conditions known as tauopathies (Mazanetz and Fischer, 2007). Tau phosphorylation at ser202 normally occurs during embryonic development, then ceases in the adult CNS; however, in AD, phosphorylation at this site is recapitulated and correlates with induction of abnormal phosphorylation states and neurofibrillary tangle formation (Goedert et al., 1998, 1993). Systemic LPS injection significantly increased tau ser202 phosphorylation levels in striatum after 24 h, and this effect was completely blocked by RAGE-Ab (Fig. 6E). Total levels of tau did not present significant variations in relation to β -actin content (Suppl. Fig. 2F). Although RAGE ligands have been previously observed to induce tau phosphorylation, the inhibitory effect of RAGE-Ab cannot be ascribed to RAGE blocking in striatum, as RAGE-Ab did not cross the BBB (Fig. 5F). It is possible that, in response to systemic inflammation and BBB disruption induced by LPS, activated microglia and astrocytes release proinflammatory mediators that activate death receptors in neurons, which in turn activate ERK1/2, GSK-3 β and CDK5-dependent tau phosphorylation, a classic neurotoxic cascade hypothesized for Alzheimer's disease (Zilka et al.,

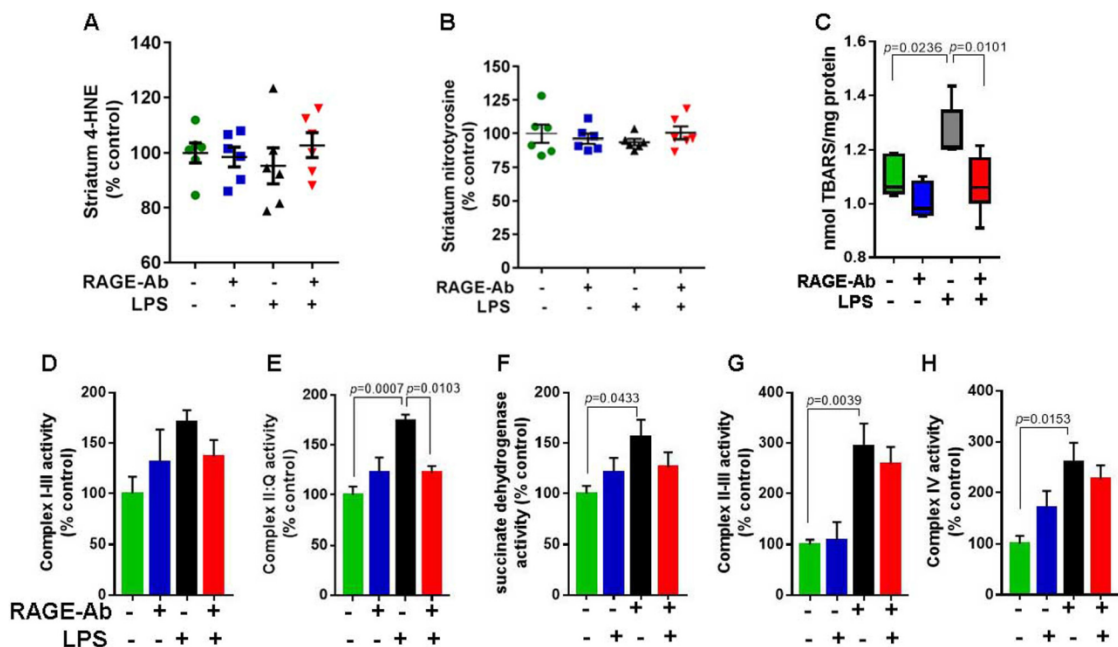


Fig. 7. Effects of systemic administration of RAGE-Ab and LPS on oxidative stress parameters and mitochondrial activity in striatum. Wistar rats received a single dose of RAGE-Ab (50 μ g/kg i.p.) followed by a single dose of LPS (5 mg/kg i.p.); control group received saline. Twenty-four hours after LPS injection, striatum was isolated. A) 4-HNE (4-hydroxynonenal) and B) nitrotyrosine relative levels were analyzed by ELISA and C) lipoperoxidation was analyzed by TBARS determination. D) Mitochondrial complex I-III, E) complex II-Q (ubiquinone), F) succinate dehydrogenase G) complex II-III and H) complex IV activities were followed spectrophotometrically. Values represent mean \pm SEM of samples obtained from six rats/group. The values are represented as percentage to control. One-way analysis of variance and Bonferroni Multiple Comparison post hoc test were applied for all data. The *p* values are embedded in figure.

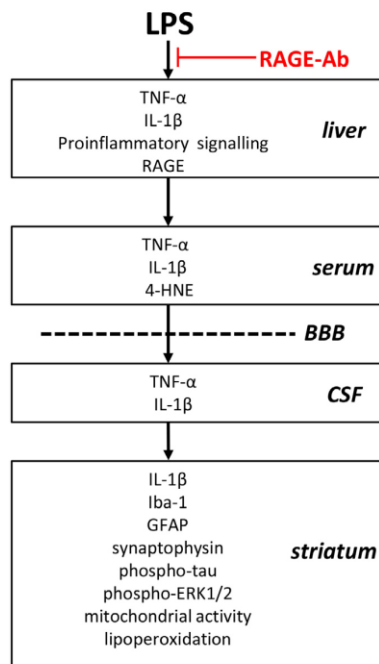


Fig. 8. Proposed mechanism of the role of RAGE on systemic inflammation and consequent BBB disruption, CSF proinflammatory cytokines and striatal damage 24 h after LPS induction. RAGE antibody pre-treatment prevents RAGE ligand binding and inhibits liver proinflammatory activation via NF- κ B pathway. Increases in serum TNF- α , IL-1 β and lipoperoxidation, as well as neuroinflammation and brain damage markers are all inhibited by systemic injection of RAGE-Ab.

2012). ERK1/2 phosphorylation was significantly increased by systemic injection of LPS and this effect was blocked by RAGE-Ab (Fig. 6F). ERK1/2 are present in all three major cell types in the striatum and an increase in ERK1/2 phosphorylation is consistent with any or all of the three cell types being activated. Overall these results suggest that LPS activates microglia, astrocytes and neurons in the striatum 24 h after injection and RAGE-Ab significantly decreased this activation without affecting striatal RAGE levels. This, along with data from Fig. 5F showing that RAGE-Ab does not translocate to the brain in LPS-treated animals, strongly suggests that systemic inhibition of RAGE activation can lead to blockade of the effects of LPS in the striatum. In a broader context, considering the effects of RAGE-Ab over parameters of inflammation and damage in all tissues analyzed, these results indicate that systemic blockade of RAGE protects the CSF and striatum by inhibiting the proinflammatory action of LPS at systemic level.

Oxidative stress is a major component in the neuronal death triggered by neuroinflammation during the progression of neurodegenerative conditions (Halliwell, 2006). To further understand the importance of systemic RAGE blocking in the acute effects of systemic inflammation on striatum, we next analyzed oxidative stress markers and there were no alterations in 4-HNE and nitrotyrosine levels, two specific markers of oxidative and nitrosative damage to lipids and proteins, respectively (Fig. 7A and B). However, TBARS levels were increased in LPS-treated animals and systemic RAGE-Ab injection prevented this effect (Fig. 7C). This result led us to analyze mitochondrial function by measuring the activity of the respiratory chain complexes in striatum, as mitochondrial activity is one of the main sources of reactive species production, along with NADPH oxidase, during an inflammatory burst

(Halliwell and Gutteridge, 2007). We observed that activities of complex II-ubiquinone, succinate dehydrogenase, complex II-III and complex IV were enhanced in LPS-treated animals. In liver LPS induced decreases in complex II activities while RAGE-Ab prevented this effect, no activities were found in other complex (Fig. 7D–H). We also analyzed parameters of antioxidant defence activation in striatum by assessing the activities of the enzymes CAT, SOD and GPx, the non-enzymatic antioxidant capacity by TRAP assay and quantification of total reduced thiol (sulfhydryl) groups. However, we did not observe any changes in these parameters (Supplementary Fig. 2A–E).

4. Conclusion

Systemic inflammation induced by LPS has been applied in diverse protocols that affect the function of the nigrostriatal axis, resulting in deficits of motor function, dopamine loss and neurodegeneration (Byler et al., 2009; Qin et al., 2013, 2007). Here we applied a protocol of acute inflammation with a single LPS injection and examined short-term effects (at 24 h after LPS injection) in blood serum, liver, CSF, prefrontal cortex, striatum, SN and VTA. A summary diagram is provided indicating the major findings (Fig. 8). Inhibiting effects induced by LPS in liver and serum, RAGE-Ab prevented LPS-related effects in CSF and striatum, but not in prefrontal cortex, SN and VTA. Our hypothesis is that systemic RAGE-Ab administration prior to LPS injection blocks the effects caused by RAGE upregulation and activation in liver, thus preventing a cascade of proinflammatory events caused by RAGE at systemic level, which include the production and release of cytokines that reach the brain and affect the striatum in less than 24 h (Fig. 8 and graphical abstract). Systemic RAGE activation contributes to BBB impairment and access of proinflammatory cytokines to the striatum, probably by stimulating the production and release of cytokines by liver. This is the first observation reporting the involvement of systemic RAGE signalling in neuroinflammation, tau phosphorylation, synaptophysin downregulation and brain redox impairment resulting from systemic inflammation. It remains to be determined, in the future, the role of RAGE in the long-term impairment of CNS functions that may evolve as consequence of systemic proinflammatory insults of different types. Also, it will be important to confirm if the involvement of RAGE in this process is restricted to CSF and striatum or if it affects other brain regions with time. In this context, evaluating neuroinflammation, oxidative stress, brain energy metabolism and parameters of neurodegeneration in longer periods after systemic LPS induction could be useful to determine the role of RAGE linking systemic and CNS inflammation. The mechanism by which RAGE exerts this role remains elusive (Fig. 8 and graphical abstract) but our data suggest that inhibition of the RAGE pathway may be an effective approach to block proinflammatory insults affecting the CNS.

Acknowledgments

This work was supported by funds from the Brazilian research agencies Conselho Nacional de Desenvolvimento Científico e Tecnológico (CNPq) #400437/2013-9, #443514/2014-3 and #401260/2014-3, Fundação de Amparo a Pesquisa do Estado do Rio Grande do Sul (FAPERGS) #2299-2551/14-6, Propesq-UFRGS and Coordenação de Aperfeiçoamento de Pessoal de Nível Superior (CAPES).

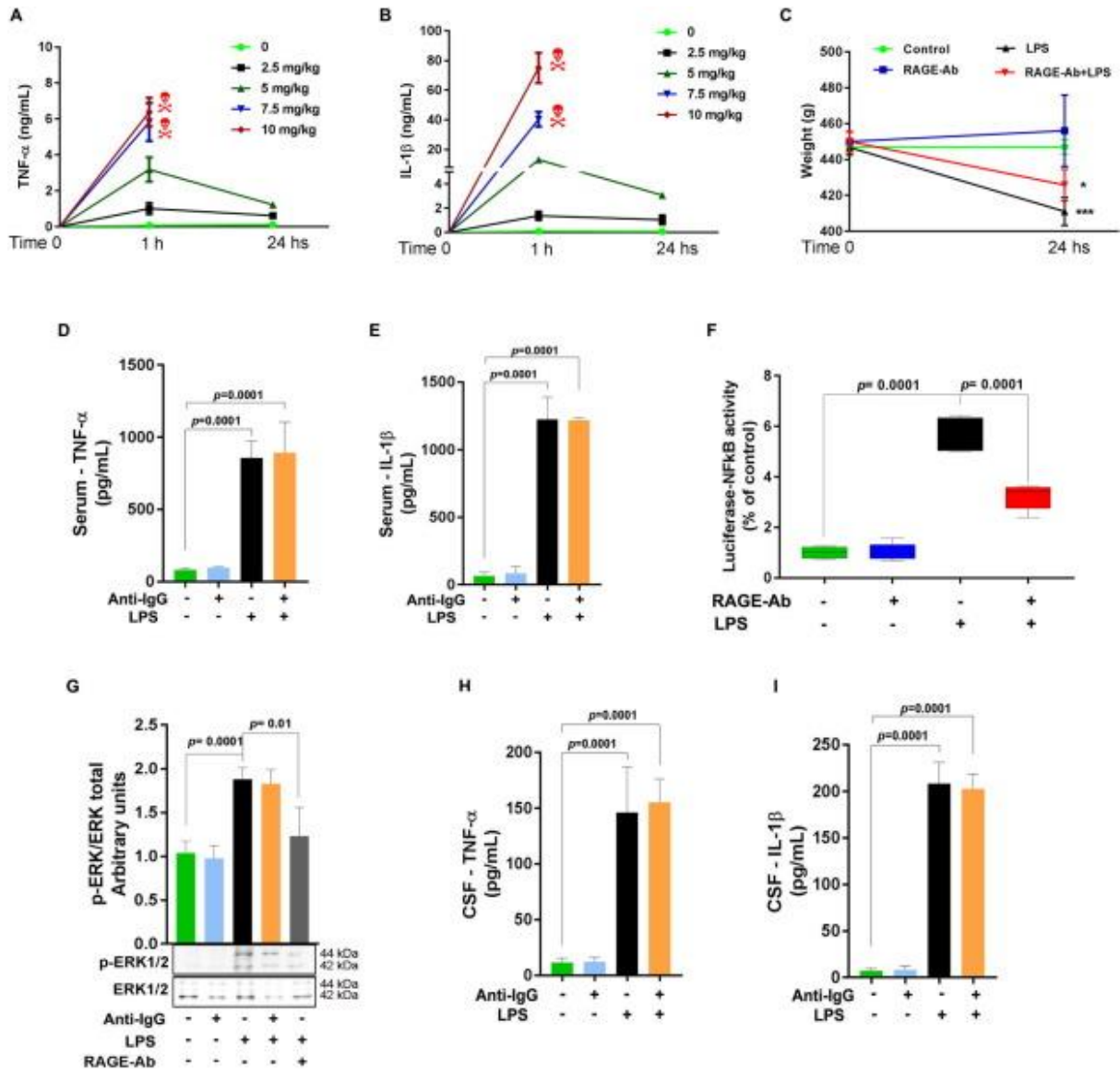
Appendix A. Supplementary data

Supplementary data associated with this article can be found, in the online version, at <http://dx.doi.org/10.1016/j.bbi.2017.01.008>.

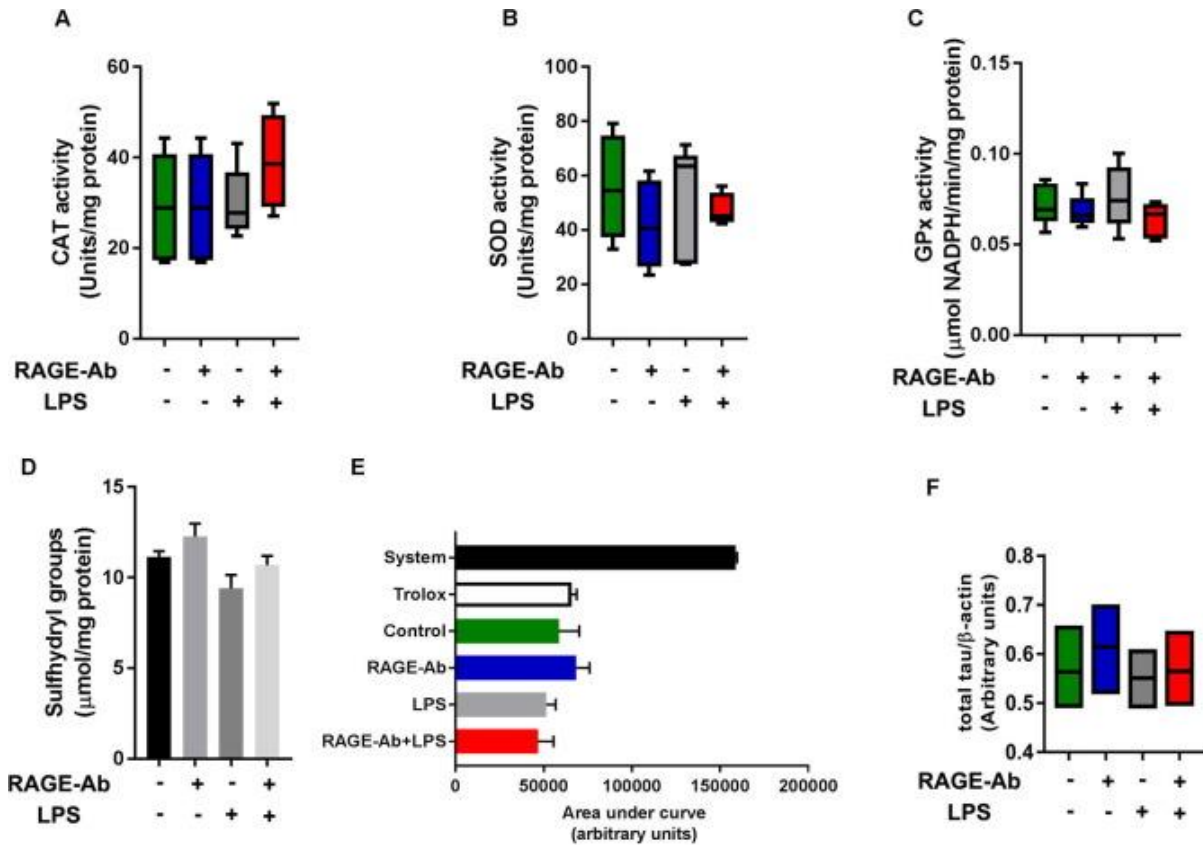
References

- Aebi, H., 1984. Catalase in vitro. *Methods Enzymol.* 105, 121–126.
- Arancio, O., Zhang, H.P., Chen, X., Lin, C., Trinchese, F., Puzzo, D., Liu, S., Hegde, A., Yan, S.F., Stern, A., Luddy, J.S., Lue, L.F., Walker, D.G., Roher, A., Buttini, M., Mucke, L., Li, W., Schmidt, A.M., Kindy, M., Hyslop, P.A., Stern, D.M., Du Yan, S.S., 2004. RAGE potentiates Abeta-induced perturbation of neuronal function in transgenic mice. *EMBO J.* 23, 4096–4105.
- Bodea, L.G., Wang, Y., Linnartz-Gerlach, B., Kopatz, J., Sinkkonen, L., Musgrove, R., Kaoma, T., Muller, A., Vallar, L., Di Monte, D.A., Balling, R., Neumann, H., 2014. Neurodegeneration by activation of the microglial complement-phagosome pathway. *J. Neurosci.* 34, 8546–8556.
- Bradford, M.M., 1976. A rapid and sensitive method for the quantitation of microgram quantities of protein utilizing the principle of protein-dye binding. *Anal. Biochem.* 72, 248–254.
- Bro, S., Flyvbjerg, A., Binder, C.J., Bang, C.A., Denner, L., Olgaard, K., Nielsen, L.B., 2008. A neutralizing antibody against receptor for advanced glycation end products (RAGE) reduces atherosclerosis in uremic mice. *Atherosclerosis* 201, 274–280.
- Byler, S.L., Boehm, G.W., Karp, J.D., Kohman, R.A., Tarr, A.J., Schallert, T., Barth, T.M., 2009. Systemic lipopolysaccharide plus MPTP as a model of dopamine loss and gait instability in C57Bl/6j mice. *Behav. Brain Res.* 198, 434–439.
- Chen, Z., Jalabi, W., Shpargel, K.B., Farabaugh, K.T., Dutta, R., Yin, X., Kidd, G.J., Bergmann, C.C., Stohman, S.A., Trapp, B.D., 2012. Lipopolysaccharide-induced microglial activation and neuroprotection against experimental brain injury is independent of hemato-genous TLR4. *J. Neurosci.* 32, 11706–11715.
- Creagh-Brown, B.C., Quinlan, G.J., Evans, T.W., Burke-Gaffney, A., 2010. The RAGE axis in systemic inflammation, acute lung injury and myocardial dysfunction: an important therapeutic target? *Intensive Care Med.* 36, 1644–1656.
- Cunningham, C., Hennessy, E., 2015. Co-morbidity and systemic inflammation as drivers of cognitive decline: new experimental models adopting a broader paradigm in dementia research. *Alzheimer Res. Ther.* 7, 33.
- da Silva, C.G., Ribeiro, C.A., Leipnitz, G., Dutra-Filho, C.S., Wyse, A.A., Wannmacher, C.M., Sarkis, J.J., Jakobs, C., Wajner, M., 2002. Inhibition of cytochrome c oxidase activity in rat cerebral cortex and human skeletal muscle by D-2-hydroxyglutaric acid in vitro. *Biochim. Biophys. Acta* 1586, 81–91.
- Dal-Pizzol, F., Rojas, H.A., Dos Santos, E.M., Vuolo, F., Constantino, L., Feier, G., Pasquali, M., Comim, C.M., Petronilho, F., Gelain, D.P., Quevedo, J., Moreira, J.C., Ritter, C., 2013. Matrix metalloproteinase-2 and metalloproteinase-9 activities are associated with blood-brain barrier dysfunction in an animal model of severe sepsis. *Mol. Neurobiol.*
- Draper, H.H., Hadley, M., 1990. Malondialdehyde determination as index of lipid peroxidation. *Methods Enzymol.* 186, 421–431.
- Dresch, M.T., Rossato, S.B., Kappel, V.D., Biegelmeier, R., Hoff, M.L., Mayorga, P., Zuanazzi, J.A., Henriques, A.T., Moreira, J.C., 2009. Optimization and validation of an alternative method to evaluate total reactive antioxidant potential. *Anal. Biochem.* 385, 107–114.
- Duty, S., Jenner, P., 2011. Animal models of Parkinson's disease: a source of novel treatments and clues to the cause of the disease. *Br. J. Pharmacol.* 164, 1357–1391.
- Ellman, G.L., 1959. Tissue sulfhydryl groups. *Arch. Biochem. Biophys.* 82, 70–77.
- Fischer, J.C., Ruitenbeek, W., Berden, J.A., Trijbels, J.M., Veerkamp, J.H., Stadhouders, A.M., Sengers, R.C., Janssen, A.J., 1985. Differential investigation of the capacity of succinate oxidation in human skeletal muscle. *Clin. Chim. Acta* 153, 23–36.
- Fischer, C.W., Elfving, B., Lund, S., Wegener, G., 2015. Behavioral and systemic consequences of long-term inflammatory challenge. *J. Neuroimmunol.* 288, 40–46.
- Flohe, L., Gunzler, W.A., 1984. Assays of glutathione peroxidase. *Methods Enzymol.* 105, 114–121.
- Gasparotto, J., Senger, M.R., Kunzler, A., Degrossoli, A., de Simone, S.G., Bortolin, R.C., Somensi, N., Girardi, C.S., de Souza, C.A.S., Calabrese, K.A.S., Dal-Pizzol, F., Moreira, J.C., Silva-Jr, F.P., Gelain, D.P., 2015. Increased tau phosphorylation and receptor for advanced glycation endproducts (RAGE) in the brain of mice infected with *Leishmania amazonensis*. *Brain Behav. Immun.* 43, 37–45.
- Gehrmann, J., Matsumoto, Y., Kreutzberg, G.W., 1995. Microglia: intrinsic immunoreactive cell of the brain. *Brain Res. Brain Res. Rev.* 20, 269–287.
- Goedert, M., Jakes, R., Crowther, R.A., Six, J., Lubke, U., Vandermeeren, M., Cras, P., Trojanowski, J.Q., Lee, V.M., 1993. The abnormal phosphorylation of tau protein at Ser-202 in Alzheimer disease recapitulates phosphorylation during development. *Proc. Natl. Acad. Sci. U.S.A.* 90, 5066–5070.
- Goedert, M., Jakes, R., Crowther, R.A., Hasegawa, M., Smith, M.J., Spillantini, M.G., 1998. Intra-neuronal filamentous tau protein and alpha-synuclein deposits in neurodegenerative diseases. *Biochem. Soc. Trans.* 26, 463–471.
- Guo, Z.J., Niu, H.X., Hou, F.F., Zhang, L., Fu, N., Nagai, R., Lu, X., Chen, B.H., Shan, Y.X., Tian, J.W., Nagaraj, R.H., Xie, D., Zhang, X., 2008. Advanced oxidation protein products activate vascular endothelial cells via a RAGE-mediated signaling pathway. *Antioxid. Redox Signal.* 10, 1699–1712.
- Halliwell, B., 2006. Oxidative stress and neurodegeneration: where are we now? *J. Neurochem.* 97, 1634–1658.
- Halliwell, B., Gutteridge, J.M.C., 2007. *Free Radicals in Biology and Medicine*. Oxford University Press, Oxford.
- Hoban, D.B., Connaughton, E., Connaughton, C., Hogan, G., Thornton, C., Mulcahy, P., Moloney, T.C., Dowd, E., 2013. Further characterisation of the LPS model of Parkinson's disease: a comparison of intra-nigral and intra-striatal lipopolysaccharide administration on motor function, microgliosis and nigrostriatal neurodegeneration in the rat. *Brain Behav. Immun.* 27, 91–100.
- Holt, E.M., Steffen, L.M., Moran, A., Basu, S., Steinberger, J., Ross, J.A., Hong, C.P., Sinaiko, A.R., 2009. Fruit and vegetable consumption and its relation to markers of inflammation and oxidative stress in adolescents. *J. Am. Diet.* 109, 414–421.
- Jaeger, L.B., Dohgu, S., Sultana, R., Lynch, J.L., Owen, J.B., Erickson, M.A., Shah, G.N., Price, T.O., Fleegal-Demotta, M.A., Butterfield, D.A., Banks, W.A., 2009. Lipopolysaccharide alters the blood-brain barrier transport of amyloid beta protein: a mechanism for inflammation in the progression of Alzheimer's disease. *Brain Behav. Immun.* 23, 507–517.
- Juranek, J., Ray, R., Banach, M., Rai, V., 2015. Receptor for advanced glycation end-products in neurodegenerative diseases. *Rev. Neurosci.* 26, 691–698.
- Kim, J., Waldvogel, H.J., Faull, R.L., Curtis, M.A., Nicholson, L.F., 2015. The RAGE receptor and its ligands are highly expressed in astrocytes in a grade-dependant manner in the striatum and subependymal layer in Huntington's disease. *J. Neurochem.* 134, 927–942.
- Kuhla, A., Norden, J., Abshagen, K., Menger, M.D., Vollmar, B., 2013. RAGE blockade and hepatic microcirculation in experimental endotoxaemic liver failure. *Br. J. Surg.* 100, 1229–1239.
- Kumar, H., Kawai, T., Akira, S., 2009. Toll-like receptors and innate immunity. *Biochem. Biophys. Res. Commun.* 388, 621–625.
- Lee, G., Goossens, K.A., 2015. Sampling Blood From the Lateral Tail Vein of the Rat. *J. Vis. Exp.*
- Lissi, E., Pascual, C., Del Castillo, M.D., 1992. Luminol luminescence induced by 2,2'-Azo-bis(2-amidinopropane) thermolysis. *Free Radic. Res. Commun.* 17, 299–311.
- Liu, M., Bing, G., 2011. Lipopolysaccharide Animal Models for Parkinson's Disease. *Parkinsons Dis.*
- Lukic, I.K., Humpert, P.M., Nawroth, P.P., Bierhaus, A., 2008. The RAGE pathway: activation and perpetuation in the pathogenesis of diabetic neuropathy. *Ann. N. Y. Acad. Sci.* 1126, 76–80.
- Lutterloh, E.C., Opal, S.M., 2007. Antibodies against RAGE in sepsis and inflammation: implications for therapy. *Expert Opin. Pharmacother.* 8, 1193–1196.
- Lutterloh, E.C., Opal, S.M., Pittman, D.D., Keith Jr., J.C., Tan, X.Y., Clancy, B.M., Palmer, H., Milarski, K., Sun, Y., Palardy, J.E., Parejo, N.A., Kessimian, N., 2007. Inhibition of the RAGE products increases survival in experimental models of severe sepsis and systemic infection. *Crit. Care* 11, R122.
- Maczurek, A., Shanmugam, K., Munch, G., 2008. Inflammation and the redox-sensitive AGE-RAGE pathway as a therapeutic target in Alzheimer's disease. *Ann. N. Y. Acad. Sci.* 1126, 147–151.
- Mandrekar, P., Szabo, G., 2009. Signalling pathways in alcohol-induced liver inflammation. *J. Hepatol.* 50, 1258–1266.
- Marsche, G., Semlitsch, M., Hammer, A., Frank, S., Weigl, B., Demling, N., Schmidt, K., Windischhofer, W., Waeg, G., Sattler, W., Malle, E., 2007. Hypochlorite-modified albumin colocalizes with RAGE in the artery wall and promotes MCP-1 expression via the RAGE-Erk1/2 MAP-kinase pathway. *FASEB J.* 21, 1145–1152.
- Martens, H.A., Nienhuis, H.L., Gross, S., van der Steege, G., Brouwer, E., Berden, J.H., de Sevaux, R.G., Derksen, R.H., Voskuyl, A.E., Berger, S.P., Navis, G.J., Nolte, I.M., Kallenberg, C.G., Bijl, M., 2012. Receptor for advanced glycation end products (RAGE) polymorphisms are associated with systemic lupus erythematosus and disease severity in lupus nephritis. *Lupus* 21, 959–968.
- Mazanec, M.P., Fischer, P.M., 2007. Untangling tau hyperphosphorylation in drug design for neurodegenerative diseases. *Nat. Rev. Drug Discovery* 6, 464–479.
- Mazarati, A., Maroso, M., Iori, V., Vezzani, A., Carli, M., 2011. High-mobility group box-1 impairs memory in mice through both toll-like receptor 4 and receptor for advanced glycation end products. *Exp. Neurol.* 232, 143–148.
- Misra, H.P., Fridovich, I., 1972. The role of superoxide anion in the autoxidation of epinephrine and a simple assay for superoxide dismutase. *J. Biol. Chem.* 247, 3170–3175.
- Nguyen, J.C., Killcross, A.S., Jenkins, T.A., 2014. Obesity and cognitive decline: role of inflammation and vascular changes. *Front. Neurosci.* 8, 375.
- NIH, 1985. *National Institutes of Health Guide for Care and Use of Laboratory Animals* <<http://grants.nih.gov/grants/olaw/Guide-for-the-care-and-use-of-laboratory-animals.pdf>>.
- Niranjan, R., Kamat, P.K., Nath, C., Shukla, R., 2010. Evaluation of guggulipid and nimesulide on production of inflammatory mediators and GFAP expression in LPS stimulated rat astrocytoma, cell line (C6). *J. Ethnopharmacol.* 127, 625–630.
- Nirogi, R., Kandikere, V., Mudigonda, K., Bhyrapuneni, G., Muddana, N., Saralaya, R., Benade, V., 2009. A simple and rapid method to collect the cerebrospinal fluid of rats and its application for the assessment of drug penetration into the central nervous system. *J. Neurosci. Methods* 178, 116–119.
- Norden, D.M., Trojanowski, P.J., Villanueva, E., Navarro, E., Godbout, J.P., 2016. Sequential activation of microglia and astrocyte cytokine expression precedes increased Iba-1 or GFAP immunoreactivity following systemic immune challenge. *Glia* 64, 300–316.
- Ong, L.K., Page, S., Briggs, G.D., Guan, L., Dun, M.D., Verrills, N.M., Dunkley, P.R., Dickson, P.W., 2016. Peripheral lipopolysaccharide challenge induces long-term changes in tyrosine hydroxylase regulation in the adrenal medulla. *J. Cell. Biochem.*
- Origlia, N., Righi, M., Capsoni, S., Cattaneo, A., Fang, F., Stern, D.M., Chen, J.X., Schmidt, A.M., Arancio, O., Yan, S.D., Domenici, L., 2008. Receptor for advanced glycation end product-dependent activation of p38 mitogen-activated protein kinase contributes to amyloid-beta-mediated cortical synaptic dysfunction. *J. Neurosci.* 28, 3521–3530.

- Origlia, N., Criscuolo, C., Arancio, O., Yan, S.S., Domenici, L., 2014. RAGE inhibition in microglia prevents ischemia-dependent synaptic dysfunction in an amyloid-enriched environment. *J. Neurosci.*, 8749–8760.
- O'Sullivan, J.B., Ryan, K.M., Curtin, N.M., Harkin, A., Connor, T.J., 2009. Noradrenergic reuptake inhibitors limit neuroinflammation in rat cortex following a systemic inflammatory challenge: implications for depression and neurodegeneration. *Int. J. Neuropsychopharmacol.* 12, 687–699.
- Ott, C., Jacobs, K., Haucke, E., Navarrete Santos, A., Grune, T., Simm, A., 2014. Role of advanced glycation end products in cellular signaling. *Redox Biol.* 2, 411–429.
- Pandharipande, P.P., Girard, T.D., Jackson, J.C., Morandi, A., Thompson, J.L., Pun, B.T., Brummel, N.E., Hughes, C.G., Vasilevskis, E.E., Shintani, A.K., Moons, K.G., Geevarghese, S.K., Canonic, A., Hopkins, R.O., Bernard, G.R., Dittus, R.S., Ely, E. W., Investigators, B.-I.S., 2013. Long-term cognitive impairment after critical illness. *N. Engl. J. Med.* 369, 1306–1316.
- Qin, L., Wu, X., Block, M.L., Liu, Y., Breese, G.R., Hong, J.S., Knapp, D.J., Crews, F.T., 2007. Systemic LPS causes chronic neuroinflammation and progressive neurodegeneration. *Glia* 55, 453–462.
- Qin, L., Liu, Y., Hong, J.S., Crews, F.T., 2013. NADPH oxidase and aging drive microglial activation, oxidative stress, and dopaminergic neurodegeneration following systemic LPS administration. *Glia* 61, 855–868.
- Rao, J.S., Kellom, M., Kim, H.W., Rapoport, S.I., Reese, E.A., 2012. Neuroinflammation and synaptic loss. *Neurochem. Res.* 37, 903–910.
- Ray, R., Juranek, J.K., Rai, V., 2016. RAGE axis in neuroinflammation, neurodegeneration and its emerging role in the pathogenesis of amyotrophic lateral sclerosis. *Neurosci. Biobehav. Rev.* 62, 48–55.
- Romero-Gomez, M., Montagnese, S., Jalan, R., 2015. Hepatic encephalopathy in patients with acute decompensation of cirrhosis and acute-on-chronic liver failure. *J. Hepatol.* 62, 437–447.
- Rustin, P., Chretien, D., Bourgeron, T., Gerard, B., Rotig, A., Saudubray, J.M., Munnich, A., 1994. Biochemical and molecular investigations in respiratory chain deficiencies. *Clin. Chim. Acta* 228, 35–51.
- Schapiro, A.H., Mann, V.M., Cooper, J.M., Dexter, D., Daniel, S.E., Jenner, P., Clark, J.B., Marsden, C.D., 1990. Anatomic and disease specificity of NADH CoQ1 reductase (complex I) deficiency in Parkinson's disease. *J. Neurochem.* 55, 2142–2145.
- Shen, D.D., Artru, A.A., Adkison, K.K., 2004. Principles and applicability of CSF sampling for the assessment of CNS drug delivery and pharmacodynamics. *Adv. Drug Delivery Rev.* 56, 1825–1857.
- Sims, G.P., Rowe, D.C., Rietdijk, S.T., Herbst, R., Coyle, A.J., 2010. HMGB1 and RAGE in inflammation and cancer. *Annu. Rev. Immunol.* 28, 367–388.
- Son, Y., Kim, S., Chung, H.T., Pae, H.O., 2013. Reactive oxygen species in the activation of MAP kinases. *Methods Enzymol.* 528, 27–48.
- Sugimoto, K., Yasujima, M., Yagihashi, S., 2008. Role of advanced glycation end products in diabetic neuropathy. *Curr. Pharm. Des.* 14, 953–961.
- Tarsa, L., Goda, Y., 2002. Synaptophysin regulates activity-dependent synapse formation in cultured hippocampal neurons. *Proc. Natl. Acad. Sci. U.S.A.* 99, 1012–1016.
- Teismann, P., Sathe, K., Bierhaus, A., Leng, L., Martin, H.L., Bucala, R., Weigle, B., Nawroth, P.P., Schulz, J.B., 2012. Receptor for advanced glycation endproducts (RAGE) deficiency protects against MPTP toxicity. *Neurobiol. Aging* 33, 2478–2490.
- Tekabe, Y., Anthony, T., Li, Q., Ray, R., Rai, V., Zhang, G., Schmidt, A.M., Johnson, L.L., 2015. Treatment effect with anti-RAGE F(ab)² antibody improves hind limb angiogenesis and blood flow in Type 1 diabetic mice with left femoral artery ligation. *Vasc. Med.* 20, 212–218.
- Van Amersfoort, E.S., Van Berkel, T.J., Kuiper, J., 2003. Receptors, mediators, and mechanisms involved in bacterial sepsis and septic shock. *Clin. Microbiol. Rev.* 16, 379–414.
- van Zoelen, M.A., van der Poll, T., 2008. Targeting RAGE in sepsis. *Crit. Care* 12, 103.
- van Zoelen, M.A., Schmidt, A.M., Florquin, S., Meijers, J.C., de Beer, R., de Vos, A.F., Nawroth, P.P., Bierhaus, A., van der Poll, T., 2009. Receptor for advanced glycation end products facilitates host defense during *Escherichia coli*-induced abdominal sepsis in mice. *J. Infect. Dis.* 200, 765–773.
- Viatour, P., Merville, M.P., Bours, V., Chariot, A., 2005. Phosphorylation of NF-kappaB and I kappaB proteins: implications in cancer and inflammation. *Trends Biochem. Sci.* 30, 43–52.
- Wang, H.L., Lai, T.W., 2014. Optimization of Evans blue quantitation in limited rat tissue samples. *Sci. Rep.* 4, 6588.
- Wang, J.Z., Xia, Y.Y., Grundke-Iqbal, I., Iqbal, K., 2012. Abnormal hyperphosphorylation of tau: sites, regulation, and molecular mechanism of neurofibrillary degeneration. *J. Alzheimer Dis.* 33, S123.
- Widmann, C.N., Heneka, M.T., 2014. Long-term cerebral consequences of sepsis. *Lancet Neurol* 13, 630–636.
- Xia, P., Deng, Q., Gao, J., Yu, X., Zhang, Y., Li, J., Guan, W., Hu, J., Tan, Q., Zhou, L., Han, W., Yuan, Y., Yu, Y., 2016. Therapeutic effects of antigen affinity-purified polyclonal anti-receptor of advanced glycation end-product (RAGE) antibodies on cholestasis-induced liver injury in rats. *Eur. J. Pharmacol.* 779, 102–110.
- Xie, J., Mendez, J.D., Mendez-Valenzuela, V., Aguilar-Hernandez, M.M., 2013. Cellular signalling of the receptor for advanced glycation end products (RAGE). *Cell. Signal.* 25, 2185–2197.
- Xu, P.B., Lou, J.S., Ren, Y., Miao, C.H., Deng, X.M., 2012. Gene expression profiling reveals the defining features of monocytes from septic patients with compensatory anti-inflammatory response syndrome. *J. Infect.* 65, 380–391.
- Yamamoto, Y., Harashina, A., Saito, H., Tsuneyama, K., Munesue, S., Motoyoshi, S., Han, D., Watanabe, T., Asano, M., Takasawa, S., Okamoto, H., Shimura, S., Karasawa, T., Yonekura, H., Yamamoto, H., 2011. Septic shock is associated with receptor for advanced glycation end products ligation of LPS. *J. Immunol.* 186, 3248–3257.
- Yu, Y., Ye, R.D., 2015. Microglial alpha receptors in Alzheimer's disease. *Cell. Mol. Neurobiol.* 35, 71–83.
- Zilka, N., Kazmerova, Z., Jadhav, S., Neradil, P., Madari, A., Obetkova, D., Bugos, O., Novak, M., 2012. Who fans the flames of Alzheimer's disease brains? Misfolded tau on the crossroad of neurodegenerative and inflammatory pathways. *J. Neuroinflamm.* 9, 47.



Supplementary Fig. 1. Pilot tests for dose determination of LPS and RAGE-Ab efficacy control experiments. Wistar rats (6 per group) received different doses of LPS: 0 (saline), 2.5, 5, 7.5, and 10 mg/kg were administered. The blood was sampled before LPS injection (time 0); then at 1 h and 24 h after LPS injection. A) TNF- α and B) IL-1 β levels were assessed by ELISA. C) Average weight before and 24 h after LPS: Wistar rats received a single dose of RAGE-Ab (50 μ g/kg i.p.) followed by a single dose of LPS (5 mg/kg i.p.); control group received saline. To evaluate the specificity of RAGE-Ab action over LPS effects, serum cytokine levels were evaluated in animals treated with isotype anti-IgG (50 μ g/kg) instead of RAGE-Ab. Serum D) TNF- α and E) IL-1 β were analyzed by ELISA. F) In RAW 264.7 macrophage cell line, a NF- κ B transactivation assay was performed to evaluate the blocking activity of RAGE-Ab over LPS-induced activation of NF- κ B. G) Comparison between blocking activity of RAGE-Ab and isotype anti-IgG on LPS-evoked liver ERK1/2 phosphorylation. The effect of anti-IgG on H) TNF- α and I) IL-1 β in CSF was also analyzed by ELISA. Values represent mean \pm SEM of samples obtained from six rats. One-way analysis of variance and Bonferroni Multiple Comparison *post-hoc* test were applied for all data. Skulls represent groups with 100% of mortality before completion of 24 h. Asterisks denote difference to control groups (** $p < 0.0001$ and * $p < 0.05$).



Supplementary Fig. 2. Effects of systemic administration of RAGE-Ab and LPS on striatum antioxidant enzymes, non-enzymatic antioxidant defense and total levels of tau. Wistar rats received a single dose of RAGE-Ab (50 $\mu\text{g}/\text{kg}$ i.p.) followed by a single dose of LPS (5 mg/kg i.p.); control group received saline. Striatum was isolated 24 h later. A) CAT (catalase) B) SOD (superoxide dismutase) activity and C) GPx (glutathione peroxidase) activities were determined. D) Reduced thiol (-SH) groups content was evaluated spectrophotometrically. E) TRAP parameter was determined by luminescence kinetic assay. F) The contents of total tau and β -actin were determined by western blot (representative gels in Fig. 6). Values of total tau were normalized in relation to β -actin. Values represent mean \pm SEM of samples obtained from six rats. One-way analysis of variance and Bonferroni Multiple Comparison post-hoc test were applied for all data. The p values are embedded in figure.

Capítulo III

Receptor for advanced glycation end products mediates sepsis-triggered amyloid- β accumulation, tau phosphorylation, and cognitive impairment

Publicado em: **Journal of Biological Chemistry (2018)**



Receptor for advanced glycation end products mediates sepsis-triggered amyloid- β accumulation, Tau phosphorylation, and cognitive impairment

Received for publication, March 16, 2017, and in revised form, November 9, 2017. Published, Papers in Press, November 10, 2017, DOI 10.1074/jbc.M117.786756

Juciano Gasparotto[‡], Carolina S. Girardi[‡], Nauana Somensi[‡], Camila T. Ribeiro[‡], José C. F. Moreira[‡], Monique Michels[§], Beatriz Sonai[§], Mariane Rocha[§], Amanda V. Steckert^{¶||***‡}, Tatiana Barichello^{¶||***‡}, João Quevedo^{¶||***‡}, Felipe Dal-Pizzol[§], and Daniel P. Gelain^{†1}

From the [‡]Centro de Estudos em Estresse Oxidativo, Departamento de Bioquímica, Instituto de Ciências Básicas da Saúde, Universidade Federal do Rio Grande do Sul, Porto Alegre 90035-003 RS, Brazil, the [§]Laboratório de Fisiopatologia Experimental, Instituto Nacional de Ciência e Tecnologia Translacional em Medicina, and [¶]Laboratório de Neurociências at Programa de Pós-Graduação em Ciências da Saúde, Unidade Acadêmica de Ciências da Saúde, Universidade do Extremo Sul Catarinense-Criciúma, Criciúma 88806-000 SC, Brazil, and the ^{||}Translational Psychiatry Program and ^{**}Center of Excellence on Mood Disorders at Department of Psychiatry and Behavioral Sciences, McGovern Medical School, University of Texas Health Science Center at Houston and ^{**}Neuroscience Graduate Program, University of Texas Graduate School of Biomedical Sciences at Houston, Houston, Texas 77030

Edited by Paul E. Fraser

Patients recovering from sepsis have higher rates of CNS morbidities associated with long-lasting impairment of cognitive functions, including neurodegenerative diseases. However, the molecular etiology of these sepsis-induced impairments is unclear. Here, we investigated the role of the receptor for advanced glycation end products (RAGE) in neuroinflammation, neurodegeneration-associated changes, and cognitive dysfunction arising after sepsis recovery. Adult Wistar rats underwent cecal ligation and perforation (CLP), and serum and brain (hippocampus and prefrontal cortex) samples were obtained at days 1, 15, and 30 after the CLP. We examined these samples for systemic and brain inflammation; amyloid- β peptide (A β) and Ser-202-phosphorylated Tau (p-Tau^{Ser-202}) levels; and RAGE, RAGE ligands, and RAGE intracellular signaling. Serum markers associated with the acute proinflammatory phase of sepsis (TNF α , IL-1 β , and IL-6) rapidly increased and then progressively decreased during the 30-day period post-CLP, concomitant with a progressive increase in RAGE ligands (S100B, Ne-[carboxymethyl]lysine, HSP70, and HMGB1). In the brain, levels of RAGE and Toll-like receptor 4, glial fibrillary acidic protein and neuronal nitric-oxide synthase, and A β and p-Tau^{Ser-202} also increased during that time. Of note, intracerebral injection of RAGE antibody into the hippocampus at days 15, 17, and 19 post-CLP reduced A β and p-Tau^{Ser-202} accumulation, Akt/mechanistic target of rapamycin signaling, levels of ionized calcium-binding adapter molecule 1 and glial fibrillary

acidic protein, and behavioral deficits associated with cognitive decline. These results indicate that brain RAGE is an essential factor in the pathogenesis of neurological disorders following acute systemic inflammation.

Sepsis is defined as a life-threatening organ dysfunction caused by dysregulated host responses to an infection (1). At admission, up to 71% of septic patients develop potentially irreversible acute cerebral dysfunction (2, 3), a condition caused by systemic inflammation without brain infection and clinically characterized by slowing of mental processes, impaired attention, disorientation, delirium, or coma (4). Recent studies have shown that long-lasting consequences following sepsis recovery often include brain disorders (5). Even after full recovery, animals subjected to sepsis induced by cecal ligation and perforation (CLP)² demonstrated significant difficulties in performing behavioral tasks, indicating cognitive deficits (6). In recovered patients, persistent deficits in functional abilities and general quality of life are observed (7), which may be associated with long-lasting impairment in cognitive capacities associated with memory and executive function (8).

This long-term impairment in brain function was suggested to result from neurodegenerative or ischemic mechanisms triggered by systemic inflammation (9). Peripherally produced cytokines can enter the central nervous system (CNS), as sepsis is able to induce transient disruption of the blood-brain barrier (BBB) (10, 11). This in turn leads to microglia/astrocyte activation and local production of pro-inflammatory mediators and

This work was supported by grants from Conselho Nacional de Desenvolvimento Científico e Tecnológico (to D. P. G., J. C. F. M., J. Q., and F. D.-P.), Fundação de Amparo à Pesquisa do Estado do Rio Grande do Sul (to D. P. G. and J. C. F. M.), Fundação de Amparo à Pesquisa e Inovação do Estado de Santa Catarina (to J. Q. and F. D.-P.), Propeq/UFRGS (to D. P. G. and J. C. F. M.), Fundação CAPES, Instituto Cérebro e Mente (to J. Q.) and UNESC (to T. B., J. Q., and F. D.-P.). The authors declare that they have no conflicts of interest with the contents of this article.

¹ To whom correspondence should be addressed: Dept. de Bioquímica, ICBS, UFRGS, Rua Ramiro Barcelos, 2600-anexo, CEP 90035-003, Porto Alegre, RS, Brazil. Tel.: 55-51-3308-5577, Fax: 55-51-3308-5535; E-mail: daniel.gelain@ufrgs.br.

² The abbreviations used are: CLP, cecal ligation and perforation; RAGE, receptor for advanced glycation end product; sRAGE, soluble form of RAGE; RAGEab, RAGE antibody; AGE, advanced glycation end product; A β , amyloid- β ; A β PP, amyloid precursor protein; BBB, blood-brain barrier; GFAP, glial fibrillary acidic protein; mTOR, mechanistic target of rapamycin; nNOS, neuronal nitric-oxide synthase; AD, Alzheimer's disease; ANOVA, analysis of variance; CML, Ne-(carboxymethyl)lysine; b.w., body weight; TBI, traumatic brain injury.

reactive species (12, 13). However, details of the molecular cascades linking systemic inflammation to neuroinflammation and brain dysfunction still need to be better understood. Comprehension of these mechanisms in detail may reveal valuable information that can be used as a basis to develop new strategies to treat sepsis co-morbidities. In addition, unveiling new details on the molecular events linking systemic inflammation to brain dysfunction may also uncover new insights to the understanding of the onset of neurodegeneration itself (14).

Neurodegenerative processes may evolve over the course of many years, and the diagnosis is generally performed only in advanced or late stages, when brain function is impaired due to significant neuronal loss. Neurodegeneration is characterized by progressive neuronal death associated with the accumulation of misfolded, aberrant forms of cellular proteins or peptides with neurotoxic activity. In Alzheimer's disease (AD), neuronal death occurs concomitant to progressive formation of neurofibrillary tangles and amyloid (senile) plaques. Neurofibrillary tangles are formed due to aberrant hyperphosphorylation of the microtubule-stabilizing protein Tau, whereas amyloid plaques originate by hydrophobic aggregates of misfolded amyloid- β peptide ($A\beta$). Hyperphosphorylation of Tau occurs in at least 22 other brain conditions, such as amyotrophic lateral sclerosis, Down's syndrome, and prion diseases (15), and because disruption of Tau homeostasis is associated with cognitive deficits (16), modulation of Tau phosphorylation by pathogenic processes may also be associated with the onset of neurodegenerative processes. Similarly, cleavage of the amyloid precursor protein (A β PP) by different secretases may generate small peptides, including a variety of $A\beta$ peptides (17). Necrotic and apoptotic neuronal death is induced by extracellular $A\beta$ both through activation of death receptors in neurons and induction of microglial pro-inflammatory activation and astrotosis (18). Pro-inflammatory activation, in turn, further induces $A\beta$ aggregation due to amino acid oxidation and peptide destabilization (19).

The receptor for advanced glycation end products (RAGE) is a multiligand pattern-recognition receptor, belonging to the immunoglobulin superfamily of proteins (20). Although it was first described to be activated by advanced glycation end products (AGEs), RAGE can interact with a number of different classes of agonists, including S100 family proteins (e.g. S100B), high-mobility group box protein 1 (HMGB1), 70-kDa heat-shock protein (HSP70), and N ϵ -(carboxymethyl)lysine (CML) (21), among others. RAGE is expressed only by lungs and endothelial cells in a constitutive fashion and is generally repressed in other tissues; however, an increase in the concentration of circulating RAGE ligands induces the expression of this receptor in most cell types (20). RAGE activation triggers different signaling cascades for immune responses, including the ERK1/2-dependent activation of NF- κ B and consequent transcriptional activation of pro-inflammatory genes (22), whereas RAGE inhibition was demonstrated to have a protective role against sepsis and LPS-induced endotoxemia (23–25). In the CNS, RAGE expression has been linked to neuroinflammation, $A\beta$ influx through the BBB, and neurodegeneration associated with AD, among other conditions (26, 27). It was previously demonstrated that HMGB1, a RAGE ligand, mediates cognitive

dysfunction in sepsis survivors (28) and that RAGE is increased in the brain of rats 30 days after sepsis induction by CLP (29, 30). Following the observation that $A\beta$ binds and activates RAGE (31), RAGE was identified as an important link in the intertwined signaling of inflammatory, amyloidogenic, and pro-apoptotic cascades during the progression of AD, as it maintains a chronic pro-inflammatory state via $A\beta$ -dependent stimulation of microglia (32). Nonetheless, a possible role of RAGE in other CNS disorders, including those associated with pro-inflammatory states, has been relatively neglected.

This study was performed to evaluate whether RAGE is associated with the changes in CNS homeostasis that arise after the recovery of the acute pro-inflammatory phase of sepsis. Therefore, the levels of pro-inflammatory markers, $A\beta$, phosphorylated Tau, and RAGE-associated molecules (including RAGE, several RAGE ligands, and intracellular downstream targets) were monitored in serum and brain from 24 h to 30 days after CLP surgery. The serum was evaluated for peripheral inflammatory markers and RAGE ligands, and the hippocampus and prefrontal cortex were evaluated because these structures are directly associated with cognitive dysfunctions observed in this rat model (6, 33). RAGE signaling was blocked by immune neutralization in the hippocampus between 15 and 19 days after CLP, and the cognitive function (inhibitory avoidance and object recognition tasks), neuroinflammatory (RAGE, Iba-1, and GFAP), and neurodegenerative markers ($A\beta$ and phosphorylated Tau) were evaluated 30–31 days after CLP. The results presented here indicate the following: (i) RAGE signaling increases as acute pro-inflammatory markers decrease over the 30 days following CLP, in serum, and CNS; and (ii) blocking of RAGE in the hippocampus inhibits neuroinflammatory and neurodegenerative markers in this brain region, as well as cognitive deficits that are observed 30 days after CLP. Overall these data suggest that RAGE signaling in the CNS exerts an important role in the progressive impairment of brain function that arises after the recovery from the acute phase of sepsis, and it may be involved in the long-term development of brain dysfunction and neurodegeneration triggered by episodes of acute systemic inflammation, including polymicrobial sepsis.

Results

Neuroinflammation and neurodegeneration markers increase after the acute phase of sepsis

Increased levels of IL-1 β , TNF- α , and IL-6 were observed in serum 24 h after sepsis induction (Fig. 1A). Fifteen days after CLP, IL-1 β and TNF- α were still increased, but no differences were detected between sham and CLP animals 30 days after surgery. These results confirmed that CLP induced an acute increase in systemic pro-inflammatory mediators and that the differences in cytokine levels between sham-operated and animals undergoing CLP decreased with time. As animals subjected to CLP often present with brain dysfunction after full recovery from inflammation, biochemical markers of neuroinflammation in hippocampus and prefrontal cortex were evaluated at early and late periods after sepsis induction. One day after CLP, IL-1 β , IL-6, and TNF- α levels were increased in the hippocampus (Fig. 1B) and the prefrontal cortex (Fig. 1C). Fif-

RAGE mediates neurodegeneration in sepsis

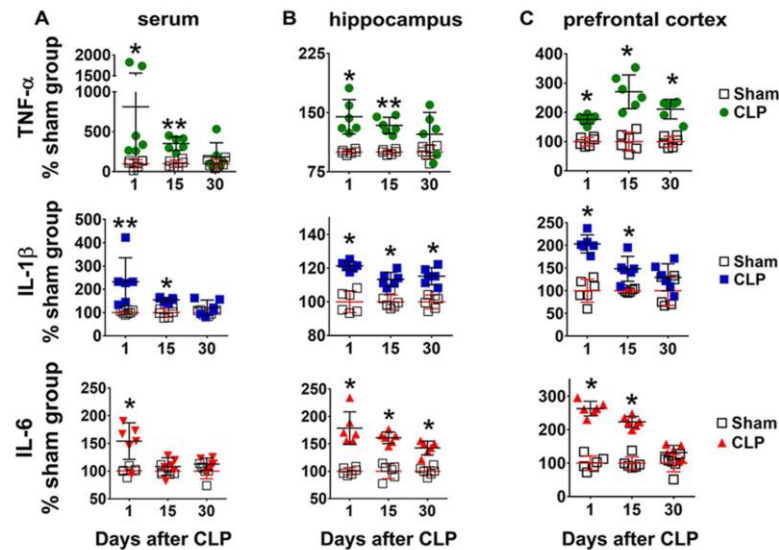


Figure 1. Content of pro-inflammatory cytokines in serum, hippocampus, and prefrontal cortex at 1, 15, and 30 days after CLP. The content of pro-inflammatory cytokines IL-1 β , IL-6, and TNF- α was assessed by ELISA in serum (A), hippocampus (B), and prefrontal cortex (C). Values represent relative quantification considering control (sham group) as 100%. Scattered individual data points ($n = 6$) and standard deviations are represented. Differences between sham and CLP groups on each day were considered significant when $p < 0.05$ according Student's t test (two-tailed) analysis (*, $p < 0.05$, and **, $p < 0.001$).

teen days after CLP, the levels of all cytokines were still increased, but 30 days after CLP, TNF- α had returned to control values in the hippocampus, whereas IL-1 β and IL-6 levels returned to values similar to sham-operated animals in the prefrontal cortex (Fig. 1, B and C). Toll-like receptor 4 (TLR4), a membrane receptor important in the modulation of pro-inflammatory responses, increased in both brain structures only at 30 days after CLP (Fig. 2, A and D). A similar profile was observed with the content of GFAP, a marker of astrocyte activation (Fig. 2, B and E). However, the neuronal nitric-oxide synthase (nNOS) content did not change in the hippocampus (Fig. 2C), although it increased in the prefrontal cortex 15 and 30 days after CLP (Fig. 2F).

Increased formation of A β from A β PP cleavage and aberrant phosphorylation of the microtubule-stabilizing protein Tau are key events leading to the formation of amyloid plaques and neurofibrillary tangles, respectively. In the hippocampus, increased A β immunodetection and enhanced Tau phosphorylation were observed only at 30 days after CLP (Fig. 3, A and B, respectively). In the prefrontal cortex, A β immunodetection increased 15 and 30 days after CLP (Fig. 3C), and Tau phosphorylation at Ser-202 transiently increased 15 days after CLP and then returned to basal levels at 30 days (Fig. 3D). Confirming this observation, immunofluorescence visualization of these markers 30 days after CLP showed increased immunostaining of A β and phospho-Tau in the hippocampus (Fig. 3E) and enhanced immunostaining of A β as well as remnant presence of phospho-Tau in the prefrontal cortex (Fig. 3F).

Circulating RAGE ligands and brain RAGE increase as animals recover from CLP

To evaluate a possible relationship between RAGE signaling and brain function impairment in sepsis, the content of several

biochemical markers associated with RAGE was assessed. The content of various RAGE ligands (CML, HMGB1, HSP70, and S100B) was determined in the serum (Fig. 4A). CML levels increased in all periods after CLP; HMGB1 increased 15 and 30 days after CLP, whereas HSP70 levels were increased only at 30 days. No differences in S100B levels were detected. Levels of the soluble form of RAGE (sRAGE) in the serum were analyzed, as RAGE shedding and release off the cell membrane is an important regulatory mechanism of signaling termination. No differences in serum sRAGE levels were detected at any period after CLP (Fig. 4A). The content of RAGE ligands and RAGE was also evaluated in the brain. In the hippocampus, CML levels were unaltered, whereas HMGB1 and HSP70 levels decreased 15 days after CLP (Fig. 4B). In the prefrontal cortex, CML levels were increased only 1 day after CLP (Fig. 4C); HMGB1 and HSP70 levels were decreased 15 days after CLP, but no differences were observed at other periods (Fig. 4C). The content of RAGE in both structures increased at 15 and 30 days after CLP (Fig. 4, B and C).

Hippocampal RAGE antibody injection inhibits neuroinflammation and neurodegeneration markers

The levels of circulating RAGE ligands and brain RAGE are more prominent after the acute phase of sepsis, when most pro-inflammatory markers are already decreased or declining to levels similar to sham-operated animals. In this context, the role of RAGE in changes observed in the brain 30 days after CLP was investigated by selective blocking of RAGE in the hippocampus with anti-RAGE antibody (RAGE ab , 100 μ g/kg). RAGE ab was administered via cannula consecutively at days 15, 17, and 19 after CLP. At 30 days after CLP, the endogenous content of RAGE in the hippocampus decreased in CLP-subjected animals receiving RAGE ab as visualized by immunoflu-

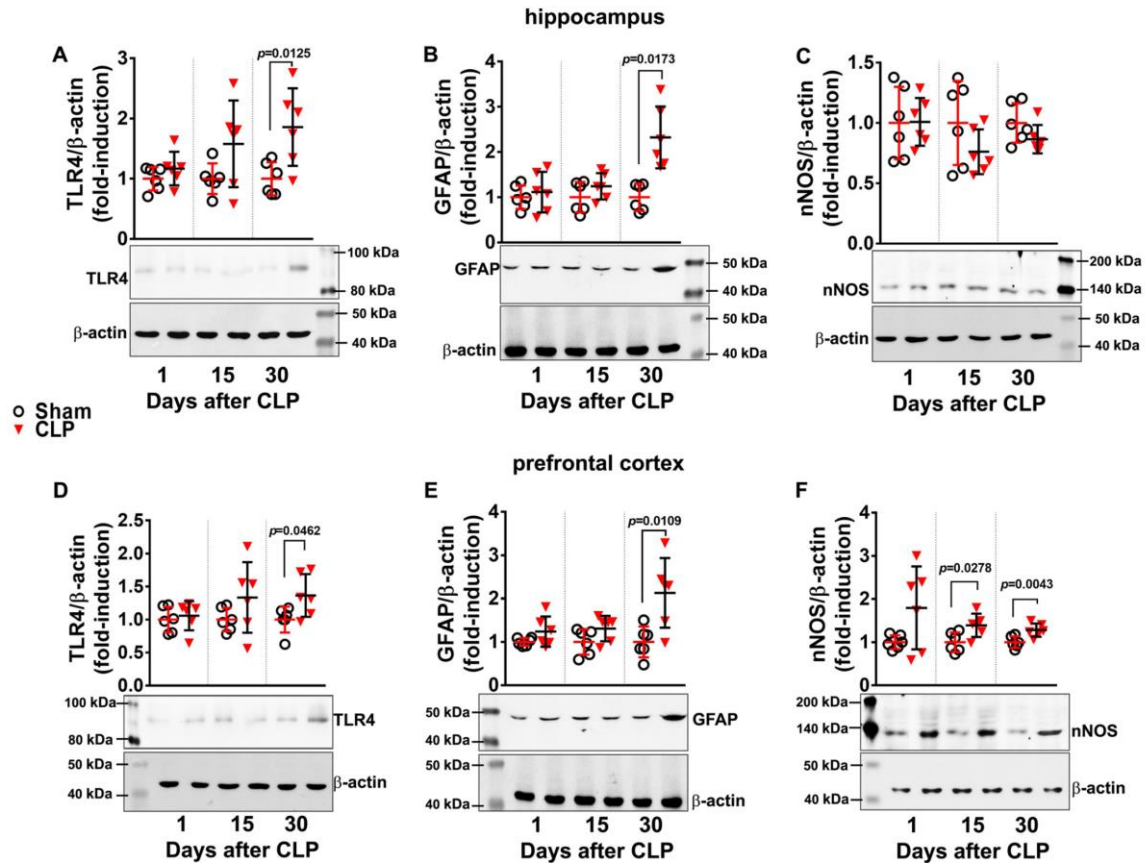


Figure 2. Content of pro-inflammatory markers in hippocampus and prefrontal cortex at 1, 15, and 30 days after CLP. TLR4, GFAP, and nNOS protein levels in hippocampus (A–C, respectively) and prefrontal cortex (D–F, respectively) were evaluated by Western blotting. Scattered individual data points ($n = 6$) and standard deviation are represented. Representative Western blots are demonstrated with graphs. Differences between sham and CLP groups in each day were considered significant when $p < 0.05$ according to Student's *t* test (two-tailed) analysis. Individual *p* values are depicted when differences were detected.

orescence microscopy (Fig. 5A). Besides, immunolocalization of Iba-1 (Fig. 5B) and GFAP (Fig. 5C) indicated that RAGE α b administration inhibited CLP-induced microglial and astrocyte activation, respectively. The increases in hippocampal A β immunostaining (Fig. 5D) and Tau phosphorylation (Fig. 5E) observed 30 days after CLP were also inhibited by RAGE α b administration to hippocampus. Quantification of fluorescence intensity of RAGE, Iba-1, GFAP, A β , and p-Tau immunostaining and statistical analysis confirmed these observations (Table 1).

Interestingly, hippocampal RAGE α b administration also had effects in the prefrontal cortex. Mean values and statistical analysis of fluorescence quantification in hippocampus are shown in Table 1. The increase in RAGE induced by CLP was inhibited in prefrontal cortex of animals treated with RAGE α b, as observed by fluorescent immunolocalization (Fig. 6A). The number of cells with positive staining for both Iba-1 (Fig. 6B) and GFAP (Fig. 6C) was also decreased by hippocampal RAGE inhibition, and a similar effect was observed with A β immunostaining (Fig. 6D). No significant effect was observed on Tau phosphorylation, as this parameter was not significantly altered

in the prefrontal cortex 30 days after CLP (Fig. 6E). To further confirm this observation, a double staining was performed with the neuronal marker NeuN. Hippocampal Tau phosphorylation is possible to observe at the subcellular level and at different magnifications along with NeuN-positive neurons. Distribution of p-Tau and NeuN staining within cells varies according to the irradiation pattern of neuritis/axons from the perinuclear area, which is the site of NeuN expression (Fig. 7A). In the prefrontal cortex, however, staining for phosphorylated Tau is not observed, although NeuN staining suggests a decrease in the number of neurons at both structures in the CLP group, which is rescued by RAGE α b (Fig. 7B and Table 1).

A β and phosphorylated Tau immunofluorescence was observed in isolated cells to identify morphological staining patterns that could be associated with extracellular deposition or intracellular accumulation. Staining of A β antibodies in isolated neurons of hippocampus and prefrontal cortex from CLP and CLP + RAGE α b groups resembles neuronal bodies and neurite projections (Fig. 8, A and B). Plaque-like structures were not observed. A similar examination was performed with

RAGE mediates neurodegeneration in sepsis

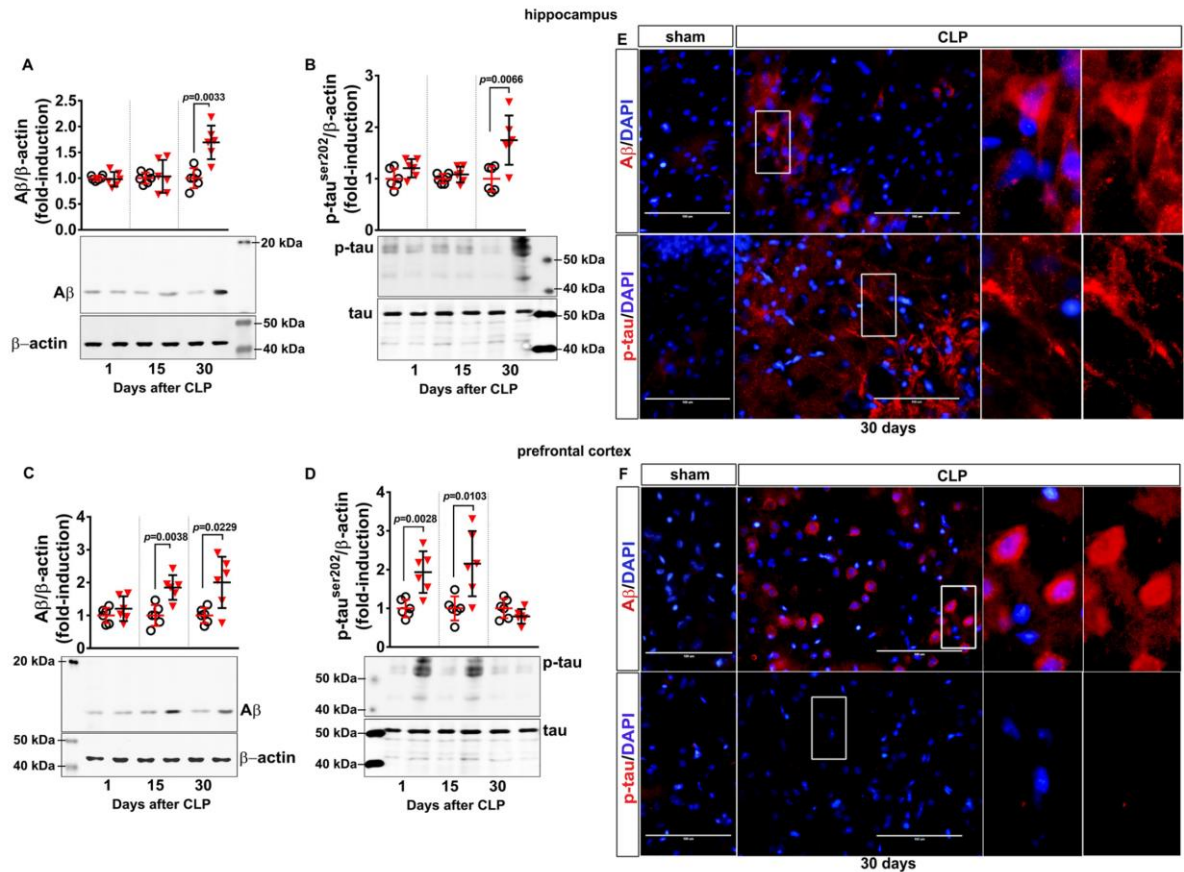


Figure 3. Content of $A\beta$ and phosphorylated Tau in hippocampus and prefrontal cortex of animals at 1, 15, and 30 days after CLP. The levels of $A\beta$ and Tau phosphorylated at Ser-202 ($p\text{-Tau}^{\text{Ser-202}}$) in hippocampus (A and B, respectively) and prefrontal cortex (C and D, respectively) were evaluated by Western blotting. Scattered individual data points ($n = 6$) and standard deviation are represented. Representative Western blots are demonstrated. Differences between sham and CLP groups in each day were considered significant when $p < 0.05$ according to Student's *t* test (two-tailed) analysis; individual *p* values are depicted. Immunofluorescence-based visualization of $A\beta$ and $p\text{-Tau}^{\text{Ser-202}}$ was performed in hippocampus (E) and prefrontal cortex (F) samples of animals 30 days after CLP. DAPI was used for nuclear staining. Magnification bar length is 100 μm . Insets show staining details.

phosphorylated Tau with double staining for NeuN. The morphological pattern displayed at a cellular level in hippocampus does not resemble extracellular deposition of structures such as neurofibrillary tangles, but they are suggestive of intracellular fibrillary constitution (Fig. 9A). Neurons of the prefrontal cortex, in contrast, do not present $p\text{-Tau}$ reactivity, as observed above (Fig. 9B).

Long-term effects of RAGE in brain involves modulation of Akt and mTOR

RAGE and TLR4 modulate inflammatory and neurodegenerative responses through activation of specific protein kinase cascades. The phosphorylation of ERK1/2 and Akt, which participate in different signal cascades evoked by RAGE and TLR4, was verified. In the hippocampus, ERK1/2 phosphorylation was increased 24 h and 15 days after CLP but returned to levels similar to sham animals 30 days after CLP (Fig. 10A). In the prefrontal cortex, ERK1/2 phosphorylation was increased 24 h after CLP but returned to basal levels at later periods (Fig. 10D).

In contrast, Akt had an opposite profile, presenting increased phosphorylation only 15 and 30 days after CLP in both structures (Fig. 10, B and E). Considering this profile of transient activation of ERK1/2 and late sustained activation of Akt, the phosphorylation state of Akt downstream target mTOR was analyzed. Phosphorylation of mTOR in the hippocampus was significantly decreased compared with sham animals at 30 days after CLP, with no alterations at earlier times (Fig. 10C). In the prefrontal cortex, mTOR phosphorylation was increased 1 day after CLP but displayed an opposite profile at 15 and 30 days following CLP, presenting decreased phosphorylation compared with sham animals (Fig. 10F). These results suggest that RAGE signaling is associated with Akt phosphorylation and mTOR dephosphorylation, as these effects occurred concomitantly after the acute inflammatory phase of sepsis.

To confirm this hypothesis, the effect of hippocampal RAGE inhibition over Akt and mTOR phosphorylation states 30 days after CLP in both structures was analyzed.

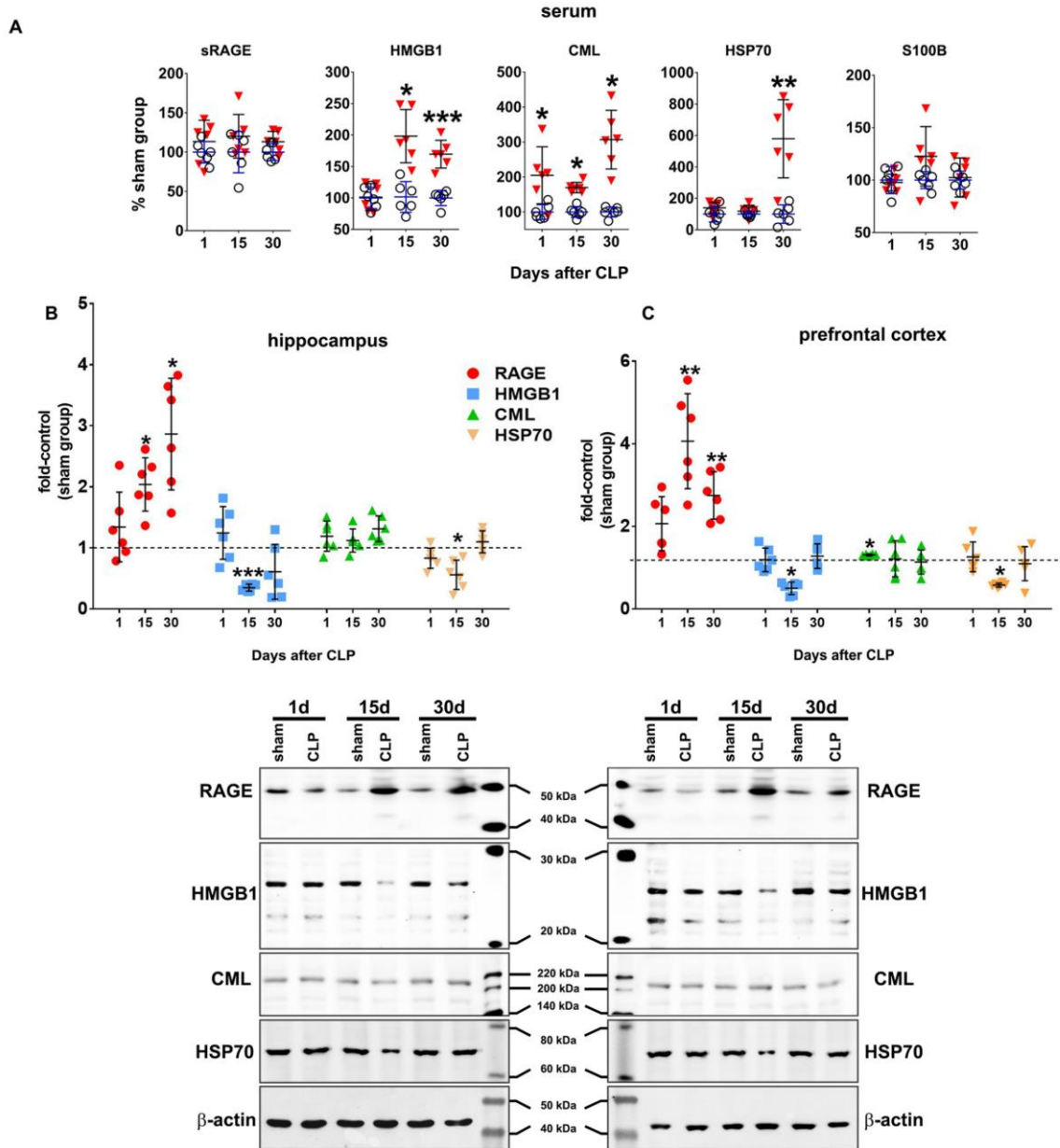


Figure 4. RAGE ligands, sRAGE, and RAGE in serum and brain. The circulating content of the RAGE ligands S100B, CML, HSP70, and HMGB1 and of the sRAGE isoform in serum was assessed by ELISA (A). Values represent relative quantification considering control (sham group) as 100%. The immunocent of CML, HMGB1, HSP70, and RAGE in hippocampus (B) and prefrontal cortex (C) was assessed by Western blotting. Representative Western blots are demonstrated. Scattered individual data points ($n = 6$) and standard deviation are represented for all data. Differences between sham and CLP groups were considered significant when $p < 0.05$ according to Student's t test (two-tailed) analysis (*, $p < 0.05$, and **, $p < 0.001$).

RAGE ab treatment to the hippocampus significantly inhibited the increase in Akt phosphorylation (Fig. 11A) and reversed the inhibition of mTOR phosphorylation (Fig. 11B) observed 30 days after CLP. Furthermore, quantification of RAGE levels in these same samples confirmed that RAGE ab injection to the hippocampus down-regulated RAGE protein levels in this structure (Fig. 11C), suggesting a link for

RAGE, Akt, and mTOR. The immunocent of A β and phosphorylated Tau was also assessed in these samples (Fig. 11, D and E, respectively). Hippocampal RAGE ab administration also affected RAGE signaling in the prefrontal cortex. Changes in prefrontal cortex Akt and mTOR observed in the CLP group were significantly reversed by RAGE ab injection into the hippocampus (Fig. 11, F and G, respectively). Simi-

RAGE mediates neurodegeneration in sepsis

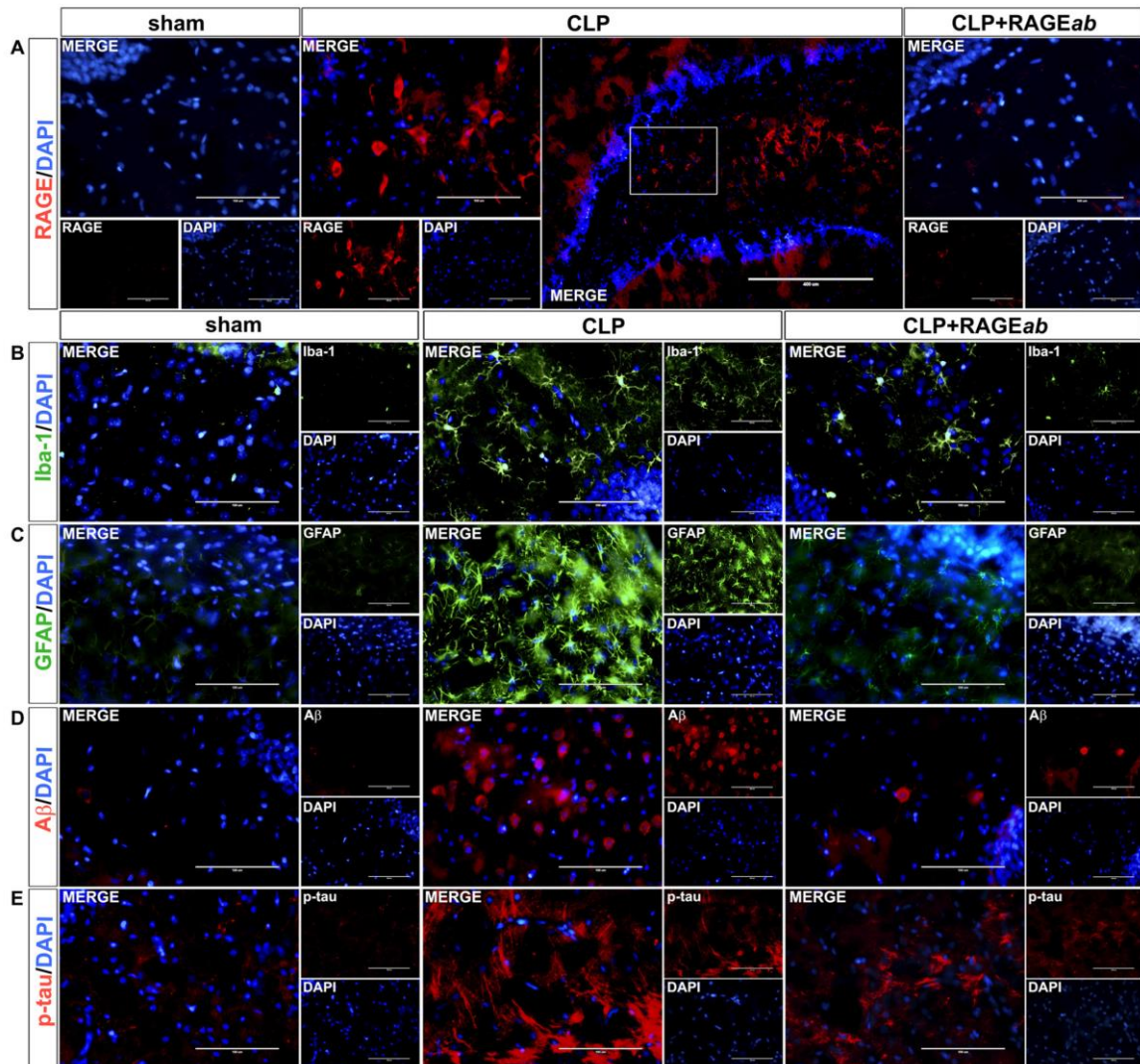


Figure 5. Effects of hippocampal RAGEab injection over RAGE and markers of neuroinflammation and neurodegeneration in hippocampus of animals submitted to CLP. RAGEab was administered bilaterally into the hippocampus at 100 $\mu\text{g}/\text{kg}$ at days 15, 17, and 19 after CLP. Control animals received 100 $\mu\text{g}/\text{kg}$ of isotype IgG. At day 30 after CLP, the hippocampus was prepared for immunofluorescence detection of RAGE (A), Iba-1 (B), GFAP (C), A β (D), and phospho-Tau (E). DAPI was used for nuclear staining. Magnification bar length is 400 μm in the bigger panel and 100 μm in all other panels.

Table 1

Values of fluorescence immunostaining intensity (fold-induction)

Mean \pm S.D. values of fluorescence intensity units from eight animals per group. ****, $p < 0.0001$, ***, $p < 0.001$, and **, $p < 0.01$ were compared with sham group. ####, $p < 0.0001$, ###, $p < 0.001$, and ##, $p < 0.01$ were compared with CLP group. One-way ANOVA was done with Tukey's post hoc test.

	Hippocampus			Prefrontal cortex		
	Sham	CLP	CLP + RAGEab	Sham	CLP	CLP + RAGEab
RAGE	1 \pm 0.44	28.5 \pm 5.29****	2.54 \pm 1.37####	1 \pm 1.02	35.39 \pm 11.7****	4.25 \pm 2.51####
Iba-1	1 \pm 0.51	28.2 \pm 2.02****	7.64 \pm 1.82####	1 \pm 0.97	4.97 \pm 2.39**	1.39 \pm 0.67##
GFAP	1 \pm 0.28	8.49 \pm 2.95****	1.58 \pm 0.14####	1 \pm 0.48	17.9 \pm 6.34****	2.15 \pm 0.68####
A β	1 \pm 0.30	53.08 \pm 10.91**	17.63 \pm 5.18####	1 \pm 0.98	28.17 \pm 13.83***	10.12 \pm 5.01##
p-Tau	1 \pm 0.14	6.08 \pm 1.45**	2.97 \pm 0.85####	1 \pm 0.57	0.99 \pm 0.64	0.65 \pm 0.38
NeuN	1 \pm 0.10	0.53 \pm 0.11****	1.01 \pm 0.15####	1 \pm 0.31	0.55 \pm 0.19**	1.18 \pm 0.20##

larly, levels of RAGE in these samples were significantly inhibited by RAGEab administration (Fig. 11H). Finally, the effect of hippocampal RAGEab injection on A β immunode-

tection (Fig. 11I) and phosphorylated Tau (Fig. 11J) levels also repeated the pattern seen in the prefrontal cortex immunolocalization.

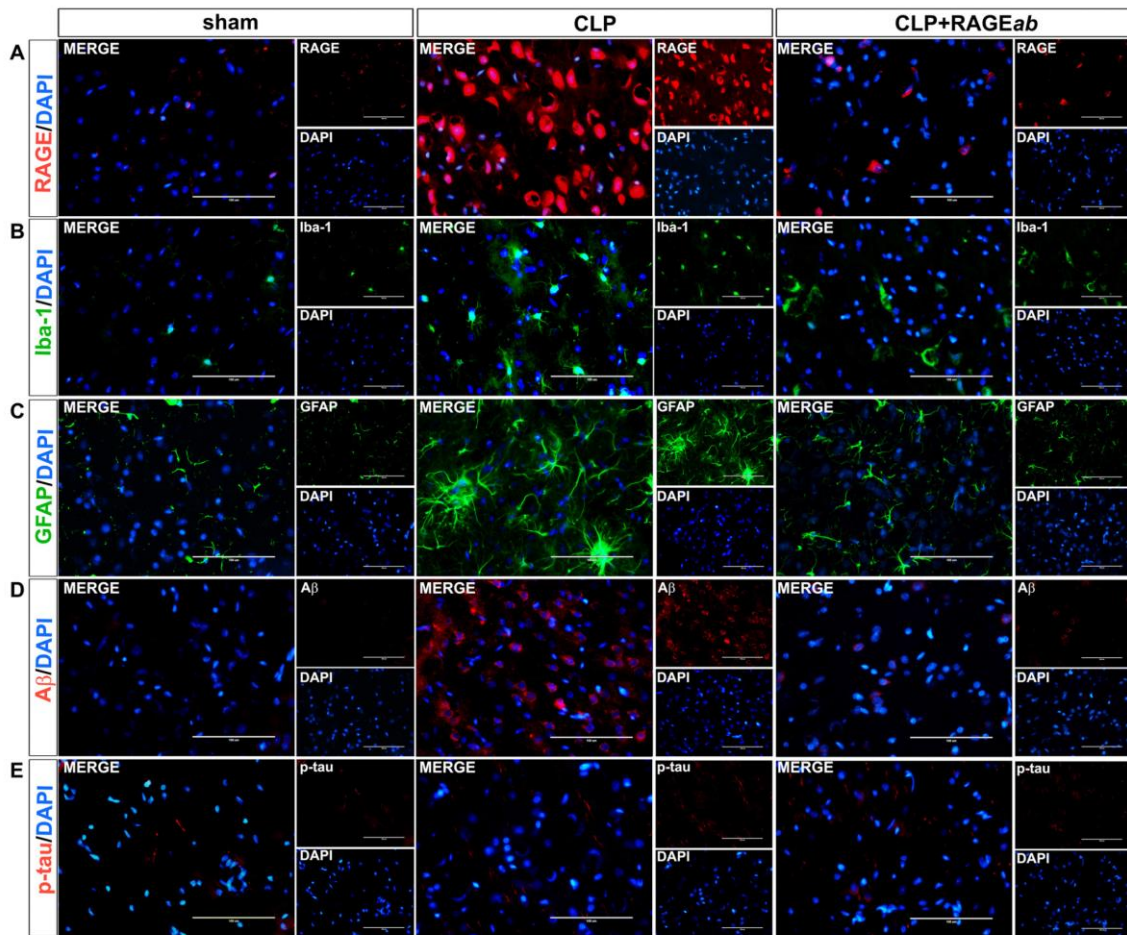


Figure 6. Effects of hippocampal RAGEab injection in prefrontal cortex RAGE and markers of neuroinflammation and neurodegeneration in animals submitted to CLP. RAGEab was administered bilaterally into the hippocampus at 100 $\mu\text{g}/\text{kg}$ at days 15, 17, and 19 after CLP. Control animals received 100 $\mu\text{g}/\text{kg}$ of isotype IgG. At day 30 after CLP, the prefrontal cortex was prepared for immunofluorescence detection of RAGE (A), Iba-1 (B), GFAP (C), A β (D), and phospho-Tau (E). DAPI was used for nuclear staining. Magnification bar length is 100 μm .

Hippocampal RAGEab injection restores impaired cognitive performance

Finally, the effect of hippocampal RAGE immune neutralization in cognitive performance was evaluated 30 days after CLP. Sepsis induces a significant impairment in memory retention tasks, and animals treated with RAGEab administration had performance similar to control animals (Fig. 12, A and B). These results, altogether, suggest that administration of RAGEab into hippocampus is able to restore some of the alterations in brain function that are observed after recovery from the acute phase of sepsis.

Discussion

In this study, animals surviving sepsis presented brain alterations commonly associated with the onset of neurodegenerative processes, and RAGE was demonstrated to play a key role in the progression of these changes. Sepsis enhances transcription of pro-inflammatory cytokines, including TNF- α , IL-1 β , and

IL-6 (4), which affect the arrangement of tight junctions in BBB endothelial cells (34–36). This increases BBB permeability, contributing to neuroinflammation and cell death (11). The present model of polymicrobial sepsis induced by CLP requires the use of antibiotics to maintain survival around 40%. However, the antibiotic therapy, as observed here and in previous works, does not prevent the progression of sepsis, although it significantly enhances survival (37, 38). The variation in pro-inflammatory cytokines at the systemic level presented a typical pattern here. Pro-inflammatory cytokines may accumulate in brain due to saturable influx transport, retrograde axonal transport systems, or simple diffusion in areas where BBB is impaired. A similar pattern was observed here, as brain pro-inflammatory markers increased, systemic cytokines decreased following acute inflammation recovery. All cytokines were elevated in the brain 24 h after CLP and decreased with time, except TNF- α in the prefrontal cortex (which peaked at 15 days and then decreased). In contrast, alterations in TLR4, GFAP,

RAGE mediates neurodegeneration in sepsis

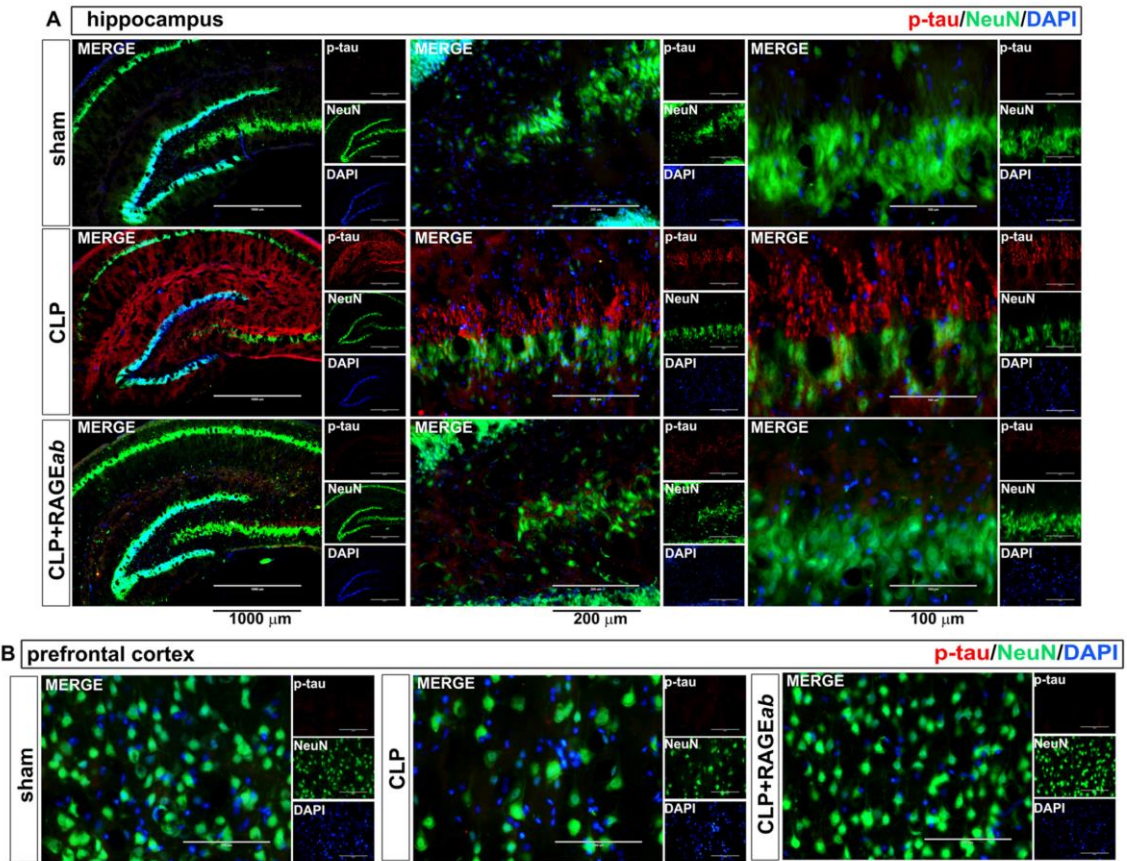


Figure 7. Effects of hippocampal RAGEab injection over phospho-Tau and NeuN staining in hippocampus and prefrontal cortex of animals submitted to CLP. RAGEab was administered bilaterally into the hippocampus at 100 $\mu\text{g}/\text{kg}$ at days 15, 17, and 19 after CLP. Control animals received 100 $\mu\text{g}/\text{kg}$ isotype IgG. At day 30 after CLP, the hippocampus (A) and the prefrontal cortex (B) were prepared for immunofluorescence detection of phospho-Tau (red) and the neuron nuclear marker NeuN (green). DAPI was used for nuclear staining. Magnification bar length in hippocampus: left panels, 1000 μm ; central panels, 200 μm ; and right panels, 100 μm . In prefrontal cortex panels, the magnification bar length is 100 μm .

and nNOS, which are markers associated with inflammatory activation in specific cells, were not observed earlier than 15 days after CLP. Indeed, TLR4 and GFAP levels were altered only 30 days after CLP. These data unveil a bimodal profile of inflammation in the CNS following sepsis, with a more prominent role of pro-inflammatory cytokines at earlier stages, probably resulting from transient BBB disruption during the acute phase of sepsis, followed by resident activation of local cells as BBB is restored and animals recover from acute inflammation. As mentioned above, BBB is disrupted during the acute phase of sepsis, but it restores its integrity and selective permeability as animals recover from acute inflammation (11, 39).

Previous work has demonstrated that CLP induces microglial activation, and this is associated with long-term cognitive dysfunction caused by sepsis (13). A similar profile was observed here for astrocytes, as GFAP levels increased late after CLP. Altogether, these observations suggest that the glia exert an important role in the chronic neuroinflammation and long-term impairments in brain function observed after sepsis recovery. In this context, the late increase in TLR4 levels (30 days after CLP) may be associated with late astrocyte/microglial

activation instead of polymicrobial-dependent up-regulation. TLR4 triggers production of cytokines, nitric oxide (NO), and reactive oxygen species in microglia and astrocytes (40). Abnormal Tau phosphorylation is associated with several neurodegenerative conditions, including AD and other tauopathies where formation of highly dense hydrophobic aggregates of misfolded proteins causes neuronal death (41). Tau presents at least 85 potential sites of phosphorylation, which are regulated by several different protein kinases and phosphatases. The specific phosphorylation of some of these sites has been associated with particular physiological processes, whereas the overstimulation of some sites has been suggested to be more critical for the induction of abnormal aggregation (42–44). Abnormal stimulation of Tau Ser-202 phosphorylation correlates with AD in adult humans and is associated with neurofibrillary tangle formation (43). The involvement of aberrant Tau phosphorylation in brain function impairment following sepsis is consistent with previous observations, including progressive decline in cognitive functions and oxidative damage to CNS (45, 46). RAGE expression in the adult CNS is more often associated with microglia and astrocytes, although it may be induced in

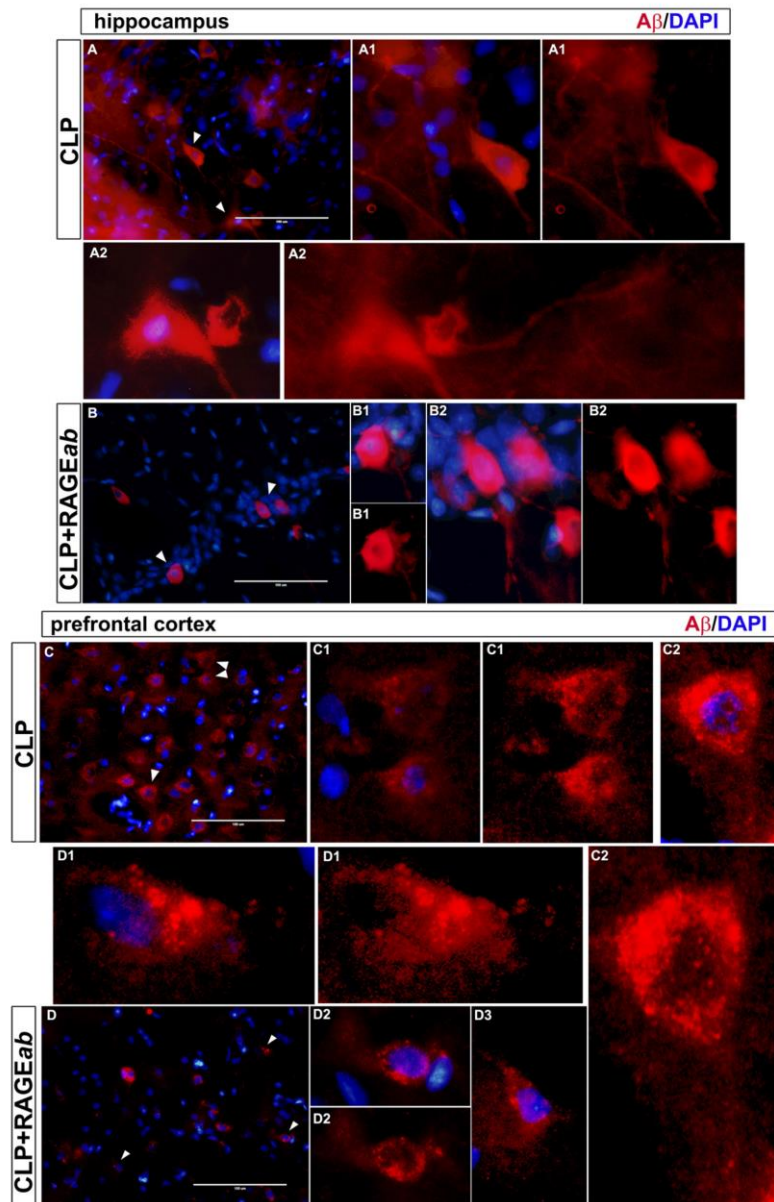


Figure 8. Morphological observation of A β immunofluorescence staining in hippocampus and prefrontal cortex 30 days after CLP. Sections of tissues from CLP and CLP + RAGEab groups are shown at *left panels* (magnification bar length is 100 μ m). *White arrows* indicate isolated cells detailed in augmented visualization. DAPI-merged and isolated A β stainings are compared. Morphology is indicative of intraneuronal localization of A β . *Letters and numbers in upper left* of images identify panels that originated the detailed images of isolated cells.

neurons as well. The mechanistic relationship between RAGE and Tau phosphorylation in the brain may involve RAGE up-regulation as a consequence of microglia and astrocyte activation, release of pro-inflammatory mediators to the extracellular milieu, and consequent activation of neurotoxic pathways in neurons, including GSK-3 β - and CDK5-regulated cascades that participate in Tau phosphorylation (47). This hypothesis is supported by our finding that in the hippocampus RAGE up-regulation precedes Tau phosphorylation at 15 days.

The immunostaining profile of phosphorylated Tau in the hippocampus is indicative of intracellular sublocalization, whereas no evident formation of tangles was detected. Extracellular accumulation of neurofibrillary tangles is characteristically observed in post-mortem analyses of AD brains, being normally associated with late stages of neurodegeneration. However, Tau abnormal phosphorylation, aggregation, and proteolysis constitute earlier steps in the formation of neurofibrillary tangles, being crucial events in the pathogenesis of AD and

RAGE mediates neurodegeneration in sepsis

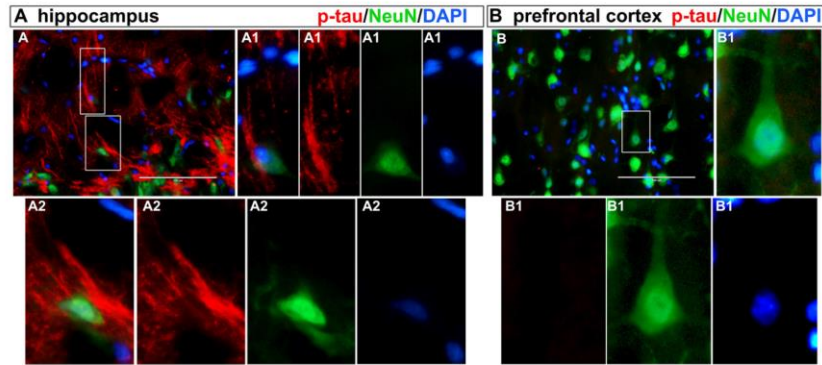


Figure 9. Morphological observation of phospho-Tau and NeuN immunofluorescence double staining in hippocampus and prefrontal cortex 30 days after CLP. Sections of tissues from CLP group are shown at upper left panels (magnification bar length is 100 μ m). Costaining with phospho-Tau (red) and the neuronal nuclear marker NeuN (green) are used to confirm neuronal localization of phospho-Tau. Details of highlighted areas are compared for each type of staining, including DAPI and merged images. Morphology is indicative of intraneuronal localization of filamentous phospho-Tau deposition in hippocampus. Prefrontal cortex did not show phospho-Tau staining, confirming Western blotting and immunofluorescence data for 30 days post-CLP animals. Letters and numbers in upper left of images identify panels that originated the detailed images of isolated cells.

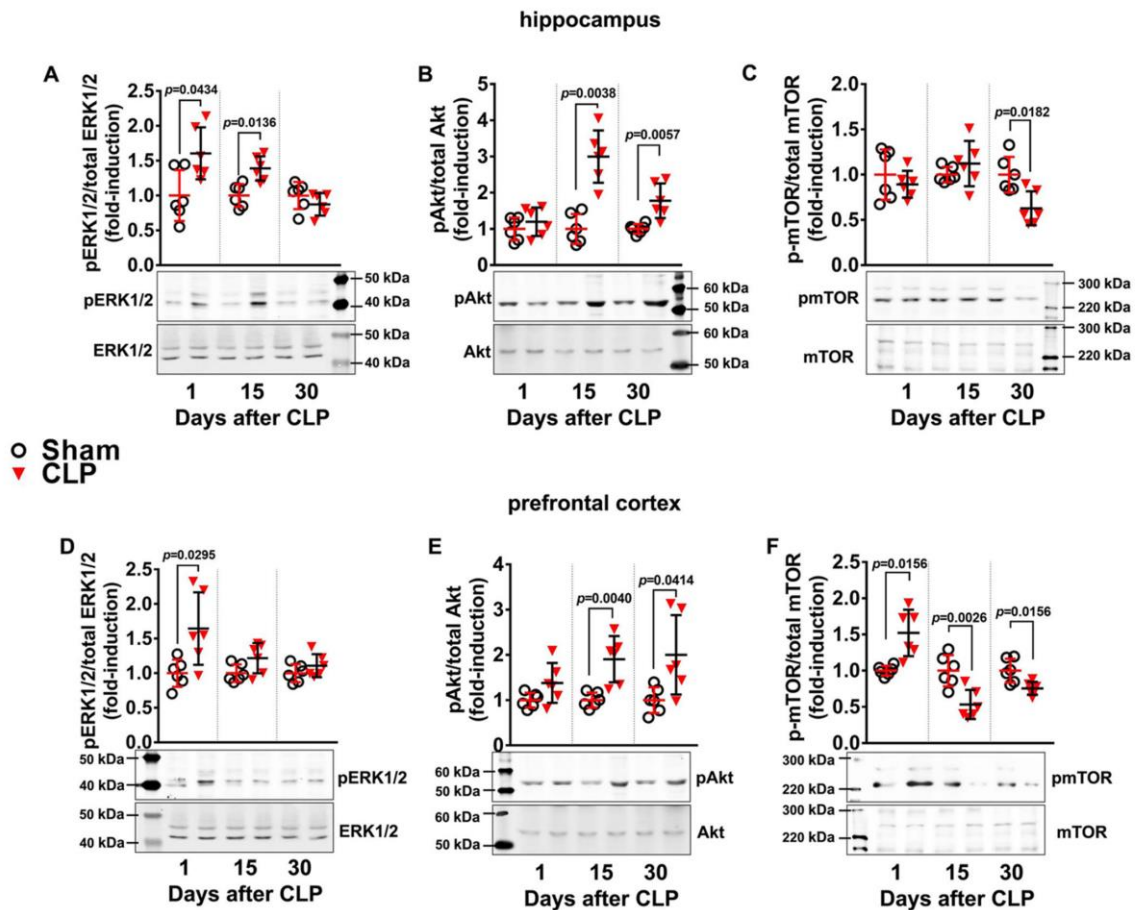


Figure 10. ERK1/2, Akt, and mTOR phosphorylation in hippocampus and prefrontal cortex of animals at 1, 15, and 30 days after CLP. The phosphorylated levels of hippocampal ERK1/2 (A), Akt (B), and mTOR (C), and the phosphorylated levels of prefrontal cortex ERK1/2 (D), Akt (E), and mTOR (F) relative to their total respective protein levels were assessed by Western blotting. Scattered individual data points ($n = 6$) and standard deviation are represented for all data. Representative Western blots are demonstrated. Differences between sham and CLP groups in each day were considered significant when $p < 0.05$ according student's t test (two-tailed) analysis; individual p values are depicted.

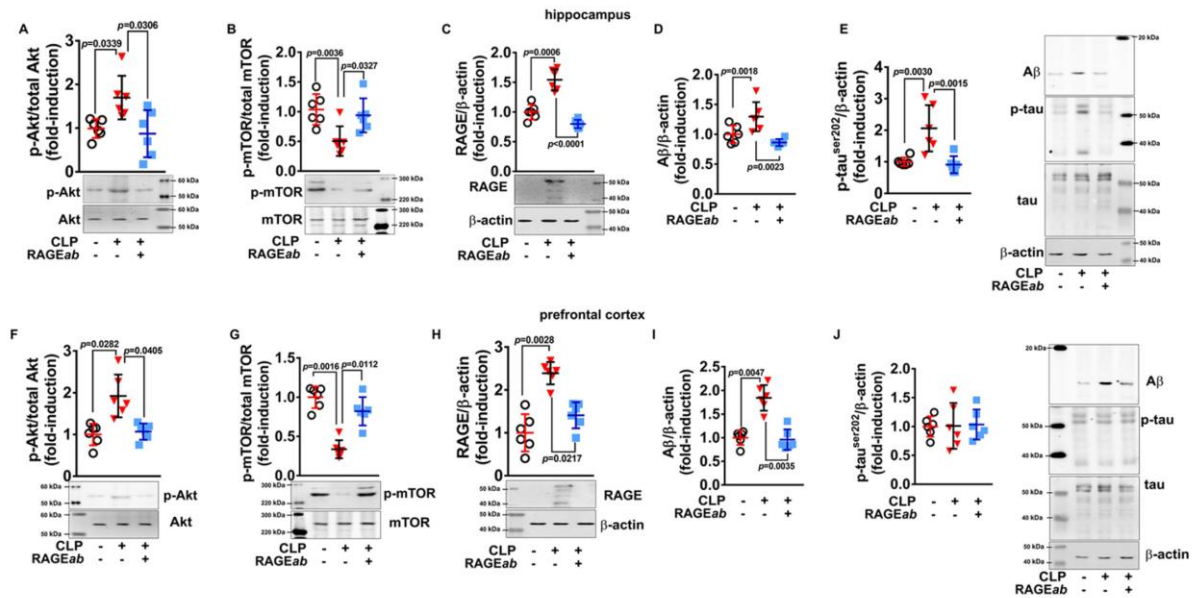


Figure 11. Akt and mTOR phosphorylation are associated with RAGE and markers of neurodegeneration in brain. RAGEab was administered bilaterally into the hippocampus at 100 μ g/kg at days 15, 17, and 19 after CLP. Hippocampus was isolated, and the levels of phosphorylated Akt (A) and mTOR (B), RAGE (C), A β (D), and phosphorylated Tau (E) 30 days after CLP were analyzed by Western blotting. Similarly, in isolated prefrontal cortex, phosphorylated Akt (F) and mTOR (G), RAGE (H), A β (I), and phosphorylated Tau (J) were assessed. Scattered individual data points ($n = 6$) and standard deviation are represented for all data. Representative Western blottings are demonstrated. Differences between groups were considered significant when $p < 0.05$ according to one-way ANOVA with Tukey's post hoc test; individual p values are depicted.

other sporadic tauopathies (48, 49). It is postulated that the process of Tau abnormal phosphorylation and aggregation in tauopathies follows a progression through three stages: pre-tangle formation, when soluble oligomers and small aggregates are observed as intracellular inclusions; intracellular neurofibrillary tangle stage, when it is possible to observe phosphorylated Tau in the form of intracellular filaments; and extraneuronal neurofibrillary tangles stage, when neurons that originated the processes are no longer viable (48). Our observations are suggestive that the first two stages are taking place in hippocampus. In prefrontal cortex, however, Tau phosphorylation had already returned to basal levels 30 days after CLP, although NeuN staining suggests a decreased number of neurons.

The progressive accumulation of A β is also consistent with this scenario. A β PP metabolism is normally accelerated in AD and related diseases and may lead to A β generation (50). However, the amyloid plaques observed in pathological analysis of AD brains are believed to take decades to form (51). Accumulation of A β in amyloid plaques is affected by transcriptional regulation of A β PP, modifications in expression and/or activity of secretases involved in A β PP cleavage, and oxidative damage resulting from glial activation (19). Interestingly, secretases responsible for A β PP cleavage also act in RAGE shedding (52, 53), indicating that RAGE and A β share important regulatory steps, and their homeostasis may be disrupted by common mechanisms. RAGE is also a major regulator of systemic A β translocation into CNS through BBB (54), and A β -RAGE interaction enhances Tau phosphorylation (27). Brain accumulation of A β following CLP recovery has been previously associated

with long-term cognitive impairment (30). Here, a progressive increase in A β immunodetection was observed with time after CLP and RAGE immune neutralization in hippocampus was able to inhibit this effect in both structures at 30 days, suggesting a link between RAGE and A β induction. This is in agreement with previous observations showing that RAGE inhibition prevented A β production, inflammation, oxidative stress, and cognitive deficits in an AD mouse model and in rats receiving intrahippocampal AGEs (31, 55).

Immunofluorescence images display a staining pattern not indicative of plaque-like structures but an intraneuronal location varying between cell bodies and neurites and, apparently, axons in some cells. Although deposition of A β in AD senile plaques is postulated to occur in the course of years, or perhaps decades, the formation, aggregation, and deposition of A β in traumatic brain injury (TBI) can be highly accelerated, taking place in a span of hours from an acute episode of trauma (56). The pattern of A β staining in hippocampus and prefrontal cortex observed here does not indicate an advanced stage of neurodegeneration commonly associated with the presence of amyloid plaques but intraneuronal accumulation of A β or, more likely, its full-length precursor protein, considering the morphological pattern of staining. Early intraneuronal accumulation of A β in neurons that are particularly vulnerable in AD were observed in AD brains, as well as Down's syndrome and numerous transgenic mouse models of AD (57). This "pre-plaque" accumulation takes place in intraneuronal endosomal vesicles, reportedly located in cell soma and, at higher extent, distal neurites and synapses (58, 59). Recently, the hypothesis that A β extracellular plaque deposits are the remnants of these

RAGE mediates neurodegeneration in sepsis

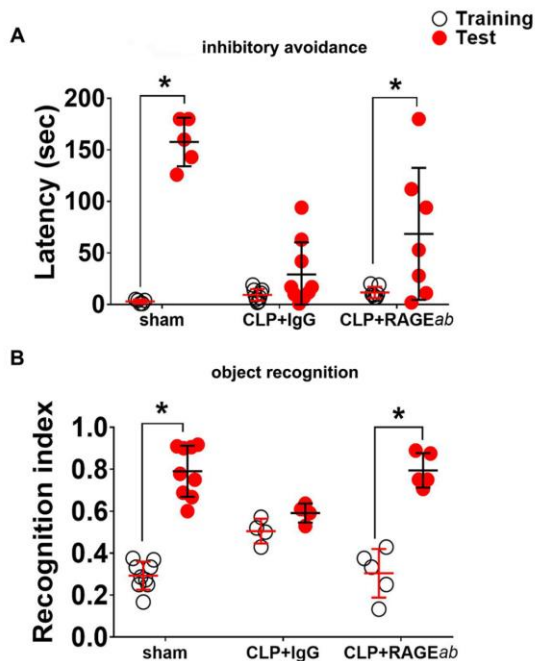


Figure 12. Effect of RAGEab injection into hippocampus over cognitive tests in animals subjected to CLP. RAGEab was administered bilaterally into the hippocampus at 100 $\mu\text{g}/\text{kg}$ at days 15, 17, and 19 after CLP. For inhibitory avoidance tasks (A), training sessions were performed at day 30 after surgery. Test sessions were carried out 24 h after training, and the step-down latency was used as a measure of retention. For object recognition task (B), training at day 30 after CLP was conducted by placing rats in the field with two identical objects (objects A1 and A2). Twenty four hours later, animals were allowed to explore the field in the presence of the familiar object A and a novel object C. A recognition index was calculated as the ratio $\text{TB}/(\text{TA} + \text{TB})$, with TA = time spent exploring the familiar object A; TB = time spent exploring the novel object B. Scattered individual data points with mean and standard deviation from animals from two different experiments are represented; comparisons among groups were performed using the Mann-Whitney *U* test. For behavioral analyses, individual groups were compared by the Wilcoxon tests. Animals that presented unusual locomotor activity or any other sign of altered behavior during training sessions were excluded from tests. Differences were considered significant when $p < 0.05$ (*).

degenerating neurites and synapses, as well as neuron cell soma (neurites and synapses also exist at neuron cell bodies), has been increasingly supported by detailed studies on subcellular localization of $A\beta$ formation, oligomerization, and subsequent deposition in the progression of neurodegeneration (57). Our results are in accordance with this hypothesis, as $A\beta$ staining in our model seems to follow a pattern of intracellular localization, not associated with plaques and not as extensive as would be expected following an acute TBI episode. Notwithstanding, in non-transgenic Wistar rats, intraneuronal $A\beta$ accumulation in response to neuroinflammation is not usually as high as observed here, especially considering the intensity of the effect and the age of the animals used in this study (3-month-old young adults). In this context, a possible cross-reactivity with full-length $A\beta\text{PP}$ in our immunofluorescence images should not be ruled out. This is a plausible hypothesis to explain why CLP induces this extent of $A\beta$ labeling in young animals at such short times after surgery. Importantly, this possibility does not invalidate the current interpretation of our observations, con-

sidering that $A\beta$ has originated from $A\beta\text{PP}$ cleavage and thus a marked increase in $A\beta\text{PP}$ could constitute an earlier step of this process. Although detailed molecular steps of these events remain to be elucidated, the occurrence of augmented $A\beta$ and Tau phosphorylation in the hippocampus and prefrontal cortex, together with previous evidence mentioned above, are highly suggestive of neurotoxic processes that potentially represent early molecular steps of neurodegenerative cascades in the course of activation. Besides, the observation that RAGE immunoneutralization inhibited $A\beta$ immunodetection and Tau phosphorylation represents valuable information concerning the sequence of events by which sepsis and systemic inflammation trigger long-term neurodegenerative processes.

Circulating RAGE ligands were increased in serum, and RAGE was up-regulated in brain structures. These data could indicate that the influx of peripheral RAGE ligands to the CNS is occurring, as sepsis-impaired BBB allows unspecific transport of pro-inflammatory mediators to the brain (10, 11, 60). Although the determination of RAGE ligands in total tissue does not reflect the extracellular content of these molecules in the CNS, they presented little or no variations, corroborating the hypothesis that RAGE in CNS is activated and up-regulated by peripherally-produced ligands and cytokines. As a consequence, intracellular effects triggered downstream RAGE activation that may take place in a similar time frame to RAGE protein up-regulation. Importantly, a correlation between Akt/mTOR and RAGE signaling is observed. Akt phosphorylation in brain is increased concomitantly with the increase in RAGE markers in serum and brain, and this relationship was further reinforced by the observation that RAGEab inhibited Akt phosphorylation. ERK1/2 and Akt are important components in neurodegenerative and inflammatory pathways and cross-talk to counteract, enhance, or suppress signaling by each other (61). In neurodegenerative diseases (especially AD), neuronal ERK1/2 activation is generally associated with GSK3- β cascade regulating Tau phosphorylation, but in glia these kinases are associated with inflammation (26, 62). A ubiquitous consequence of RAGE binding is NF- κB activation through ERK1/2, which in turn activates inflammatory cytokines and RAGE transcription. Alternatively, Akt activation is associated with survival responses, including inhibition of pro-inflammatory activation and autophagic clearance of protein aggregates (63, 64). Nonetheless, both exhibit differential states of basal activity and response to stimuli in different brain areas. Recently, it was observed that ERK1/2- and Akt-mediated pathways share little common regulation in different brain structures of $A\beta\text{PP}/\text{PS1}$ transgenic mice, despite simultaneous dysfunctional processes (65). ERK1/2 phosphorylation was increased in earlier periods and returned to basal levels later; in contrast, Akt phosphorylation exhibited a pattern of progressive increase. These data point to a shift from ERK1/2-mediated pathways, in earlier periods, to Akt signaling in later periods. Also, these results are in accordance with the decrease in acute pro-inflammatory markers observed during CLP recovery. Thus, a scenario where pro-inflammatory cytokines increase in the CNS causing ERK1/2 phosphorylation during the acute phase of sepsis followed by a second phase where RAGE up-regulation evokes Akt-dependent responses as pro-inflammatory cytokines

decrease is consistent with our data. In neurodegenerative conditions, mTOR is generally associated with control of autophagy and apoptosis in response to protein misfolding and aggregation. Akt and ERK1/2 affect mTOR by modulating the activation of the mTOR-inhibitory TSC1–TSC2 complex (66). Akt also controls mTOR by phosphorylation (67, 68). Here, mTOR phosphorylation decreased concomitant to stimulation of Akt. It is possible that the late effect of CLP on mTOR phosphorylation in brain is related to inhibitory feedback mechanisms of RAGE involving Akt late phosphorylation. The observation that RAGE ab reversed the effects of CLP on mTOR and Akt phosphorylation states after 30 days is consistent with this interpretation. Besides, it is also important to note that HSP70 levels in both structures were decreased 15 days after CLP. HSP70 is a molecular chaperone important for the control of autophagy as its function is directly related to protein misfolding and turnover. Decreased levels of HSP70 could be related to a deficit in autophagic processing, and this, in turn, could contribute to enhance the accumulation of damaged or misfolded proteins.

The time course of events observed here indicates a trend pattern. The decrease in acute systemic inflammation characteristic of sepsis occurs with progressive increase in RAGE-associated markers in serum and brain over time, suggesting a shift from acute inflammation toward chronic neuroinflammation. In different chronic diseases related to organ function degeneration, RAGE expression is elevated and associated with the support of a chronic inflammatory state (20, 69). The results presented here suggest that RAGE signaling increases as the acute pro-inflammatory signaling decreases as animals recover from sepsis. The spatial and temporal differences in the expression of markers associated with acute inflammation, RAGE, and neurodegenerative signaling may be related to the systemic origin of inflammation, which may affect CNS structures at different extents depending on their localization, contact area with blood vessels, and relative constitution of different cell types. However, LPS-induced systemic inflammation was reported to cause loss of neurons in both hippocampus and prefrontal cortex, with substantial loss of cholinergic innervations, resembling a neurodegenerative process; and different types of cognitive deficits were observed in this model (70). Previous works demonstrated several different cognitive deficits in sepsis survivors, and these deficits were associated with the prefrontal cortex and hippocampus inflammation (6, 13, 71). Here, it was demonstrated that blocking RAGE signaling in the hippocampus inhibited long-term cognitive dysfunction. All these data taken together suggest that systemic inflammation induces long-term hippocampal and prefrontal alterations that are somehow similar to a neurodegenerative process. These molecular and structural alterations are linked to a phenotype of cognitive dysfunction that is dependent on hippocampus and prefrontal connections.

Antagonism of RAGE signaling using RAGE antibodies or sequestering RAGE ligands with sRAGE have been previously undertaken in models of inflammation and sepsis. The use of monoclonal, polyclonal, or Fab fragments has been extensively applied as a pharmacological inhibitor was available only very recently. RAGE inhibition by these approaches has a significant

impact on sepsis, mainly through attenuation of pro-inflammatory signaling (24). Utilization of Fab fragments or monoclonal antibodies instead of polyclonal antibodies used here could represent a practical advantage as they would not bind to other scavenger receptors sharing similar epitopes. A necessary step for development of a clinical protocol based on immune neutralization of RAGE, in this context, is the rational design of a selective RAGE antibody for human utilization in a clinical trial. Besides, the delivery of an anti-RAGE molecule to specific brain regions should be considered another essential step, which could demand a surgical approach. A clinical trial with a synthetic RAGE inhibitor, PF-04494700 (Azelaion or TTP488), indicated no consistent effect on plasma levels of A β , inflammatory biomarkers, or secondary cognitive outcomes in phase II (72). However, a follow-up examination, conducted after treatment was suspended, suggested a possible clinical benefit for a low dose, but as these data became evident only long after discontinuation of the treatment based on preliminary results, they remain inconclusive (73). Currently, a phase III clinical trial is ongoing for efficacy and safety in mild AD (NCT02080364). Nonetheless, in an experimental context, blocking of RAGE with polyclonal antibodies has been successfully demonstrated in different rodent models of systemic inflammation, and effects caused by unspecific binding have not been observed (74–76). Systemic blocking of RAGE previous to sepsis attenuated the effects of endotoxemic shock (23, 25, 77). Here, RAGE ab was used to evaluate the role of RAGE in brain dysfunction occurring 30 days after CLP. Importantly, the hippocampal administration of RAGE ab was performed from 15 to 19 days after CLP, to establish the importance of CLP-induced up-regulation of RAGE in changes emerging after the acute pro-inflammatory phase of sepsis. Blocking RAGE prior to CLP, or using constitutive RAGE knock-out models, would result in an overall inhibition of systemic inflammation, as demonstrated previously (77), whereas the main goal of the current approach was to identify a molecular link connecting systemic inflammation and brain dysfunction that may be involved in long-term brain impairment caused by sepsis. This allowed identifying RAGE as an important molecular component in the course of CNS signaling events often associated with the onset and progression of neurodegeneration, such as A β accumulation, Tau phosphorylation, astrocyte/microglia activation, and modulation of Akt and mTOR. Also, the participation of RAGE in cognitive impairment as animals recover from an episode of sepsis could also be identified.

In conclusion, the results presented here demonstrate a prominent role of RAGE in the development of biochemical and behavioral changes commonly associated with the onset of neurodegenerative processes. Although the limitations of the current model do not allow an extrapolation of a more important role for RAGE in the evolution of characteristic neurodegenerative conditions (such as AD and other tauopathies, for instance), this study provided valuable insight to the understanding of mechanistic links that could associate episodes of acute systemic inflammation to the activation of neurodegenerative-associated signaling in the CNS in later periods of life. Besides, the development of a clinical protocol for RAGE immune neutralization in a specific brain region could be

RAGE mediates neurodegeneration in sepsis

designed to be applied in early steps of neurodegenerative diseases, such as AD, in future clinical studies. The results presented here indicate that inhibition of RAGE in the hippocampus and prefrontal cortex by injection of RAGE α B in hippocampus is able to counteract the degenerative process triggered by sepsis. Clinical strategies that treat the cause of neuronal death in neurodegenerative diseases are currently scarce, as most therapeutic approaches focus on alleviating or retarding the symptoms of neurodegeneration.

Experimental procedures

Chemicals

Electrophoresis and immunoblot reagents were from Bio-Rad, Thermo Fisher Scientific Pierce Protein Biology Products, and GE Healthcare Brazilian Headquarter (São Paulo, Brazil). Polyclonal and monoclonal antibodies from Abcam (Cambridge, UK) were as follows: TNF- α (ab6671); IL-1 β (ab9722); IL-6 (ab9324); CML (ab27684); nitrotyrosine (ab7048); RAGE (ab37647); and TLR4 (ab22048). Antibodies against S100B (catalog no. 9550), HSP70 (catalog no. 4872), HMGB1 (catalog no. 3935), GFAP (catalog no. 3670), p-Tau (Ser-202) (catalog no. 11834), Tau (catalog no. 4019), A β (catalog no. 2454), p-ERK-44/42 (Thr-202/Tyr-204) (catalog no. 9101), ERK-44/42 (catalog no. 9102), RAGE (catalog no. 4679), p-Akt (Ser-308) (catalog no. 13038), Akt (catalog no. 9272), p-mTOR (catalog no. 2971), and mTOR (catalog no. 4517) were from Cell Signaling Technology. Polyclonal antibody against nNOS (AB5380) and NeuN (MAB377) was from Merck Millipore. β -Actin (A1978) monoclonal antibody was from Sigma. Anti-Iba-1 (catalog no. 019-19741) was from Wako Chemicals. Antibody concentrations were used as indicated by the manufacturers. Biotinylated ladder protein marker was from Cell Signaling Technology. Anti-rabbit IgG peroxidase-conjugated (catalog no. AP132P) and anti-mouse IgG peroxidase-conjugated (catalog no. AP124P) were from Merck Millipore. Immunoblot chemiluminescence detection was carried out with the West Pico detection kit from Thermo Fisher Scientific Pierce Protein Biology Products (Rockford, IL). MilliQ-purified H₂O was used for preparing solutions. For RAGE immune neutralization, anti-RAGE rat IgG (SC5563) from Santa Cruz Biotechnology, Inc. (Dallas, TX), was used. All other reagents used in this study were of analytical or HPLC grade.

CLP

Adult (60-day-old) male Wistar rats were used in this study. Animals were subjected to CLP or sham-surgery as described previously (78). In brief, rats were anesthetized with a mixture of ketamine (80 mg/kg) and xylazine (10 mg/kg) given intraperitoneally. A 3-cm midline laparotomy was performed to expose the cecum with adjoining intestine, under aseptic conditions. The cecum was tightly ligated with a 3.0 silk suture at its base, below the ileocecal valve, and perforated with a 14-gauge needle. The cecum was then gently squeezed to extrude a small amount of feces from the perforation site. The cecum was then returned to the peritoneal cavity, and the laparotomy was closed with 4.0 silk sutures. A sham operation (laparotomy and cecal exposure without further manipulation) was performed as control. After surgery, animals were resuscitated with nor-

mal saline (50 ml/kg b.w. subcutaneously as bolus injection) and received 30 mg/kg ceftriaxone and 25 mg/kg clindamycin in saline (50 ml/kg b.w.) subcutaneously every 6 h for a total of 3 days. Sodium dipyrone was used as analgesic due to its high gastric tolerability and to avoid opioid analgesics that could have any possible influence in behavior tests. Besides, there are no reported effects of sodium dipyrone over sepsis aggravation to date. Administration of 80 mg/kg was performed at the end of surgery, and 0.5% flavored dipyrone suspension was provided in the water for 3 days after surgery. All these drugs were equally administered to sham and CLP animals. It is relevant to cite that even flavored dipyrone could alter water taste, although evident changes in water consumption were not observed. To minimize variability between different experiments, the CLP procedure was always performed by the same investigator. For each experiment, every group had an initial number of 22 animals, with a survival rate of 100% in the sham group and around 40% in the sepsis group, which was in accordance with our previous observations (30, 79). A minimum of six animals per group (sham *versus* CLP) on each day (1, 15, or 30 days after surgery) was used for individual biochemical and behavioral analyses. For behavioral analyses, animals that were unable to complete tasks within a maximum time were excluded. To collect samples for biochemical analyses, animals were euthanized by decapitation, and samples (tissues and blood) were collected immediately. The whole blood was collected in a centrifuge tube, and the serum was immediately separated by centrifugation while the brain was dissected. Brain was dissected in a Petri's dish containing isotonic PBS placed on ice. After surgical isolation of the hippocampus and prefrontal cortex, these samples were immediately homogenized in ice-cold RIPA buffer containing a complete protease and phosphatase inhibitor mixture (CST catalog no. 5872). For histology preparation, the procedure is provided below. All experimental procedures were performed in accordance with the National Institutes of Health, Guide for the Care and Use of Laboratory Animals (NRC80), and the Brazilian Society for Neuroscience and Behavior recommendations for animal care (80). The experimental protocols were approved by Committee of Ethics for the Use of Animals under protocol number 068/2014-2 (Universidade do Extremo Sul Catarinense) and the Universidade Federal do Rio Grande do Sul Committee of Ethics for the Use of Animals under protocol number 22629.

RAGE immune neutralization

Rats were bilaterally implanted with guide cannulas under anesthesia with isoflurane (1.0–2.0% delivered in O₂). Fourteen days after CLP, the rat was anesthetized with 2.0% isoflurane and placed in a Kopf stereotaxic frame and a stainless steel guide cannula (27 gauge, 9-mm length) aimed 1 mm above the hippocampus coordinates: anteroposterior, 2.2 mm, lateral \pm 2.0 mm, and ventral -3.7 (81) was inserted. Isoflurane (1.0–2.0%) was delivered during the entire procedure. Anchoring screws and dental acrylic secured the guide cannula to the skull. The skin was approximated around the implant and sutured in place. The solutions were infused through an injection needle of 10 mm length, thus extending 1 mm beyond the length of guide cannula. The needle had a flat extremity and was con-

nected to a 10- μ l Hamilton syringe, and infusions were carried out over 30 s, first on one side and then on the other. In each case the infusion cannula was left in place for 15 s after the infusion had been completed. Rat polyclonal RAGE α was administered bilaterally into the hippocampus at 100 μ g/kg saline at days 15, 17, and 19 after CLP. Control animals received 100 μ g/kg of isotopic IgG.

Behavior tests

Animals were subjected to inhibitory avoidance tasks 30 days after CLP. The behavioral procedures were conducted between 13:00 and 16:00 h in a sound-isolated room. All behavioral tests were performed by the same person who was blind to the animal group. The inhibitory avoidance procedure was described in a previous report (82). Training sessions were performed 30 days after surgery. Immediately after stepping down on the grid, animals received a foot shock of 0.3 mA for 2 s. In test sessions carried out 24 h after training, no foot shock was given, and the step-down latency (maximum of 180 s) was used as a measure of retention. Animals that failed to step down on the grid or presented any signs of unusual locomotor activity were excluded. During object recognition habituation, session animals were allowed to explore an open field. Training was conducted by placing rats in the field, in which two identical objects (objects A1 and A2; both being cubes) were positioned. Twenty four hours after training, animals were allowed to explore the field in the presence of the familiar object A and a novel object B (a sphere with a square-shaped base). A recognition index was calculated and was reported as the ratio TB/(TA + TB) (TA = time spent exploring the familiar object A; TB = time spent exploring the novel object B). Animals that presented unusual locomotor activity during training session were excluded.

ELISA measurements

To determine TNF- α , IL1- β , IL-6, and CML concentrations in serum and TNF- α , IL-1 β , IL-6, S100B, CML, HSP70, and HMGB1 in tissues, we used an indirect enzyme-linked immunosorbent assay (ELISA) procedure. Samples were normalized according to protein content (83) and added to ELISA microplates. The antigen was incubated for 24 h at room temperature. The immunoreactivity (1:1) was detected using a spectrophotometric detection kit from BD Biosciences. The reaction was stopped with sulfuric acid (2 M), and samples were read at 450 nm. Purified proteins were used for standard curve calculation.

Western blotting

To perform immunoblot experiments, the tissue was homogenized with 1 \times RIPA buffer, centrifuged 14,000 \times g for 10 min at 4 $^{\circ}$ C, and supernatant proteins were measured by the Bradford method (83). Laemmli sample buffer was added to complete volume according to the protein content of each sample, and equal amounts of cell protein (30 μ g/well) were fractionated by SDS-PAGE and electroblotted onto nitrocellulose membranes with Trans-Blot[®] SD Semi-Dry Electrophoretic Transfer Cell, Bio-Rad. Membranes were incubated for 20 min at room temperature in SNAP i.d.[®] 2.0 Protein Detection System, Merck Millipore, with each primary antibody. Anti-rabbit

or -mouse IgG peroxidase-linked secondary antibody was incubated with membranes for an additional 20 min in SNAP (1:2000 dilution range), and the immunoreactivity was detected by enhanced chemiluminescence using Supersignal West Pico Chemiluminescent kit from Thermo Fisher Scientific. Molecular weight was accessed with a biotinylated protein ladder (5 μ l per well). Densitometric analysis of the images was performed with ImageJ software (ImageJ version 1.49, National Institutes of Health). Blots were developed to be linear in the range used for densitometry.

Perfusion fixation of tissue for histology

Animals (eight per group) were anesthetized with thiopental and lidocaine (120 and 10 mg/kg i.p.). Once the animal was unresponsive to toe pinch-response (anesthesia validation test), it was placed on the operating table with its back down. A scalpel was used to make an incision through the abdomen at the length of the diaphragm, followed by a cut of the rib cage up to the collarbone on both sides of the ribs providing a clear view of the heart. A small incision was made in the posterior end of the left ventricle and an olive-tipped perfusion needle was inserted through the ventricle to extend straight up about 5 mm. An incision to the rat right atrium was made to create an outlet for free flow of the solution. A hemostat was used to stabilize the needle and to clamp the descendent aorta to optimize perfusion in the CNS. Eight animals per group were perfused with 0.9% sterile saline during 10 min (flow rate 20 ml/min) followed by 10 min with paraformaldehyde solution 4% in PBS (pH 7.4) (flow rate 20 ml/min). The brains were then carefully extracted and maintained in 4% paraformaldehyde for 24 h at 4 $^{\circ}$ C, then placed in sucrose 15% for 24 h at 4 $^{\circ}$ C, and placed in sucrose 30% for 24 h at 4 $^{\circ}$ C. Brains were slightly dried and frozen in -20 $^{\circ}$ C. After 24 h the prefrontal cortex and the hippocampus were sectioned in slices of 15 μ m on the coronal plane using a cryostat at -20 $^{\circ}$ C (Jung Histoslide 2000R; Leica; Heidelberg, Germany). A total of 20–30 slices per rat containing the structures was collected in PBS containing 0.1% Triton X-100 (PBS-0.1%). The free-floating sections were incubated with 5% albumin during 2 h to block non-specific binding sites. The antibody was incubated during 48 h at 4 $^{\circ}$ C. Anti-RAGE, anti-Iba-1, anti-GFAP, anti-A β , and anti-phospho-Tau were used at 1:500 dilution. DAPI was used for nucleic acid staining (1:500; D9542, Sigma). Antibodies were diluted in PBS containing bovine serum albumin (2%). After washing four times with PBS-0.1%, tissue sections were incubated with secondary antibody according to reactive species (anti-rabbit or mouse Alexa 488 or 555 from Cell Signaling Technology), all diluted 1:500 in PBS and 2% BSA. After 1 h at room temperature, the slices were washed several times in PBS-0.1%, transferred to gelatinized slides, mounted with FluorSave[™] (345789, Merck Millipore), and covered with coverslips. The images were obtained with a Microscopy EVOS[®] FL Auto Imaging System (AMAFD1000, Thermo Fisher Scientific). Quantitative analysis of immunofluorescence staining was performed with ImageJ software (ImageJ version 1.49, National Institutes of Health). Results are expressed as fold relative to control (sham) group.

RAGE mediates neurodegeneration in sepsis

Statistical analysis

Statistical analysis was performed with GraphPad 5.0 software (GraphPad Software Inc., San Diego). Student's *t* test (one-tailed) was applied for simple comparisons between sham and CLP animals in each assay and one-way analysis of variance (ANOVA) followed by Tukey's post hoc test in assays with more groups. For behavioral analyses, individual groups were compared by the Wilcoxon tests, and comparisons among groups in inhibitory avoidance tasks were performed using the Mann-Whitney *U* test. Differences were considered significant when $p < 0.05$.

Author contributions—J. G. performed experiments, analyzed all data, elaborated the figures, and wrote the majority of the manuscript. C. S. G., N. S., and C. T. R. performed Western blottings and ELISA measurements. M. M., B. S., M. R., and A. V. S. performed surgical procedures (CLP and hippocampal cannulation), RAGEab administration, and behavioral tests plus analyses. J. C. F. M. designed experiments, discussed data, and helped to write the manuscript. T. B. and J. Q. designed behavioral experiments, analyzed and discussed data, and helped to write the manuscript. F. D. P. and D. P. G. provided the aims, design, and setting of the study, analyzed data, and wrote and reviewed the manuscript. All authors read and approved the final manuscript.

Acknowledgments—The Translational Psychiatry Program is funded by the Department of Psychiatry and Behavioral Sciences, McGovern Medical School, University of Texas Health Science Center at Houston. Laboratory of Neurosciences and Fisiopatologia Experimental (Brazil) are one of the members of the Center of Excellence in Applied Neurosciences of Santa Catarina (NENASC).

References

1. Singer, M., Deutschman, C. S., Seymour, C. W., Shankar-Hari, M., Annane, D., Bauer, M., Bellomo, R., Bernard, G. R., Chiche, J. D., Cooper-Smith, C. M., Hotchkiss, R. S., Levy, M. M., Marshall, J. C., Martin, G. S., Opal, S. M., et al. (2016) The Third International Consensus Definitions for Sepsis and Septic Shock (Sepsis-3). *JAMA* **315**, 801–810 CrossRef Medline
2. Wilson, J. X., and Young, G. B. (2003) Progress in clinical neurosciences: sepsis-associated encephalopathy: evolving concepts. *Can. J. Neurol. Sci.* **30**, 98–105 CrossRef Medline
3. Widmann, C. N., and Heneka, M. T. (2014) Long-term cerebral consequences of sepsis. *Lancet Neurol.* **13**, 630–636 CrossRef Medline
4. Semmler, A., Herrmann, S., Mormann, F., Weberpals, M., Paxian, S. A., Okulla, T., Schäfers, M., Kummer, M. P., Klockgether, T., and Heneka, M. T. (2008) Sepsis causes neuroinflammation and concomitant decrease of cerebral metabolism. *J. Neuroinflammation* **5**, 38 CrossRef Medline
5. Winters, B. D., Eberlein, M., Leung, J., Needham, D. M., Pronovost, P. J., and Sevransky, J. E. (2010) Long-term mortality and quality of life in sepsis: a systematic review. *Crit. Care Med.* **38**, 1276–1283 CrossRef Medline
6. Barichello, T., Martins, M. R., Reinke, A., Feier, G., Ritter, C., Quevedo, J., and Dal-Pizzol, F. (2005) Cognitive impairment in sepsis survivors from cecal ligation and perforation. *Crit. Care Med.* **33**, 221–223 CrossRef Medline
7. Yende, S., Austin, S., Rhodes, A., Finfer, S., Opal, S., Thompson, T., Bozza, F. A., LaRosa, S. P., Ranieri, V. M., and Angus, D. C. (2016) Long-term quality of life among survivors of severe sepsis: analyses of two international trials. *Crit. Care Med.* **44**, 1461–1467 CrossRef Medline
8. Iwashyna, T. J., Ely, E. W., Smith, D. M., and Langa, K. M. (2010) Long-term cognitive impairment and functional disability among survivors of severe sepsis. *JAMA* **304**, 1787–1794 CrossRef Medline
9. Annane, D., and Sharshar, T. (2015) Cognitive decline after sepsis. *Lancet. Respir. Med.* **3**, 61–69 CrossRef Medline
10. Varatharaj, A., and Galea, I. (2017) The blood-brain barrier in systemic inflammation. *Brain Behav. Immun.* **60**, 1–12 Medline
11. Dal-Pizzol, F., Rojas, H. A., dos Santos, E. M., Vuolo, F., Constantino, L., Feier, G., Pasquali, M., Comim, C. M., Petronilho, F., Gelain, D. P., Quevedo, J., Moreira, J. C., and Ritter, C. (2013) Matrix metalloproteinase-2 and metalloproteinase-9 activities are associated with blood-brain barrier dysfunction in an animal model of severe sepsis. *Mol. Neurobiol.* **48**, 62–70 CrossRef Medline
12. Michels, M., Steckert, A. V., Quevedo, J., Barichello, T., and Dal-Pizzol, F. (2015) Mechanisms of long-term cognitive dysfunction of sepsis: from blood-borne leukocytes to glial cells. *Intensive Care Med. Exp.* **3**, 30 CrossRef Medline
13. Michels, M., Vieira, A. S., Vuolo, F., Zepelini, H. G., Mendonça, B., Mina, F., Domingui, D., Steckert, A., Schuck, P. F., Quevedo, J., Petronilho, F., and Dal-Pizzol, F. (2015) The role of microglia activation in the development of sepsis-induced long-term cognitive impairment. *Brain Behav. Immun.* **43**, 54–59 CrossRef Medline
14. Cunningham, C., and Hennessy, E. (2015) Co-morbidity and systemic inflammation as drivers of cognitive decline: new experimental models adopting a broader paradigm in dementia research. *Alzheimers Res. Ther.* **7**, 33 CrossRef Medline
15. Spires-Jones, T. L., Stoothoff, W. H., de Calignon, A., Jones, P. B., and Hyman, B. T. (2009) Tau pathophysiology in neurodegeneration: a tangled issue. *Trends Neurosci.* **32**, 150–159 CrossRef Medline
16. Gendron, T. F., and Petrucelli, L. (2009) The role of Tau in neurodegeneration. *Mol. Neurodegener.* **4**, 13 CrossRef Medline
17. Multhaup, G., Huber, O., Buée, L., and Galas, M. C. (2015) Amyloid precursor protein (APP) metabolites APP intracellular fragment (AICD), Aβ42, and tau in nuclear roles. *J. Biol. Chem.* **290**, 23515–23522 CrossRef Medline
18. Nalivaeva, N. N., and Turner, A. J. (2013) The amyloid precursor protein: a biochemical enigma in brain development, function and disease. *FEBS Lett.* **587**, 2046–2054 CrossRef Medline
19. Zuo, L., Hemmelgarn, B. T., Chuang, C. C., and Best, T. M. (2015) The role of oxidative stress-induced epigenetic alterations in amyloid-β production in Alzheimer's disease. *Oxid. Med. Cell. Longev.* **2015**, 604658 Medline
20. Creagh-Brown, B. C., Quinlan, G. J., Evans, T. W., and Burke-Gaffney, A. (2010) The RAGE axis in systemic inflammation, acute lung injury and myocardial dysfunction: an important therapeutic target? *Intensive Care Med.* **36**, 1644–1656 CrossRef Medline
21. Batkulwar, K. B., Bansode, S. B., Patil, G. V., Godbole, R. K., Kazi, R. S., Chinnathambi, S., Shanmugam, D., and Kulkarni, M. J. (2015) Investigation of phosphoproteome in RAGE signaling. *Proteomics* **15**, 245–259 CrossRef Medline
22. Tóbon-Velasco, J. C., Cuevas, E., and Torres-Ramos, M. A. (2014) Receptor for AGEs (RAGE) as mediator of NF-κB pathway activation in neuroinflammation and oxidative stress. *CNS Neurol. Disord. Drug Targets* **13**, 1615–1626 CrossRef Medline
23. Lutterloh, E. C., Opal, S. M., Pittman, D. D., Keith, J. C., Jr, Tan, X. Y., Clancy, B. M., Palmer, H., Milarski, K., Sun, Y., Palardy, J. E., Parejo, N. A., and Kessimian, N. (2007) Inhibition of the RAGE products increases survival in experimental models of severe sepsis and systemic infection. *Crit. Care* **11**, R122 CrossRef Medline
24. van Zoelen, M. A., Schmidt, A. M., Florquin, S., Meijers, J. C., de Beer, R., de Vos, A. F., Nawroth, P. P., Bierhaus, A., and van der Poll, T. (2009) Receptor for advanced glycation end products facilitates host defense during *Escherichia coli*-induced abdominal sepsis in mice. *J. Infect. Dis.* **200**, 765–773 CrossRef Medline
25. van Zoelen, M. A., and van der Poll, T. (2008) Targeting RAGE in sepsis. *Crit. Care* **12**, 103 CrossRef Medline
26. Srikanth, V., Maczurek, A., Phan, T., Steele, M., Westcott, B., Juskiw, D., and Münch, G. (2011) Advanced glycation end products and their receptor RAGE in Alzheimer's disease. *Neurobiol. Aging* **32**, 763–777 Medline
27. Li, X. H., Lv, B. L., Xie, J. Z., Liu, J., Zhou, X. W., and Wang, J. Z. (2012) AGEs induce Alzheimer-like tau pathology and memory deficit via

- RAGE-mediated GSK-3 activation. *Neurobiol. Aging* **33**, 1400–1410 Medline
28. Chavan, S. S., Huerta, P. T., Robbiati, S., Valdes-Ferrer, S. I., Ochani, M., Dancho, M., Frankfurt, M., Volpe, B. T., Tracey, K. J., and Diamond, B. (2012) HMGB1 mediates cognitive impairment in sepsis survivors. *Mol. Med.* **18**, 930–937 Medline
 29. Dal-Pizzol, F., Pasquali, M., Quevedo, J., Gelain, D. P., and Moreira, J. C. (2012) Is there a role for high mobility group box 1 and the receptor for advanced glycation end products in the genesis of long-term cognitive impairment in sepsis survivors? *Mol. Med.* **18**, 1357–1358 Medline
 30. Schwalm, M. T., Pasquali, M., Miguel, S. P., Dos Santos, J. P., Vuolo, F., Comim, C. M., Petronilho, F., Quevedo, J., Gelain, D. P., Moreira, J. C., Ritter, C., and Dal-Pizzol, F. (2014) Acute brain inflammation and oxidative damage are related to long-term cognitive deficits and markers of neurodegeneration in sepsis-survivor rats. *Mol. Neurobiol.* **49**, 380–385 CrossRef Medline
 31. Deane, R., Singh, I., Sagare, A. P., Bell, R. D., Ross, N. T., LaRue, B., Love, R., Perry, S., Paquette, N., Deane, R. J., Thiyagarajan, M., Zarcone, T., Fritz, G., Friedman, A. E., Miller, B. L., and Zlokovic, B. V. (2012) A multimodal RAGE-specific inhibitor reduces amyloid β -mediated brain disorder in a mouse model of Alzheimer disease. *J. Clin. Invest.* **122**, 1377–1392 CrossRef Medline
 32. Yu, Y., and Ye, R. D. (2015) Microglial A β receptors in Alzheimer's disease. *Cell. Mol. Neurobiol.* **35**, 71–83 CrossRef Medline
 33. Barichello, T., Martins, M. R., Reinke, A., Constantino, L. S., Machado, R. A., Valvassori, S. S., Moreira, J. C., Quevedo, J., and Dal-Pizzol, F. (2007) Behavioral deficits in sepsis-surviving rats induced by cecal ligation and perforation. *Braz. J. Med. Biol. Res.* **40**, 831–837 CrossRef Medline
 34. Gutierrez, E. G., Banks, W. A., and Kastin, A. J. (1993) Murine tumor necrosis factor α is transported from blood to brain in the mouse. *J. Neuroimmunol.* **47**, 169–176 CrossRef Medline
 35. Yarlagadda, A., Alfson, E., and Clayton, A. H. (2009) The blood brain barrier and the role of cytokines in neuropsychiatry. *Psychiatry* **6**, 18–22 Medline
 36. Pan, W., Stone, K. P., Hsueh, H., Manda, V. K., Zhang, Y., and Kastin, A. J. (2011) Cytokine signaling modulates blood-brain barrier function. *Curr. Pharm. Des.* **17**, 3729–3740 CrossRef Medline
 37. Dal-Pizzol, F., Di Leone, L. P., Ritter, C., Martins, M. R., Reinke, A., Pens Gelain, D., Zanutto-Filho, A., de Souza, L. F., Andrades, M., Barbeiro, D. F., Bernard, E. A., Cammarota, M., Bevilacqua, L. R., Soriano, F. G., Cláudio, J., et al. (2006) Gastrin-releasing peptide receptor antagonist effects on an animal model of sepsis. *Am. J. Respir. Crit. Care Med.* **173**, 84–90 CrossRef Medline
 38. Ritter, C., Andrades, M. E., Reinke, A., Menna-Barreto, S., Moreira, J. C., and Dal-Pizzol, F. (2004) Treatment with *N*-acetylcysteine plus deferoxamine protects rats against oxidative stress and improves survival in sepsis. *Crit. Care Med.* **32**, 342–349 CrossRef Medline
 39. du Moulin, G. C., Paterson, D., Hedley-Whyte, J., and Broitman, S. A. (1985) *E. coli* peritonitis and bacteremia cause increased blood-brain barrier permeability. *Brain Res.* **340**, 261–268 CrossRef Medline
 40. Lee, J. Y., Lee, J. D., Phipps, S., Noakes, P. G., and Woodruff, T. M. (2015) Absence of toll-like receptor 4 (TLR4) extends survival in the hSOD1G93A mouse model of amyotrophic lateral sclerosis. *J. Neuroinflammation* **12**:90 Medline
 41. Wang, J. Z., Xia, Y. Y., Grundke-Iqbal, I., and Iqbal, K. (2013) Abnormal hyperphosphorylation of Tau: sites, regulation, and molecular mechanism of neurofibrillary degeneration. *J. Alzheimers Dis.* **33**, S123 Medline
 42. Goedert, M., Jakes, R., Crowther, R. A., Six, J., Lübke, U., Vandermeeren, M., Cras, P., Trojanowski, J. Q., and Lee, V. M. (1993) The abnormal phosphorylation of tau protein at Ser-202 in Alzheimer disease recapitulates phosphorylation during development. *Proc. Natl. Acad. Sci. U.S.A.* **90**, 5066–5070 CrossRef Medline
 43. Goedert, M., Jakes, R., Crowther, R. A., Hasegawa, M., Smith, M. J., and Spillantini, M. G. (1998) Intraneuronal filamentous tau protein and α -synuclein deposits in neurodegenerative diseases. *Biochem. Soc. Trans.* **26**, 463–471 CrossRef Medline
 44. Šimić, G., Babić Leko, M., Wray, S., Harrington, C., Delalle, I., Jovanov-Milošević, N., Bažadona, D., Buée, L., de Silva, R., Di Giovanni, G., Wischik, C., and Hof, P. R. (2016) Tau protein hyperphosphorylation and aggregation in Alzheimer's disease and other tauopathies, and possible neuroprotective strategies. *Biomolecules* **6**, 6 CrossRef Medline
 45. Sharshar, T., Gray, F., Lorin de la Grandmaison, G., Hopkinson, N. S., Ross, E., Dorandeu, A., Orlikowski, D., Raphael, J. C., Gajdos, P., and Annane, D. (2003) Apoptosis of neurons in cardiovascular autonomic centres triggered by inducible nitric-oxide synthase after death from septic shock. *Lancet* **362**, 1799–1805 CrossRef Medline
 46. Barichello, T., Fortunato, J. J., Vitali, A. M., Feier, G., Reinke, A., Moreira, J. C., Quevedo, J., and Dal-Pizzol, F. (2006) Oxidative variables in the rat brain after sepsis induced by cecal ligation and perforation. *Crit. Care Med.* **34**, 886–889 CrossRef Medline
 47. Zilka, N., Kazmerova, Z., Jadhav, S., Neradil, P., Madari, A., Obetkova, D., Bugos, O., and Novak, M. (2012) Who fans the flames of Alzheimer's disease brains? Misfolded tau on the crossroad of neurodegenerative and inflammatory pathways. *J. Neuroinflammation* **9**, 47 Medline
 48. Šimić, G., Babić Leko, M., Wray, S., Harrington, C., Delalle, I., Jovanov-Milošević, N., Bažadona, D., Buée, L., de Silva, R., Di Giovanni, G., Wischik, C., and Hof, P. R. (2016) Tau protein hyperphosphorylation and aggregation in Alzheimer's disease and other tauopathies, and possible neuroprotective strategies. *Biomolecules* **6**, 6 CrossRef Medline
 49. Simic, G. (2002) Pathological tau proteins in argyrophilic grain disease. *Lancet Neurol.* **1**, 276 CrossRef Medline
 50. O'Brien, R. J., and Wong, P. C. (2011) Amyloid precursor protein processing and Alzheimer's disease. *Annu. Rev. Neurosci.* **34**, 185–204 CrossRef Medline
 51. Edwards, G., 3rd, Moreno-Gonzalez, I., and Soto, C. (2017) Amyloid- β and tau pathology following repetitive mild traumatic brain injury. *Biochem. Biophys. Res. Commun.* **483**, 1137–1142 CrossRef Medline
 52. Cho, H. J., Son, S. M., Jin, S. M., Hong, H. S., Shin, D. H., Kim, S. J., Huh, K., and Mook-Jung, I. (2009) RAGE regulates BACE1 and A β generation via NFAT1 activation in Alzheimer's disease animal model. *FASEB J.* **23**, 2639–2649 CrossRef Medline
 53. Takuma, K., Fang, F., Zhang, W., Yan, S., Fukuzaki, E., Du, H., Sosunov, A., McKhann, G., Funatsu, Y., Nakamichi, N., Nagai, T., Mizoguchi, H., Ibi, D., Hori, O., Ogawa, S., et al. (2009) RAGE-mediated signaling contributes to intraneuronal transport of amyloid- β and neuronal dysfunction. *Proc. Natl. Acad. Sci. U.S.A.* **106**, 20021–20026 CrossRef Medline
 54. Candela, P., Gosselet, F., Saint-Pol, J., Sevin, E., Boucay, M. C., Boulanger, E., Cecchelli, R., and Fenart, L. (2010) Apical-to-basolateral transport of amyloid- β peptides through blood-brain barrier cells is mediated by the receptor for advanced glycation end-products and is restricted by P-glycoprotein. *J. Alzheimers Dis.* **22**, 849–859 CrossRef Medline
 55. Hong, Y., Shen, C., Yin, Q., Sun, M., Ma, Y., and Liu, X. (2016) Effects of RAGE-specific inhibitor FPS-ZM1 on amyloid- β metabolism and AGEs-induced inflammation and oxidative stress in rat hippocampus. *Neurochem. Res.* **41**, 1192–1199 CrossRef Medline
 56. Johnson, V. E., Stewart, W., and Smith, D. H. (2010) Traumatic brain injury and amyloid- β pathology: a link to Alzheimer's disease? *Nat. Rev. Neurosci.* **11**, 361–370 Medline
 57. Gouras, G. K., Willén, K., and Faideau, M. (2014) The inside-out amyloid hypothesis and synapse pathology in Alzheimer's disease. *Neurodegener. Dis.* **13**, 142–146 Medline
 58. Takahashi, R. H., Almeida, C. G., Kearney, P. F., Yu, F., Lin, M. T., Milner, T. A., and Gouras, G. K. (2004) Oligomerization of Alzheimer's β -amyloid within processes and synapses of cultured neurons and brain. *J. Neurosci.* **24**, 3592–3599 CrossRef Medline
 59. Capetillo-Zarate, E., Gracia, L., Yu, F., Banfelder, J. R., Lin, M. T., Tampellini, D., and Gouras, G. K. (2011) High-resolution 3D reconstruction reveals intra-synaptic amyloid fibrils. *Am. J. Pathol.* **179**, 2551–2558 CrossRef Medline
 60. Opp, M. R., George, A., Ringgold, K. M., Hansen, K. M., Bullock, K. M., and Banks, W. A. (2015) Sleep fragmentation and sepsis differentially impact blood-brain barrier integrity and transport of tumor necrosis factor- α in aging. *Brain Behav. Immun.* **50**, 259–265 CrossRef Medline
 61. Dent, P. (2014) Crosstalk between ERK, AKT, and cell survival. *Cancer Biol. Ther.* **15**, 245–246 CrossRef Medline

RAGE mediates neurodegeneration in sepsis

62. Kamat, P. K., Rai, S., Swarnkar, S., Shukla, R., and Nath, C. (2014) Molecular and cellular mechanism of okadaic acid (OKA)-induced neurotoxicity: a novel tool for Alzheimer's disease therapeutic application. *Mol. Neurobiol.* **50**, 852–865 CrossRef Medline
63. Shi, S., Liang, D., Bao, M., Xie, Y., Xu, W., Wang, L., Wang, Z., and Qiao, Z. (2016) Gx-50 inhibits neuroinflammation via $\alpha 7$ nAChR activation of the JAK2/STAT3 and PI3K/AKT pathways. *J. Alzheimers Dis.* **50**, 859–871 CrossRef Medline
64. Heras-Sandoval, D., Pérez-Rojas, J. M., Hernández-Damián, J., and Pedraza-Chaverri, J. (2014) The role of PI3K/AKT/mTOR pathway in the modulation of autophagy and the clearance of protein aggregates in neurodegeneration. *Cell. Signal.* **26**, 2694–2701 CrossRef Medline
65. Guillot, F., Kemppainen, S., Lavoisier, G., Miettinen, P. O., Laroche, S., Tanila, H., and Davis, S. (2016) Brain-specific basal and novelty-induced alternations in PI3K-Akt and MAPK/ERK signaling in a middle-aged A β PP/PS1 mouse model of Alzheimer's disease. *J. Alzheimers Dis.* 2016; 51(4):1157–1173 CrossRef Medline
66. Maiese, K. (2016) Targeting molecules to medicine with mTOR, autophagy, and neurodegenerative disorders. *Br. J. Clin. Pharmacol.* **82**, 1245–1266 Medline
67. Asati, V., Mahapatra, D. K., and Bharti, S. K. (2016) PI3K/Akt/mTOR and Ras/Raf/MEK/ERK signaling pathways inhibitors as anticancer agents: Structural and pharmacological perspectives. *Eur. J. Med. Chem.* **109**, 314–341 CrossRef Medline
68. Chiang, G. G., and Abraham, R. T. (2005) Phosphorylation of mammalian target of rapamycin (mTOR) at Ser-2448 is mediated by p70S6 kinase. *J. Biol. Chem.* **280**, 25485–25490 CrossRef Medline
69. Lukic, I. K., Humpert, P. M., Nawroth, P. P., and Bierhaus, A. (2008) The RAGE pathway: activation and perpetuation in the pathogenesis of diabetic neuropathy. *Ann. N.Y. Acad. Sci.* **1126**, 76–80 CrossRef Medline
70. Semmler, A., Frisch, C., Debeir, T., Ramanathan, M., Okulla, T., Klockgether, T., and Heneka, M. T. (2007) Long-term cognitive impairment, neuronal loss and reduced cortical cholinergic innervation after recovery from sepsis in a rodent model. *Exp. Neurol.* **204**, 733–740 CrossRef Medline
71. Barichello, T., Martins, M. R., Reinke, A., Feier, G., Ritter, C., Quevedo, J., and Dal-Pizzol, F. (2005) Long-term cognitive impairment in sepsis survivors. *Crit. Care Med.* **33**, 1671 CrossRef Medline
72. Sabbagh, M. N., Agro, A., Bell, J., Aisen, P. S., Schweizer, E., and Galasko, D. (2011) PF-04494700, an oral inhibitor of receptor for advanced glycation end products (RAGE), in Alzheimer disease. *Alzheimer Dis. Assoc. Disord.* **25**, 206–212 CrossRef Medline
73. Galasko, D., Bell, J., Mancuso, J. Y., Kupiec, J. W., Sabbagh, M. N., van Dyck, C., Thomas, R. G., Aisen, P. S., and Alzheimer's Disease Cooperative Study. (2014) Clinical trial of an inhibitor of RAGE-A β interactions in Alzheimer disease. *Neurology* **82**, 1536–1542 CrossRef Medline
74. Origlia, N., Righi, M., Capsoni, S., Cattaneo, A., Fang, F., Stern, D. M., Chen, J. X., Schmidt, A. M., Arancio, O., Yan, S. D., and Domenici, L. (2008) Receptor for advanced glycation end product-dependent activation of p38 mitogen-activated protein kinase contributes to amyloid- β -mediated cortical synaptic dysfunction. *J. Neurosci.* **28**, 3521–3530 CrossRef Medline
75. Kuhla, A., Norden, J., Abshagen, K., Menger, M. D., and Vollmar, B. (2013) RAGE blockade and hepatic microcirculation in experimental endotoxaemic liver failure. *Br. J. Surg.* **100**, 1229–1239 CrossRef Medline
76. Xia, P., Deng, Q., Gao, J., Yu, X., Zhang, Y., Li, J., Guan, W., Hu, J., Tan, Q., Zhou, L., Han, W., Yuan, Y., and Yu, Y. (2016) Therapeutic effects of antigen affinity-purified polyclonal anti-receptor of advanced glycation end-product (RAGE) antibodies on cholestasis-induced liver injury in rats. *Eur. J. Pharmacol.* **779**, 102–110 CrossRef Medline
77. Lutterloh, E. C., and Opal, S. M. (2007) Antibodies against RAGE in sepsis and inflammation: implications for therapy. *Expert Opin. Pharmacother.* **8**, 1193–1196 CrossRef Medline
78. Ritter, C., Andrades, M., Frota Júnior, M. L., Bonatto, F., Pinho, R. A., Polydoro, M., Klamt, F., Pinheiro, C. T., Menna-Barreto, S. S., Moreira, J. C., and Dal-Pizzol, F. (2003) Oxidative parameters and mortality in sepsis induced by cecal ligation and perforation. *Intensive Care Med.* **29**, 1782–1789 CrossRef Medline
79. Barichello, T., Machado, R. A., Constantino, L., Valvassori, S. S., Réus, G. Z., Martins, M. R., Petronilho, F., Ritter, C., Quevedo, J., and Dal-Pizzol, F. (2007) Antioxidant treatment prevented late memory impairment in an animal model of sepsis. *Crit. Care Med.* **35**, 2186–2190 CrossRef Medline
80. National Research Council (2011) Committee for the Update of the Guide for the Care and Use of Laboratory Animals. 8th Ed., National Academies Press, Washington, D. C.
81. Paxinos, G., and Watson, C. (2005) *The Rat Brain in Stereotaxic Coordinates*, 5th Ed., pp. 181–207, Elsevier Academic Press, Amsterdam
82. Roesler, R., Vianna, M. R., de-Paris, F., and Quevedo, J. (1999) Memory-enhancing treatments do not reverse the impairment of inhibitory avoidance retention induced by NMDA receptor blockade. *Neurobiol. Learn. Mem.* **72**, 252–258 CrossRef Medline
83. Bradford, M. M. (1976) A rapid and sensitive method for the quantitation of microgram quantities of protein utilizing the principle of protein-dye binding. *Anal. Biochem.* **72**, 248–254 CrossRef Medline

Capítulo IV

**Targeted inhibition of RAGE in substantia nigra of rats blocks
6-OHDA–induced dopaminergic denervation**

Publicado em: **Scientific Reports (2017)**

Targeted inhibition of RAGE in *substantia nigra* of rats blocks 6-OHDA-induced dopaminergic denervation

Juciano Gasparotto¹, Camila Tiefensee Ribeiro¹, Rafael Calixto Bortolin¹, Nauana Somensi¹, Thallita Kelly Rabelo¹, Alice Kunzler¹, Natália Cabral Souza², Matheus Augusto de Bittencourt Pasquali³, José Claudio Fonseca Moreira¹ & Daniel Pens Gelain¹

The receptor for advanced glycation endproducts (RAGE) is a pattern-recognition receptor associated with inflammation in most cell types. RAGE up-regulates the expression of proinflammatory mediators and its own expression via activation of NF- κ B. Recent works have proposed a role for RAGE in Parkinson's disease (PD). In this study, we used the multimodal blocker of RAGE FPS-ZM1, which has become available recently, to selectively inhibit RAGE in the substantia nigra (SN) of rats intracranially injected with 6-hydroxydopamine (6-OHDA). FPS-ZM1 (40 μ g per rat), injected concomitantly with 6-OHDA (10 μ g per rat) into the SN, inhibited the increase in RAGE, activation of ERK1/2, Src and nuclear translocation of NF- κ B p65 subunit in the SN. RAGE inhibition blocked glial fibrillary acidic protein and Iba-1 upregulation as well as associated astrocyte and microglia activation. Circulating cytokines in serum and CSF were also decreased by FPS-ZM1 injection. The loss of tyrosine hydroxylase and NeuN-positive neurons was significantly inhibited by RAGE blocking. Finally, FPS-ZM1 attenuated locomotor and exploratory deficits induced by 6-OHDA. Our results demonstrate that RAGE is an essential component in the neuroinflammation and dopaminergic denervation induced by 6-OHDA in the SN. Selective inhibition of RAGE may offer perspectives for therapeutic approaches.

Parkinson's disease (PD) is a progressive neurodegenerative disorder characterized by the specific loss of the nigrostriatal dopaminergic neurons, causing locomotor and postural deficits. Chronic neuroinflammation has been reported as a major contributor to PD¹. The defense mechanisms in brain are able to protect against inflammatory processes. However, when inflammatory stressors accumulate beyond a threshold, which has not been defined until date, signaling pathways for neuronal death are triggered.

The amount of evidence linking RAGE to neurodegenerative diseases such as Alzheimer's disease, PD, and Huntington's disease has been increasing in the last few years². RAGE belongs to the superfamily of immunoglobulins, which are present on the surface of many types of cells such as neurons, microglia, brain endothelial cells³ and astrocytes⁴. RAGE is a very promiscuous receptor binding many proteins such as S100b, HMGB1, HSP70, AGEs, β -amyloid and LPS among many others. New proteins with the capacity to bind RAGE are reported continuously.

Many animal models have been used to elucidate the mechanisms that trigger neurodegenerative diseases. We chose the rat model, where 6-hydroxydopamine (6-OHDA) is administered unilaterally. This model has been studied extensively and the dopaminergic denervation in this rat model is similar to that in PD^{5,6}.

In the present work, we used a pharmacological antagonist, FPS-ZM1, for blocking RAGE in the SN to investigate potential neuroprotective effects against 6-OHDA-induced dopaminergic denervation. FPS-ZM1 is able to penetrate BBB and acts as a high affinity, multimodal blocker of RAGE through V domain-mediated ligand

¹Centro de Estudos em Estresse Oxidativo, Departamento de Bioquímica, Instituto de Ciências Básicas da Saúde, Universidade Federal do Rio Grande do Sul, Porto Alegre, RS, Brazil. ²Instituto de Medicina Tropical, Departamento de Bioquímica, Universidade Federal do Rio Grande do Norte, Natal, RN, Brazil. ³Unidade Acadêmica de Engenharia de Alimentos, Centro de Tecnologia e Recursos Naturais, Universidade Federal de Campina Grande – UFCG, Campina Grande, Paraíba, Brazil. Correspondence and requests for materials should be addressed to J.G. (email: Juciano).

Received: 2 February 2017

Accepted: 19 July 2017

Published online: 18 August 2017

binding³. FPS-ZM1 treatment has been employed to study neurotoxicity models^{7,8}. FPS-ZM1 was injected into the same site of 6-OHDA. Proinflammatory, oxidative and neurotoxic effects of 6-OHDA in serum, CSF, and SN were evaluated. The results demonstrate a relationship between RAGE and 6-OHDA induced dopaminergic denervation in the SN. FPS-ZM1 was able to protect against most of the 6-OHDA-induced effects, suggesting that RAGE plays a pivotal role in the propagation/amplification of inflammatory effects and dopaminergic denervation consequent from 6-OHDA injection.

Results

RAGE is increased in the SN of 6-OHDA-treated rats. The content of immunoreactive RAGE increased in the SN region of 6-OHDA-administered rats as shown by immunofluorescence analysis (Fig. 1a). Injection of RAGE blocking peptide FPS-ZM1 into the SN concomitantly with 6-OHDA inhibited the increase in RAGE content. Relative quantification by western blotting showed that RAGE increased by 50% in animals administered with 6-OHDA, which was inhibited by FPS-ZM1 by 46% (Fig. 1b). RAGE content and immunolocalization in the contralateral (not showed) SN was not affected, as expected (Fig. 1a). Interestingly, rats injected with FPS-ZM1 + 6-OHDA had increased RAGE localization in blood vessels as show detailed in Fig. 1a. In Control and FPZ-ZM1 groups, RAGE was not detected (Fig. 1a). To identify the cells in which RAGE was induced, we conducted co-immunostaining of RAGE with glial fibrillary acidic protein (GFAP - astrocyte marker), Iba-1 (microglial marker), or TH (dopaminergic neuron marker). The results showed the induction of RAGE mainly in TH+ cells, but not in astrocytes or microglia (Fig. 2a and b). Confocal microscopy scanning of Z-axis confirmed the co-localization of TH and RAGE staining in the same cells (Fig. 2c), demonstrating a different pattern of staining from rats treated with FPS-ZM1 and 6-OHDA, in which RAGE is typically localized in endothelial cells and absent in TH+ neurons (Fig. 2d). Details of Z-axis scanning are shown in supplementary figure S1a and b.

NF-κB activation in SN of 6-OHDA-injected rats is mediated by RAGE. Following ligand binding, the intracellular machinery activated by RAGE induces the dissociation of p65 and p50 subunits from the inhibitory IκB subunit of the NF-κB complex in the cytoplasm, leading to p65 nuclear translocation. This results in transcriptional activation of proinflammatory genes and up-regulation of RAGE expression, as the RAGE gene (*AGER*) is also responsive to NF-κB transcriptional activity⁹. The immunofluorescence images of the transcriptional subunit, p65 of NF-κB show the translocation of p65 from cytoplasm to nucleus in many cells in 6-OHDA-induced group (Fig. 3a and detail in Fig. 3b). FPS-ZM1 completely blocked the 6-OHDA-induced translocation of p65 to nuclei. There were negligible number of p65+ nuclei in control group (2.3 ± 1.5) or animals receiving only FPS-ZM1 (3.4 ± 1.6) (Fig. 3c).

ERK1/2 and Src activation in SN of 6-OHDA-injected rats are mediated by RAGE. RAGE ligand binding on cell membrane results in the activation of different protein phosphorylation cascades leading to the activation of transcription factors such as NF-κB¹⁰. We therefore examined the phosphorylation/activation of MAPKs, which are regulatory signaling molecules in inflammation and cell death and might be activated upon RAGE ligand binding. 6-OHDA induced the phosphorylation of ERK1/2 and Src (Fig. 4a and d), and the antagonist FPS-ZM1 suppressed ERK1/2 and Src activation. p38 was not inhibited to a significant extent by FPS-ZM1 and JNK phosphorylation was not significantly altered by 6-OHDA (Fig. 4b and c). These data suggest that ERK1/2 and Src phosphorylation in the SN of 6-OHDA-treated rats are evoked via a RAGE-dependent pathway.

RAGE inhibition in SN blocks 6-OHDA-induced neuroinflammation. We also measured pro-inflammatory cytokines in CSF and serum (Fig. 5a and b). TNF-α and IL-1β were increased in CSF (110% and 130% respectively) and serum (70% and 150% respectively) of 6-OHDA-injected rats. FPS-ZM1 blocked the IL-1β increase in CSF (Fig. 5a), whereas both cytokines were blocked in serum (Fig. 5b). The administration of 6-OHDA triggers an inflammatory process that contributes to dopaminergic denervation. RAGE is a major regulator of chronic inflammation in several tissues, including CNS¹¹. In order to assess the effect of RAGE inhibition on the inflammation of SN in 6-OHDA-injected rats, we evaluated the effect of RAGE inhibition on glial activation by assessing GFAP and Iba-1 immunostaining (Fig. 5c) and immunoblotting (Fig. 5d and e). The increases in the number of GFAP+ cells and the content of GFAP were inhibited by the presence of FPS-ZM1, indicating that RAGE inhibition decreases 6-OHDA-induced astrocyte activation (Fig. 5c and e). Similar effect was observed with Iba-1, suggesting the involvement of RAGE in 6-OHDA-induced microglia activation (Fig. 5c and d).

RAGE inhibition in SN blocks 6-OHDA-induced dopaminergic denervation. Tyrosine hydroxylase (TH) is the rate-limiting enzyme in catecholamine synthesis and is the golden marker for dopaminergic neurons in the SN¹². Death of dopaminergic neurons is a hallmark of PD. Therefore, we evaluated the effect of RAGE inhibition over dopaminergic neurons by immunostaining TH+ neurons and on other neurons by assessing a general neuronal marker, neuronal nuclear antigen (NeuN). The immunofluorescence analysis for neuronal markers revealed a significant loss of TH+ and NeuN+ cells in the SN of animals treated with 6-OHDA (Fig. 6a). Western blot analysis confirmed these observations (Fig. 6b and c). The RAGE inhibitor, FPS-ZM1 blocked the loss of TH and NeuN positive cells when administered concomitantly with 6-OHDA (Fig. 6a–c) and rescued the protein content. The blocking effect of RAGE inhibition in 6-OHDA-induced dopaminergic denervation is shown in nigrostriatal axis (Sup. Fig. S2). In addition, the TH-immunoreactivity images are shown in whole SN and striatum (caudate–putamen unit) (Sup. Fig. S3).

RAGE inhibition in SN rescues locomotor, rotational and exploratory deficits induced by 6-OHDA. Dopaminergic denervation induced by 6-OHDA is characterized by locomotor and exploratory deficits that can be assessed in behavioral tests. General motor performance was assessed 14 days after surgery, using the constant (21 RPM) rotarod test. Animals injected with 6-OHDA displayed significant reduction in the

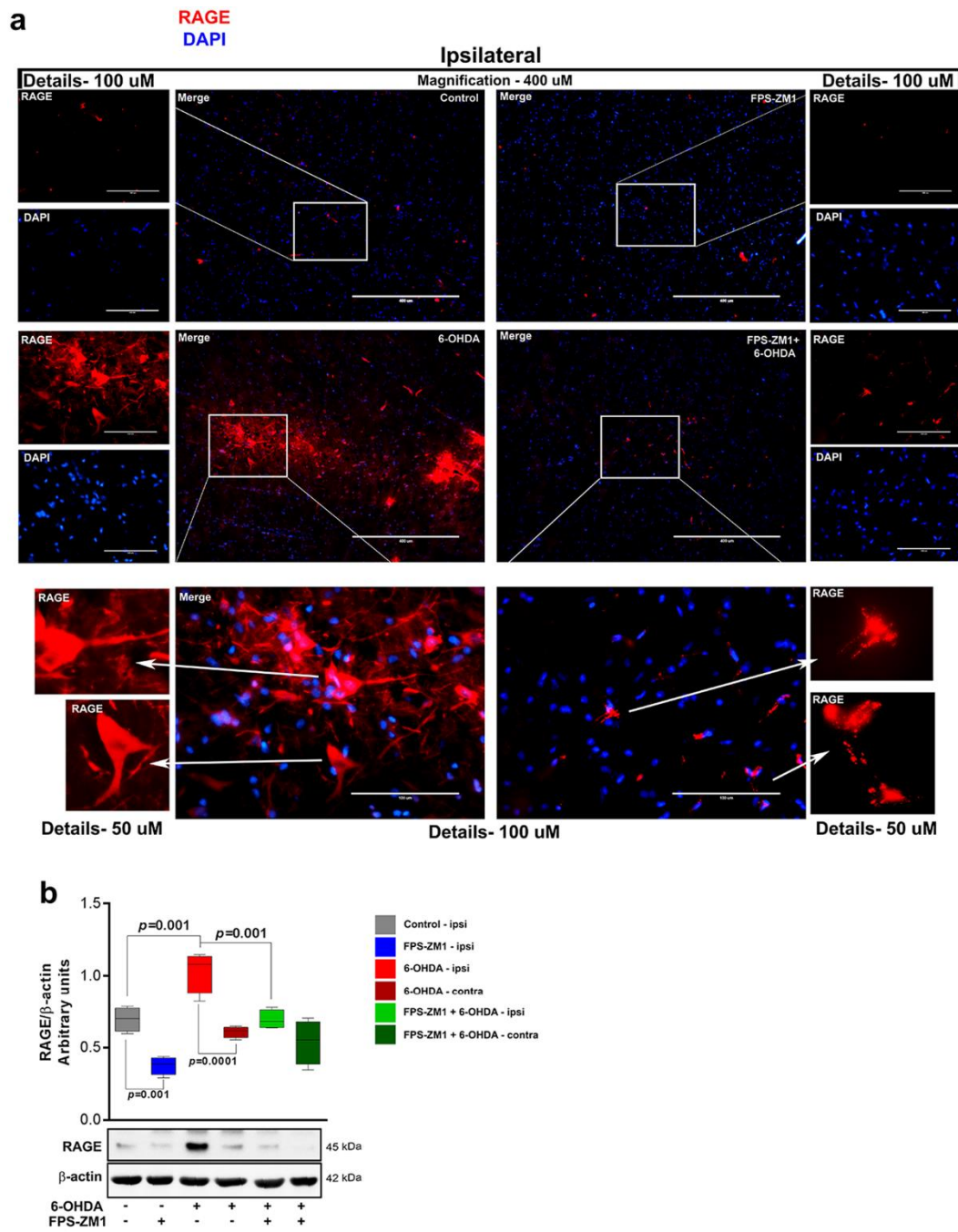


Figure 1. FPS-ZM1 blocked the increase in the levels of RAGE in rats administered with 6-OHDA. Rats were prepared for immunofluorescence and western blotting 15 days after the injection of 6-OHDA. **(a)** Representative immunofluorescence images of SN immunostained for RAGE and DAPI ($n = 10$ per group). The ipsilateral sides are shown. The microscopy images were taken with 400 μ m of magnification and the squares represents the location of the approximation of 100 μ m. **(b)** Representative western blots and quantification of RAGE ($n = 6$ per group). Each color in the graph represents a group and a brain location: gray - control/ipsilateral side; blue - FPS-ZM1/ipsilateral side; red - 6-OHDA/ipsilateral side; dark red - 6-OHDA/contralateral side; green - FPS-ZM1 + 6-OHDA/ipsilateral side; dark green - FPS-ZM1 + 6-OHDA/contralateral side. Values represent mean \pm SD. One-way analysis of variance and Bonferroni Multiple Comparison *post-hoc* test were applied to all data. p values are embedded in the figure.

time on rotarod (60% of the control (Fig. 7a). Rats administered with both FPS-ZM1 and 6-OHDA presented an improved motor ability on rotarod test (10% higher than that of 6-OHDA group).

To evaluate the effectiveness and precision of the 6-OHDA injection the rotational behavior was assessed. The apomorphine-induced rotation is shown in Fig. 7b. The data demonstrate that 6-OHDA administration

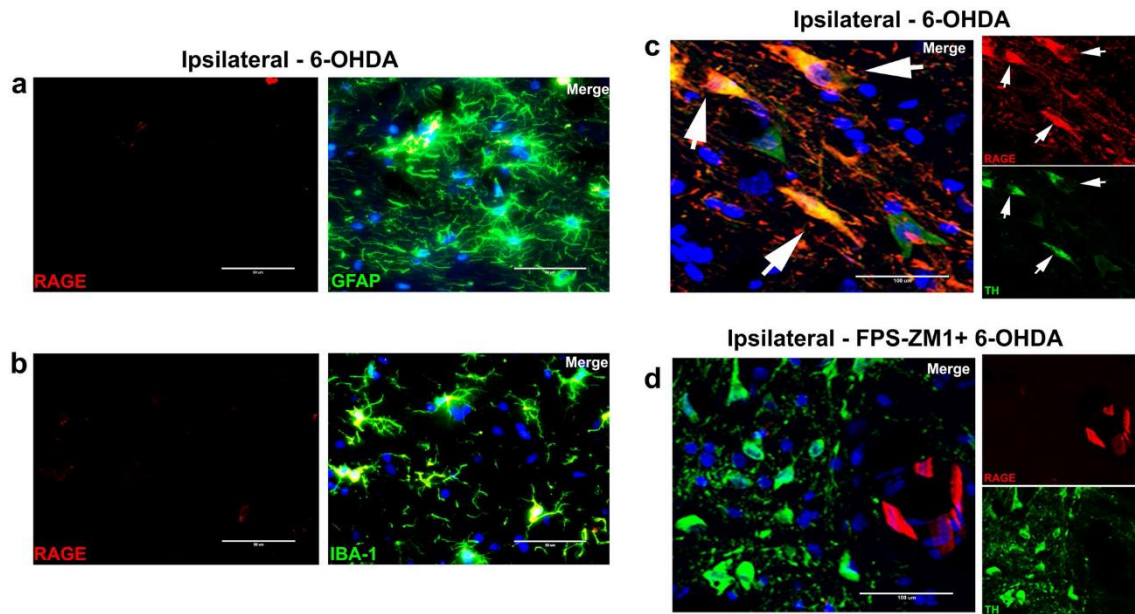


Figure 2. RAGE preferentially binds to dopaminergic neurons. Rats were prepared for immunofluorescence 15 days after 6-OHDA administration. The sections were co-immunostained for markers specific to different cell types and RAGE to evaluate the morphology and co-localization. (a) GFAP + RAGE, (b) IBA-1 + RAGE. The microscopy images were taken with 50 μm of magnification. (c) Confocal representative immunofluorescence images of SN co-immunostained for TH, RAGE and DAPI to ipsilateral 6-OHDA-induced and (d) ipsilateral FPS-ZM1 + 6-OHDA. The confocal microscopy images were taken with 100 μm of magnification and the z-axis layers are detailed in Sup. Fig. S1a and b. Representative immunofluorescence images of SN co-immunostained for different cell types ($n = 10$ per group): Only ipsilateral sides are showed.

induced a rotational asymmetry, with rats displaying significant increase in continuous contralateral rotations following apomorphine injection (mean rates of 12 ± 1.5). Animals receiving FPS-ZM1 + 6-OHDA had significantly lower rotation rates (4.6 ± 1.2) induced by apomorphine injection. Control and FPS-ZM1 groups did not show any significant spontaneous rotation. The lesion severity of 6-OHDA model was established according to apomorphine-induced rotation¹³. The present model is characterized as severe, since rats exhibited more than 3 contralateral turns/minute. This magnitude of impairment is expected to display $> 85\%$ TH+ cell loss in SN and $> 45\%$ TH+ cell loss in VTA¹³.

We also evaluated the exploratory activity. Animals administered with FPS-ZM1 + 6-OHDA presented a higher exploratory activity in an open field test of rearing events, compared to animals receiving only 6-OHDA (Fig. 7c). Notably, 6-OHDA reduced the number of rearing episodes (50% of control), whereas rats exposed to FPS-ZM1 + 6-OHDA displayed a higher number of rearing episodes compared to the control group (Fig. 7c).

Discussion

Although 6-OHDA-induced dopaminergic denervation has been a useful model largely utilized for understanding motor and biochemical dysfunctions associated to PD, it is not clear, whether dopaminergic cell death induced by this toxin shares common molecular mechanisms to those observed in patients. In this context, it must be considered that the 6-OHDA model does not replicate several pathological characteristics of PD, which poses limitations in relation to the interpretations of molecular mechanisms underlying the progression of dopaminergic cell death when using this model. For instance, animal models of 6-OHDA injection do not display Lewy bodies in the brain, a histopathological hallmark of PD^{14,15}. Besides, the dopaminergic denervation is localized and rapidly induced if compared to PD. In this disease, a progressive neuronal death evolves in the course of years and its consequence is not restricted to dopaminergic denervation, although this is the main cause of the characteristic motor symptoms¹⁴. Nonetheless, animal models of PD present different limitations regarding the multiple dysfunctions of the disease, and the 6-OHDA animal model is still considered a valid model to investigate behavioral and cellular features of PD¹⁴. Here, we performed a localized inhibition of RAGE with FPS-ZM1 (RAGE antagonist) to understand the involvement of RAGE in dopaminergic denervation and to test a potential strategy to prevent and neuronal death. RAGE interacts with a variety of ligands¹ that may lead to inflammatory response causing brain injury and cell death¹⁶. To investigate the role of RAGE in SN, we administered 6-OHDA to induce neuronal death and co-administered FPS-ZM1 to inhibit the action of RAGE.

RAGE is a receptor with bad reputation², fittingly so. RAGE is implicated in numerous neurodegenerative disorders such as Alzheimer's disease, Parkinson's disease, and Huntington's disease². Although there is ample evidence demonstrating the involvement of RAGE in neurodegenerative diseases¹⁷, the mechanism by which RAGE

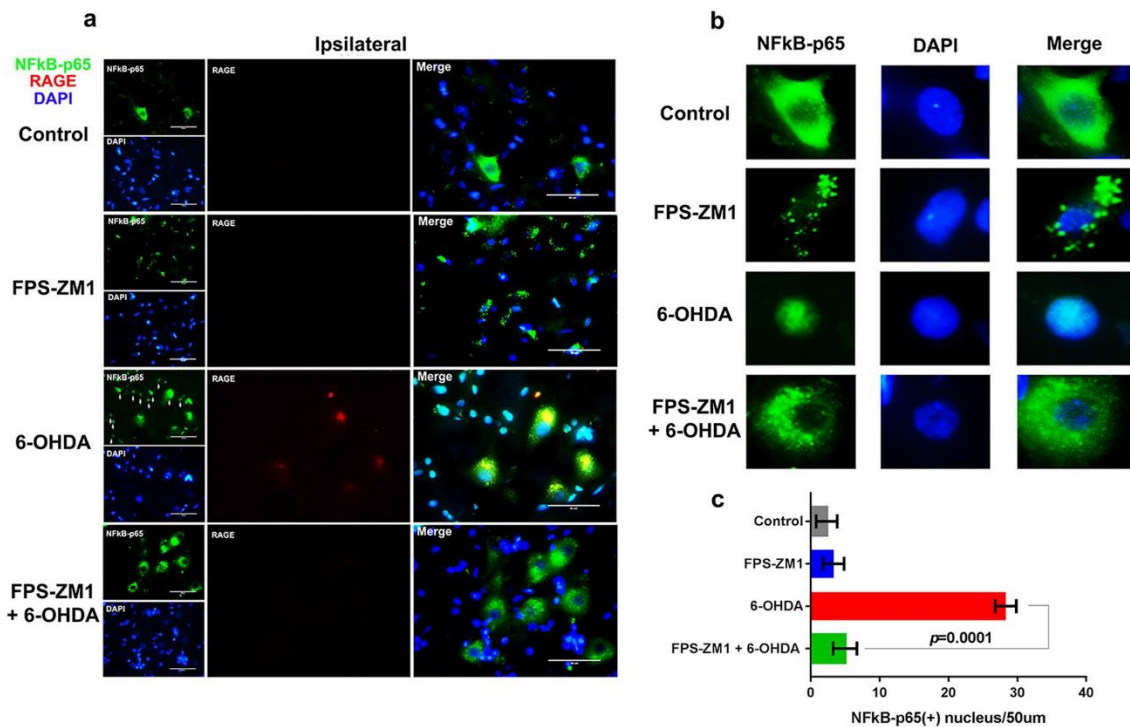


Figure 3. FPS-ZM1 blocked the 6-OHDA-induced nuclear translocation of NF- κ B-p65. Rats were prepared for immunofluorescence 15 days after 6-OHDA administration. (a) Representative co-immunofluorescence images of SN immunostained for NF- κ B-p65, RAGE and DAPI ($n = 10$ per group). The ipsilateral sides are showed. The microscopy images were taken with 50 μ m of magnification. (b) Cell details. (c) p65+ nucleus quantification/picture with 50 μ m magnification area. Values represent mean \pm SD from 6 rats per group. One-way analysis of variance and Bonferroni Multiple Comparison *post-hoc* test were applied to all data. p values are embedded in the figure.

causes neuronal death remains unclear. Our results have demonstrated that 6-OHDA increased the number of RAGE-positive cells specifically in SN (Fig. 1a). Immunofluorescence visualization of a larger area in SN gives a general picture of the capacity of RAGE antibody to bind to various cell types. However, when we approximate the image magnification (Fig. 2c) it is possible to observe an accentuated presence of RAGE in dopaminergic neurons compared to that in astrocytes (Fig. 2a) and microglia (Fig. 2b).

Astrocytes are stellate-like cells and represent the most abundant cell type in most parts of the brain. The morphological changes induced in astrocytes by 6-OHDA (Sup. Fig. S1c) may result from changes of cytoskeletal proteins in microfilaments, intermediate filaments, and/or microtubules¹⁸. Microglia are highly dynamic cells, presenting a functional phenotype. Under both physiological and pathological conditions, they scan their environment and regulate tissue homeostasis¹⁹. In response to 6-OHDA lesion, microglia displayed a morphology associated to an activated phenotype (Sup. Fig. S1d) Furthermore, 6-OHDA reduced the number of TH+ neurons and induced characteristic morphological changes in surviving cells. The remaining TH+ cells showed a spherical format in comparison to the normal spindle forms presenting a well-designed axodendritic network (Sup. Fig. S1e and f). The neuroplasticity induced by 6-OHDA or derived toxins is unclear, however altered cell morphology may be an informative tool in documenting the changes caused by the neurotoxic insults to neuronal and nucleolar volume²⁰.

NF- κ B is a critical factor transducing a variety of inflammatory and pro- or anti-apoptotic signals in the cell, depending on the stimulus²¹. There was a massive presence of NF- κ B-p65 in the nuclei of the SN cells of rats receiving 6-OHDA, indicating a transcriptional effect (Fig. 3b). NF- κ B translocation also promotes the expression of proinflammatory cytokines¹¹. The gene encoding RAGE contains functional binding elements for NF- κ B. RAGE can also upregulate itself, perpetuating the neuroinflammation^{21, 22}. FPS-ZM1 significantly suppresses the ERK1/2 phosphorylation and NF- κ B translocation to the nuclei of the cells in the SN of rats injected with 6-OHDA (Fig. 3a-c). This strongly suggests that inhibiting RAGE activation blocked the signaling cascade and consequently blocked the inflammation and damage caused by 6-OHDA.

RAGE activation triggers MAPK-controlled phosphorylation cascades. Our results show that 6-OHDA significantly increased ERK1/2 and Src activation (Fig. 4a and d). ERK 1/2 is the main component of the MAPK pathway and when enhanced by prior Src phosphorylation, it plays a key role in RAGE signal, which may result in the upregulation of NF- κ B²³. In addition RAGE directly binds to ERK by a D-like domain, this interaction does

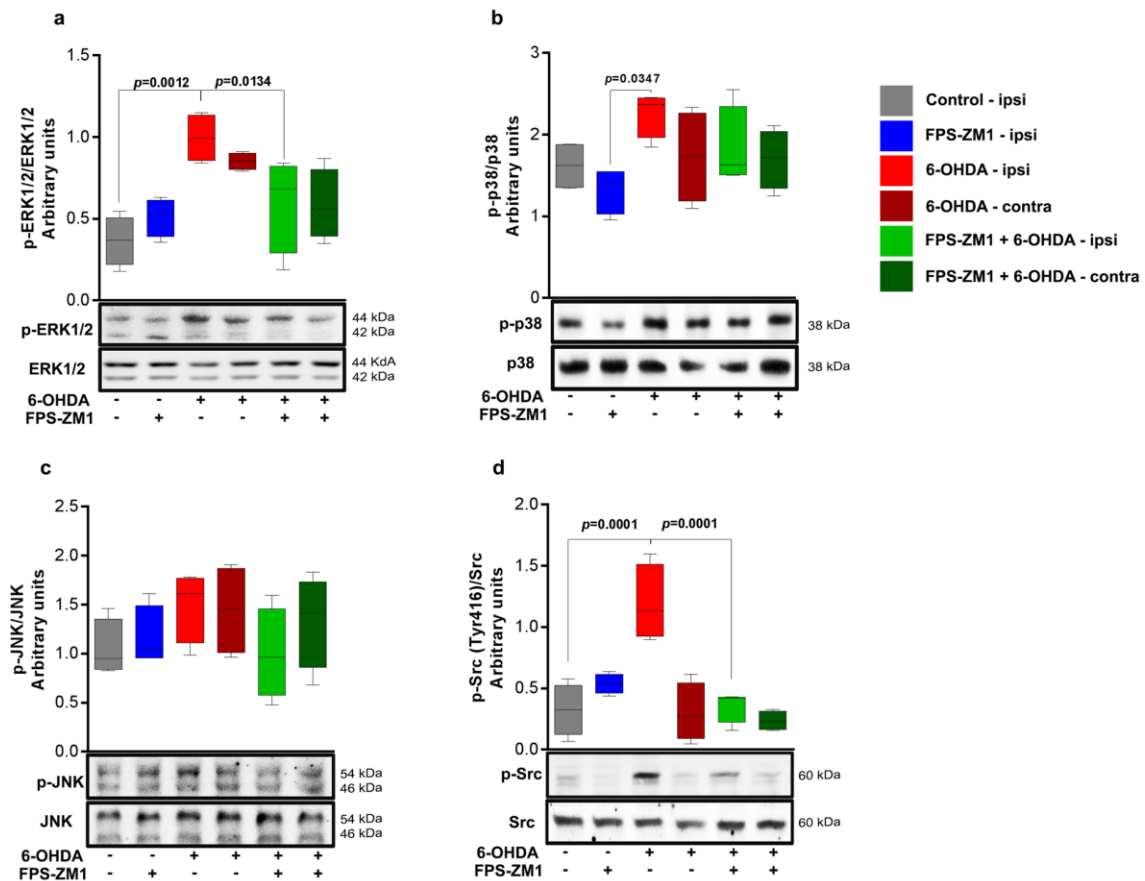


Figure 4. FPS-ZM1 inhibited 6-OHDA-induced MAPK-ERK 1/2 and Src phosphorylation. Tissue samples were prepared for western blotting assay 15 days after 6-OHDA-injection. (a) p-ERK 1/2. (b) p-p38. (c) p-JNK. (d) p-Src. The representative western blots of phosphorylated protein and total protein are shown below the graphs. Values represent mean \pm SD from 6 rats per group. One-way analysis of variance and Bonferroni Multiple Comparison *post-hoc* test were applied to all data. *p* values are embedded in the figure.

not occur with others MAPKs as for p38 and JNK²³. RAGE seems to have an important effect in this pathway, whereas FPS-ZM1 blocked the 6-OHDA-induced signaling otherwise activated by RAGE.

We observed an increase in TNF- α and IL-1 β in 6-OHDA-induced rats, as demonstrated by the ELISA measurements in CSF and serum (Fig. 5a and b). The increases in these cytokines originate from many cells stimulated by 6-OHDA, mainly astrocytes and microglia, which overproduce and release TNF- α and IL-1 β into CSF and serum. 6-OHDA generates a strong pro-inflammatory response and inflammatory condition in distinct cell types. Inhibiting RAGE with FPS-ZM1 blocked the release of cytokines (TNF- α in CSF was the exception) and the activation of astrocytes and microglia in SN (Fig. 5c-e). Taking these results together, RAGE seems to be a crucial factor that mediates the 6-OHDA-induced inflammatory process and contributes to neuronal degeneration.

Research with animal models and clinical studies suggested that RAGE⁴, protein S100B²⁴ and HMGB1²⁵ are potential contributors to the development of PD. These data are in accordance with our results and support our research focus to block RAGE, since inflammatory signaling and neuronal damage seem to occur through this receptor.

6-OHDA administration, as expected, reduced the number of TH and NeuN positive neurons (Fig. 6a-c). FPS-ZM1 protected against 6-OHDA-induced effects. These results provide strong evidence for the hypothesis that RAGE inhibition blocks all signaling cascades involved in neuroinflammation and dopaminergic denervation. The neuronal death in SN manifested in locomotor deficit was confirmed by rotarod test and apomorphine-induced rotations (Fig. 7a and b). In addition, the animals displayed depression-like behavior and decrease in exploratory interest (Fig. 7c) that is correlated with DA impairments²⁶. FPS-ZM1 also protects against 6-OHDA-induced behavioral changes. There was an increase in exploratory interest, probably because there was an increase in the expression of neurotransmitters. The behavioral impairments along with reduced number of neurons in the SN provide concrete evidence for the progressive death of DA neurons. FPS-ZM1 protects against this effect of 6-OHDA.

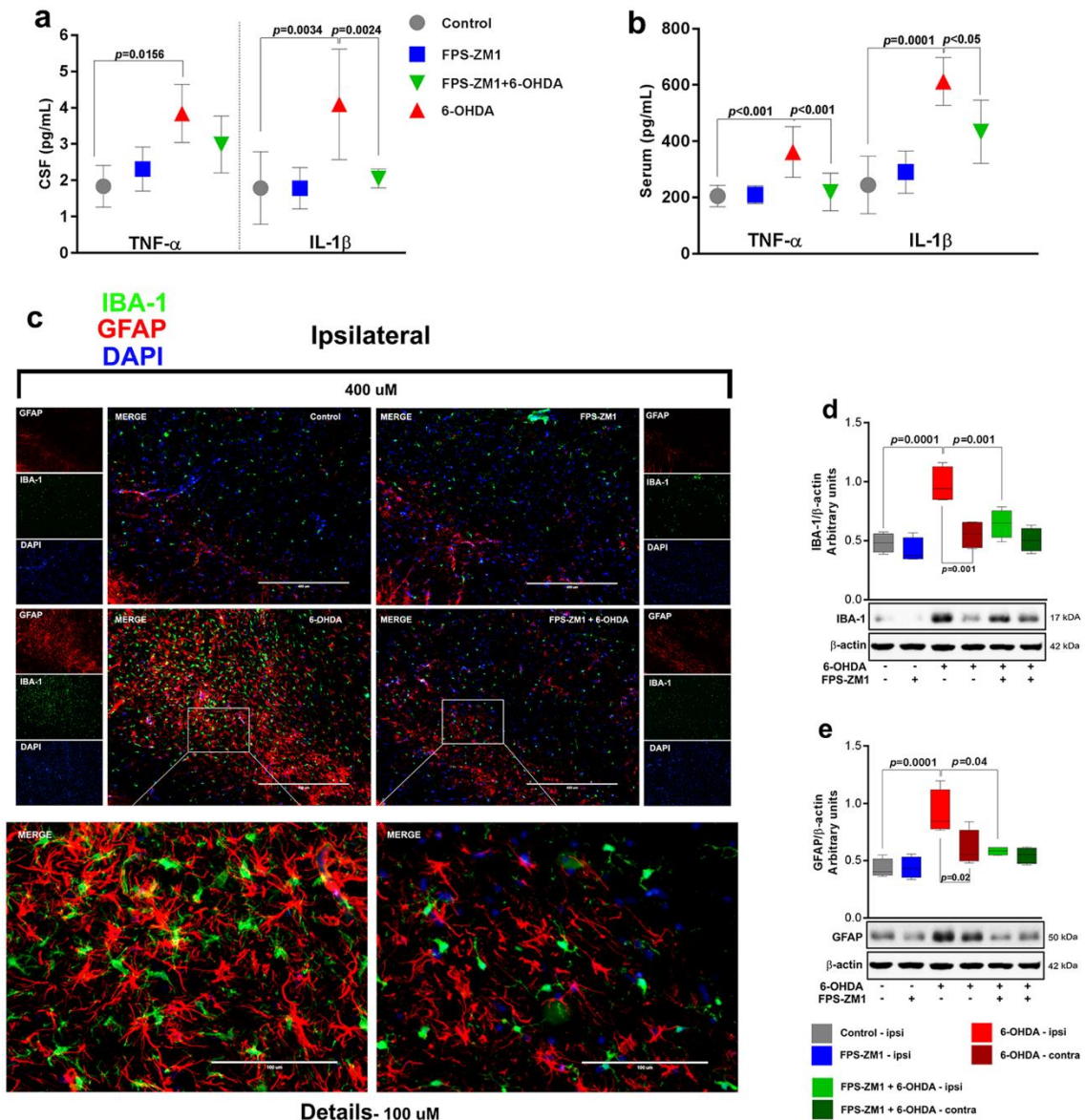


Figure 5. FPS-ZM1 protected rats from 6-OHDA-induced neuronal inflammation. CSF and serum were analyzed by ELISA assay 15 days after 6-OHDA administration. (a) Cerebrospinal fluid was analyzed for TNF- α and IL-1 β . TNF- α and IL-1 β levels are expressed in pg/mL. (b) Serum samples were analyzed for TNF- α and IL-1 β . (c) Representative immunofluorescence images of SN co-immunostained for IBA-1, GFAP and DAPI ($n = 10$ per group). The ipsilateral sides are shown. The microscopy images were taken with 400 μ m of magnification and the squares represents the location of the approximation of 100 μ m. Representative western blots and quantification of (d) IBA-1 ($n = 6$ per group) and (e) GFAP ($n = 6$ per group). Each color in the graph represents a group and a brain location: gray - control/ipsilateral side; blue - FPS-ZM1/ipsilateral side; red - 6-OHDA/ipsilateral side; dark red - 6-OHDA/green - FPS-ZM1 + 6-OHDA/ipsilateral side; dark green - FPS-ZM1 + 6-OHDA/contralateral side. Values represent mean \pm SD. One-way analysis of variance and Bonferroni Multiple Comparison *post-hoc* test were applied to all data. p values are embedded in the figure.

Conclusion

The multimodal blocker of RAGE, FPS-ZM1, shows a neuroprotective activity in the rat model of 6-OHDA-induced PD. FPS-ZM1 injected in the SN blocked dopaminergic denervation, neuroinflammation, and locomotor/exploratory deficits induced by 6-OHDA. The probable chain of events triggered by 6-OHDA in the SN of rats, according to our results, includes RAGE activation and upregulation, followed by activation of downstream signaling that involves ERK1/2 and Src, leading to p65 nuclear translocation and consequent pro-inflammatory response. This latter effect results in activation of astrocytes and microglia and increased

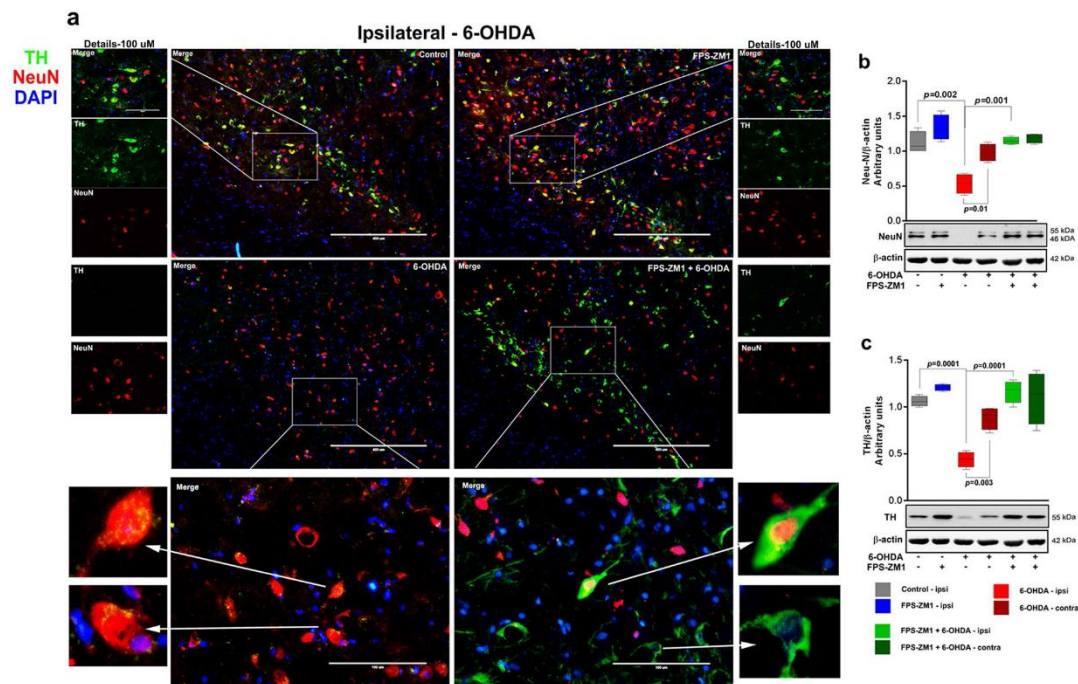


Figure 6. FPS-ZM1 inhibited 6-OHDA-induced neuronal death. Tissues were prepared for immunofluorescence and western blotting 15 days after 6-OHDA administration. (a) Representative immunofluorescence images of SN immunostained for TH, NeuN, and DAPI ($n = 10$ per group). The ipsilateral sides are shown. The microscopy images were taken with 400 μ m of magnification and the squares represents the approximation to 100 μ m. (b) Representative western blots and quantification of NeuN ($n = 6$ per group) and c) TH ($n = 6$ per group). Each color in the graph represents a group and a brain location: gray - control/ipsilateral side; blue - FPS-ZM1/ipsilateral side; red - 6-OHDA/ipsilateral side; dark red - 6-OHDA/contralateral side; green - FPS-ZM1 + 6-OHDA/ipsilateral side; dark green - FPS-ZM1 + 6-OHDA/contralateral side. Values represent mean \pm SD. One-way analysis of variance and Bonferroni Multiple Comparison *post-hoc* test were applied to all data. p values are embedded in the figure.

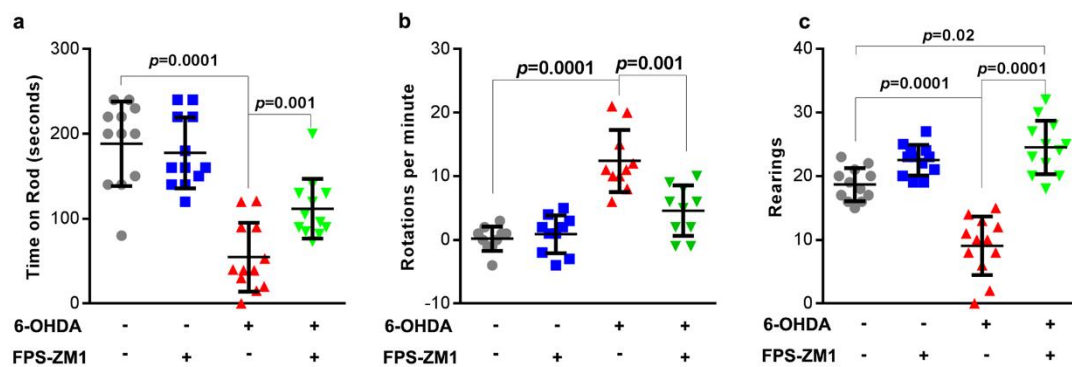


Figure 7. FPS-ZM1 protects rats from 6-OHDA-induced motor deficits. Locomotor abilities of rats injected with 6-OHDA were examined 14 days after the injection. (a) Rotarod test - total time on the rod limited to 4 min. (b) Rotational activity after apomorphine challenging. (c) Open field rearing test - duration limited to 5 min. Values represent mean \pm SD from ten rats per group. One-way analysis of variance and Bonferroni Multiple Comparison *post-hoc* test were applied to all data. p values are embedded in the figure. $n = 12$ per group was used for rotarod and rearing test, $n = 10$ per group was used to measure the rotational activity.

circulating cytokines in CSF and serum. This, in turn, contributes to cell death and consequent loss of dopaminergic neurons (neurodegeneration), which is reflected in the deficits in locomotor and exploratory behavior. FPS-ZM1 was effective in blocking the dopaminergic denervation induced by 6-OHDA. However, it did not bring back the rotarod performance to control levels, indicating that molecular pathways other than RAGE also contribute to locomotor deficits caused by 6-OHDA, which is expected. Co-localization immunofluorescence results indicate that neurons are the main cells expressing RAGE in the SN of 6-OHDA-injected rats. Despite the limitations of this model, the present results indicate that the potential application of RAGE pharmacological inhibition in PD and the understanding of the role of this receptor in the pathophysiology of this disease must be investigated in more details.

Methods

Chemicals. Electrophoresis and immunoblotting apparatus were from Bio-Rad (Hercules, USA) and GE Healthcare Brazilian Headquarter (Sao Paulo, Brazil), respectively. The antibody information is listed in the descriptions of each technique. All other reagents used in this study were of analytical or HPLC grade.

Ethics Statement. Our research protocol was approved under project number 27683 by the Ethical Committee for Animal Experimentation of the Universidade Federal do Rio Grande do Sul-Brazil (CEUA-UFRGS). All experimental procedures were performed in accordance with the guidelines of the National Institutes of Health²⁷ and the Brazilian Society for Neuroscience and Behavior recommendations for animal care. All efforts were made to minimize animal suffering.

Animals. Male Wistar rats (60 days old) bred in our facilities were maintained at constant temperature of $21 \pm 1^\circ\text{C}$ and 12-hour light–dark cycle. They were caged in groups of four animals with free access (*ad libitum*) to water and standard commercial food (Chow Nuvilab CR-1 type; PR, Brazil). The rats were anesthetized with a single dose of ketamine (100 mg/kg; i.p.) and xilazine (10 mg/kg; i.p.) for all surgical procedures.

FPS-ZM1 and 6-hydroxydopamine (6-OHDA) preparation. FPS-ZM1 ($\text{C}_{20}\text{H}_{22}\text{ClNO}$) is a non-toxic, tertiary amide compound that acts as a high affinity multimodal blocker of RAGE V domain-mediated ligand binding ($K_i = 25, 148, \& 230 \text{ nM}$)³. It was dissolved in a small amount of dimethylsulfoxide (DMSO) and then diluted with saline to 10 $\mu\text{g}/\mu\text{L}$ stock solution. The final DMSO concentration was 0.02%. FPS-ZM1 was purchased from Merck Millipore (MA, USA). Each rat received injection with 40 μg of FPS-ZM1 into the SN. 6-OHDA is a neurotoxic synthetic organic compound that destroys catecholaminergic terminals. It was prepared as a 5 $\mu\text{g}/\mu\text{L}$ solution in 0.02% ascorbic acid dissolved in sterile saline, protected from heat and light. 6-OHDA was purchased from Sigma-Aldrich® (MO, USA). Each rat was administered with 10 μg ²⁸ of 6-OHDA.

Experimental design. The rats were randomly divided into four groups:

- Group 1: control group received intranigral injection of saline solution.
- Group 2: received FPS-ZM1 (intranigral injection).
- Group 3: received 6-OHDA (intranigral injection).
- Group 4: received FPS-ZM1 + 6-OHDA (intranigral injection).

Fourteen days after the induction of the SN lesion (see below), behavior tests were performed. On the 15th day, all the animals were anaesthetized and CSF was sampled. Six animals from each group were decapitated and serum was collected, followed by dissection of the SN for analysis. Ten animals in each group were intracardially perfused for immunofluorescence assessment.

Surgical Procedure. Anesthetized rats were immobilized by securing via ear and nose bars on a stereotaxic apparatus (Insight-EFF 338, SP, BRA). Fur was shaved with a pet clipper (SKU #: 09160-210 – Wahl; IL, USA) and 10% povidone-iodine solution was applied to sterilize the incision site. The skulls were trepanned with a dental drill (3 mm) at the appropriate location. A single dose (2 μL) of 6-OHDA²⁸ or FPS-ZM1³ or saline was injected into the left SN at the following stereotaxic coordinates: antero-posterior (AP): –5.0 mm from bregma; medio-lateral (ML): ± 2.1 mm from the midline; dorso-ventral (DV): –8.0 mm from skull, according to the Rat Brain Atlas in Stereotaxic Coordinates Paxinos²⁹, using a 10- μL Hamilton® syringe 701SN, needle size 23s ga (Sigma-Aldrich®, MO, USA). Syringes were lowered into the brain at a rate of 2 mm/min. The chemicals were injected at a rate of 0.5 $\mu\text{L}/\text{min}$ and the syringe was left in place for 2 min after injection, before drawing back at a rate of 2 mm/min. The incision was thoroughly cleaned with povidone-Iodine solution and closed using three sutures. Lactated Ringer's solution (1 mL) was injected subcutaneously to replenish electrolytes. Nebacetin (Medley; RS, BRA) was applied topically to the incision to prevent infections. The animals were removed from stereotaxic frame and placed in a controlled temperature recovery cage (37°C) until they regained consciousness. The animals were returned to the housing facility 2 h after the surgery.

Immunofluorescence microscopy. Fifteen days after the surgery, rats were perfused via the vascular system with descending aorta clamped. Sterile saline was administered for 10 min followed by perfusion with 4% paraformaldehyde (PFA) solution in PBS, pH 7.4, for 10 more minutes. The brains were then carefully recovered and maintained in 4% PFA for 24 h at 4°C . The brains were then transferred into 15% sucrose solution for 24 h at 4°C followed by immersion in 30% sucrose for additional 24 h at 4°C . Brains were lightly dried and frozen at -20°C . After 24 h, the SN region was sectioned into slices of 15 μm thickness on the coronal plane using a cryostat at -20°C (Jung Histoslide 2000R; Leica; Heidelberg, Germany). A total of 20–30 slices per rat containing SN were collected in PBS containing 0.1% triton $\times 100$. The free-floating sections were incubated in 5%

albumin for 2 h to block nonspecific binding. The sections were then incubated with antibodies for 48 h at 4 °C. The details of the antibody source and dilutions are as follows. Anti-GFAP (1:500- G6171) and DAPI for nucleic acid staining (1:500; D9542) were from Sigma-Aldrich® (MO, USA). Anti-IBA-1 (1:500; 019-19741) was from Wako Chemicals USA, Inc. (VA, USA). Anti-RAGE (1:200; PA1-84173) was from Thermo Fisher Scientific (MA, USA). Anti-NeuN (1:500; MAB377) was from Merck Millipore (MA, USA). Anti-NF- κ B -p65 (1:200; 6956) and Anti-TH (1:200; 2792 S) were from Cell Signaling Technology® (MA, USA). Antibodies were diluted in PBS containing 2% bovine serum albumin. Primary antibodies were excluded from the incubation of negative controls. After washing four times with 0.1% PBS, tissue sections were incubated with secondary antibodies, which included anti-rabbit Alexa 488 or 555; anti-mouse Alexa 488 or 555 and Alexa anti-goat 555 from Cell Signaling Technology® (MA, USA), all of them diluted 1:500 in PBS containing 2% BSA. After incubation in secondary antibodies for 1 h at room temperature (21 ± 3 °C), the sections were washed several times in 0.1% PBS, transferred to gelatinized slides, mounted with FluorSave™ (345789- Merck Millipore; MA, USA) and covered with coverslips. The images were acquired using a Microscopy EVOS® FL Auto Imaging System (AMAFD1000 - Thermo Fisher Scientific; MA, USA). The Z-axis images were collected using a Laser-scanning confocal microscopy (Olympus FV 1000, Tokyo, Japan).

Enzyme-linked immunosorbent assay (ELISA) determination of cytokines. TNF- α (RAB0479-1KT) and IL-1 β (RAB0272-1KT) were quantified with commercial kits from Sigma-Aldrich® (MO, USA). The CSF from *cisterna magna* and blood serum samples were incubated in ELISA plates and processed further according to the manufacturer's protocol.

Western blotting. For immunoblotting experiments, tissues were prepared using a radioimmunoprecipitation assay buffer protocol³⁰. Total proteins (30 μ g/well) were fractionated by SDS-PAGE and electroblotted onto nitrocellulose membranes with Trans-Blot Semi-Dry Electrophoretic Transfer Cell (Bio-Rad; CA, USA). Protein loading and electroblotting efficiency were verified through Ponceau S staining. After washing with TTBS (100 mM Tris - HCl, pH 7.5, containing 0.9% NaCl, and 0.1% Tween-20), the membranes were incubated with primary antibodies (1:500 dilutions) for 20 min at room temperature in SNAP i.d. 2.0 Protein Detection System (Merck Millipore; MA, USA). The membranes were washed again with TTBS. Polyclonal and monoclonal antibodies used were from Cell Signaling Technology® (MA, USA) and included the following: anti-p-ERK-44/42 (Thr202/Tyr204) (9101), anti-ERK-44/42 (9102), anti-p-Src (Tyr416) (2101), anti-Src (2108), p-p38 (4511), anti-p38 (8690), anti-p-SAPK/JNK (Thr183/Tyr185) (9255), and anti-SAPK/JNK (9252). The blots were incubated with anti-rabbit, goat or mouse peroxidase-linked secondary antibody for an additional 20 min in SNAP (1:5000 dilution) and washed again. The immunoreactivity was detected by enhanced chemiluminescence using Supersignal West Pico Chemiluminescent kit from Thermo Fisher Scientific (MA, USA). The chemiluminescence was captured with an ImageQuant LAS 4000 (GE Healthcare; SP, Brazil). Densitometric analysis of the images were performed using ImageJ software (ImageJ v1.49, National Institute of Health, USA). Blots were developed to be linear in the range used for densitometry. All results were expressed as relative ratio to β -actin (A1978) from Sigma-Aldrich® (MO, USA) or total protein content.

Behavioral tests (locomotor, rotational and exploratory activities). The motor system was evaluated using the rotarod test. The protocol was performed at a constant speed of 21 rpm. The cut-off time was 240 s³¹. The animals were acclimated to the apparatus with three prior training sessions at one-hour intervals. The duration on rotarod during experimental sessions was measured. The mean of 3 attempts were used for the statistical analyses.

Apomorphine-induced rotation test was performed to study the hypersensitivity of the lesioned SN. Apomorphine 0.1 mg/kg (dissolved in a 0.2 mg/mL ascorbic acid in 0.9% saline solution) was subcutaneously injected and tested over a 40 min session. Animals were allowed to habituate for 5 min after injection before the recording of rotations began in cylinder rotameter (400 mm diameter). Full body ipsilateral and contralateral side rotations were counted by an observer who was blind to the animal pretreatments. The data were expressed as the net (contralateral - ipsilateral turns) average rotations per min (RPM)³². Apomorphine was purchased from Sigma-Aldrich®; MO, USA.

The other parameter evaluated was the number of rearing events. In an open field test, the rearing episodes were scored when the animal displayed a vertical exploratory activity³³.

Protein assay. Total protein was quantified by Bradford assay and used to normalize all data³⁴.

Statistical analysis. Statistical analysis was performed using GraphPad Prism version 7 (GraphPad Software Inc., CA, USA). Data were evaluated by one-way ANOVA followed by Bonferroni multiple comparison *post-hoc* test. The results are expressed as mean \pm SD. Differences were considered significant when $p < 0.05$.

References

1. Wang, Q., Liu, Y. & Zhou, J. Neuroinflammation in Parkinson's disease and its potential as therapeutic target. *Transl Neurodegener* **4**, doi:10.1186/s40035-015-0042-0 (2015).
2. Juranek, J. K. *et al.* Receptor for Advanced Glycation End Products and its Inflammatory Ligands are Upregulated in Amyotrophic Lateral Sclerosis. *Front Cell Neurosci* **9**, doi:10.3389/fncel.2015.00485 (2015).
3. Deane, R. *et al.* A multimodal RAGE-specific inhibitor reduces amyloid beta-mediated brain disorder in a mouse model of Alzheimer disease. *J Clin Invest* **122**, 1377–1392, doi:10.1172/jci58642 (2012).
4. Teismann, P. *et al.* Receptor for advanced glycation endproducts (RAGE) deficiency protects against MPTP toxicity. *Neurobiology of aging* **33**, 2478–2490, doi:10.1016/j.neurobiolaging.2011.12.006 (2012).

5. De Jesus-Cortes, H. *et al.* Protective efficacy of P7C3-S243 in the 6-hydroxydopamine model of Parkinson's disease. *NPJ Parkinsons Dis* **1**, doi:10.1038/nnpjarkd.2015.10 (2015).
6. Thiele, S. L., Warre, R. & Nash, J. E. Development of a unilaterally-lesioned 6-OHDA mouse model of Parkinson's disease. *J Vis Exp*. doi:10.3791/3234 (2012).
7. Hong, Y. *et al.* Effects of RAGE-Specific Inhibitor FPS-ZM1 on Amyloid-beta Metabolism and AGEs-Induced Inflammation and Oxidative Stress in Rat Hippocampus. *Neurochem Res* **41**, 1192–1199, doi:10.1007/s11064-015-1814-8 (2016).
8. Yang, F. *et al.* Receptor for advanced glycation end-product antagonist reduces blood-brain barrier damage after intracerebral hemorrhage. *Stroke* **46**, 1328–1336, doi:10.1161/strokeaha.114.008336 (2015).
9. Maczurek, A., Shanmugam, K. & Munch, G. Inflammation and the redox-sensitive AGE-RAGE pathway as a therapeutic target in Alzheimer's disease. *Annals of the New York Academy of Sciences* **1126**, 147–151, doi:10.1196/annals.1433.026 (2008).
10. Xie, J., Mendez, J. D., Mendez-Valenzuela, V. & Aguilar-Hernandez, M. M. Cellular signalling of the receptor for advanced glycation end products (RAGE). *Cellular signalling* **25**, 2185–2197, doi:10.1016/j.cellsig.2013.06.013 (2013).
11. Tobon-Velasco, J. C., Cuevas, E. & Torres-Ramos, M. A. Receptor for AGEs (RAGE) as mediator of NF- κ B pathway activation in neuroinflammation and oxidative stress. *CNS & neurological disorders drug targets* **13**, 1615–1626 (2014).
12. Dunkley, P. R., Bobrovskaya, L., Graham, M. E., von Nagy-Felsobuki, E. I. & Dickson, P. W. Tyrosine hydroxylase phosphorylation: regulation and consequences. *Journal of neurochemistry* **91**, 1025–1043, doi:10.1111/j.1471-4159.2004.02797.x (2004).
13. Grealish, S., Mattsson, B., Draxler, P. & Bjorklund, A. Characterisation of behavioural and neurodegenerative changes induced by intranigral 6-hydroxydopamine lesions in a mouse model of Parkinson's disease. *Eur J Neurosci* **31**, 2266–2278, doi:10.1111/j.1460-9568.2010.07265.x (2010).
14. Simola, N., Morelli, M. & Carta, A. R. The 6-hydroxydopamine model of Parkinson's disease. *Neurotox Res* **11**, 151–167 (2007).
15. Dauer, W. & Przedborski, S. Parkinson's disease: mechanisms and models. *Neuron* **39**, 889–909 (2003).
16. Zhang, H. *et al.* Genetic deficiency of neuronal RAGE protects against AGE-induced synaptic injury. *Cell death & disease* **5**, e1288, doi:10.1038/cddis.2014.248 (2014).
17. Ray, R., Juranek, J. K. & Rai, V. RAGE axis in neuroinflammation, neurodegeneration and its emerging role in the pathogenesis of amyotrophic lateral sclerosis. *Neuroscience and biobehavioral reviews* **62**, 48–55, doi:10.1016/j.neubiorev.2015.12.006 (2016).
18. Safavi-Abbasi, S., Wolff, J. R. & Missler, M. Rapid morphological changes in astrocytes are accompanied by redistribution but not by quantitative changes of cytoskeletal proteins. *Glia* **36**, 102–115 (2001).
19. Avignone, E., Lepleux, M., Angibaud, J. & Nägerl, U. V. Altered morphological dynamics of activated microglia after induction of status epilepticus. *J Neuroinflammation* **12**, doi:10.1186/s12974-015-0421-6 (2015).
20. Healy-Stoffel, M., Ahmad, S. O. & Stanford, J. A. & Levant, B. Altered nucleolar morphology in substantia nigra dopamine neurons following 6-hydroxydopamine lesion in rats. *Neurosci Lett* **546**, 26–30, doi:10.1016/j.neulet.2013.04.033 (2013).
21. Ramasamy, R. *et al.* Advanced glycation end products and RAGE: a common thread in aging, diabetes, neurodegeneration, and inflammation. *Glycobiology* **15**, 16r–28r, doi:10.1093/glycob/cwi053 (2005).
22. Li, J. & Schmidt, A. M. Characterization and functional analysis of the promoter of RAGE, the receptor for advanced glycation end products. *The Journal of biological chemistry* **272**, 16498–16506 (1997).
23. Ishihara, K., Tsutsumi, K., Kawane, S., Nakajima, M. & Kasaoka, T. The receptor for advanced glycation end-products (RAGE) directly binds to ERK by a D-domain-like docking site. *FEBS letters* **550**, 107–113 (2003).
24. Sathe, K. *et al.* S100B is increased in Parkinson's disease and ablation protects against MPTP-induced toxicity through the RAGE and TNF- α pathway. *Brain: a journal of neurology* **135**, 3336–3347, doi:10.1093/brain/aws250 (2012).
25. Santoro, M. *et al.* In-vivo evidence that high mobility group box 1 exerts deleterious effects in the 1-methyl-4-phenyl-1,2,3,6-tetrahydropyridine model and Parkinson's disease which can be attenuated by glycyrrhizin. *Neurobiol Dis* **91**, 59–68, doi:10.1016/j.nbd.2016.02.018 (2016).
26. Santiago, R. M. *et al.* Depressive-like behaviors alterations induced by intranigral MPTP, 6-OHDA, LPS and rotenone models of Parkinson's disease are predominantly associated with serotonin and dopamine. *Progress in neuro-psychopharmacology & biological psychiatry* **34**, 1104–1114, doi:10.1016/j.pnpbp.2010.06.004 (2010).
27. National Institutes of Health Guide for Care and Use of Laboratory Animals. Eighth Edition. Available in <https://grants.nih.gov/grants/olaw/Guide-for-the-Care-and-Use-of-Laboratory-Animals.pdf> Accessed 15 Jan 2017 (1985).
28. Lima, M. M. *et al.* Motor and non-motor features of Parkinson's disease - a review of clinical and experimental studies. *CNS & neurological disorders drug targets* **11**, 439–449 (2012).
29. Paxinos, G. & Watson, C. *The Rat Brain in Stereotaxic Coordinates*. Sixth edition. Academic Press (2007).
30. Gasparotto, J. *et al.* Increased tau phosphorylation and receptor for advanced glycation endproducts (RAGE) in the brain of mice infected with *Leishmania amazonensis*. *Brain Behav Immun* **43**, 37–45, doi:10.1016/j.bbi.2014.06.204 (2015).
31. Colle, D. *et al.* Probulcol Increases Striatal Glutathione Peroxidase Activity and Protects against 3-Nitropropionic Acid-Induced Pro-Oxidative Damage in Rats. *PLoS One* **8**, doi:10.1371/journal.pone.0067658 (2013).
32. Boix, J., Padel, T. & Paul, G. A partial lesion model of Parkinson's disease in mice—characterization of a 6-OHDA-induced medial forebrain bundle lesion. *Behav Brain Res* **284**, 196–206, doi:10.1016/j.bbr.2015.01.053 (2015).
33. Schallert, T., Fleming, S. M., Leasure, J. L., Tillerson, J. L. & Bland, S. T. CNS plasticity and assessment of forelimb sensorimotor outcome in unilateral rat models of stroke, cortical ablation, parkinsonism and spinal cord injury. *Neuropharmacology* **39**, 777–787 (2000).
34. Bradford, M. M. A rapid and sensitive method for the quantitation of microgram quantities of protein utilizing the principle of protein-dye binding. *Anal Biochem* **72**, 248–254 (1976).

Acknowledgements

This work was supported by Conselho Nacional de Desenvolvimento Científico e Tecnológico (CNPq) #400437/2013-9, #443514/2014-3 and #401260/2014-3; FAPERGS #2299-2551/14-6; Propesq-UFRGS and Coordenação de Aperfeiçoamento de Pessoal de Nível Superior (CAPES).

Author Contributions


J.G. conducted the experiments, designed the study, analyzed the data and drafted the manuscript. C.T.R. and R.C.B. performed western blots. T.K.R. and N.S. performed immunofluorescence microscopy. A.K. and N.C.S. performed Behavioral tests. M.A.B.P. and J.C.F.M. performed data evaluation. D.P.G. supervised and coordinated this work. All authors reviewed the manuscript.

Additional Information

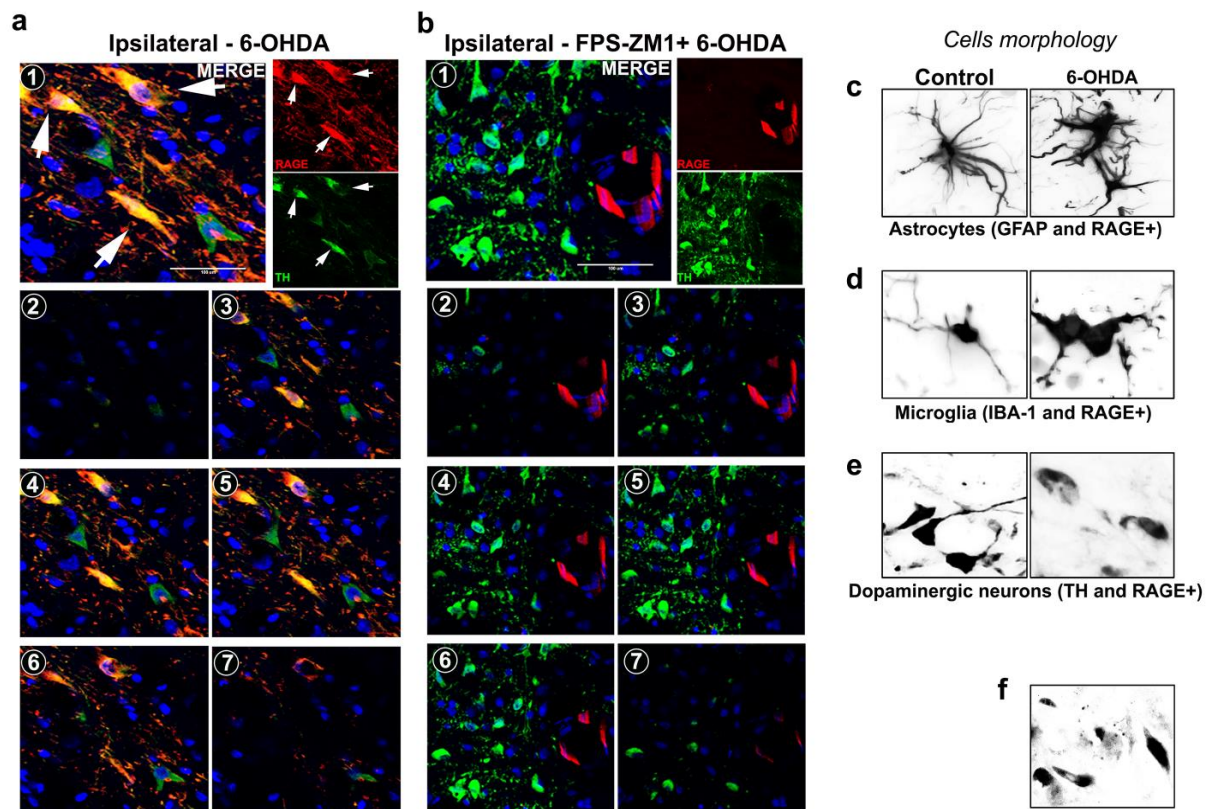
Supplementary information accompanies this paper at doi:10.1038/s41598-017-09257-3

Competing Interests: The authors declare that they have no competing interests.

Publisher's note: Springer Nature remains neutral with regard to jurisdictional claims in published maps and institutional affiliations.

 **Open Access** This article is licensed under a Creative Commons Attribution 4.0 International License, which permits use, sharing, adaptation, distribution and reproduction in any medium or format, as long as you give appropriate credit to the original author(s) and the source, provide a link to the Creative Commons license, and indicate if changes were made. The images or other third party material in this article are included in the article's Creative Commons license, unless indicated otherwise in a credit line to the material. If material is not included in the article's Creative Commons license and your intended use is not permitted by statutory regulation or exceeds the permitted use, you will need to obtain permission directly from the copyright holder. To view a copy of this license, visit <http://creativecommons.org/licenses/by/4.0/>.

© The Author(s) 2017



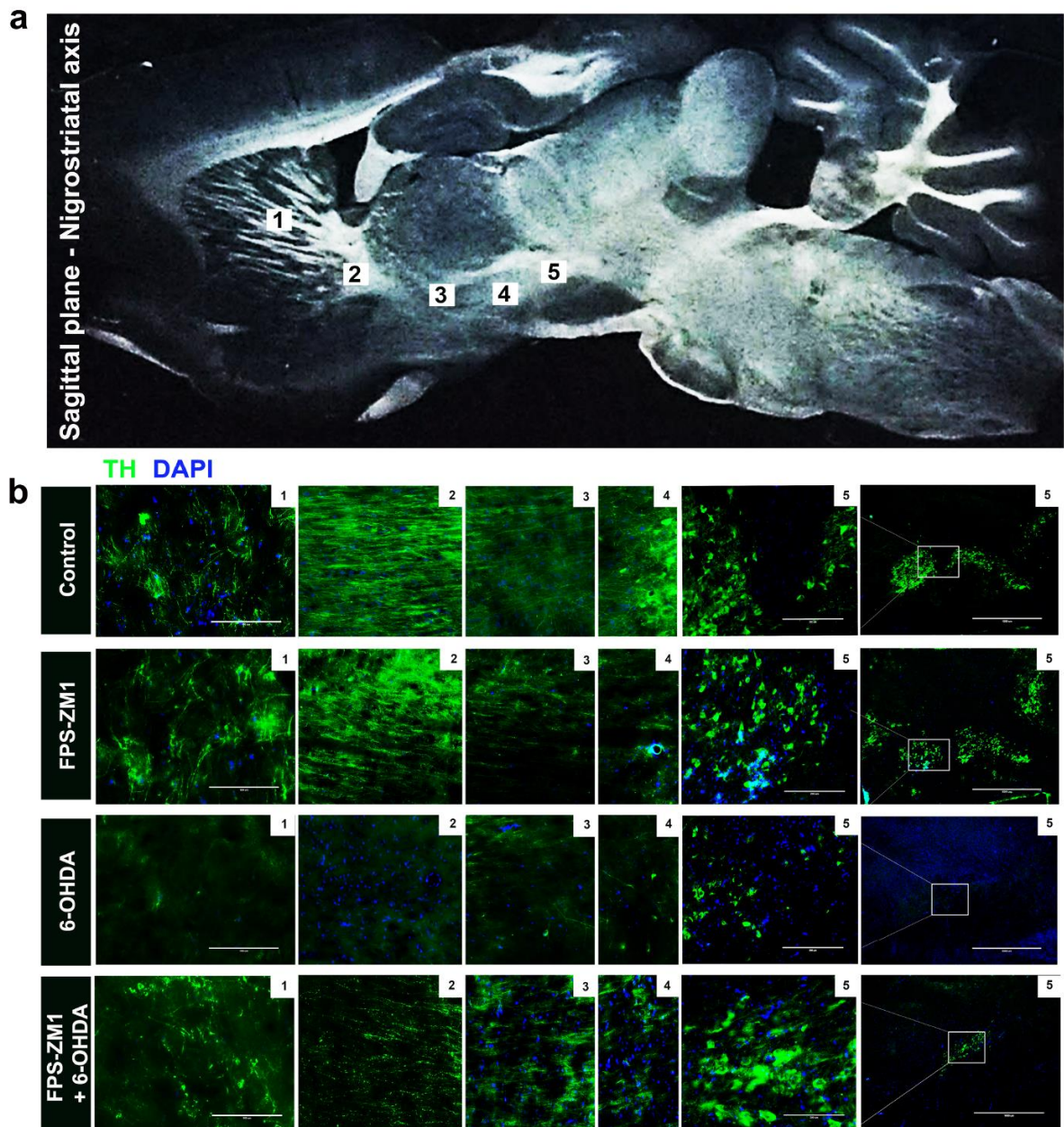
Supplementary figure S1. RAGE is localized to TH(+) neurons.

SN were prepared for immunofluorescence 15 days after the administration of 6-OHDA.

a) Confocal representative immunofluorescence images of SN co-immunostained for TH, RAGE and DAPI to ipsilateral 6-OHDA-induced and **b)** ipsilateral FPS-ZM1+6-OHDA (n=10 per group): Only ipsilateral sides are showed.

The confocal microscopy images were taken with 100 um of magnification and the z-axis layers (1-7) are detailed. Detailed cell morphology focused in one cell and shown in black and white:

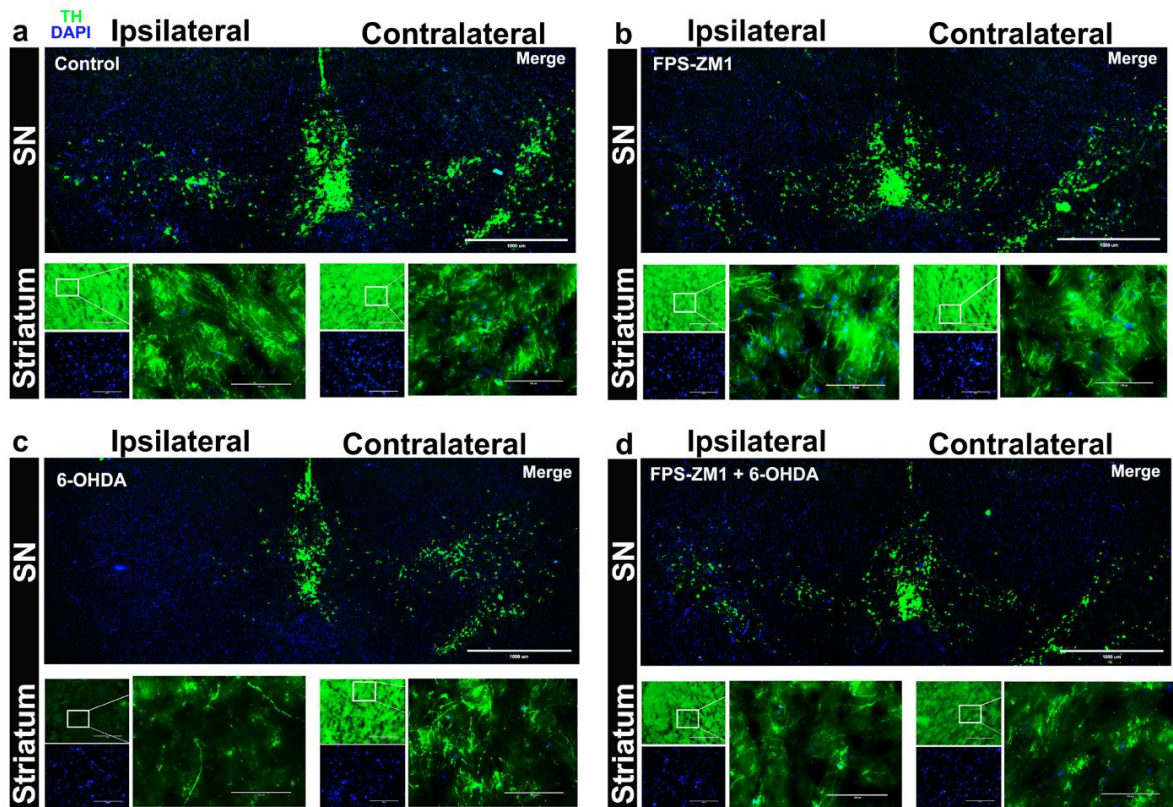
c) Astrocytes. **d)** Microglia. **e)** Dopaminergic neurons. **f)** Cells immunostained only with RAGE.



Supplementary figure S2. FPS-ZM1 blocked denervation 6-OHDA-induced in nigrostriatal axis

Rats were prepared for immunofluorescence 15 days after the injection of 6-OHDA.

a) Picture of rat brain, the numbers (1-5) represents the location of the image microscopy (100 or 400 um of magnification). **b)** The extent of damage to the nigrostriatal axis immunostained for TH and DAPI. The ipsilateral sides are shown ($n=3$ per group).



Supplementary figure S3. FPS-ZM1 blocked denervation 6-OHDA-induced in SN and striatum
 SN and striatum were prepared for immunofluorescence 15 days after the injection of 6-OHDA.
 a) control, b) FPS-ZM1, c) 6-OHDA and d) FPS-ZM1+6-OHDA representative immunofluorescence images of SN and striatum co-immunostained for TH and DAPI (n=10 per group). The ipsilateral and contralateral sides are shown. The microscopies magnification is detail in each image.

Parte 3.

Discussão

Inicialmente nomeado como receptor para AGEs, o RAGE apresenta muito mais funções do que a atividade que lhe foi primeiramente descrita. Atualmente o RAGE é o foco de investigação de diversos grupos de pesquisa, tal interesse é resultado da capacidade deste receptor em reconhecer padrões e de ligar inúmeras moléculas identificadas como ligantes do RAGE. Este receptor é essencial em mamíferos e tem como principal função mediar a composição da estrutura celular nos períodos do desenvolvimento. Após este período e em condições saudáveis, RAGE apresenta níveis basais reprimidos, porém perante a algum estímulo, por exemplo, o aumento de seus ligantes, o RAGE se torna nocivo para as células (Uttara *et al.*, 2009; Chuah *et al.*, 2013; Juranek *et al.*, 2015).

O RAGE é muito eficiente em desempenhar suas funções de mediador de sinais múltiplos, pois possui alta capacidade de adaptação a diferentes estímulos, o *splicing* alternativo, a oligomerização, a dimerização e até mesmo a multimerização são exemplos desta resposta altamente dinâmica de interagir com seus ligantes. Não bastasse a habilidade de adaptação e ligação, o RAGE parece ter preferência por moléculas que possuem características de auto-agregação como o peptídeo β -amilóide (Chuah *et al.*, 2013).

O descobrimento da presença do RAGE em vários tipos celulares no cérebro e sua relação com diversas patologias destaca este receptor como um dos principais responsáveis pelo eixo da sinalização inflamatória, possuindo uma função que pode ser caracterizada como mediador pró-inflamatório.

A expressão do RAGE no SNC foi observada pela primeira vez em neurônios motores corticais no sistema nervoso de bovinos (Brett *et al.*, 1993) e muito já foi especulado sobre a função do RAGE desde então, mas poucas constatações concretas foram estabelecidas. Nosso foco central desta tese é investigar a relação mediadora do RAGE na neuroinflamação e morte neuronal. Nos capítulos (I-IV) desta tese utilizamos diferentes modelos experimentais *in vivo* para indução de inflamação sistêmica e neuroinflamação com o intuito de investigar e elucidar o envolvimento do RAGE na neuroinflamação e neurodegeneração.

Primeiramente, no capítulo I utilizamos a *L. amazonensis* para investigar a modulação do RAGE no cérebro de camundongos (BALB/c) em resposta a um agente patogênico periférico. Nosso estudo demonstrou que a infecção periférica induzida por *L. amazonensis* afeta a fosforilação de tau e o conteúdo do RAGE no córtex de camundongos (BALB/c), além de induzir estresse e dano oxidativo. É importante salientar que, no modelo utilizado, não há presença de parasitas no sistema nervoso central. Estes resultados somados com outros publicados por nosso grupo (De Oliveira *et al.*, 2013; Gasparotto, Kunzler, *et al.*, 2017) destacam o envolvimento do RAGE nas doenças infecciosas induzida por parasitas.

Existem múltiplos relatos em medicina humana e veterinária relacionando a *L. amazonensis* com manifestações neurológicas (Nieto *et al.*, 1996; Gontijo *et al.*, 2002; Abreu-Silva *et al.*, 2003). Pacientes de leishmaniose apresentam alterações neurológicas induzidas pela doença (Petersen e Greenlee, 2011), porém o mecanismo pelo qual a doença afeta o SNC é pouco investigada. Considerando nossos resultados, é possível que os sintomas neurológicos associados à leishmaniose crônica sejam mediados por RAGE.

No capítulo II realizamos um mapeamento entre a inflamação sistêmica e a neuroinflamação utilizando LPS como agente indutor de inflamação aguda e anti-RAGE como método de neutralização imune do RAGE. A administração sistêmica de LPS (i.p.) tem sido usada repetidamente em modelos com ratos e camundongos a fim de determinar o papel da inflamação na degeneração dos neurônios dopaminérgicos localizados no eixo nigro-estriatal (Liu e Bing, 2011; Reinert *et al.*, 2014). Os neurônios dopaminérgicos destas regiões são vulneráveis a processos de inflamação e estresse oxidativo (Dunkley *et al.*, 2004; Damanhuri *et al.*, 2012). Estudos anteriores demonstram que, independentemente da idade do animal, a injeção sistêmica de LPS causa danos severos no sistema dopaminérgico (Qin *et al.*, 2007; Liu *et al.*, 2008).

Nossa investigação teve como objetivo principal verificar como o bloqueio do RAGE afeta a resposta aguda ao LPS no soro, fígado, líquido cefalorraquidiano e principalmente em diferentes estruturas do cérebro (estriado, córtex pré-frontal, área tegmental ventral e substância negra) de ratos Wistar. A compreensão do mecanismo e as vias que ocorrem os primeiros sinais de inflamação e estresse oxidativo no SNC são essenciais para elucidação de como o RAGE aumenta e acumula cronicamente em diferentes estruturas do SNC.

Nossos resultados disponibilizaram evidências de que a inflamação sistêmica induz a disfunção transitória ou permanente no cérebro expondo-o a mediadores inflamatórios solúveis. Ainda, forneceu evidências do envolvimento da sinalização do RAGE na neuroinflamação, fosforilação de tau, regulação da sinaptofisina e comprometimento do estado redox cerebral resultante de inflamação sistêmica. O bloqueio sistêmico do RAGE é capaz de proteger o estriado de danos causados pela injeção sistêmica de LPS, reduzindo a ativação microglial e astrocitária bem como parâmetros de dano neuronal (Gasparotto, Tiefensee Ribeiro, *et al.*, 2017). Este efeito

foi observado ocorrer de forma aguda (até 24 horas após a indução de inflamação) e o bloqueio de RAGE inibiu a ativação sistêmica de NF- κ B e liberação de citocinas pró-inflamatórias na circulação.

Os efeitos encontrados estão diretamente relacionados com o RAGE, visto que os ratos que tiveram seus receptores bloqueados não apresentaram a resposta inflamatória encontrada nos animais que receberam apenas LPS. Além dos resultados publicados no capítulo II, também investigamos outros órgãos como pulmões, baço, rins e coração, porém não foram constatadas alterações significativas (dados não publicados). Investigações de longo prazo utilizando este modelo ainda estão em andamento pelo nosso grupo.

No capítulo III, utilizamos o modelo de sepse com intuito de investigar os efeitos do RAGE na neuroinflamação, neurodegeneração e na disfunção cognitiva tempo-dependente em ratos Wistar. Ratos Wistar foram submetidos a ligadura cecal (CLP), e perfuração. Amostras de soro e cérebro (hipocampo e córtex pré-frontal) foram obtidas nos dias 1, 15 e 30 após o CLP. RAGE e seus ligantes foram investigados. Os animais que sobrevivem a sepse apresentam alterações cerebrais comumente associado ao início de processos neurodegenerativos (Gasparotto *et al.*, 2018). Para determinar o papel do RAGE na disfunção neuronal, administramos anti-RAGE diretamente no hipocampo dos ratos como intervenção terapêutica para os efeitos causados pela sepse. Ratos que receberam o anti-RAGE tiveram diminuição do acúmulo do peptídeo β -amilóide, diminuição da fosforilação da tau^{Ser202} e níveis de sinalização de Akt /mTOR igual a grupos controle, além da diminuição dos déficits comportamentais associados ao declínio cognitivo. Estes resultados indicam que o RAGE é fator essencial na patogênese de transtornos neurológicos após inflamação sistêmica aguda induzida por sepse.

Pacientes que se recuperam de sepse têm taxas mais altas de comprometimento das funções cognitivas, incluindo doenças neurodegenerativas (Semmler *et al.*, 2008) como a doença de Alzheimer. Estudos imuno-histoquímicos com tecido cerebral humano demonstraram que os níveis do RAGE são aumentados em pacientes com a doença de Alzheimer em relação a grupo controle (Sasaki *et al.*, 2001; Miller *et al.*, 2008). A expressão do RAGE está presente em células endoteliais cerebrais, astrócitos, neurônios do hipocampo, córtex entorrinal e giro frontal superior, de pacientes com a doença (Jeynes e Provias, 2008; Miller *et al.*, 2008).

Como RAGE permanece ativado enquanto o β -amilóide está presente (Yan *et al.*, 1996), RAGE está diretamente envolvido na iniciação e amplificação da toxicidade neuronal de β -amilóide onde RAGE também contribui para a translocação de β A1-40 do espaço extracelular para o intracelular, difundindo-se entre as células e causando danos neuronais (Takuma *et al.*, 2009). A inibição da atividade do RAGE leva a uma queda pronunciada nos níveis *in vitro* e *in vivo* de ERO cerebral, bem como uma função cognitiva melhorada em animais e pacientes com doença de Alzheimer (Deane *et al.*, 2012; Hong *et al.*, 2016).

O estresse oxidativo é um indutor de aumento do RAGE, assim como RAGE pode induzir estresse oxidativo, esta relação foi observada em diferentes doenças, onde o aumento da produção de ERO é uma característica, incluindo diabetes, aterosclerose e doença de Parkinson (Guo *et al.*, 2008; Zhang *et al.*, 2008; Zhang *et al.*, 2009).

Em análises pós-morte realizadas em pacientes diagnosticados com doença de Parkinson, foi evidenciado o acúmulo de AGEs nos corpos de Lewy, o que aconteceu provavelmente devido a glicação das proteínas desempacotadas que constituem esses aglomerados (Munchau e Bhatia, 2000). O aumento do conteúdo do

RAGE em corpos de Lewy foi demonstrado até mesmo em condições pré-sintomáticas à doença de Parkinson, destacando a presença do receptor mesmo sem haver os sintomas clássicos da doença (Dalfo *et al.*, 2005).

Para melhorar o entendimento de mecanismo de ação do RAGE nas doenças neurodegenerativas, optamos por uma abordagem mais direta de indução de morte neuronal, injetando 6-OHDA diretamente na substância negra de ratos Wistar. 6-OHDA é um composto orgânico sintético neurotóxico que destrói terminais catecolaminérgicos (Lima *et al.*, 2012). FSP-ZM1 (figura 4), um eficiente antagonista farmacológico do RAGE foi utilizado para bloquear o receptor, injetando-o no mesmo local que a 6-OHDA foi administrada. O tratamento com FPS-ZM1 vem sendo empregado para estudar modelos de neurotoxicidade (Deane *et al.*, 2012; Yang *et al.*, 2015; Hong *et al.*, 2016; Bongarzone *et al.*, 2017).

Efeitos pró-inflamatórios, oxidativos e neurotóxicos induzidos pela 6-OHDA foram bloqueados pelo antagonista do RAGE, no soro, no líquido cefalorraquidiano e na substância negra. Os resultados demonstram uma relação mediadora entre RAGE e a morte neuronal, onde RAGE desempenha um papel fundamental na propagação / amplificação de efeitos inflamatórios e na denervação dopaminérgica induzida por 6-OHDA na substância negra de ratos.

O RAGE é capaz de induzir um desequilíbrio oxidativo severo nos neurônios dopaminérgicos, pelo elevado número de mitocôndrias nestas células, apresentando uma predisposição ao consumo elevado de oxigênio (Dal-Pizzol *et al.*, 2001) e consequente vulnerabilidade maior ao estresse oxidativo. Apesar dos neurônios dopaminérgicos estarem adaptados às altas taxas de metabolismo oxidativo, componentes das defesas antioxidantes endógenas desses neurônios parecem ser comprometidos em algum estágio de progressão da doença de Parkinson, uma vez

que a análise *post-mortem* de tecidos cerebrais de pacientes demonstra o acúmulo de marcadores de dano oxidativo (Dal-Pizzol *et al.*, 2001).

O capítulo IV nos trouxe informações importantes da localização do RAGE. Até o momento, informações da presença do RAGE nos neurônios eram escassas (Sasaki *et al.*, 2001; Miller *et al.*, 2008). Nossos resultados demonstram a presença do RAGE no corpo dos neurônios. Este achado é fator crucial para compreensão do mecanismo de morte neuronal, visto que o receptor faz a mediação entre o meio extracelular para intracelular de diversas moléculas com potencial neurodegenerativo.

Os modelos animais contribuem para aumentar o conhecimento sobre a fisiopatologia das doenças neurodegenerativas. Todos os quatro modelos investigados para a construção desta tese apresentam envolvimento do RAGE. Esses modelos reproduzem diferentes aspectos de uma dada doença, bem como as lesões histopatológicas e seus principais sintomas. A investigação em diferentes modelos experimentais nos proporciona um melhor entendimento da abrangência de ação do RAGE em diferentes casos.

O modelo de *L. Amazonensis* nos disponibilizou a primeira informação quanto a presença do RAGE no córtex pré-frontal de camundongos induzido por uma infecção periférica. Os modelos utilizando o LPS ou a sepse (mimetizam um ambiente de infecção bacteriana) foram utilizados para investigar o papel do RAGE nas respostas iniciais dos processos inflamatórios. Nossos resultados demonstraram que os processos inflamatórios e degenerativos em diferentes estruturas do SNC foram mediados por RAGE. O modelo utilizando a 6-OHDA é um método clássico de infusão intracraniana que induz a destruição maciça à nível celular dos neurônios dopaminérgicos do eixo nigrostriatal, este modelo é amplamente utilizado para investigar disfunções motoras e bioquímicas semelhantes as observadas na doença

de Parkinson. Neste modelo o RAGE foi o principal mediador da morte neuronal. Portanto, apesar dos insultos pró-inflamatórios iniciais serem diferentes, a presença do RAGE é marcante em todos os modelos e é o responsável por mediar processos neuroinflamatórios e neurodegenerativos.

Levando em conta nossos resultados, o desenvolvimento da morte neuronal é tempo dependente e tende a seguir uma ordem cronológica de eventos. Cada modelo experimental que utilizamos para comprovar o papel do RAGE na mediação da neurodegeneração apresenta no primeiro momento respostas fisiológicas distintas, por exemplo: a *L. amazonensis* desencadeia febre leve nas primeiras 48 horas sem mortalidade (capítulo I); injeção de LPS desencadeia febre intensa nas primeiras 24 horas acompanhado de sangramento pelo nariz e mortalidade de 15% (capítulo II); sepse desencadeia febre intensa nas primeiras 48 horas e mortalidade acima de 40% (capítulo III); denervação induzida por 6-OHDA na substância negra, nas primeiras horas não apresenta nenhum sintoma visível e não há mortalidade (capítulo IV).

Passado o período mais crítico da inflamação (de 24 a 48 horas após o insulto) os animais se recuperam e de acordo com o tempo, alterações em nível bioquímico (parâmetros de estresse oxidativo e dano oxidativo) e molecular (expressão de proteínas) são detectados. Em diferentes janelas de tempo, uma maior concentração dos ligantes do RAGE pode ser detectado tanto na circulação sanguínea quanto nos órgãos.

Estudos com modelos animais demonstram que passado os sintomas após infecções (LPS) ou administração de α -sinucleína, marcadores de neurodegeneração tendem a levar mais da metade da vida do animal para serem detectados em regiões do cérebro (Qin *et al.*, 2007; Hansen *et al.*, 2013; Rey *et al.*, 2016). Por mais que as primeiras respostas fisiológicas e bioquímicas de um organismo frente a infecções

possuam sintomas distintos, em longo prazo encontramos similaridades como aumento de conteúdo do RAGE.

De acordo com os resultados obtidos até o momento, o RAGE parece ter papel importante nas patogêneses degenerativas, uma vez que estímulos que desencadeiam a ativação da expressão desse receptor invariavelmente resultam na instalação de um processo crônico de inflamação local associado a estresse oxidativo, dano oxidativo em biomoléculas, acúmulo de α -sinucleína e consequente progressão de morte celular no tecido afetado.

Uma vez aumentado o mecanismo de retroalimentação da expressão do RAGE fará com que mais moléculas do RAGE sejam sintetizadas. Quanto maior a quantidade do RAGE na célula maior será a sinalização pró-inflamatória e a produção de espécies reativas, atingindo níveis que a célula não suporta e acaba perdendo função ou morrendo. As estratégias de bloqueio apresentadas nesta tese forem eficazes em bloquear os efeitos deletérios mediados pelo RAGE (figura 5) induzidos por diferentes modelos.

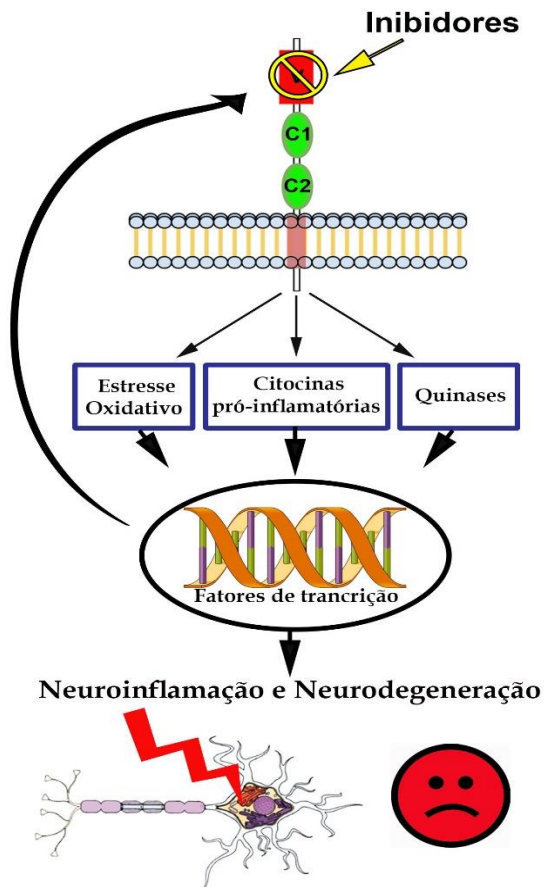


Figura 5. A inibição do RAGE bloqueia a neuroinflamação e a neurodegeneração, induzida pela interação com seus ligantes. Tanto o anti-RAGE quanto o FPS-ZM1 foram eficientes em bloquear a ligação dos ligantes do RAGE. O bloqueio do receptor inibe toda a cascata de sinalização, evitando o estresse oxidativo, a ativação de cinases e a produção de citocinas pró-inflamatórias.

Existem outros receptores de membrana, além do RAGE, que podem modular a ativação pró-inflamatória no cérebro, por exemplo o TLR-4 (Lehnardt *et al.*, 2003; Takeda *et al.*, 2003). Este receptor já foi sugerido por fazer *cross-talk* com RAGE (Qin *et al.*, 2009), porém o mecanismo não é detalhado. De fato, nossas atenções estão voltadas para o RAGE, nossos resultados suportam a hipótese que RAGE é fundamental no desenvolvimento da inflamação e da neurodegeneração.

Inevitavelmente, não são apenas processos patológicos que afetam o aumento do RAGE. O envelhecimento apresenta um declínio progressivo na eficiência dos processos fisiológicos (não necessariamente tudo ao mesmo tempo) após a fase de reprodução. A capacidade de células e organismos para se recuperar de um insulto, como lesão traumática (ou estresse oxidativo) também diminui com a idade (Gutteridge e Halliwell, 2015). De fato, o envelhecimento vem acompanhado de

inúmeras disfunções celulares, são processos naturais, o qual aumentos do conteúdo do RAGE faz parte.

Em um estudo comparando ratos idosos que passaram por treinamento com exercícios de intensidade moderada com ratos da mesma idade que receberam a administração do FPS-ZM1, ambos os grupos tiveram resultados semelhantes. Reduziram os níveis de AGEs e de múltiplos marcadores de estresse oxidativo, diminuíram a expressão do RAGE e suprimiram a ativação de NF- κ B em aortas de ratos (Gu *et al.*, 2014). Este resultado demonstra que o exercício induziu a inativação de AGE/RAGE e que o RAGE está diretamente relacionado com estresse oxidativo e inflamação durante o processo de envelhecimento (Gu *et al.*, 2014).

O estilo de vida também é um componente que pode afetar diretamente o eixo AGE-RAGE. O efeito de nove meses de ingestão de dietas enriquecidas com CML foi testado em camundongos controle e camundongos RAGE ^(-/-). As dietas com alto índice de CML afetaram aortas dos camundongos selvagens enquanto que os RAGE ^(-/-) não tiveram alterações. Os AGEs podem conduzir anormalidades na vasculatura semelhante à do envelhecimento, pelo menos em parte através do RAGE (Grossin *et al.*, 2015). RAGE é expresso em maiores níveis em indivíduos obesos em comparação com indivíduos magros, principalmente em macrófagos e adipócitos (Gaens *et al.*, 2014). Dietas com alto teor de gordura para humanos e/ou em modelos com animais geram ligantes do RAGE, como CML, modificações de fosfoetanolamina de isolevuglandinas, HMGB1 e S100B, que se acumulam em tecidos metabólicos na obesidade (Fujiya *et al.*, 2014; Gaens *et al.*, 2014; Uribarri *et al.*, 2015).

O aumento da disponibilidade de ligantes do RAGE seja pelo processo de envelhecimento ou pela ingestão exacerbada de AGEs associado com rotinas sedentárias aumentam a presença do RAGE nas células. Somado a isso a exposição

de um organismo a estímulos deletérios como por exemplo, infecções, estresse oxidativo e inflamação são componentes que podem agravar ainda mais os níveis do RAGE levando a neurodegeneração.

Adicionado aos fatores externos listados acima, a neurogênese na fase adulta é comprometida (Riddle e Lichtenwalner, 2007), a maquinaria para produção de novas células neuronais (hormônios, fatores de crescimento, neurotransmissores, etc...) nesta fase é debilitada em comparação aos períodos do desenvolvimento (Riddle e Lichtenwalner, 2007; Urbán e Guillemot, 2014). Este efeito acarreta em déficit na reposição de neurônios essenciais para o funcionamento correto do cérebro.

A origem das doenças neurodegenerativas ainda é pouco conhecida, porém sabe-se que o envelhecimento faz parte do processo da vida, as células se desenvolvem cumprem suas funções e morrem, com neurônios não é diferente. Todos os organismos serão oxidados pelo tempo, porém este efeito pode variar entre eles, esta variação parece estar relacionada com hábitos e fatores genéticos que podem delinear caminhos opostos ou a favor às doenças neurodegenerativas.

Conclusões

As doenças neurodegenerativas em estágios iniciais são altamente silenciosas, são imperceptíveis por anos e de difícil diagnóstico. No momento que os sintomas surgem, grandes áreas do cérebro estão comprometidas. RAGE contribui de maneira direta para isso, o qual parece atuar como um gatilho que frente a um estímulo dispara cascatas de sinalização que levam à morte dos neurônios. Nossos resultados apontam o RAGE como o principal mediador para aumento do estado pró-inflamatório e progressão neurodegenerativa. Além disso, uma vasta gama de evidências

disponíveis na literatura, tanto em estudos *in vitro* quanto *in vivo*, sugerem que a inibição do RAGE pode ser uma ferramenta útil para o gerenciamento de patologias imunoinflamatórias.

Independente do modelo experimental que utilizamos nesta tese, a inibição do RAGE resulta na redução: **a)** do acúmulo do RAGE nas células; **b)** de proteínas relacionadas a neuroinflamação; **c)** da morte neuronal. Dado o papel crucial do RAGE em muitas doenças, a descoberta de drogas que inibam o RAGE pode acarretar benefícios para doenças neurodegenerativas e também outras doenças que RAGE seja o agente mediador.

A diversidade da sinalização do RAGE pode ser um fator limitante para o bloqueio do receptor, pois além de ser ativado por diversos ligantes, é necessário que sejam considerados para investigação bloqueadores com afinidade para diferentes domínios, oligômeros e isoformas do RAGE. Dada a importância deste alvo em múltiplas doenças, o desenvolvimento de uma nova geração de intervenções terapêuticas é emergente.

Por mais promissores que os resultados sejam, é necessário investigar mais a fundo os efeitos fisiológicos do RAGE, visto que a longo prazo os efeitos do bloqueio do RAGE são desconhecidos.

Perspectivas

Com base nos resultados observados neste trabalho, as perspectivas futuras são:

A) Investigar a janela de tempo necessária para que haja o aumento do conteúdo do RAGE após indução de neuroinflamação induzida por LPS em ratos Wistar.

B) Investigar os efeitos do bloqueio do RAGE após ter aumento constatado significativamente (período que será estabelecido na opção A) em um protocolo de neurodegeneração crônica (6 a 10 meses) induzida por LPS em ratos Wistar.

C) Averiguar por qual mecanismo (apoptose, senescência, autofagia) o RAGE leva a morte dos neurônios dopaminérgicos induzido por LPS em ratos Wistar.

D) Enquanto a metodologia de experimentação animal visa principalmente esclarecer os mecanismos celulares e moleculares na associação entre o RAGE e a neurodegeneração, vamos complementar nosso estudo sobre o RAGE com a investigação de dados bioquímicos e clínicos coletados em pacientes com a doença de Parkinson. Isso nos fornecerá uma medida de validação do estudo experimental e propiciará o desenvolvimento de uma ferramenta analítica de diagnóstico quantitativo.

E) Investigar qual a relação entre RAGE e seus ligantes nos diferentes estágios clínicos da doença de Parkinson, no grau de envolvimento neurológico e na indução de declínio cognitivo

F) Quantificar os níveis de ligantes de RAGE e moduladores do estado inflamatório (citocinas pró- e anti-inflamatórias) na circulação (sangue periférico) nos modelos animais e também nos pacientes, afim de determinar possíveis correlações

e a potencial utilização do RAGE e de seus moduladores como marcadores periféricos preditivos da evolução da doença de Parkinson

Referências Bibliográficas

ABREU-SILVA, A. L. et al. Central nervous system involvement in experimental infection with *Leishmania (Leishmania) amazonensis*. **Am J Trop Med Hyg**, v. 68, n. 6, p. 661-5, Jun 2003. ISSN 0002-9637 (Print)0002-9637.

ALAM, M. Z. et al. Infectious Agents and Neurodegenerative Diseases: Exploring the Links. **Curr Top Med Chem**, v. 17, n. 12, p. 1390-1399, 2017. ISSN 1568-0266.

BIERHAUS, A. et al. Loss of pain perception in diabetes is dependent on a receptor of the immunoglobulin superfamily. **J Clin Invest**, v. 114, n. 12, p. 1741-51, Dec 2004. ISSN 0021-9738 (Print)0021-9738.

BONGARZONE, S. et al. Targeting the Receptor for Advanced Glycation Endproducts (RAGE): A Medicinal Chemistry Perspective. **J Med Chem**, v. 60, n. 17, p. 7213-7232, Sep 14 2017. ISSN 0022-2623.

BRETT, J. et al. Survey of the distribution of a newly characterized receptor for advanced glycation end products in tissues. **Am J Pathol**, v. 143, n. 6, p. 1699-712, Dec 1993. ISSN 0002-9440 (Print)0002-9440.

BUCKLEY, S. T.; EHRHARDT, C. The receptor for advanced glycation end products (RAGE) and the lung. **J Biomed Biotechnol**, v. 2010, p. 917108, 2010. ISSN 1110-7243.

CARY, B. P. et al. Synthesis and Evaluation of [18F]RAGER: A First Generation Small-Molecule PET Radioligand Targeting the Receptor for Advanced Glycation Endproducts. **ACS Chem Neurosci**, v. 7, n. 3, p. 391-8, Mar 16 2016. ISSN 1948-7193 (Electronic).

CHAVAKIS, T. et al. The pattern recognition receptor (RAGE) is a counterreceptor for leukocyte integrins: a novel pathway for inflammatory cell recruitment. **J Exp Med**, v. 198, n. 10, p. 1507-15, Nov 17 2003. ISSN 0022-1007 (Print)0022-1007.

CHEN, C. et al. Abeta-AGE aggravates cognitive deficit in rats via RAGE pathway. **Neuroscience**, v. 257, p. 1-10, Jan 17 2014. ISSN 0306-4522.

CHEN, X. et al. RAGE: a potential target for Abeta-mediated cellular perturbation in Alzheimer's disease. **Curr Mol Med**, v. 7, n. 8, p. 735-42, Dec 2007. ISSN 1566-5240 (Print)1566-5240.

CHEN, Y. et al. Blockade of late stages of autoimmune diabetes by inhibition of the receptor for advanced glycation end products. **J Immunol**, v. 173, n. 2, p. 1399-405, Jul 15 2004. ISSN 0022-1767 (Print)0022-1767.

CHENG, C. et al. Expression profiling of endogenous secretory receptor for advanced glycation end products in human organs. **Mod Pathol**, v. 18, n. 10, p. 1385-96, Oct 2005. ISSN 0893-3952 (Print)0893-3952.

CHO, H. J. et al. RAGE regulates BACE1 and Abeta generation via NFAT1 activation in Alzheimer's disease animal model. **Faseb j**, v. 23, n. 8, p. 2639-49, Aug 2009. ISSN 0892-6638.

CHUAH, Y. K. et al. Receptor for advanced glycation end products and its involvement in inflammatory diseases. **Int J Inflam**, v. 2013, p. 403460, 2013. ISSN 2090-8040 (Print)2042-0099.

DAL-PIZZOL, F. et al. Neonatal iron exposure induces oxidative stress in adult Wistar rat. **Brain Res Dev Brain Res**, v. 130, n. 1, p. 109-14, Sep 23 2001. ISSN 0165-3806 (Print)0165-3806.

_____. Is there a role for high mobility group box 1 and the receptor for advanced glycation end products in the genesis of long-term cognitive impairment in sepsis survivors? In: (Ed.). **Mol Med**. United States, v.18, 2012. p.1357-8; author reply 1359. ISBN 1528-3658 (Electronic)1076-1551 (Linking).

DALFO, E. et al. Evidence of oxidative stress in the neocortex in incidental Lewy body disease. **J Neuropathol Exp Neurol**, v. 64, n. 9, p. 816-30, Sep 2005. ISSN 0022-3069 (Print)0022-3069.

DAMANHURI, H. A. et al. Tyrosine hydroxylase phosphorylation in catecholaminergic brain regions: a marker of activation following acute hypotension and glucoprivation. **PLoS One**, v. 7, n. 11, p. e50535, 2012. ISSN 1932-6203.

DATTILO, B. M. et al. The extracellular region of the receptor for advanced glycation end products is composed of two independent structural units. **Biochemistry**, v. 46, n. 23, p. 6957-70, Jun 12 2007. ISSN 0006-2960 (Print)0006-2960.

DE CHIARA, G. et al. Infectious Agents and Neurodegeneration. In: (Ed.). **Mol Neurobiol**, v.46, 2012. p.614-38. ISBN 0893-7648 (Print)1559-1182 (Electronic).

DE OLIVEIRA, R. B. et al. Schistosoma mansoni infection causes oxidative stress and alters receptor for advanced glycation endproduct (RAGE) and tau levels in multiple organs in mice. **Int J Parasitol**, v. 43, n. 5, p. 371-9, Apr 2013. ISSN 1879-0135.

DEANE, R. et al. A multimodal RAGE-specific inhibitor reduces amyloid beta-mediated brain disorder in a mouse model of Alzheimer disease. **J Clin Invest**, v. 122, n. 4, p. 1377-92, Apr 2012. ISSN 0021-9738.

DING, K. H. et al. Disordered osteoclast formation in RAGE-deficient mouse establishes an essential role for RAGE in diabetes related bone loss. **Biochem Biophys Res Commun**, v. 340, n. 4, p. 1091-7, Feb 24 2006. ISSN 0006-291X (Print)0006-291x.

DING, Q.; KELLER, J. N. Evaluation of rage isoforms, ligands, and signaling in the brain. **Biochim Biophys Acta**, v. 1746, n. 1, p. 18-27, Oct 30 2005. ISSN 0006-3002 (Print)0006-3002.

DUNKLEY, P. R. et al. Tyrosine hydroxylase phosphorylation: regulation and consequences. **J Neurochem**, v. 91, n. 5, p. 1025-43, Dec 2004. ISSN 0022-3042 (Print)0022-3042.

FALCONE, C. et al. Plasma levels of soluble receptor for advanced glycation end products and coronary atherosclerosis: possible correlation with clinical presentation. **Dis Markers**, v. 35, n. 3, p. 135-40, 2013. ISSN 0278-0240.

FUJII, E. Y.; NAKAYAMA, M. The measurements of RAGE, VEGF, and AGEs in the plasma and follicular fluid of reproductive women: the influence of aging. **Fertil Steril**, v. 94, n. 2, p. 694-700, Jul 2010. ISSN 0015-0282.

FUJIYA, A. et al. The role of S100B in the interaction between adipocytes and macrophages. **Obesity (Silver Spring)**, v. 22, n. 2, p. 371-9, Feb 2014. ISSN 1930-7381.

GAENS, K. H. et al. Nepsilon-(carboxymethyl)lysine-receptor for advanced glycation end product axis is a key modulator of obesity-induced dysregulation of adipokine expression and insulin resistance. **Arterioscler Thromb Vasc Biol**, v. 34, n. 6, p. 1199-208, Jun 2014. ISSN 1079-5642.

GASPAROTTO, J. et al. Receptor for advanced glycation end products mediates sepsis-triggered amyloid- β accumulation, Tau phosphorylation, and cognitive impairment. **J Biol Chem**, v. 293, n. 1, p. 226-244, Jan 2018. ISSN 1083-351X.

_____. N-acetyl-cysteine inhibits liver oxidative stress markers in BALB/c mice infected with *Leishmania amazonensis*. **Mem Inst Oswaldo Cruz**, v. 112, n. 2, p. 146-154, Feb 2017. ISSN 0074-0276.

_____. Anti-RAGE antibody selectively blocks acute systemic inflammatory responses to LPS in serum, liver, CSF and striatum. **Brain Behav Immun**, Jan 2017. ISSN 1090-2139.

GEROLDI, D. et al. High levels of soluble receptor for advanced glycation end products may be a marker of extreme longevity in humans. **J Am Geriatr Soc**, United States, v. 54, n. 7, p. 1149-50, 2006. ISSN 0002-8614 (Print)0002-8614 (Linking).

GONTIJO, C. M. et al. Concurrent cutaneous, visceral and ocular leishmaniasis caused by *Leishmania (Viannia) braziliensis* in a kidney transplant patient. **Mem Inst Oswaldo Cruz**, v. 97, n. 5, p. 751-3, Jul 2002. ISSN 0074-0276 (Print)0074-0276.

GROSSIN, N. et al. Dietary CML-enriched protein induces functional arterial aging in a RAGE-dependent manner in mice. **Mol Nutr Food Res**, v. 59, n. 5, p. 927-38, May 2015. ISSN 1613-4125.

GU, Q. et al. Contribution of receptor for advanced glycation end products to vasculature-protecting effects of exercise training in aged rats. **Eur J Pharmacol**, v. 741, p. 186-94, Oct 15 2014. ISSN 0014-2999.

GUO, Z. J. et al. Advanced oxidation protein products activate vascular endothelial cells via a RAGE-mediated signaling pathway. **Antioxid Redox Signal**, v. 10, n. 10, p. 1699-712, Oct 2008. ISSN 1557-7716.

HALLIWELL, B.; GUTTERIDGE, J. M. C. **Free Radicals in Biology and Medicine**. 5th. New York: Oxford University Press, 2015.

HANSEN, C. et al. A novel alpha-synuclein-GFP mouse model displays progressive motor impairment, olfactory dysfunction and accumulation of alpha-synuclein-GFP. **Neurobiol Dis**, v. 56, p. 145-55, Aug 2013. ISSN 0969-9961.

HOFMANN, M. A. et al. RAGE mediates a novel proinflammatory axis: a central cell surface receptor for S100/calgranulin polypeptides. **Cell**, v. 97, n. 7, p. 889-901, Jun 25 1999. ISSN 0092-8674 (Print)0092-8674.

HONG, Y. et al. Effects of RAGE-Specific Inhibitor FPS-ZM1 on Amyloid-beta Metabolism and AGEs-Induced Inflammation and Oxidative Stress in Rat Hippocampus. **Neurochem Res**, v. 41, n. 5, p. 1192-9, May 2016. ISSN 0364-3190.

HORI, O. et al. The receptor for advanced glycation end products (RAGE) is a cellular binding site for amphoterin. Mediation of neurite outgrowth and co-expression of rage and amphoterin in the developing nervous system. **J Biol Chem**, v. 270, n. 43, p. 25752-61, Oct 27 1995. ISSN 0021-9258 (Print)0021-9258.

HUDSON, B. I. et al. Interaction of the RAGE cytoplasmic domain with diaphanous-1 is required for ligand-stimulated cellular migration through activation of Rac1 and Cdc42. **J Biol Chem**, v. 283, n. 49, p. 34457-68, Dec 5 2008. ISSN 0021-9258 (Print)0021-9258.

HUTTUNEN, H. J. et al. Coregulation of neurite outgrowth and cell survival by amphoterin and S100 proteins through receptor for advanced glycation end products (RAGE) activation. **J Biol Chem**, v. 275, n. 51, p. 40096-105, Dec 22 2000. ISSN 0021-9258 (Print)0021-9258.

JANSSEN-HEININGER, Y. M.; POYNTER, M. E.; BAEUERLE, P. A. Recent advances towards understanding redox mechanisms in the activation of nuclear factor kappaB. **Free Radic Biol Med**, v. 28, n. 9, p. 1317-27, May 1 2000. ISSN 0891-5849 (Print)0891-5849.

JEYNES, B.; PROVIAS, J. Evidence for altered LRP/RAGE expression in Alzheimer lesion pathogenesis. **Curr Alzheimer Res**, v. 5, n. 5, p. 432-7, Oct 2008. ISSN 1567-2050 (Print)1567-2050.

JURANEK, J. et al. Receptor for advanced glycation end-products in neurodegenerative diseases. **Rev Neurosci**, v. 26, n. 6, p. 691-8, 2015. ISSN 0334-1763 (Print)0334-1763.

KIM, S. J. et al. Two beta-strands of RAGE participate in the recognition and transport of amyloid-beta peptide across the blood brain barrier. **Biochem Biophys Res Commun**, v. 439, n. 2, p. 252-7, Sep 20 2013. ISSN 0006-291x.

KISLINGER, T. et al. Receptor for advanced glycation end products mediates inflammation and enhanced expression of tissue factor in vasculature of diabetic apolipoprotein E-null mice. **Arterioscler Thromb Vasc Biol**, v. 21, n. 6, p. 905-10, Jun 2001. ISSN 1079-5642.

KOCH, M. et al. Structural basis for ligand recognition and activation of RAGE. **Structure**, v. 18, n. 10, p. 1342-52, Oct 13 2010. ISSN 0969-2126.

LECLERC, E. et al. S100B and S100A6 differentially modulate cell survival by interacting with distinct RAGE (receptor for advanced glycation end products) immunoglobulin domains. **J Biol Chem**, v. 282, n. 43, p. 31317-31, Oct 26 2007. ISSN 0021-9258 (Print)0021-9258.

LEHNARDT, S. et al. Activation of innate immunity in the CNS triggers neurodegeneration through a Toll-like receptor 4-dependent pathway. **Proc Natl Acad Sci U S A**, v. 100, n. 14, p. 8514-9, Jul 8 2003. ISSN 0027-8424 (Print)0027-8424.

LI, J.; SCHMIDT, A. M. Characterization and functional analysis of the promoter of RAGE, the receptor for advanced glycation end products. **J Biol Chem**, v. 272, n. 26, p. 16498-506, Jun 27 1997. ISSN 0021-9258 (Print)0021-9258.

LILIENSIEK, B. et al. Receptor for advanced glycation end products (RAGE) regulates sepsis but not the adaptive immune response. **J Clin Invest**, v. 113, n. 11, p. 1641-50, Jun 2004. ISSN 0021-9738 (Print)0021-9738.

LIMA, M. M. et al. Motor and non-motor features of Parkinson's disease - a review of clinical and experimental studies. **CNS Neurol Disord Drug Targets**, v. 11, n. 4, p. 439-49, Jun 1 2012. ISSN 1871-5273.

LIU, M.; BING, G. Lipopolysaccharide Animal Models for Parkinson's Disease. **Parkinsons Dis**, v. 2011, 2011. ISSN 2042-0080 (Electronic).

LIU, Y. et al. Endotoxin induces a delayed loss of TH-IR neurons in substantia nigra and motor behavioral deficits. **Neurotoxicology**, v. 29, n. 5, p. 864-70, Sep 2008. ISSN 0161-813X (Print)0161-813x.

LOPEZ-DIEZ, R. et al. Complex tissue-specific patterns and distribution of multiple RAGE splice variants in different mammals. **Genome Biol Evol**, v. 5, n. 12, p. 2420-35, 2013. ISSN 1759-6653.

LUTTERLOH, E. C. et al. Inhibition of the RAGE products increases survival in experimental models of severe sepsis and systemic infection. **Crit Care**, v. 11, n. 6, p. R122, 2007. ISSN 1364-8535.

MACKIC, J. B. et al. Human blood-brain barrier receptors for Alzheimer's amyloid-beta 1-40. Asymmetrical binding, endocytosis, and transcytosis at the apical side of brain microvascular endothelial cell monolayer. **J Clin Invest**, v. 102, n. 4, p. 734-43, Aug 15 1998. ISSN 0021-9738 (Print)0021-9738.

MATSUMOTO, S. et al. Solution structure of the variable-type domain of the receptor for advanced glycation end products: new insight into AGE-RAGE interaction. **Biochemistry**, v. 47, n. 47, p. 12299-311, Nov 25 2008. ISSN 0006-2960.

MATTSON, M. P.; CAMANDOLA, S. NF-kappaB in neuronal plasticity and neurodegenerative disorders. **J Clin Invest**, v. 107, n. 3, p. 247-54, Feb 2001. ISSN 0021-9738 (Print)0021-9738.

MILLER, I. N.; CRONIN-GOLOMB, A. Gender differences in Parkinson's disease: clinical characteristics and cognition. **Mov Disord**, v. 25, n. 16, p. 2695-703, Dec 15 2010. ISSN 0885-3185.

MILLER, M. C. et al. Hippocampal RAGE immunoreactivity in early and advanced Alzheimer's disease. **Brain Res**, v. 1230, p. 273-80, Sep 16 2008. ISSN 0006-8993 (Print)0006-8993. D

MUNCHAU, A.; BHATIA, K. Pharmacological treatment of Parkinson's disease. **Postgrad Med J**, v. 76, n. 900, p. 602-10, Oct 2000. ISSN 0032-5473 (Print)1469-0756 (Electronic).

NEEPER, M. et al. Cloning and expression of a cell surface receptor for advanced glycosylation end products of proteins. **J Biol Chem**, v. 267, n. 21, p. 14998-5004, Jul 25 1992. ISSN 0021-9258 (Print)0021-9258.

NIETO, C. G. et al. Detection of Leishmania infantum amastigotes in canine choroid plexus. **Vet Rec**, v. 139, n. 14, p. 346-7, Oct 5 1996. ISSN 0042-4900 (Print)0042-4900.

PETERSEN, C. A.; GREENLEE, M. H. W. Neurologic Manifestations of Leishmania spp. Infection. **J Neuroparasitology**, v. 2, 2011. ISSN 2090-2344 (Print)2090-2352 (Electronic).

PIRAS, S. et al. RAGE Expression and ROS Generation in Neurons: Differentiation versus Damage. **Oxid Med Cell Longev**, v. 2016, 2016. ISSN 1942-0900 (Print)1942-0994 (Electronic).

QIN, L. et al. Systemic LPS causes chronic neuroinflammation and progressive neurodegeneration. **Glia**, v. 55, n. 5, p. 453-62, Apr 1 2007. ISSN 0894-1491 (Print)0894-1491.

QIN, Y. H. et al. HMGB1 enhances the proinflammatory activity of lipopolysaccharide by promoting the phosphorylation of MAPK p38 through receptor for advanced glycation end products. **J Immunol**, v. 183, n. 10, p. 6244-50, Nov 15 2009. ISSN 0022-1767.

RAI, V. et al. Signal transduction in receptor for advanced glycation end products (RAGE): solution structure of C-terminal rage (ctRAGE) and its binding to mDia1. **J Biol Chem**, v. 287, n. 7, p. 5133-44, Feb 10 2012. ISSN 0021-9258.

RAMASAMY, R.; SHEKHTMAN, A.; SCHMIDT, A. M. The multiple faces of RAGE--opportunities for therapeutic intervention in aging and chronic disease. **Expert Opin Ther Targets**, v. 20, n. 4, p. 431-46, 2016. ISSN 1472-8222.

RAMASAMY, R. et al. Receptor for Advanced Glycation End Products: Fundamental Roles in the Inflammatory Response: Winding the Way to the Pathogenesis of Endothelial Dysfunction and Atherosclerosis. **Ann N Y Acad Sci**, v. 1126, p. 7-13, Apr 2008. ISSN 0077-8923 (Print)1749-6632 (Electronic).

REINERT, K. R. et al. Short-term effects of an endotoxin on substantia nigra dopamine neurons. **Brain Res**, v. 1557, p. 164-70, Apr 4 2014. ISSN 0006-8993.

REY, N. L. et al. Widespread transneuronal propagation of alpha-synucleinopathy triggered in olfactory bulb mimics prodromal Parkinson's disease. **J Exp Med**, v. 213, n. 9, p. 1759-78, Aug 22 2016. ISSN 0022-1007.

RIDDLE, D. R.; LICHTENWALNER, R. J. Neurogenesis in the Adult and Aging Brain. In:Brain Aging: Models, Methods, and Mechanisms. Chapter 6. (Ed.): CRC Press/Taylor & Francis, 2007.

RODRIGUEZ GONZALEZ-MORO, J. M. et al. Impact of COPD severity on physical disability and daily living activities: EDIP-EPOC I and EDIP-EPOC II studies. **Int J Clin Pract**, v. 63, n. 5, p. 742-50, May 2009. ISSN 1368-5031.

RONG, L. L. et al. Antagonism of RAGE suppresses peripheral nerve regeneration. **Faseb j**, v. 18, n. 15, p. 1812-7, Dec 2004. ISSN 0892-6638.

_____. RAGE modulates peripheral nerve regeneration via recruitment of both inflammatory and axonal outgrowth pathways. **Faseb j**, v. 18, n. 15, p. 1818-25, Dec 2004. ISSN 0892-6638.

RUDERMAN, N. B.; WILLIAMSON, J. R.; BROWNLEE, M. Glucose and diabetic vascular disease. **Faseb j**, v. 6, n. 11, p. 2905-14, Aug 1992. ISSN 0892-6638 (Print)0892-6638.

SARNICO, I. et al. NF-kappaB and epigenetic mechanisms as integrative regulators of brain resilience to anoxic stress. **Brain Res**, v. 1476, p. 203-10, Oct 2 2012. ISSN 0006-8993.

SASAKI, N. et al. Immunohistochemical distribution of the receptor for advanced glycation end products in neurons and astrocytes in Alzheimer's disease. **Brain Res**, v. 888, n. 2, p. 256-262, Jan 12 2001. ISSN 0006-8993 (Print)0006-8993.

SATHE, K. et al. S100B is increased in Parkinson's disease and ablation protects against MPTP-induced toxicity through the RAGE and TNF-alpha pathway. **Brain**, v. 135, n. Pt 11, p. 3336-47, Nov 2012. ISSN 0006-8950.

SCHMIDT, A. M. et al. RAGE: a novel cellular receptor for advanced glycation end products. **Diabetes**, v. 45 Suppl 3, p. S77-80, Jul 1996. ISSN 0012-1797 (Print)0012-1797.

_____. Isolation and characterization of two binding proteins for advanced glycosylation end products from bovine lung which are present on the endothelial cell surface. **J Biol Chem**, v. 267, n. 21, p. 14987-97, Jul 25 1992. ISSN 0021-9258 (Print)0021-9258.

_____. Regulation of human mononuclear phagocyte migration by cell surface-binding proteins for advanced glycation end products. **J Clin Invest**, v. 91, n. 5, p. 2155-68, May 1993. ISSN 0021-9738 (Print)0021-9738.

SEMMLER, A. et al. Sepsis causes neuroinflammation and concomitant decrease of cerebral metabolism. **J Neuroinflammation**, v. 5, p. 38, 2008. ISSN 1742-2094.

SESSA, L. et al. The Receptor for Advanced Glycation End-Products (RAGE) Is Only Present in Mammals, and Belongs to a Family of Cell Adhesion Molecules (CAMs). **PLoS One**, v. 9, n. 1, 2014. ISSN 1932-6203 (Electronic). Disponível em: < <http://dx.doi.org/10.1371/journal.pone.0086903> >.

SIMM, A. et al. Age associated changes of AGE-receptor expression: RAGE upregulation is associated with human heart dysfunction. **Exp Gerontol**, v. 39, n. 3, p. 407-13, Mar 2004. ISSN 0531-5565 (Print)0531-5565.

SONG, J. et al. Receptor for Advanced Glycation End Products (RAGE) and Its Ligands: Focus on Spinal Cord Injury. **Int J Mol Sci**, v. 15, n. 8, p. 13172-91, 2014. ISSN 1422-0067 (Electronic).

SRIKANTH, V. et al. Advanced glycation endproducts and their receptor RAGE in Alzheimer's disease. **Neurobiol Aging**, v. 32, n. 5, p. 763-77, May 2011. ISSN 0197-4580.

TAGUCHI, A. et al. Blockade of RAGE-amphoterin signalling suppresses tumour growth and metastases. **Nature**, v. 405, n. 6784, p. 354-60, May 18 2000. ISSN 0028-0836 (Print)0028-0836.

TAKEDA, K.; KAISHO, T.; AKIRA, S. Toll-like receptors. **Annu Rev Immunol**, v. 21, p. 335-76, 2003. ISSN 0732-0582 (Print)0732-0582.

TAKUMA, K. et al. RAGE-mediated signaling contributes to intraneuronal transport of amyloid-beta and neuronal dysfunction. **Proc Natl Acad Sci U S A**, v. 106, n. 47, p. 20021-6, Nov 24 2009. ISSN 0027-8424.

TEISMANN, P. et al. Receptor for advanced glycation endproducts (RAGE) deficiency protects against MPTP toxicity. **Neurobiol Aging**, v. 33, n. 10, p. 2478-90, Oct 2012. ISSN 0197-4580.

URBÁN, N.; GUILLEMOT, F. Neurogenesis in the embryonic and adult brain: same regulators, different roles. **Front Cell Neurosci**, v. 8, 2014. ISSN 1662-5102 (Electronic). D

URIBARRI, J. et al. Elevated serum advanced glycation endproducts in obese indicate risk for the metabolic syndrome: a link between healthy and unhealthy obesity? **J Clin Endocrinol Metab**, v. 100, n. 5, p. 1957-66, May 2015. ISSN 0021-972x.

UTTARA, B. et al. Oxidative Stress and Neurodegenerative Diseases: A Review of Upstream and Downstream Antioxidant Therapeutic Options. **Curr Neuropharmacol**, v. 7, n. 1, p. 65-74, Mar 2009. ISSN 1570-159X (Print)1875-6190 (Electronic).

VALENTE, T. et al. Immunohistochemical analysis of human brain suggests pathological synergism of Alzheimer's disease and diabetes mellitus. **Neurobiol Dis**, v. 37, n. 1, p. 67-76, Jan 2010. ISSN 0969-9961.

WIDMANN, C. N.; HENEKA, M. T. Long-term cerebral consequences of sepsis. **Lancet Neurol**, v. 13, n. 6, p. 630-6, Jun 2014. ISSN 1474-4422.

XUE, J. et al. The receptor for advanced glycation end products (RAGE) specifically recognizes methylglyoxal-derived AGEs. **Biochemistry**, v. 53, n. 20, p. 3327-35, May 27 2014. ISSN 0006-2960.

YAN, S. D. et al. RAGE and Alzheimer's disease: a progression factor for amyloid-beta-induced cellular perturbation? **J Alzheimers Dis**, v. 16, n. 4, p. 833-43, 2009. ISSN 1387-2877 (Print)1387-2877.

_____. RAGE and amyloid-beta peptide neurotoxicity in Alzheimer's disease. **Nature**, v. 382, n. 6593, p. 685-91, Aug 22 1996. ISSN 0028-0836 (Print)0028-0836.

_____. Receptor-dependent cell stress and amyloid accumulation in systemic amyloidosis. **Nat Med**, v. 6, n. 6, p. 643-51, Jun 2000. ISSN 1078-8956 (Print)1078-8956.

YANG, F. et al. Receptor for advanced glycation end-product antagonist reduces blood-brain barrier damage after intracerebral hemorrhage. **Stroke**, v. 46, n. 5, p. 1328-36, May 2015. ISSN 0039-2499.

YATIME, L.; ANDERSEN, G. R. Structural insights into the oligomerization mode of the human receptor for advanced glycation end-products. **Febs j**, v. 280, n. 24, p. 6556-68, Dec 2013. ISSN 1742-464x.

ZHANG, L. et al. Receptor for advanced glycation end products is subjected to protein ectodomain shedding by metalloproteinases. **J Biol Chem**, v. 283, n. 51, p. 35507-16, Dec 19 2008. ISSN 0021-9258 (Print)0021-9258.

ZHANG, L.; POSTINA, R.; WANG, Y. Ectodomain shedding of the receptor for advanced glycation end products: a novel therapeutic target for Alzheimer's disease. **Cell Mol Life Sci**, v. 66, n. 24, p. 3923-35, Dec 2009. ISSN 1420-682x.

ZHOU, Z. et al. Regulation of osteoclast function and bone mass by RAGE. **J Exp Med**, v. 203, n. 4, p. 1067-80, 2006. ISSN 0022-1007 (Print)1540-9538 (Electronic).

ZONG, H. et al. Homodimerization is essential for the receptor for advanced glycation end products (RAGE)-mediated signal transduction. **J Biol Chem**, v. 285, n. 30, p. 23137-46, Jul 23 2010. ISSN 0021-9258.